SYNTHESIS AND STUDY OF NOVEL NANOCOMPOSITES WITH POLYMER MATRIX (FOSSIL-BASED AND BIO-BASED RESINS) AND GRAPHENE OR RELATED LAYERED MATERIALS (GRMs) FOR LIGHTWEIGHT AUTOMOTIVE APPLICATIONS.

Sheikh, Rehman

Doctoral thesis

University of Sunderland,

September 2022

SYNTHESIS AND STUDY OF NOVEL NANOCOMPOSITES WITH POLYMER MATRIX (FOSSIL-BASED AND BIO-BASED RESINS) AND GRAPHENE OR RELATED LAYERED MATERIALS (GRMS) FOR LIGHTWEIGHT AUTOMOTIVE APPLICATIONS

SHEIKH MUHAMMAD AMEER UR REHMAN

A thesis submitted in partial fulfilment of the requirements of the University of Sunderland for the degree of Doctor of Philosophy

September 2022

Abstract

Novel nanocomposites were synthesized and studied, comprising of graphene nanoplatelets (GNPs) or reduced graphene oxide (rGO) or 3-glycidoxypropyltrimethoxysilane (GLYMO-rGO) as nanofillers, dispersed in epoxy resin matrices. Due to limited petrochemical resources and environmental concerns, biopolymers are becoming increasingly attractive, allowing a more sustainable production and growth. Therefore, both fossil-based and bio-based epoxy resins were studied. New graphene/epoxy nanocomposites were developed, following a facile solvent-free approach, adding the above graphene related materials (GRMs) in the amine hardener, simplifying the experimental procedure, and lowering manufacturing cost. The addition of GRMs caused an increase in the degree of curing of the epoxy systems, a reduction in activation energy, improved thermal stability, mechanical properties, and lap shear strength. More specifically, in the fossil-based resin, an increase in thermal stability by the addition of GNPs was identified in the range of 360–580°C using TGA. In terms of mechanical properties, addition of an optimum amount of 0.5%wt of GNPs improved the Young's Modulus by 37%. Nanoindentation measurements showed a 9.4% improvement in hardness at 0.7%wt GNPs. In the bio-based resin, addition of 1.5wt% of GLYMO-rGO into the epoxy matrix was found to increase the degree of cure by up to 12% and glass transition temperature by 14°C. Mechanical testing showed that the addition of 0.05wt% GLYMO-rGO improves young's modulus and tensile strength by 60% and 16%, respectively, compared to neat epoxy. The resins enhanced with GRMs were also used as an adhesive to bond CFRP/CFRP and CFRP/aluminium adherents. The addition of 0.1wt% GLYMO-rGO into the adhesive and CRFP adherents showed improved lap shear strength by 23.6% compared to neat resin, while in the case of CFRP/Aluminium joints the increase was 21.2%. These novel nanocomposite materials can be used to design lightweight materials for energy-efficient and safe vehicles.

Extended summary Chapter

The thesis consists of seven chapters, presenting the work performed during this PhD research. Chapter 1 introduces the research questions, including the identification of optimum dispersion methodologies of GRMs (GNPs, rGO, GLYMO-rGO) into different epoxies (Epilok 60-566 and Epilok 60-600G); the identification of suitable curing conditions; investigations of property enhancements (mechanical and thermal) and joining performance improvements between similar or dissimilar materials. It also includes the rationale for developing new lightweight nanocomposite materials and contributing to knowledge.

Chapter 2 detailed literature review is presented, which aims to inform the reader about graphene/epoxy nanocomposites. This chapter discusses thoroughly epoxy polymer systems, GRMs and their composites reported in the literature, different processing variables that affect the dispersibility of GRMs into polymer matrices and their relationship to the final properties of nanocomposites. A detailed review of the adhesive bonding for improving the lap shear strength of joints is provided.

In chapter 3, an overview of materials used in the automotive industry is provided. First, the traditional materials, i.e. steel, aluminium, magnesium, are analysed, which potentially could be replaced by lighter polymer nanocomposite materials, i.e. GRM enhanced carbon fibre-reinforced polymers (CFRPs). Then, in chapter 4, the experimental methods used are discussed. Experimental methods include techniques that were used for materials synthesis using bath ultrasonication and wet lay-up process also materials characterisation techniques using differential scanning calorimetry (DSC), cure kinetic models, thermogravimetric analysis(TGA), scanning electron microscopy (SEM), and others.

Chapter 5 reports the formulation and characterisation of new graphene/polymer nanocomposites using graphene nanoplatelets (GNPs) and the epoxy system Epilok 60–

566/Curamine 32–494. In a suggested solvent-free approach, GNPs were first dispersed into the curamine hardener using bath ultrasonication, followed by the addition of the epoxy resin. The cure kinetics were studied by DSC under nonisothermal and under isothermal conditions. The kinetic parameters of the curing process were determined using the nonisothermal Kissinger and Ozawa-Flynn-Wall models. It is found that the degree of curing increased with the addition of GNPs, while the activation energy decreased by 13.7% for the primary amine reaction and by 6.6% for the secondary amine reaction with epoxy groups as obtained from the Kissinger model. An increase in thermal stability by adding GNPs was identified in the range of 360-580℃ using TGA. An amount of 0.5wt% of GNPs in the hardener improved Young's Modulus by 37%. Nanoindentation measurements showed a 9.4% improvement in hardness at 0.7wt% nanofiller.

Chapter 6 reports the synthesis and study of novel nanocomposites using a biobased epoxy/amine (Epilok 60-600G/Curamine 30-952) matrix, reinforced with reduced graphene oxide (rGO) or functionalised with 3- glycidoxypropyltrimethoxysilane (GLYMO-rGO). Epilok 60-600G and Curamine 30-952 have 36% and 66% bio-based renewable content, respectively. The addition of 1.5 wt% of GLYMO-rGO into the epoxy matrix has increased the degree of cure by up to 12% and the glass transition temperature by 14℃, which shows improvement in thermal stability. Mechanical testing showed that adding 0.05 wt% GLYMO-rGO improves Young's modulus and Ultimate tensile strength by 60% and 16%, respectively, compared to neat epoxy. The GRM enhanced resin was used as a matrix system to prepare CFRP laminates and adhesive to prepare lap shear joints; CFRP/CFRP (similar adherents), and CFRP/Aluminium (dissimilar adherents). The addition of 0.1 wt% GLYMO-rGO into the adhesive and the CRFP adherents showed improved lap shear strength by 23.6% compared to the neat resin, while in the case of CFRP/Aluminium joints, the increase was 21.2%. This

improved lap shear strength can be beneficial in lightweight automotive applications where CFRP and aluminium parts are required to assemble and bonded.

Chapter 7 presents a discussion of this research, conclusions, and suggestions for future research.

Acknowledgements

First and foremost, I would like to give definitive thanks to Allah for everything he has given me in my life. I would like to thank my supervisors, Director of Studies Dr Panagiotis Karagiannidis and co-supervisor Prof. David Baglee, for their guidance, encouragement, efforts and cooperation. I am happy to have them as my supervisors, which has benefited me greatly. I would also acknowledge my fellow research colleagues' valuable advice and encouragement throughout my research.

I want to thank all the staff at the Engineering Lab, the University of Sunderland, especially David Wilson, Chris Rowan, David Winter and David Harrison and Timothy Betterton from The National Glass Centre, who were supportive and encouraging.

I would like to thank Bitrez Ltd (UK), Thomas Swan & Co. Ltd (UK), Avanzare (Spain) and Inter-Química (Spain) for providing epoxy resins, GNPs and rGOs. I appreciate their generosity.

I owe special thanks to my parents, who were supportive and encouraging during my lows and highs times.

I want to express my gratitude to my siblings for their continuous support and understanding throughout my research journey, which has enabled me to achieve many research goals. I would also like to thank my well-wisher and mentor, Dr Muhammad Sheikh.

Finally, I would like to give special thanks and acknowledgement for the tremendous and continuous help, patience, and inspiration that I received from my wife.

Published Papers Detail

- Bio-based epoxy/amine reinforced with reduced graphene oxide (rGO) or GLYMO-rGO: study of curing kinetics, mechanical properties, lamination and bonding performance.

  Sheikh Rehman, Julio Gomez, Elvira Villaro, Dwane Cossey, Panagiotis Karagiannidis.

  Nanomaterials 2022, 12(2), 222, doi.org/10.3390/nano12020222

- Development of new graphene/epoxy nanocomposites and study of cure kinetics, thermal and mechanical properties

  Sheikh Rehman, Sufyan Akram, Antonios Kanellopoulos, Ahmed Elmarakbi, Panagiotis G. Karagiannidis.

  Thermochimica Acta Volume 694, December 2020, 178785,

  doi.org/10.1016/j.tca.2020.178785

Research Seminar

- ‘’Development of new graphene/epoxy nanocomposites: Study of cure kinetics, thermal and mechanical properties, lamination and bonding performance’’ Engineering Research Seminar Series 2021-22, University of Sunderland, 15th December 2021.

List of Symbols

GRMs	Graphene related materials
GNP	Graphene Nanoplatelet
rGO	Reduced Graphene Oxide
GO	Graphene Oxide
f-rGO	Functionalised reduced graphene oxide
GLYMO	3-glycidoxypropyltrimethoxysilane
Na-MMT	Sodium montmorillonite
LDH	Layered double hydroxide
EG	Exfoliated graphite
CNT	Carbon nanotubes
CNF	Carbon nanofibers
CO_2	Carbon dioxide
DCB	Dichlorobenzene
DMF	Dimethylformamide
PVA	Polyvinyl Alcohol
SDS	Sodium dodecyl sulphate
GA	Gum Arabic
CF	Carbon fibre
CFRP	Carbon fibre-reinforced polymer
DSC	Differential Scanning Calorimetry
2D	two-dimensional
TGA	Thermogravimetric analysis
SEM	Scanning Electron Microscopy
TEM	Transmission electron microscopy
DGEBA	Diglycidyl ether of bisphenol A
DDM	Diaminodiphenylmethane
TGDDM	Tetraglycidyl-4,4’-diaminodiphenylmethane
DDS	Diamine 4,4’-diaminodiphenylsulfone
FTIR	Fourier Transform Infrared Spectroscopy
LSS	Lap shear strength
FWHM	Full width at half maximum

Al	Aluminium
EAA	European Aluminum Association
MD	Molecular Dynamics
EU	European Union
LULUCF	Land use, land-use change and forestry activities
EEW	Epoxide equivalent weight
AHEW	Amine hydrogen equivalent weight
ΔH_{iso}	Total heat of curing recorded isothermally
ΔH_{dyn}	Residual heat of curing recorded dynamically
α	Degree of curing
XPS	X-ray photoelectron spectroscopy
T_{init}	Initial curing temperature
T_{peak}	Peak curing temperature
T_{final}	Final curing temperature
ΔH_{ult}	Ultimate heat of curing
ASTM	American Society for Testing and Materials
GUI	Graphical user interface
(S)	Shape index
SSA	Specific surface area
BPA	Bisphenol A
CB	Carbon black
E_a	Activation energy
k	Rate constant
A	Pre-exponential factor
β, φ	Heating rate
Ti	Isoconversion temperature
f(α)	Conversion function
Tg	Transition temprature
(ΔH)	Heat of cure
E	Young's modulus
UTS	Ultimate tensile strength
σ	Stress

ε	Strain
wt. %	Weight fraction percent
vol.%	Volume fraction percent
ω	Angular frequency
ε^2	Dielectric permittivity
C_p	Heat capacity at constant pressure
R	Gas constant
T	Temperature
T_d	Degradation temperature
v	Velocity
min	Minute
τ	Ultimate shear strength
P	Applied load
b	Joint width
l	Overlap length

Unit Abbreviations

nm	Nanometre
µm	Micrometre
mm	Millimetre
cm	Centimetre
m	Metre
s	Second
N	Newton
g	Gram
mg	Milligram
Kg	Kilogram
Pa	Pascal
L	Litre
MPa	Megapascal
GPa	Gigapascal
°C	Degrees Celsius
°K	Degrees Kelvin
W	Watt
eV	Electron volt
mol	Mole
J	Joule
KHz	Kilohertz

Table of Contents

List of Figures

List of Tables

Chapter 1

1.1 Introduction

This thesis covers the identification of optimum dispersion methodologies of GRMs (GNPs, rGO, GLYMO-rGO) into different epoxies (Epilok 60-566 and Epilok 60-600G); the identification of suitable curing conditions; investigations of property enhancements (mechanical and thermal) and joining performance improvements between similar or dissimilar materials. It is noted that the addition of GRMs caused an increase in the degree of curing of the epoxy system, reduction in activation energy of curing reactions, improved thermal stability and increased mechanical properties. Furthermore, the incorporation of GRMs also improved the lap shear strength of CFRP/CFRP and CFRP/Aluminium joints. This chapter also details the rationale for developing new lightweight nanocomposite materials and contributing to knowledge.

1.2 Background and motivation for the research

The selection of materials for vehicle components is essential because it affects vehicle performance, cost, emission levels and fuel economy (Fentahun & Savas, 2018). In addition, the number of automotive units manufactured globally is rising and is expected to reach 117 million cars yearly by 2030 (• Global Vehicle Production Forecast 2030 _ Statista, n.d.), which can negatively impact the environment, air quality and citizen health due to carbon emissions (Milner et al., 2020). Figure 1. 1 presents a global vehicle production forecast between 2025 and 2030, which is expected to rise by 7 million units in five years (Global Vehicle Production Forecast 2030 Statista, n.d.).

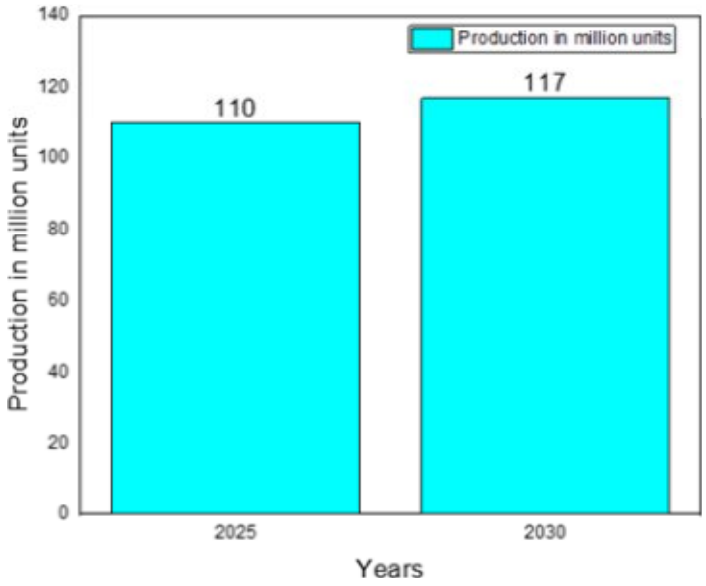

Figure1. 1: Global vehicle production forecast between 2025 and 2030 (million units) (Global Vehicle Production Forecast 2030 Statista, n.d.).

The weight of a vehicle is directly linked to fuel consumption and carbon emissions; the transport industry's need to reduce fuel consumption and carbon emissions urges multi-material design strategies to maximise weight reduction (Taub et al., 2019). Many vehicles where heavy metals are used could be replaced with polymer-matrix composite materials, which offer good mechanical properties at reduced weight, lowering fuel consumption at the use phase (Koffler, 2014). A vehicle's weight reduction of 100 kg reduces carbon dioxide emissions by 1.2 kg and fuel consumption by 0.5 litres over a distance of 100 km (Overview: Lightweighting Matters - Just-Auto Magazine | Issue 6 | June 2020, n.d.). In addition, a 10% reduction in vehicle weight can result in a 6% - 8% fuel economy improvement (Gene Liao & State University, 2017).

For this reason, intense research is undertaken to design lightweight materials for vehicle components (Rosenthal et al., 2020). However, the cost should also be considered during component design and materials selection. Due to the abundance and ease of fabrication, lightweight materials such as carbon fibres, aluminium, and magnesium are more costly than

traditional heavier materials, e.g. cast iron and steel. However, the transition to electric vehicles still necessitates lightweight as the heavy battery packs increase vehicle weight and energy consumption. With tighter regulations on CO_2 emissions, the demand for electric vehicles (EVs) has surged recently. Both battery electric vehicles (BEVs) and plug-in hybrid electric vehicles (PHEVs) are currently regarded as crucial routes to achieving future environmental impact standards and sustainable transport. For these technologies to be competitive alternatives to conventional cars (powered by internal combustion engines) for long-distance transportation the EV drive range needs to increase (Gao et al., 2019). This can be done by lightening the vehicle. An alternative design approach is to use multi-materials or structures; thus, multi-material composites can be employed to generate tailored materials for specific purposes when single homogenous materials, like in some EVs components, cannot match overall design requirements (Delogu et al., 2017). In the future, high-strength steel for EVs bodies-in-white and other structural parts is likely to be used in both polymer-based and metal matrix composites (Lipman & Maier, 2021). The top manufacturers in the world have over 100 new battery electric vehicle (BEV) models planned for release by 2024, which would boost EVs sales to 30-35% of passenger vehicles by 2030 (*Electric Vehicles to Increase Aluminum Demand | Secondary A356.2*, n.d.). It is widely recognised that lightweight will remain a priority even as the industry transitions from Internal Combustion engines (ICE) to EVs (Kumanan et al., 2021). With prospects in the optimization of the weight of the battery carrier, more energy-dense battery chemistries, and range management, electric vehicle makers are currently driving the demand for lightweight materials (*FEATURE: Light Speed – How Electric Cars Are Driving a New Wave of Lightweighting*, n.d.). In comparison to a typical ICE vehicle, the powertrain of a full-battery BEV with a 35.8 kWh battery pack and 100 kW electric motor is about 125 percent heavier. In addition, lightweighting has a significant effect on the price of BEVs due to the possible savings from secondary weight reductions and

downsizing of both the battery and drivetrain components while maintaining the same range (How Lightweight Design Saves Costs in Battery-Electric Vehicles, n.d.).

In 2020, the worldwide transportation sector emitted around 7.3 billion metric tonnes of carbon dioxide, making it a significant polluter. Passenger cars were the significant contributors that year, accounting for nearly 41% of all CO2 emissions from transportation. Surface transportation is responsible for roughly 20% of worldwide CO2 emissions (• Global Transport CO2 Emissions Breakdown 2020 Statista, n.d.). Figure 1. 2 represents the distribution of CO2 emissions produced by the transportation sector worldwide in 2020 by subsector.

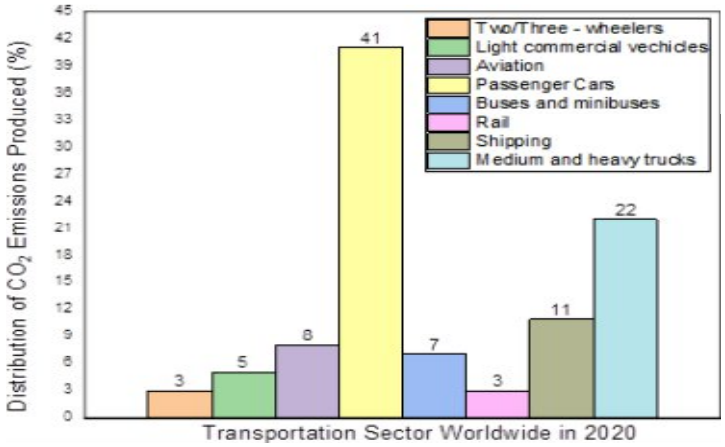

Figure1. 2: Distribution of CO_2 emissions produced by the transportation sector worldwide in 2020, by subsector, data from (• Global Transport CO_2 Emissions Breakdown 2020 Statista, n.d.).

Lightweight material innovation is a great challenge for many manufacturers; it includes raw material selection, modelling and manufacturing (Czerwinski, 2021). The automotive industry's use of structural composite materials began in the 1950s; composites are lightweight, fatigue resistant, and easily moulded to shape from those early days, making them an appealing alternative to metals. However, there has been no widespread transition from metals to composites in the car industry. Despite significant research efforts in the area of composite manufacturing, there is still a huge opportunity to create cutting-edge production methods that

work with automation to boost material productivity. Further research should be done into the composite structure that is created by combining natural, biodegradable components with synthetic materials to increase the strength and stiffness of the material while still being environmentally friendly (Rajak et al., 2019).

It started with a fibreglass body shell and air suspension and then was implemented by various automotive manufacturers for various parts, including panels, chassis and other components. However, due to the continuous need for improved lightweight components, the automotive industry looks into innovative materials and solutions. Polymer matrix composites are a mixture of two or more distinct components that, when combined, have properties that are superior to the separate constituents (Agrawal & Mirzaeifar, 2019; Saboori et al., 2017; Urbańczyk et al., 2019). The significant advantage of modern polymer composite materials is that they are both light and strong (Sherwani et al., 2021). A unique material that precisely satisfies the requirements of a particular application can be created by selecting an optimal combination of matrix and reinforcement material. Because many composites may be moulded into complicated shapes, allowing design freedom (Design Flexibility - Benefits of Composites| Composites Lab, n.d.). Nowadays, Nanotechnology has been introduced to nanomaterials; the term nanotechnology generally refers to the developments in science and engineering at the nanometre scale to fabricate novel materials, structures, and devices (J. K. Patel et al., 2021). The features of these devices have been created to satisfy specific scientific and technological goals. The application scope of nanocomposites is extensive; it covers aerospace (James Njuguna & Pielichowski, 2003), automotive (Naskar et al., 2016), packaging (Kausar, 2020), biomedical (Qi et al., 2018)(Lu et al., 2019), marine, sports, construction, devices, thermal management systems, adhesives, paints and coatings, industrial tooling, general consumer products, and many others(D. Galpaya et al., 2012) (X. Huang et al., 2012).

Numerous automotive parts are made using polymer composites like fibre-reinforced polymers (FRP). When compared to many other materials, they are more effective. FRPs have boosted battery-driven vehicle range, reduced pollution, improved soundproofing, and other aspects of the vehicle (Samyal et al., 2021). FRPs are used in a variety of fields such as Brake pads and discs, Body parts, Door panels, Engine compartments and Interiors.

Brake pads and discs:

The body's whole kinetic energy is transformed into heat while braking because of friction that occurs between the brake disc and brake pads. Sometimes, this heat is so powerful that it significantly raises the temperature of the braking system. As a result, FRPs are frequently employed to fabricate these parts due to their high specific heat capacity and melting point (Chhipa et al., 2021).

Body parts:

Different body elements including dashboards, engine hoods, etc are made from reinforcing fibres like jute, flax, and hemp. They are suitable substitutes for the lightweight metal alloys that are typically utilised because of their light weight and great strength. The reliability and strength of these materials have been tested in a variety of ways, and the outcomes have largely been impressive (Kong et al., 2016).

Door panels:

The car door panels are made from composite materials made of bamboo fibres and polymers. Additionally, it results in these panels' soundproofing and sound absorption being improved (Suhaib Kamran et al., 2022).

Engine compartment:

These materials are frequently utilised as insulating materials inside the engine compartment because they are good sound absorbers and excellent heat insulators. In order to prevent heat

buildup and vibrations from the engine from entering the car's cabin. Today, many top automakers use composite materials blended with natural fibres to construct the interiors of their cars, including the dashboard, seat coverings, and car roof, among other interior components. These substances can absorb sound and vibrations and are biodegradable (Bahl et al., 2020).

Nanocomposites are manufactured by inserting nanoscale reinforcements inside a material matrix such as a polymer (Showaib & Elsheikh, 2020), and they are a class of materials that evolved from these breakthroughs in nanotechnology; they are called polymer nanocomposites. Polymers are utilised as a matrix for nanoparticles to form nanocomposite materials, which attracted the attention of many researchers (Abu-Okail et al., 2021)(El-Kassas & Elsheikh, 2021). Nanofillers inserted in the polymer matrix demonstrate significant improvements in attributes such as strength, modulus, chemical stability, and thermal stability. The volume proportion of nanofiller, aspect ratio, matrix alignment, and other geometrical parameters all influence the properties of polymer nanocomposites (Hussain et al., 2006). Polymer-based nanocomposites show improved mechanical, thermal, and electrical properties compared to polymer-based composites and their related conventional fillers (Tutunchi et al., 2015). The application of nanofillers has a significant impact on the interfacial load transfer levels of multifunctional nanocomposite materials. The interfacial area between a nanofiller and a polymer matrix varies according to the dimension and structure of the nanofillers (Chiu et al., 2016)(Punetha et al., 2017).

Epoxy polymers are a class of high-performance crosslinked polymers. However, epoxy polymers are among the most broadly utilised polymers in the industry, and their high adhesion has incited the use of these materials in the formation of composites and nanocomposites (Chatterjee et al., 2012; Kamarian et al., 2019; Maleki Moghadam et al., 2016; Saber- Samandari et al., 2007). Numerous researchers utilised epoxy polymers to manufacture composites and nanocomposites through their broad applications (Ayatollahi et al., 2019; H. Gu et al., 2016; J. Gu et al., 2017; Maghsoudlou et al., 2019; Marouf et al., 2016). They have widespread

applications as the main component for adhesives and matrices for structural composites in various industries. A pre-polymer oligomer is usually based on bisphenol A (BPA) and is cured with the addition of a curing agent, which can be a variety of compounds such as diamines or polyamines, polyamides and acid anhydrides (Odian, 2004). At the moment, almost 75% of the world's production of epoxy pre-polymers is produced by the condensation reaction of BPA and epichlorohydrine, yielding the diglycidyl ether of BPA (DGEBA), as shown in Figure 1. 3.

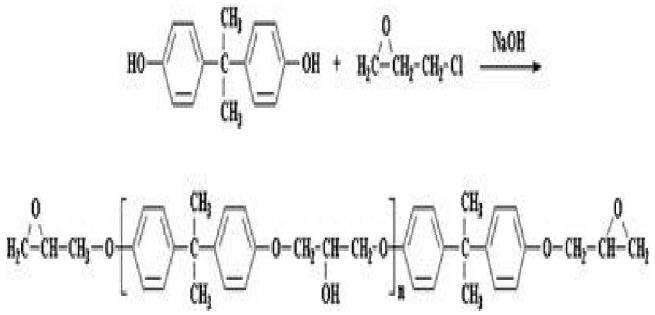

Figure 1.3: Epoxy resin DGEBA; preparation reaction from bisphenol A (BPA) and epichlorhydrin.

The epoxy resins and the curing agents commonly used today are derived from petroleum sources. However, pressing environmental concerns and finite petrochemical resources urge industries towards sustainable products; hence, more research and development on bio-based polymers derived from naturally occurring raw materials are needed (Baroncini et al., 2016). A product that is entirely or partially made from biomass is referred to as a "bio-based product." - Furthermore, these new materials must be tested and developed further to replace conventional ones. To meet application requirements, the new biobased resins need to be combined with state-of-the-art reinforcing agents, such as nanofillers. Graphene and related materials have attracted significant attention as advanced carbon nanofillers in polymer matrix nanocomposites (H. Kim, Abdala, et al., 2010; Potts et al., 2011; Wei et al., 2015).

An important application area of epoxies is adhesive bonding offering unique advantages compared to other joining methods, e.g. superior damping, reduced noise, corrosion resistance,

reduced stress concentrations and design flexibility.

Nanotechnology is particularly attractive due to the low filler needed in composite materials to improve mechanical, electrical and thermal properties. For example, carbon fibre reinforced polymer (CFRP) composite materials comprise carbon fibres as the strong and stiff reinforcing agent combined with a tough polymer matrix, typically a thermoset polymer. One of the main thermosets dominating the CFRPs market is epoxies, a class of high-performance crosslinked polymers with a broad range of applications, e.g. paints and coatings, adhesives, and composite matrix (Gibson, 2017).

1.3 Graphene Structure

Graphene is a single layer (monolayer) of carbon atoms, it is a two-dimensional material made up of bonded and densely packed sp^2 carbon atoms in a honeycomb crystal lattice (Szeluga et al., 2015) have attracted significant academic and industrial interest in the last decade due to their exciting properties, Graphite is made up of layers of graphene stacked on top of each other with a 0.335nanometer interplanar spacing. The individual graphene layers in graphite are held together by Van der Waals forces, which can be overcome during graphite exfoliation. Graphene is the thinnest and lightest substance known to man(*Graphene - What Is It? | Graphenea*, n.d.). Because of the higher close or tight packing of atoms in the crystal lattice of graphene and similar materials, graphene is one of the most stable materials (Tiwari et al., 2018)(Tiwari et al., 2020). The properties of graphene have been thoroughly assessed since it was separated in 2004 (Novoselov et al., 2004). Due to its unique properties, i.e. mechanical, electrical, and thermal properties. Graphene, in particular, has Young's Modulus(E) of 1TPa(Young et al., 2012), the Ultimate tensile strength (UTS) of 130GPa (C. Lee et al., 2008a) and a surface area of 2630 m^2/g(Stoller et al., 2008), which qualifies it as an excellent nanoscale filler in polymer-matrix nanocomposites. Furthermore, graphene is chosen over other traditional nanofillers such as metal oxides, carbon nanotubes (CNTs), carbon black

(CB), layered silicates, and carbon nanofibers (CNF) (Abbasi et al., 2019). According to Park et al., graphene can be classified according to three different characteristics: (i) the number of layers, (ii) the average lateral size, and (iii) the carbon/oxygen ratio (M. V. D. Z. Park et al., 2017). Some properties of graphene are explained in figure 1.4.

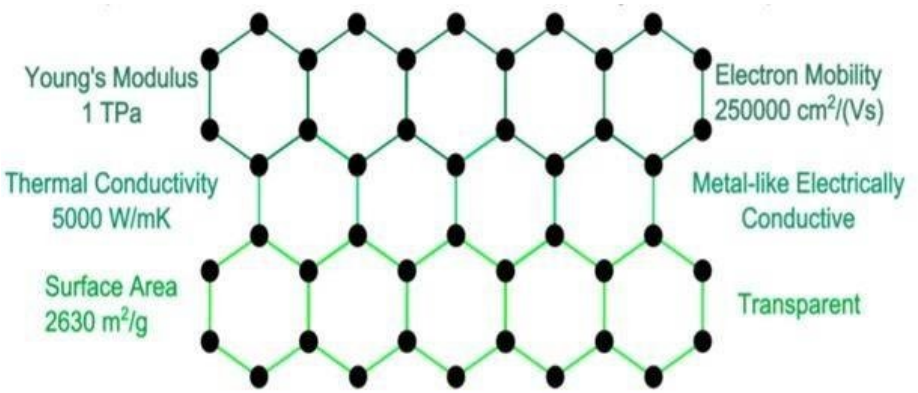

Figure 1.4: Graphene hexagonal honeycomb chemical structure and its extraordinary physical properties. The black dots are carbon atoms(Cataldi et al., 2018).

Graphene was discovered by Andre Geim and Konstantin Novoselov of the University of Manchester. In 2010, the Nobel Prize in Physics was given to them for their remarkable contributions to science and technology (Tiwari et al., 2016). Furthermore, due to the tremendous reputation of graphene, large research communities have paid much attention to the design and development of graphene materials for various industrial applications (Rudrapati, 2020). Different forms of graphene include GO (graphene oxide), GNP (graphene nanoplate), rGO (reduced graphene oxide) (Y. Peng et al., 2015).

1.4 Graphene derivatives as potential filler nanomaterials

Perhaps the most common graphene derivative is graphene oxide (GO); graphene oxide can be used to produce polymer-graphene oxide nanocomposites and derivatives with outstanding mechanical and controlled chemical properties. In addition, graphene oxide has better dispersibility and processability in an aqueous environment, so mostly used as an alternative for graphene materials (Compton et al., 2012; C. Li et al., 2012; D. Li et al., 2008). Graphene

oxide (GO) is formed from mineral graphite flakes by a thermal oxidation process developed by Hummers and modified by successors (Hummers & Offeman, 1958).

One of the highly used methods of joining different mechanical parts is adhesive bonding technology (R. D. Adams, 2005). Because of the possibility of lighter-weight vehicles, fuel savings, and decreased emissions, the usage of adhesively bonded joints in the automobile industry has expanded dramatically in recent years (M. D. Banea et al., 2018). However, improving the safety of structures, increasing the lifetime, and reducing the costs are highly needed nowadays and can show a significant tolerance to damage. This technique can also build dissimilar joints (E. C. Botelho et al., 2004; Hasheminia et al., 2019; A. M. G. Pinto et al., 2009). The ability to join construction materials of different physical and chemical properties (B. He & Ge, 2017)(Anyfantis & Tsouvalis, 2012), as well as of considerably different sizes (e.g. thickness) (M. D. Banea et al., 2018; Edson Cocchieri Botelho et al., 2006; L. F. M. da Silva & Adams, 2007; B. He & Ge, 2017), is helpful for various applications. Adhesive bonding can virtually join all types of materials and combinations of materials and is growingly used in the automotive industry (Budhe et al., 2017). However, combining dissimilar materials brings significant challenges to the body car assembly process (Banea et al., 2018). Thus, an adequate understanding of the behaviour of multi-material adhesively bonded joints is crucial to ensure the efficiency, reliability and safety of such joints. Adhesive joints have significant advantages compared to other joining techniques such as spot welding and mechanical joining (L. F. M. da Silva et al., 2018a)(Robert D. Adams & Wake, 1984). The usage of adhesive bonding as an alternative to mechanical fasteners offers the potential for reduced weight and cost (Marques et al., 2020)(Mariana D. Banea et al., 2014)(Advantages of Adhesive Bonding over Mechanical Fasteners, n.d.)(Advantages of Structural Adhesives over Welding, Rivets and Traditional Fastening Methods, n.d.)(High-Strength Adhesives Are Replacing Mechanical Fasteners for Durable, Low-Cost Bonds, n.d.). The most proficient

utilisation of adhesives in manufacturing activity relies upon enhancing adhesives selection, joint design, and procedure conditions (Marques et al., 2020).

1.5 Research Methods:

In this research various fabrication and characterisation methods are used, where material fabrication techniques, including ultrasonication and wet lay/hand-up processes. To characterise thermal and mechanical properties, characterisation techniques include differential scanning calorimetry (DSC), Thermogravimetric analysis (TGA), Scanning Electron Microscopy (SEM), Tensile test, Hardness through Nanoindentation and Shear Lap joint test. TGA was used to investigate the effects of graphene on the thermal stability of the epoxies while DSC was utilised to study the curing kinetics of the chemical reaction between the resin and the amine. Mechanical characterisation included stress-strain curves record, analysis and determination of mechanical properties (Young's Modulus, Ultimate Tensile Strength, hardness) and Shear Lap joint test for bond strength. Fabrication and characterisation methods are discussed in chapter 4.

1.6 Life cycle and Sustainability analysis

Life cycle Analysis (LCA) plays an important role in assessing the potential impact of these new technologies and various end-of-life (EoL) treatment management options (Arvidsson et al., 2018b). In this way, LCA supports the collaboration of research and innovation activities aimed at achieving environmentally friendly and sustainable products that fit into the framework of the circular economy (Arvidsson et al., 2018a). This research designed novel nanocomposite material for lightweight automotive applications. Its expensive material as compared to traditional automotive materials due to the high cost of raw materials such as Carbon Fibre. It can benefit if we use it for higher miles journeys rather than a lower miles journey, so it will improve fuel efficiency and reduce gas emission. Bulk production of vehicles from this material can decrease the material's cost.

In addition, the environmental impact of filler loading on various matrices is combined with the nanocomposite performance expected from a mechanical and joint strength improvement to choose the compounding with the least required performance and environmental impact. As a result, the purpose of this study is to highlight key open difficulties that must be solved by designing lightweight materials for energy-efficient and safe vehicles.

1.7 Aims of the thesis

The aims of this research are as follows:

- To develop novel polymer (fossil-based and bio-based resins)/graphene and related layered materials (GRMs) nanocomposite materials aiming for property enhancement (mechanical and thermal)
- Develop experimental methodologies for improved dispersion quality of GRMs within epoxy matrices, allowing better components with fewer steps and costs
- Investigates the functionalisation of graphene and compatibility with specific epoxies suitable for automotive applications (high Tg, low viscosity)
- Developing 3-phase (graphene/carbon fibre/epoxy) for bonding performance aims to improve joining technology towards a multi-material lightweight design

Overall, this research aims to contribute to designing lightweight materials for energy-efficient and safe vehicles.

1.8 Research Questions

Based on the research aims discussed in the previous section, the following research questions are formulated

1. Which are the optimum dispersion methodologies of GRMs (GNPs, rGO, f-rGO with GLYMO) into different epoxies (Epilok 60-566 and Epilok 60-600G)?

2. How GRMs affect the curing kinetics of epoxy systems?
3. How to improve mechanical properties (Young's Modulus, Tensile strength, Lap Shear Strength) of GRMs/epoxy resin due to GRM fillers?
4. Can biobased resins be combined with GRMs to replace conventional composite systems for sustainable development?
5. How do develop lap shear joints between similar or dissimilar materials using GRMs and identify process parameters that affect the response of the joints?

1.9 Contribution to the knowledge

- New GRMs/epoxy nanocomposites were developed following a facile solvent-free approach
- Cure kinetics was studied by DSC non-isothermally, using Kissinger and Ozawa-Flynn-Wall models, which showed that the addition of graphene caused an increase in the degree of curing and reduction in activation energy
- Cure kinetics of these materials is performed where GRMs (rGO/GLYMO-rGO) are dispersed into a bio-based epoxy without solvent and used ultrasonication, which showed that the addition of GRMs (rGO/GLYMO-rGO) caused an increase in the degree of curing and glass transition (Tg)
- GRMs/Bio-based resin was also used as adhesive and adherents to bond CFRP/CFRP and CFRP/Aluminium adherents
- The addition of GRMs/Bio-based into the adhesive led to a significant increase in joint strength compared to that of the pure epoxy

A breakdown of the structure of the remaining chapters is provided below.

In Chapter 2, a detailed literature review aims to inform the reader on the state of the art in the area of graphene/epoxy nanocomposites. The chapter discusses thoroughly epoxy polymer

systems, GRMs and their composites reported in the literature, and reviews different processing variables that affect the dispersibility of GRMs into polymer matrices and their relationship to the final properties of nanocomposites. It also gives a detailed review of adhesive bonding for improving the lap shear strength of joints.

In chapter 3, an overview of materials used in the automotive industry is provided. First, the traditional materials, i.e. steel, aluminium, magnesium, are mentioned, which potentially could be replaced by lighter polymer nanocomposite materials, i.e. GRM enhanced carbon fibre-reinforced polymers (CFRPs).

In chapter 4, the experimental methods that were used in this thesis are discussed. These include techniques that were used for materials synthesis, e.g. bath ultrasonication, wet lay-up process, and materials characterisation techniques, e.g. differential scanning calorimetry (DSC), cure kinetic models, thermogravimetric analysis (TGA), scanning electron microscopy (SEM) and many others.

Chapter 5 reports the formulation and characterisation of new graphene/polymer nanocomposites using graphene nanoplatelets (GNPs) and the epoxy system Epilok 60–566/Curamine 32–494. In a suggested solvent-free approach, GNPs were first dispersed into the curamine hardener using bath ultrasonication, followed by the addition of the epoxy resin. The cure kinetics were studied by DSC under nonisothermal and under isothermal conditions. The kinetic parameters of the curing process were determined using the nonisothermal Kissinger and Ozawa-Flynn-Wall models. Thermal stability was analysed by Thermogravimetric analysis (TGA). In terms of mechanical properties, performed the tensile test, Nanoindentation measurements and hardness.

The epoxy resins and the curing agents commonly used today are derived from finite petrochemical resources. Biopolymers are becoming increasingly attractive, allowing a more

sustainable production and growth.

Chapter 6 reports the synthesis and study of novel nanocomposites using a biobased epoxy/amine (Epilok 60-600G/Curamine 30-952) matrix, reinforced with rGO or functionalised with GLYMO-rGO. Epilok 60-600G and Curamine 30-952 have 36% and 66% bio-based renewable content, respectively. These graphene-related materials (GRMs) were first dispersed into the curamine hardener using bath ultrasonication, followed by the addition of the epoxy resin. Curing kinetics were studied by DSC under non-isothermal and under isothermal conditions. A scanning electron microscope (SEM) analysed the morphology of nanocomposite material. Performed mechanical testing for examined *E* and *UTS*. Carbon fibre reinforced polymer (CFRP) laminates were prepared via hand lay-up, using the nanocomposite system GRM/Epilok/Curamine as a matrix, and were cut as CFRP adherents for lap shear joints. The GRM/Epilok/Curamine was also used as adhesive to bond the CFRP/CFRP and CFRP/aluminium adherents.

Chapter 7 presents a general discussion of this research, general conclusions and suggestions for future research.

The potential applications emerging from the knowledge developed in this study on low loading of GRMs with carbon fibre/epoxy are beneficial to designing lightweight materials with better mechanical properties for automotive applications.

1.10 Summary

In summary, new graphene/epoxy nanocomposites are developed following a facile solvent-free approach, simplifying the experimental procedure and lowering manufacturing costs. The addition of GRMs caused an increase in the degree of curing of the studied epoxy systems, reduced activation energy, improved thermal stability and increased mechanical properties. The incorporation of GRMs also improved the lap shear strength of CFRP/CFRP and CFRP/Aluminium joints.

Chapter 2 Literature Review

Literature review is conducted to inform on the research background and to identify research gaps and challenges in the research area of GRM/epoxy nanocomposites. Firstly, automotive materials are introduced, highlighting the necessity to develop better and lighter polymer composites. Then, GRM nanofillers and epoxy polymers are introduced. This literature review focuses on key findings from the current research published in the journal articles and reports, highlighting the importance of dispersion of GRMs into epoxy polymer matrices, the effect of the addition of GRMs on the polymer cure kinetics, and resultant physical properties, i.e. mechanical properties, thermal stability. Material properties will be analysed to understand the importance of bonding lightweight components with similar or dissimilar materials in the car structure, and hence literature on lap shear tests will also be reviewed.

2.1 Introduction

The selection of materials for vehicle components is crucial because it affects vehicle performance, cost, carbon emission levels and fuel economy.

Lightweighting improves fuel efficiency and reduces environmental impact by reducing emissions, particularly carbon dioxide. The EU (European Union) has set a mandatory target for reducing greenhouse gas emissions: 40% below 1990 levels by 2030 (2030 Climate & Energy Framework - Climate Action, 2018); in June 2019, the UK made a legally binding commitment, CO_2 and other greenhouse gas emissions should be reduced to zero by 2050 (Gov.uk, 2019); however, the transport sector, which includes road transport, railways, domestic aviation, shipping, fishing, and aircraft support vehicles, is estimated to be responsible for around 27% of total emissions in the UK (Gov.UK 2019), represents in figure 2. 1. Because increased road traffic has vastly outweighed gains in car fuel economy, transportation emissions are only 4.6% lower than in 1990 (BEIS, 2020).

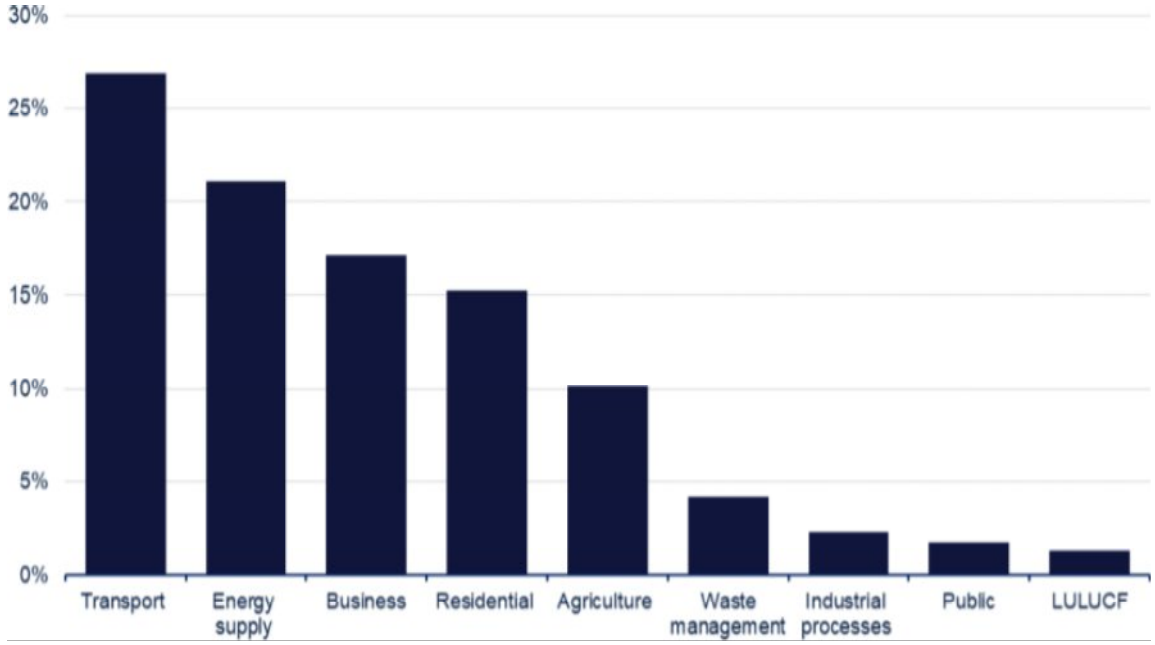

Figure 2. 1: Territorial UK greenhouse gas emissions by National Communication sector, 2019 (%) (BEIS, 2020).

Dow Automotive Systems reports that a 100 kg weight reduction reduces emissions by 5.0 to 12.5g of CO_2 (3 to 7 %) per driven kilometre (Dow Automotive Systems, 2015). The weight of a vehicle has a significant impact on how much fuel it will use. The heavier the vehicle, the more energy it needs to get moving. Additional weight increases a vehicle's rolling resistance, which is a force that opposes forward motion created as the wheels roll over the road. This indicates that lowering a vehicle's weight is a highly effective technique to reduce fuel usage (*Vehicle Weight*, n.d.). Efforts toward improved fuel efficiency in the automotive sector are fundamental to ensuring sustainable transport (Deepak & Senal, 2019; Ferreira et al., 2019; Giampieri et al., 2019; Jasiński et al., 2016; Rajagopal et al., 2017). For these reasons, the new production of vehicles is required to be lighter and energy-efficient (Elmarakbi & Azoti, 2018); also, during the component design and materials selection, cost should be considered. Lightweight materials such as carbon fibre reinforced polymer composites, aluminium and magnesium are more costly than traditional heavier materials such as cast iron and steel (Prasad et al., 2022), which are cheaper due to their abundance and ease of fabrication (Liu et

al., 2018). In Table 2.1 provides estimated fuel cost savings for a range of weight reductions (*Vehicle Weight*, n.d.)

Table 2. 1: Estimated fuel cost savings for a range of weight reductions (*Vehicle Weight*, n.d.)

Weight Reduction (Kg)	**Fuel cost savings over 200,000 (km)***	
	Cars ($)	**Trucks ($)**
10	60	80
25	150	200
50	300	400
100	600	800
200	1200	1600
400	2400	3200
1000	6000	8000

*Estimated savings are based on a fuel price of $1.00/L and the average fuel consumption and weight relationship reported by the Massachusetts Institute of Technology (MIT).

A polymer matrix reinforced with fibres is the most common composite material in the automotive industry (M. Patel et al., 2018). Around 65% of the average vehicle is made up of steel and iron (*Recycling - WorldAutoSteel*, n.d.). Cast iron and conventional steel components can be replaced with lighter alternatives such as high-strength steel, magnesium (Mg) alloys, aluminium (Al) alloys, carbon fibre, and polymer composites to reduce weight by up to 50% and consequently fuel consumption. By 2030, one-quarter of the U.S. fleet may save more than 5 billion gallons of fuel annually by using lightweight components and high-efficiency engines made possible by new materials (*Lightweight Materials for Cars and Trucks | Department of Energy*, n.d.). Polymer molecules consist of many similar repeating units (monomers), making a

homopolymer or different monomers combined, making a copolymer. The topology of these large molecules is often linear, branched, or cross-linked, and the structure develops into an extensive three-dimension network is highly interconnected chains. Thermoplastic polymers are linear or branched polymers that are not cross-linked and can be reprocessed by exposing them to heat or dissolving them in a suitable solvent. A thermosetting polymer has a crosslinked three-dimensional network and, unlike thermoplastics, cannot be melted or moulded without the permanent destruction of the chemical bonds. Due to the distinctive combination of features they provide, such as high tensile strength and modulus, thermal stability, chemical and corrosion resistance, thermosetting epoxy resins continue to be the preferred material choice for industrial and structural fields, including coatings, electronic devices, adhesives, maritime systems, and aerospace parts (Reghat et al., 2021). Epoxy materials do have some important disadvantages, though, such as their brittle nature and sensitivity to defects. Further study and development of epoxy-based nanocomposites are needed to address these issues and enable their use in commercial applications (Mirabedini et al., 2022). The combination of a reinforcement agent with the polymer matrix can be tuned to meet the required final properties of a component. Polymer matrix composite materials play a vital role in the automotive industry, reducing vehicle weight and fuel consumption by replacing many steel components (Osokoya, 2017). According to the US Department of Energy, utilizing more lightweight materials, e.g. polymer composites, magnesium and aluminium, will decrease steel production by 20% by 2035 (Prucha, 2012a). While aluminium is considered the most standard vehicle material for lightweight purposes, plastics are much lighter (the density of aluminium is 2.7g/cm^3 while the density of plastics is 1.1 g/cm^3) but are rarely used for structural components because of their lower mechanical properties compared to the metals. Due to their structural stiffness and crashworthiness, iron and steel materials have been well established in vehicle manufacturing. Polymer composites, however, offer lightweight, ease of processing and design flexibility. A unique material that precisely

satisfies the needs of a specific application can be created by selecting the right combination of polymer matrix and reinforcing agent. Polymer matrix composites (PMCs) are sophisticated composite materials with a wide range of possible uses, including the replacement of conventional materials (such as wood, concrete, aluminium, steel, etc.) for a variety of reasons (such as economies, corrosion resistance, bio-resistance, light-weighting, etc.), as well as the creation of goods that were previously impractical (Tewatia et al., 2017). As shown in figure 2. 2, which compares the weight reduction between steel and different kinds of materials for example High strength steel, Aluminum, Magnesium and Carbon Fibre composites. For example, carbon Fibre composite materials can reduce weight up to 60% compared with steel, while High strength steel, Aluminum and Magnesium reduced 20%, 40% and 50%, respectively (Gene Liao & State University, 2017).

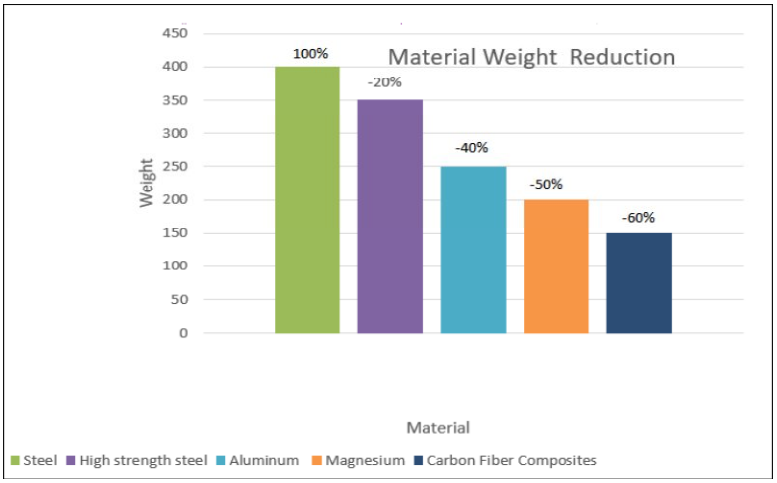

Figure 2. 2: Weight Reduction comparison using different materials (Gene Liao & State University, 2017).

Carbon fibre (CF) reinforced polymer composites have been reliable in gaining high importance in the area of composite science and technology (Mirabedini et al., 2020)(Rajak et al., 2019), particularly in aerospace (Soutis, 2005), automotive industries (Friedrich & Almajid, 2013)and sports goods (Tong, 2019). The mixture of polymer matrix and reinforcing fibres results in high-performance materials that offer more than 50% weight reduction compared to aluminium and steel, respectively (Mirabedini et al., 2020). As a result, many types of reinforcements have been developed to increase the mechanical properties of epoxy-based composites (Johnsen et al., 2007)(Ajayan et al., 2000). As a result, nano-carbon materials like CNT and GNP are frequently employed to improve the mechanical properties of polymer composites and fibre-reinforced composite laminates.

CFRP contains carbon fibres (CFs) of about 0.005-0.010 mm in width in polymeric matrices prompting lightweight composite structures (Pramanik et al., 2017). CFRP requires joining together with metal edges to frame total structures in most genuine applications, which assume a significant role in a hybrid design. Hybrid multi-material design configuration is a rising procedure of joining composites and metals with attractive and exceptional material qualities, for example, higher strength and stiffness, resistance to physical damage due to cracks, resistance to radiation damage, design versatility etc. The popularity of such specific functional properties can fulfil tremendous needs towards better structures than exploit the best execution of both metals and composites.

Consequently, it is essential to comprehend the issues related to fabricating, machining and joining composite materials (Pramanik, 2014). The yearly global demand for carbon fibre (CF) has surged from around 16,000 to 72,000 tonnes in the last decade. It is expected to rise to 140,000 tonnes, which is around 9 times its initial demand by 2020 (Dr Elmar Witten, 2014).

On the other hand, Nano-carbon compounds are difficult to disperse into polymer matrices, resulting in polymer agglomeration and limiting characteristics and uses. The reason for this is that the van der Waals forces between carbon nanomaterials can produce agglomeration, necessitating the employment of complicated methods to achieve a homogenous dispersion in a polymer matrix (Hsieh et al., 2018; Kuan et al., 2018; Shen et al., 2013; P. N. Wang et al., 2015).

Nowadays, Nanotechnology has introduced nanomaterials that are particularly attractive due to the low amount of filler needed to improve polymer matrix's mechanical, electrical, and thermal properties. The primary difference between nanocomposites and traditional composites is the size of fillers. Nanotechnology offers new materials processed at the nanoscale (<100nm), e.g. nanoparticles, nanosheets, nanowires producing nanocomposites. They have been employed in various applications, for instance, automotive, aerospace, electronics, flexible sensors and biotechnology (V. B. Mohan et al., 2015) (Bulut, 2017; Phiri et al., 2017; Zakaria et al., 2017). According to Bao et al., due to their improved mechanical properties and new nanostructures, it is obvious that using nano-fillers to reinforce a matrix material will result in greater reinforcement effectiveness than using micro-fillers. The goal of filler size reduction is to achieve a uniform distribution of filler throughout the matrix, reducing the stress concentrations in the composite structure (M. Huang & Li, 2006), which subsequently improves its mechanical properties (Le et al., 2020). Furthermore, more minor fillers can obtain higher surface energy, making stronger bonding with the matrix (Zhou et al., 2008) improving the system's stiffness and strength (Chisholm et al., 2005). The above highlight the necessity of developing novel composite materials with advanced nanofillers, which will offer lightweight and good mechanical properties at a competitive cost with competing with conventional materials by using new material fabrication and processing techniques.

Adhesive bonding is the process of using an adhesive substance to attach two or more solid materials. The materials of the joined parts (adherents, substrates) may be different or similar. As a versatile and efficient bonding technology, Adhesive bonding has been widely used in industrial applications where structures with a combination of lightweight and excellent mechanical performance are required. Due to the rapid advancement of adhesive technology, adhesively bonded joints are gradually used in the automotive, aerospace, marine and medical fields (Gültekin et al., 2016) due to practical advantages over previous bonding methods. Unlike most traditional joining methods, adhesive bonding does not necessitate drilling holes in the structure, allowing for more uniform stress distribution and avoiding stress concentration (Carbas et al., 2021). As evident from the literature, adhesives can join metals, polymers, ceramics, rubber, and combinations of any of these materials. Many advantages of adhesive joints have contributed to their widespread use in the automotive industry (M. R. G. Silva et al., 2016)(Galvez et al., 2017). Furthermore, dissimilar material joints with a structure, such as composite materials joints with lightweight metals, have been widely used in the automotive industries to address fuel economy and weight reduction issues(M. D. Banea et al., 2018; Mariana D. Banea et al., 2017; Hasheminia et al., 2019).

2.2 Graphene and related layered materials (GRMs)

Graphene and related layered materials (GRMs) have attracted significant academic and industrial interest in the last decade due to their exciting properties, i.e. mechanical, electrical and thermal. Graphene is being researched widely to improve daily life, and according to statistics given in (Dadkhah et al., 2019), articles containing the keyword graphene are increasing every year, and at the beginning of the last quarter of 2019, this keyword can be found in more than 17000 publications. Figure 2.3 shows detailed statistics of these publications. The application scope of nanocomposites is vast; it covers automotive, aerospace, marine, sports, construction, biomedical devices, adhesives, thermal management

systems, industrial tooling, paints and coatings, and general consumer products, as well as many others (Özgül & Bektaş, 2019) (*APPLICATIONS OF GRAPHENE POLYMER MATRIX COMPOSITES - The Graphene Council*, n.d.) D. Galpaya et al., 2012; X. Huang et al., 2012; Wei et al., 2015). From these motives, nowadays, many researchers are trying to include graphene and its related materials into polymers to design new GRM/polymer-based nanocomposites (Xusheng Du et al., 2017; Yunfeng Li, Zhu, Wei, Ryu, Sun, et al., 2011).

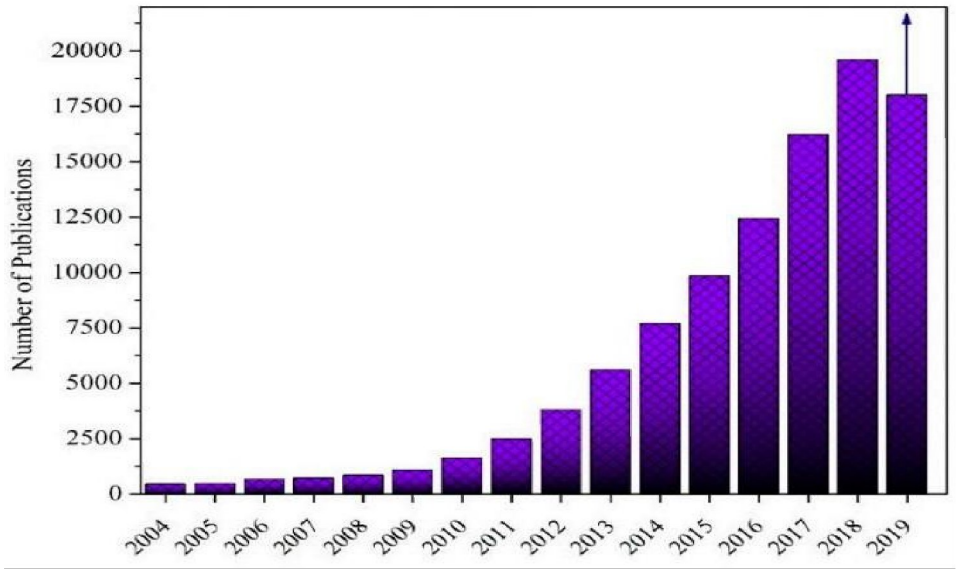

Figure 2. 3: Statistics of articles containing the keyword graphene (Dadkhah et al., 2019).

Figure 2. 4: Statistical data of articles on 2D materials and 2D material composites published during 2000–2018 based on the Web of Science database (Ji et al., 2020). The use of nanofillers to reinforce epoxy resins has recently received a lot of attention. (Barua et al., 2015; Bedsole et al., 2015; Bindu Sharmila et al., 2016; S. Liu et al., 2016).

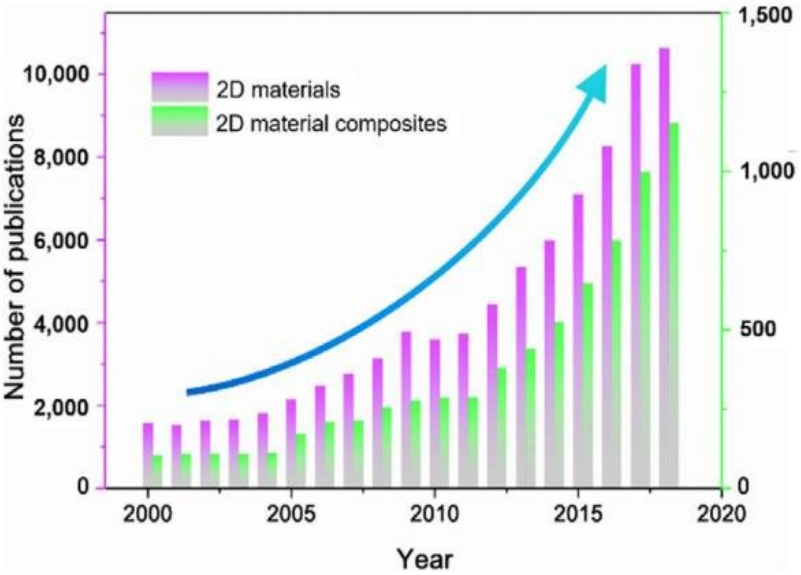

Figure 2. 4: Statistical data of articles on 2D materials and 2D material composites published during 2000–2018 based on the Web of Science database (Ji et al., 2020).

2.3 Epoxy Polymer

Epoxy resin oligomers are thermosetting polymers with two or more epoxide groups per monomer. Epoxies are one of the most high-performance materials, and their outstanding thermal stability, mechanical performance, and ease of processing have led to their employment in a variety of applications. However, like most thermosetting polymers, epoxies have several drawbacks, including intrinsic brittleness, low fracture toughness, and high electrical resistivity, limiting their use in various high-performance applications. Furthermore, several researchers (Garg & Mai, 1988)(Chang & Brittain, 1982) have concluded that high cross-link density reduces the fracture toughness of pristine epoxies due to internal stresses induced during epoxy curing, where crack initiation resistance is low and void growth due to plastic deformation is limited. To address this problem, numerous researchers have employed nano-sized organic and inorganic particles as fillers to reinforce the epoxy matrix and create advanced polymer composites with enhanced characteristics. The conversion of renewable

biomass into useful polymeric materials and composites is receiving increasing attention these days, focus on finding alternatives to petroleum polymers and minimising pollution, scientists are increasingly focusing their efforts on developing polymeric materials from renewable resources such as proteins, oils, and carbohydrates (C. Zhang et al., 2017)(Fertier et al., 2013).

2.4 GRMs Nanofillers

Inorganic nanoparticles were initially exploited as reinforcement agents in polymer nanocomposites because of their unique features and wide potential applications (P. Li et al., 2009) (Kuila et al., 2008) (Z. Zhang et al., 2006) (Ray & Okamoto, 2003) (Leroux & Besse, 2001)(Godovsky, 2000). The research was mainly focused on layered materials of natural origin, such as sodium montmorillonite (Na-MMT) or synthetic clay, such as layered double hydroxide (LDH) (Alexandre & Dubois, 2000) (Giannelis et al., 1999) (Pavlidou & Papaspyrides, 2008). However, clay minerals' electrical and thermal conductivities are pretty poor (García & Bazán, 2009)(Bao et al., 2008). In order to overcome these shortcomings, carbon-based nanofillers such as carbon black (Q. Li et al., 2009), exfoliated graphite (EG) (Debelak & Lafdi, 2007), carbon nanotubes (CNT) (Spitalsky et al., 2010), and carbon nanofibers (CNF) (Khanna & Bakshi, 2009) have been used. Graphene may be preferred over other conventional nanofillers (Na-MMT, LDH, CNT, CNF, EG, e.t.c.) owing to its high aspect ratio, the large theoretical surface area of 2630 m2/g (Bhattacharya, 2016; Whitby, 2014; Yang et al., 2011; Zhu et al., 2010), UTS of 130 GPa (C. Lee et al., 2008b) (Young et al., 2012), an E of 1TPa (Whitby, 2014)(Xu Du et al., 2008; C. Lee et al., 2008b; J. U. Lee et al., 2012; Young et al., 2012), thermal conductivity (5000 W m-1K-1) (Balandin et al., 2008)(S. Park & Ruoff, 2009), electrical conductivity (6000 S/cm) (Xu Du et al., 2008). Graphene has a hardness of 200 times steel and 30 times diamond (Geim & Novoselov, 2007). Graphene is the strongest and lightest substance known to man. (C. Lee et al., 2008b), thinnest (adsorbing 2% of light) (Nair et al., 2008), and it is the only material in which the reaction can

be carried out on both sides(Eigler & Hirsch, 2014). Graphene and related materials have attracted significant attention as advanced carbon nanofillers in polymer matrix nanocomposites (H. Kim, Abdala, et al., 2010; Potts et al., 2011; Wei et al., 2015). Graphene flakes can be produced from exfoliation of graphite via solution processing using ultrasonication (Hernandez et al., 2008), high shear mixing (Paton et al., 2014) or microfluidization (Karagiannidis et al., 2017). Another approach is the production of graphene oxide (GO) from graphite oxide and the subsequent reduction of GO to restore its properties

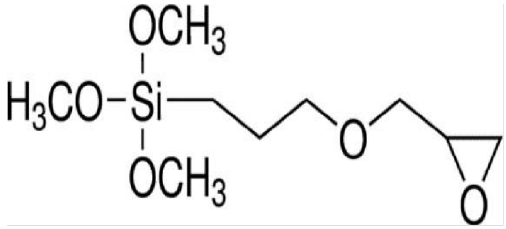

Figure 2. 5: Chemical structure of 3-glycidoxypropyltrimethoxysilane (GLYMO).

(Pei & Cheng, 201)(A. T. Smith et al., 2019). The resultant reduced graphene oxide (rGO) has improved properties compared to the defective GO and contains a small number of oxide groups which may be beneficial in its interaction with polymer matrices. To improve further dispersion and interfacial interaction between rGO and resin matrix, which leads to better load transfer, certain chemical functionalisation have been reported using organic amines (YAN et al., 2012), isocyanates (Stankovich, Piner, Nguyen, et al., 2006), azide compounds (H. He & Gao, 2010), and organosilane compounds (Bhowmik et al., 2012; Lei et al., 2016; Z. Liu et al., 2013; Y.-J. Wan et al., 2014; Xin Wang et al., 2013) such as 3-glycidoxypropyltrimethoxysilane, GLYMO (Figure 2. 5). The epoxy group of GLYMO can react with the epoxy groups of GO to form ether -C-O-C- bonds. Also, the hydrolysis of methoxy groups -OCH3 leads to the formation of silanol groups -Si-OH, which can also react with hydroxyl -OH groups and epoxy groups (Y.-J. Wan et al., 2014)(Bhowmik et al., 2012).

For all of these reasons, graphene is recognized as one of the best carbon nanofillers available, and it is used in every technology field (Agius Anastasi et al., 2016; Alamusi et al., 2018; Bonaccorso et al., 2010; Ferrari et al., 2015; Geim, 2009; A. Kumar et al., 2020). The effectiveness of graphene as a nanofiller in various polymeric systems such as epoxy, polystyrene, polyaniline, polyurethane, poly(vinylidene fluoride), Nafion, polycarbonate, poly(ethylene terephthalate) has been reported in a detailed review by Kuilla et al. (Kuilla et al., 2010). Epoxies, in particular, are a class of high-performance crosslinked polymers with widespread applications as the main component of adhesives and matrices for structural composites in various industries. Recent developments in graphene/epoxy nanocomposites are well reported in recent reviews (Wei et al., 2015)(Shah et al., 2015)(Rasheed Atif et al., 2016)(Kausar, Anwar, et al., 2016).

2.5 Processing of the graphene-polymer nanocomposites

The final properties of graphene/polymer nanocomposites strongly depend on the processing conditions (Dikin et al., 2007; Ramanathan et al., 2008; Stankovich, Dikin, et al., 2006). Many critical factors are involved in processing the graphene polymer nanocomposites, i.e. %wt amount of filler, the method of dispersing graphene into the polymer matrix, and the curing conditions. The capacity to improve epoxy's strength and fracture toughness with the addition of GNPs at low filling content is a route embraced by numerous researchers to face the engineering challenges of producing strong, lightweight materials (Crosby & Lee, 2007)(Sainsbury et al., 2017). However, the dispersion of the GRMs embedded in the polymer matrix significantly affects the physical properties of the resulting composite material. Ultrasonication, mechanical, and chemical pre-treatments have been used to increase nanofiller dispersion in the polymer matrix to address this dispersion issue. (Shahdan et al., 2013). Graphene/epoxy nanocomposites are typically prepared via in-situ curing in which graphene is dispersed within the liquid epoxy oligomer, and then the curing agent is added. The high

viscosity of epoxy may hinder the uniform dispersion of the nanofiller. For this reason, a solvent is used to facilitate dispersion (Wei et al., 2015). Even though the latter method is widely adopted, the necessary solvent removal step consists of a drawback, adding manufacturing steps while any solvent residues can deteriorate mechanical properties (R. Atif et al., 2016).

2.6 Dispersion of Nanofiller Effect on Mechanical Properties

Most of the academic work so far on graphene/epoxy nanocomposites targeted to enhance the mechanical properties of the polymer matrix (an increase of matrix toughness, improve strength and stiffness of matrix) coupled with the possibility of improving other properties, for example, electrical conductivity (Ramos-Galicia et al., 2013a) or thermal stability (D. Wang et al., 2013). A literature review is conducted for different GRMs, dispersion methods and mechanical properties. As shown in Table 2.1, various approaches used by researchers are valid and provide better accuracy based on properties, but it is not easy to support or oppose any of these methods. For example, although king et al. (J. A. King et al., 2013) and Hashim et al. (Hashim & Jumahat, 2019) have shown a significant increase in mechanical properties, a more detailed study is still needed to prove these methods are viable for more comprehensive applications.

The dispersion degree (or quality) of graphene shows a vital part in the final properties of graphene nanocomposites (Bai & Shen, 2012). However, inadequate dispersibility and the low interfacial interaction of nanofillers in polymer matrices have limited their applications. A uniform dispersion provides much-improved load conveyance from the matrix to the filler material, enhancing mechanical properties(Chandrasekaran et al., 2014). Tang et al. (Tang et al., 2013) studied the effects of graphene dispersion on the properties of polymer composites. It has been observed that highly dispersed graphene has produced better mechanical and electrical properties of composites.

In this manner, a uniform distribution of nanofillers is frequently required to accomplish great load transfer between the matrix and nano-fillers, resulting in a more uniform stress distribution (Gong et al., 2015). However, poor dispersion of nanofillers in the polymer composites decreases the properties considerably (Coleman et al., 2006)(Thostenson et al., 2001). Poor dispersibility and the low interfacial strength of nanofillers in polymer matrices have constrained their applications (Cha et al., 2019). Besides, van der Waals forces between low dimensional carbon nanomaterials can prompt agglomeration and, subsequently, challenges acquiring homogeneous dispersion in a polymer matrix (X. C. Zhang et al., 2014). However, GRMs (due to their chemically inert nature) do not mix well with polymers (e.g. epoxies), and specific functionalisation approaches (i.e. attachment of -OH, -COOH, -Si, etc.) have been proposed to improve dispersion in polymer matrices. Such chemistries need to be carefully optimised since they can significantly deteriorate the properties of GRMs.

Moreover, the functionalisation of GRMs should consider the chemistry (degree of functionalisation) of the particular resin matrix, which is usually a commercial product with proprietary non-disclosed chemistry. Uniform dispersion of nanofillers in the epoxy is a significant factor in polymer composites creation. The dispersion quality depends on the experimental protocols; different dispersion techniques and functionalisation have been tried; for example, Table 2.2 and Table 2.3 present essential references in the current academic literature. Different dispersion techniques and GRM functionalisation have been tried. In (Rafiee et al., 2009), Rafiee et al. used shear mixing and tip sonication and achieved good results with 31% improvement of young modulus at 0.1wt% of graphene in epoxy nanocomposites.

The best improvement in the mechanical properties of polymer matrices can only be accomplished if the nanofillers are homogeneously dispersed (Kango et al., 2013). Authors have tried to add solvents to aid dispersion. According to Wei et al., improved *UTS* was achieved by using dichlorobenzene (DCB) solvent to disperse graphene in the resin; *UTS* was improved from 64.46MPa to 69.32MPa (Wei et al., 2017). Dichlorobenzene is mainly used as a precursor compound in the production of agrochemicals, as a favourite chemical for solving and working with fullerenes and dissolving and removing carbon-based impurity on metal surfaces. Nevertheless, the use of additional solvent increases the processing steps as they need to be finally removed. Dimethylformamide is an organic chemical with the formula $(CH_3)_2NC(O)H$. The main expenditure of DMF is as a solvent with a low evaporation rate. DMF is used in the manufacture of plastics and acrylic fibres. DMF is also used as a solvent and produces adhesives, artificial leathers, fibres, films, and surface coatings. DCB proved more operative than ethanol and Dimethylformamide (DMF) for making homogenous and stable dispersions (Wei et al., 2017). DCB and DMF solvents are quite toxic and are not ideal for manufacturing. Hashim et al. (Hashim & Jumahat, 2019) prepared the GNP/epoxy polymer composite using a mixture of solution compounding and high-shear milling techniques. Epoxy resin was combined with three different GNP loadings (0.1, 0.2, and 0.3 wt%). GNP was initially added to acetone using a mechanical stirrer at 400 rpm for 15 minutes. The epoxy resin was then put into the mixture and vigorously stirred for another 15 minutes with the stirrer. To remove the acetone, a three-roll mill machine was used to mix the mixture for five cycles at 2000 rpm and heated to 70°C. The addition of 0.3wt% GNP improved the *E* by 32.59% and *UTS* by 14.9%. Other authors have used chemical additives (e.g. ionic or non-ionic surfactants) instead of solvents to aid dispersion. Liang et al. (Liang, Huang, et al., 2009) added 0.7wt% graphene oxide in Polyvinyl Alcohol (PVA), which increased *E* from 2.13GPa to 3.45GPa and the *UTS* by 76% (from 49.9 to 87.6MPa) PVA has the formula

$[CH_2CH(OH)]_n$. PVA is used in textiles, papermaking and a range of coatings. It is white and odourless. PVA is a resin, an ordinary or artificial organic compound. Klimek- McDonald et al. (Klimek-McDonald et al., 2018) used Asbury Carbon's TC307 (graphite nanoplatelets) with epoxy (EPON 862 with EPIKURE curing agent W) and 1 to 4 wt% (0.6 to 2.44 vol%) graphene nanoplatelets (GNPs) and reported improved *UTS* from 77.6 to 80.9MPa and *E* 2.72GPa to 2.93GPa; optimal strength falls between 1 and 2wt% for GNPs (Klimek-McDonald et al., 2018). Wei et al. (Wei & Inam, 2017) used epoxy/graphene with sodium dodecyl sulphate (SDS) surfactant and epoxy/graphene with Gum Arabic (GA). The sample with GA provided better results than other samples and improved *UTS* from 57.23MPa to 70.40MPa and *E* from 0.87GPa to 1.29Gpa. According to King et al. (J. A. King et al., 2013), an aerospace epoxy (EPON 862 with Curing Agent W) was synthesised in epoxy composites with 1 to 6 wt% of two different types of graphene nanoplatelets (XG Sciences xGnPM-5 and xGnPC-300). Typical macroscopic measurements were used to examine the tensile properties of these materials. Nanoindentation was also used to calculate the modulus and creep compliance. The *E* increased from 2.72 GPa for neat epoxy to 3.35 GPa for 6wt% t xGnPM-5/epoxy composite and 3.10 GPa for 6wt% xGnPC-300/epoxy composite, according to macroscopic measurements. The *UTS* of the formulation incorporating 6.0wt% XGnPM-5 in epoxy fell from 77.6MPa (neat epoxy) to 36.4MPa. According C. Salom et al. added 0.7wt% graphene oxide in Polyvinyl Alcohol (PVA), which increased *E* from 2.13GPa to 3.45GPa and the *UTS* by 76% (from 49.9 to 87.6MPa) (Liang, Huang, et al., 2009). The authors speculated that the difference in the molecular structure of the epoxy monomer and hardener molecules at the interface caused the drop, based on data from relevant Molecular Dynamics (MD) simulations. Improvements in *E* and *UTS* of epoxies with the addition of rGO have been reported (Rafiee et al., 2009)(Olowojoba et al., 2017). Functionalised graphene nanoplatelets (GNPs, multilayer graphene) (2.0 wt%) are used by Kim et al. (J. Kim et al.,

2018) and reported *E* of 4.08 ± 0.32 GPa also ultimate *UTS* 80.75 ± 4.41 MPa. These values are way higher than the unreinforced epoxy matrix, reported as 94.3% and 35.3% higher. Domun et al. (Domun et al., 2017) dispersed plasma functionalized graphene nanoplatelets (f-GNP) with low viscosity epoxy, Araldite® LY 564 resin using bath sonication and methanol used as a solvent. They improved *E* from 2.49 to 2.63GPa with the loading of 0.25wt% of f-GNP and *UTS* from 71 to 74Mpa with the loading of 0.75wt% of f-GNP. The more common dispersion procedure utilized is ultra-sonication; its main advantages are straightforwardness and easy implantation at an industrial scale (Anwar et al., 2016). Long-Cheng Tang et al. (Tang et al., 2013) studied the influence of graphene dispersion state on the mechanical characteristics of graphene/epoxy composites. The thermal reduction was used to exfoliate the graphene sheets from graphite oxide (GO) (thermally Reduced GO, rGO). Various dispersions of rGO sheets were prepared with and without the use of a ball mill. The composites with highly dispersed rGO had a greater glass transition temperature (T_g) and strength than those with weakly dispersed rGO, despite the fact that there were no significant variations in the tensile and flexural modulus. With the addition of 0.2 wt% well-dispersed rGO to epoxy, the T_g was enhanced by about 11°C.

Table 2. 2: Literature data of different GRMs, dispersion methods and mechanical properties.

Reference number and year	**Preparation methods and experimental conditions**	**Type of GRM and polymer used**	**Type of additive Used (solvent)**	**GRM Filler Content wt%**	**ASTM used**	**Mechanical properties**		**T_g (°C)**
						***E* (GPa) (% increase)**	***UTS* (MPa) (% increase)**	
(Hashim & Jumahat, 2019)	solution compounding and high-shear mixing	GNP, epoxy	Acetone	0.3	D638	3.58 (32.5%)	79.8 (14.9%)	N/A
(Cha et al., 2019)	planetary centrifugal mixer	GNP, epoxy		2	D638	4.65 (38.%)	83.5 (2.9% decrease)	N/A
(J. Kim et al., 2018)	Magnetic stirrer	GNP, epoxy	Acetone	2	NA	3.49±0.31 (66.2%)	63.32±0.5 (6.1%)	N/A
(Manta, 2019)	shear mixing	GNP, epoxy	Acetone	5 VOL%	D638	2.78 (17.79%)	35 (45.38% decrease)	N/A
(Krieg et al., 2018)	Speed Mixer	GNP, epoxy		20	D638	3.69±0.08 (35.66%)	49.9 (35.69% decrease)	N/A

(Pullicino et al., 2017)	shear mixing	GNP, epoxy	Acetone	5	D638	3.02 (16.23%)	74 (39.18% decrease)	N/A
(Wei et al., 2017)	bath sonication	GNP epoxy	DCB	0.3	D638	NA	69.32 (7.53%)	76.5
(Wei & Inam, 2017)	bath sonication	GNP epoxy	SDS	0.3	D638	1.21 (39%)	67.2 (17%)	72.1
			GA	0.3	D638	1.29 (48%)	70.4 (23%)	76.9
(Klimek-McDonald et al., 2018)	Shear mixing and bath sonication	Asbury Carbon's TC307 (GNPs) epoxy	NA	4	D638	2.93 (7.7%)	80.9 (6.57%)	N/A
(M. G. Prolongo et al., 2016a)	mechanical stirring, sonication.	GNP, epoxy	NA	5% mass	NA	3.20±0.15 (28%)	42±5 (39.13% decrease)	158
(J. A. King et al., 2013)	high-shear mixer H	GNP, epoxy	NA	6	D638	3.36 (23.7%)	36.4 (53.09% decrease)	N/A

(Liang, Huang, et al., 2009)		GO,	PVA	0.7		3.45 (62%)	87.6 (76%)	N/A
(Cha et al., 2019)	planetary centrifugal mixer	f-GNP epoxy	NA	2	D638,	5.76 (71%)	105.91 (23%)	N/A
(J. Kim et al., 2018)	Magnetic stirrer	f-GNP epoxy	Acetone	2	NA	4.08±0.32 (94.3%)	80.75±4.4 (35.3%)	N/A
(Domun et al., 2017)	bath sonication	f-GNP, epoxy	methanol	0.25	D638	2.63 (5.6%)	72 (1.4%)	N/A

2.7 Curing Process

The final properties of GRMs/epoxy nanocomposites also depend on the curing process. Understanding the curing mechanism is essential for the effective design of processing operations and control of the final properties of the cured resin. Differential Scanning Calorimetry (DSC) has been utilised to monitor the curing process of epoxy resins (Prime, 1997). DSC can provide an excellent determination of the onset of cure, heat of cure (ΔH), maximum rate of cure, completion of cure, degree of cure and glass transition temperature (T_g). Although there are several DSC studies on graphene oxide (GO)/epoxy systems up to date (D. G. D. Galpaya et al., 2015)(Xiao Wang et al., 2016)(Qiu et al., 2011)(Monteserín et al., 2017), very few studies are reported on the effects of pristine graphene on the cure kinetics of epoxy systems (M. G. Prolongo et al., 2016b).

The type of graphene used (i.e. geometry and surface chemistry) affects the cure kinetics of the particular resin system in use. Prolong et al. (M. G. Prolongo et al., 2016b) used GNPs (XG Science M25) with an average thickness of 6 nm and average lateral size of 25 μm with diglycidyl ether of bisphenol A (DGEBA) (Araldite F, Ciba) and 4,40-diaminodiphenylmethane (DDM) (Acros Organics). They found that the curing reaction becomes less exothermic with GNPs as the nanofiller hindered the epoxy-amine reaction. Qiu et al. studied the effects of GOs on tetrafunctional epoxy resin tetraglycidyl-4,4'-diaminodiphenylmethane (TGDDM) cured with the aromatic diamine 4,4'-diaminodiphenylsulfone (DDS) and found that GO increased the enthalpy of the cure reaction and decreased the activation energy (Ea). Wang et al. observed a maximum reduction of 28.8% in E_a in the system diglycidyl ether of bisphenol-A (DGEBA)/DDS with the addition of GO.

On the contrary, an increase in E_a was reported for GO/epoxy nanocomposites by Jouyandeh et al. (Jouyandeh et al., 2019) and Ryu et al. (Ryu et al., 2014). It was attributed to viscosity increase with the addition of the nanofiller hindering the chemical reactions. The disparity in results suggests that nanocomposites are sensitive to the detailed chemistry of the epoxy resin system as well as the functional groups on the surface of the graphene (D. G. D. Galpaya et al., 2015). Despite the improved compatibility of GO with polymer matrices, the preparation of GO requires extensive use of solvents, and its properties are inferior to graphene. Hence, new approaches that use unaltered graphite would have significant advantages in properties, cost, and environmental impact (Woltornist et al., 2015). Prolong et al. used GNPs (XG Science M25) with an average thickness of 6 nm lateral and average size 25 μm with diglycidyl ether of bisphenol A (DGEBA) (Araldite F, Ciba) and 4,40-diaminodiphenylmethane (DDM) (Acros Organics) and found that the curing reaction becomes less exothermic with the presence of GNPs.

2.7.1 Cure Monitoring Techniques

There are various methods used for investigating the curing kinetics of polymers, for example, differential scanning calorimetry (DSC) (Granado et al., 2018; J. Hu et al., 2014; J. Xu et al., 2019; G. Yamini et al., 2019; Zolghadr et al., 2019), Fourier Transform Infrared Spectroscopy (FTIR) (G. Yamini et al., 2019) and rheology estimation (J. Hu et al., 2014)(Zhongliang et al., 2019). Among them, one of the most commonly utilized procedures is DSC. It can explore the curing behaviour by estimating the difference in heat flow with temperature and time during the curing process. In past examinations, DSC was generally utilized to investigate thermosetting polymers, for example, epoxy resin (Zolghadr et al., 2019)(G. Yamini et al., 2019). This research used DSC for cure kinetics, which is detail discussed in chapter 4.

2.7.2 Joining for lightweight vehicles

The structural performance of a joint relies upon the joining technique, joint geometry and joint quality(Mallick, 2021a) (Mariana D. Banea, 2019). The joining strategy regularly relies upon the materials being joined; however, under large-scale manufacturing conditions, it should likewise be fast, less subject to fit, and dimensional varieties of the parts being joined. Joining requires a significant consideration in the design of a vehicle since joints are typically the weaker zones in the structure, and they are routinely the failure-initiating zones in the structure. Joining turns out to be increasingly significant as the body material changes from a single material to a blend of materials, since the similarity between various materials as far as their shared joinability, surface characteristics, corrosion, assembly, etc. may introduce various specific challenges and ought to be considered in the arrangement strategy and assurance of materials.

2.8 Adhesive Bonding

The process of adhering two surfaces together, usually with the production of a smooth bond, is known as adhesive bonding. This may entail the use of epoxy, glue or any of a variety of plastic agents that bond by the evaporation of a solvent or the curing of the material using heat or pressure. It is feasible to provide more extraordinary load transmission, stiffness, and fatigue resistance by using a continuous bond. Adhesives also help reduce the completed construction weight, which is vital in the transportation industry. Adhesive Bonding technology is used to join various constructional materials (R. D. Adams, 2005) such as (metals, ceramics, polymers, and composites) (Panigrahi & Zhang, 2011). However, improving the safety of structures, increasing the lifetime, and reducing the costs are highly needed nowadays and can show a significant tolerance to damage (M. D. Banea & Da Silva, 2009). This technique can also build dissimilar joints (E. C. Botelho et al., 2004; Hasheminia et al., 2019; A. M. G. Pinto et al., 2009). The ability to join construction materials of different physical and chemical properties (B. He & Ge, 2017)(Anyfantis & Tsouvalis, 2012), as well as of considerably different sizes (e.g. thickness) (M. D. Banea et al., 2018; Edson Cocchieri Botelho et al., 2006; L. F. M. da Silva & Adams, 2007; B. He & Ge, 2017) is valid for various applications. Adhesive joints have approximately significant advantages compared to other joining techniques such as spot welding and mechanical joining (L. F. M. da Silva et al., 2018a)(Robert D. Adams & Wake, 1984). Instead of mechanical bonding, adhesive bonding offers the potential for reduced weight and cost (Mariana D. Banea et al., 2014).

Due to outstanding performance, adhesive bonding is widely acceptable in the automotive sector due to its advantages over other bonding technologies such as bolts and riveting (M. R. G. Silva et al., 2016)(Galvez et al., 2017). To improve the vehicle structure where fuel efficiency and weight reduction are important, dissimilar material joints with a structure, for example,

composite materials combined with light-weight metals, have to be(M. D. Banea et al., 2018; Mariana D. Banea et al., 2017; Hasheminia et al., 2019). Epoxy resins are the most broadly utilized adhesives to bond dissimilar materials in advanced automotive and aerospace applications because of their superb adhesion property and a combination of mechanical properties and corrosion resistance (Higgins, 2000)(Burkholder et al., 2011). Various investigations have focused on further improving the performance of epoxy adhesives through the use of nanofillers. It has been shown that using different nano-fillers can significantly improve the epoxy resin system's cohesive strength and bond strength (Jojibabu et al., 2017). In order to construct an adhesive joint that achieves the appropriate levels of mechanical strength and durability, five critical processes must be considered during the design process. The primary processes are the adhesive selection process, joint design phase, surface treatment selection, manufacturing process, and control (Carbas et al., 2021). Because of its properties, aluminium is a near-ideal option for adhesive bonding because it has high surface energy, enabling the organic adhesives to wet it easily (Lathabai, 2011).

2.8.1 Properties of adhesive bonding

The chemical and physical properties of the adhesive are significant factors in adhesive joint performance. The kinds of adherents (that is, the components being joined—e.g., composite material, metal alloy, plastic) and the nature of the surface pre-treatment or primer are also essential in deciding whether the adhesive bond will operate satisfactorily. These three factors (adhesive, adherend, and surface) influence the bonded structure's service life (Adhesive | Definition, Types, Uses, Materials, & Facts | Britannica, n.d.). The intricacies of the joint design and how the applied loads are carried from one adherend to the other determine the mechanical behaviour of the bonded structure. Bulk adhesives have lower strength than metals, but when used to bond surfaces, the adhesive strength is sufficiently high for structural joints

(L. F. M. da Silva et al., 2018b), and its validity corresponds to joining surface regions. Bonding strengths of structures made of polymer composite and metals are significantly affected by the arrangement of composite surfaces just as metallic structures (Baker & Chester, 1992; Rhee & Yang, 2003; Schubbe & Mall, 1999). An adhesive can fail in the event where the strength of adhesive materials turns out to be a lot more fragile when contrasted with that of the adherents for a perfectly bonded adhesive joint (Pramanik et al., 2017). The bonded area and the thickness of the adhesive layer are the key components of adhesive sizes. Bond strength can be considerably improved by increasing the bonded area. However, because the adhesive layer is thicker, bonding performance is not always better, and in some cases, it is even preferable to decrease it. The stiffness of adhesive joints may be reduced by increasing the thickness of the adhesive layer (L. Guo et al., 2021).

2.9 GRMs /epoxy adhesives

The improvement of nanoparticle reinforced adhesive materials is one of the most investigated areas in materials science and engineering; it has been discovered that nano-fillers to epoxy resins could expand the strength and stiffness of the epoxy (Gkikas et al., 2012, 2014; Shadlou et al., 2014), which thus can expand the strength of the joint (Nemati Giv et al., 2018). The rise of nanocomposites as adhesives has pulled in incredible importance, and studies have shown that nano-fillers can improve bulk mechanical properties, joint strength and toughness of epoxy adhesives extensively (Jojibabu et al., 2017; Srivastava, 2011; Wichmann et al., 2008).

2.10 Parameters that affect the performance of the bonded joints

Several parameters affect the performance of adhesively bonded joints, for example, surface preparation, geometrical parameters (overlap length, adhesive thickness, ply angle, stacking sequence, filler content) and material parameters (adhesive & adherend properties) (Mokhtari et al., 2013)(Stazi et al., 2015). All these should be considered during the design of bonded

joints for a better result of the bonded structure. These parameters will be discussed in the following subsections.

2.10.1 Surface Preparation

Surface preparation performs a critical role in accomplishing a high bond strength and improving the durability and life of bonded joints. To get a durable and strong joint, surface preparation of adherents must make sure the following elements: removal of all contaminants (lubricants, dust, loose corrosion layers, micro-organisms) from the surfaces (Encinas et al., 2014; Iqbal et al., 2010; Kanerva & Saarela, 2013). These contaminants adversely have an effect on the adhesion and wetting of the adhesive, and if they are now not eliminated properly before applying the adhesive, they may cause bond failure. There are different chemical and physical surface treatment methods, and the correct choice of surface treatment method is crucial (Iqbal et al., 2010; J. Mohan et al., 2014; Palmieri et al., 2016). To accomplish this goal, state-of-the-art manipulating of the peel-off layer technique or various mechanical treatments (Encinas et al., 2014)(Kreling et al., 2013). The peeling layer is a technique that protects the surface from contamination (moisture, dryness, dust) and produces and provides a specific texture of the surface(Kanerva & Saarela, 2013)(Kanerva et al., 2015). It was observed that the composite matrix resin interacts with the peel layer material, and the interface or residue from the peel layer remains on the surface of the composite (Budhe et al., 2017). Also, in terms of fracture toughness or shear strength, the joint strength after peel layer treatment barely matches the strength of joints pre-treated by abrasive mechanical treatment (Kanerva et al., 2015). Due to these problems, it is necessary to carefully select type peel layer products and peel ply removal to achieve adhesive bonding successfully.

It is vital to remember that the entering aluminium surface usually has numerous surface chemistries due to past processing. This can comprise both inorganic and organic contaminants

such as lubricants, oxides, dirt and dust. These contaminants will inhibit the adhesive from bonding to the base material and must be eliminated to prepare the surface for bonding. If the adhesive were merely placed on a typical aluminium surface, it would build a long-term bond with impurities and reaction products on the surface rather than the base material. Surface contamination reduces bond strength by interfering with the adhesive's capacity to make a suitable bond (resulting in a weaker bond or a decreased bond area) (Systems, 2015).

2.10.2 Effect of filler content on shear strength

Zheng et al. (R. Zheng et al., 2015)(Prucha, 2012b)and Xu et al. (W. Xu & Wei, 2012) demonstrate that joint strength is not just related to the adhesive properties but also emphasises the bond between the adhesive and adherend. Moreover, a superior bond adhesion consistently shows an improvement in durability (Boutar et al., 2016; Sorrentino et al., 2018; H. Wan et al., 2018); Gültekin et al. (Gültekin et al., 2016) studied the effect of different GNP wt% content on the failure load of adhesive joints. They used high shear mixing and ultrasonication to disperse GNPs into the epoxy. From the research, it is obvious that the amount of GNPs in the epoxy adhesive affected the failure load of the adhesive joints, where it is also evident that with the average failure load increasing with GNP content and maximum failure load occurred in joints with 1%wt GNP content. Increased GNP fraction is also analysed and reported that with a higher fraction of GNP (2%wt), the failure load decreased, with 2%wt of GNPs, the GNPs formed as agglomerates and caused a decrease in lap shear strength. With double, the GNP/EP joint fraction from 0.5%wt to 1%wt, a 5% increment was achieved which was 15% for 0.5%wt.

On the other hand, when the GNP reinforcement was increased to 2%wt, the average failure load decreased by 7%. Jojibabu et al. analysed the effect of different GNP content such as 0,0.2,0.5, 1 and 2%wt on lap shear strength of epoxy adhesive joints; joint strength increased

and attained the highest value of 20.7 MPa for 0.5%wt GNP/epoxy, which corresponds to a 49% increase in the strength compared to the neat epoxy join(Jojibabu et al., 2016a). The expansion of GNPs into the adherents prompted a considerable increment in joint strength contrasted with the neat epoxy adherents. It was found that the 1wt.% of GNP/epoxy indicated a most extreme joint strength, which was more than twice that of the neat epoxy adhesive joints (Liberata Guadagno et al., 2015). According to Jojibabu et al., The greatest lap shear strength was achieved for the 0.5 wt.% GNP/epoxy joints were 48% higher than the pure epoxy joints, using a high shear mixer for dispersion (Jojibabu et al., 2016a). Gültekin et al. (Gültekin et al., 2016) considered the impact of GNP proportion on the failure load of the adhesive joint; the GNPs were dispersed into the epoxy using high shear blending and ultrasonication. It was found that the quantity of GNPs in the epoxy adhesive influenced the failure load of the adhesive, with the average failure load increasing with GNP content (Gültekin et al., 2016). Recently, a few studies reported improvements in the adhesion strength of epoxy adhesives with the incorporation of rGO. G. Marami et al. used rGO/Araldite2011 adhesive to bond aluminium alloy 7075-T6 adherents and found that joints with 0.5wt% rGO exhibited 27% higher lap shear strength (*LSS*) compared to joints connected with neat adhesive (Marami et al., 2016). Aradhana et al. used rGO/Araldite GY250 to bond aluminium adherents and showed ~50% increment compared to pristine epoxy (Aradhana et al., 2018). Several studies also reported improvements in epoxies using GO (Xue et al., 2019) or graphene nanoplatelets (Jojibabu et al., 2016b)(Moriche et al., 2016)(Salom et al., 2018)(Han et al., 2019)(Jee et al., 2020)(Nascimento et al., 2021).

In reality, a few studies have indicated a reduction in adhesion strength with the consolidation of GNPs into an epoxy adhesive. Moriche et al. (Moriche et al., 2016) observed a drop-off in the lap shear strength of epoxy adhesive joints modified with GNPs.

Aradhana et al. (Aradhana et al., 2018) used epoxy/GRMs (rGO & GO) with acetone solvent. The incorporation of 0.5 wt% GRMs (rGO & GO) enhanced the shear strength of the pristine epoxy adhesive. The neat epoxy showed a shear strength of 5.43 MPa. Incorporation of 0.5 wt% GRMs (rGO & GO) in epoxy resin extended shear strength up to 7.803MPa, and 8.136 MPa, which is 43.7% and 49.8% higher as compared to the neat epoxy, respectively. It also reported that with a higher fraction of GRMs (rGO & GO) (1wt%), the failure load decreased 6.174 ± 0.58MPa and 6.36 ± 0.74MPa, respectively.

It is observed that the nano-filler content is crucial; at high contents (e.g. >1% wt), agglomeration is caused, which acts as defects sites resulting in a reduction in adhesion strength(Jojibabu et al., 2020). The advancement and procedures for simple recycling, heal, or self-heal of bonded structures are happening to incredible enthusiasm for the industry. Adhesives are presented to a broad scope of service loading conditions, such as thermal cycling in space conditions, creep and weakness forced by structural joint arrangements, and residual stress due to thermal expansion mismatch between adhesive and substrates. All these service-loading conditions cause damage in adhesives limiting their structural performance and other functional characteristics.

2.10.3 Geometric parameters

One of the highly essential geometrical aspects defining an adhesive joint is the thickness of the adhesive layer. The consistency of the adhesive bonded joints must be fully considered in the design process. The strength of bonded joints relies on many structural and technical aspects and conditions of use. The geometry of the adhesive joint, the type of bonded joint material used (both adhesive and adherents) and the form of loading are all structural aspects. Much research has been accomplished to determine the effect of adhesive thickness on the strength of adhesive joints (Grant et al., 2009)(W. Xu & Wei, 2013)(Marzi et al., 2011).

However, even in single-lap joints, the effect of adhesive thickness on bond strength is still poorly known (Rośkowicz et al., 2021). The effect of adhesive thickness on bonding performance has been studied extensively in experimental and numerical investigations. However, the experimental procedures may become increasingly problematic if the adhesive layer thickness drops to tens or even a few microns (X. Chen et al., 2018). It has been a critical matter about the effect of adhesive thickness on the shear strength. According to Adams et al. (R. D. Adams & Peppiatt, 1974), the strength of epoxy adhesive joins reduces as the adhesive layer thickness increases from 0.1 to 0.2 mm. This could be attributed to increased pores and micro-crack flaws in the adhesive layer, leading to premature failure. Shokrian et al. (Shokrian et al., 2019) made adhesive joints with thicknesses of 0.3, 0.5, and 1 mm, and the results showed that the shear strength decreased slightly as the thickness increased. Silva et al. (L. F. M. da Silva et al., 2006)(Campilho et al., 2015) noticed that when the thickness of the adhesive layer rises, the shear strength reduces. However, Aydin et al. (Aydin et al., 2005) investigated aluminium-alloy single-lap joints with various thicknesses and lap lengths and found that the shear strength of the adhesive layer increases with thickness, and the failure process begins at the edge of the adhesive layer due to tensile stress caused by peeling. According to Liao et al. (Liao, Huang, and Sawa 2013), the impact of the thickness of the adhesive layer on bond strength is related to the type of adhesive. The brittle adhesive decreases with the increase of the adhesive thickness, while the tough adhesive shows an opposite response. Table 2. 3 shows lap shear strengths and type of failures of all adhesive systems.

Table 2. 3: Lap shear strengths and type of failures of reported rGO and epoxy adhesive systems.

Reference number and year	**Preparation methods and experimental conditions**	**Type of GRM and polymer used**	**Type of additive Used (solvent)**	**GRM Filler Content wt%**	**Type of substrates**	**ASTM used**	**Lap Shear Strength (MPa) increase**	**Type of Failure**
(Aradhana et al., 2018)	mechanical stirring, sonication	rGO, epoxy	acetone	0.5	Aluminium	D1002	7.803 ± 0.94 (43.7%)	Partially Cohesive
		GO, epoxy	acetone	0.5	Aluminium	D1002	8.136 ± 0.66 (49.8%)	Fully Cohesive
(Jojibabu et al., 2016a)	mechanical stirring,	GNP, epoxy		0.5	AA6061 sheets	D1002	20.7 (49%)	cohesive failure
(Marami et al., 2016)	Ball-Mill machine, bath sonicated	rGO, epoxy		0.5	2 mm thick aluminium alloy 7075-T6	D1002	30.06 ± 1.10 (26%)	cohesive failure

2.11 Summary

The literature review reveals that the GRM type used and the dispersion quality into epoxy are significant for property enhancement. The type and degree of functionalisation and the processing methodology play a vital role in dispersion quality. Additional studies are needed to clarify the optimum material combinations (i.e. chemistry and geometry of flakes and resin chemistry) and their processing. In this research, we investigate novel non-functionalised as well as functionalised GRMs combined with epoxies with low and low/medium viscosity suitable for impregnation (resin infusion) of carbon fibre tapes.

Chapter 3 Overview of Materials used in the Automotive Industry

3.1 Introduction

The primary materials used for vehicles, and their parts and components are steel, aluminium, glass, plastics, rubber, magnesium, copper, and carbon fibre composites. Stricter requirements for better fuel efficiency, weight reduction, environmental regulations, and customer needs force automotive manufacturing companies to develop new materials and structures or redesign existing ones. Many factors are involved in selecting automotive materials, such as cost, weight, safety, and recyclability/reuse (Lightweight Materials for Cars and Trucks Department of Energy, n.d.). Lightweight materials can improve fuel efficiency and reduce emissions and also, and raw material cost affects the total vehicle cost and thus is an essential parameter in materials selection.

It determines whether any new material has an opportunity to be selected for a vehicle component. However, most lightweight materials, such as aluminium, magnesium, and carbon fibre reinforced polymers, are more expensive than heavier materials like steel and cast iron for reasons that include abundance and ease of fabrication. In the decision-making process of the design, a compromise is often met, balancing cost and weight requirements. Safety and impact resistance is a vital element for an automotive component; materials should have the ability to absorb impact energy during a crash.

3.2 Current trends for reducing vehicle weight

Several methods for weight reduction are available. The most fundamental approaches are the use of low-density materials and multi-material lightweight design. These approaches are further discussed in the following sections.

3.2.1 Use of low-density materials

This design method makes use of the material's advantages. Varied materials achieve different levels of strength and/or stiffness depending on their density and material qualities. The use of low-density materials instead of high-density materials such as aluminium, magnesium and polymer matrix composites, instead of steels without reducing stiffness and durability, can improve vehicle structure(Fentahun & Savas, 2018). In addition, these lighter materials can carry high loads without increasing the vehicle's weight. Modern composite technology provides many benefits over conventional materials in the automotive industry. Composite materials have recently emerged as materials with great potential. Fibre-reinforced polymer composites, one of these material categories, are lightweight and provide the automotive industry with several benefits due to their low density and potential for weight reduction in automobiles. Composites are a perfect replacement for metallic structures in automobiles and military applications to absorb impact energy because of their enhanced impact performance features, energy-absorbing capacities, lightweight design, and anti-corrosion properties (Evci & Gülgeç, 2012). The exceptional corrosion resistance and other chemical qualities can assist manufacturers in extending the lifespan of both individual parts and complete vehicles (Gardyński et al., 2018). The automotive industry has seen tremendous growth in the use of polymer composites due to improved vehicle designs, changes in regulatory requirements, concerns about sustainability, and an emphasis on using lightweight materials in cars (Pradeep et al., 2017). The expanding use of polymer composites and their use in both interior and exterior car components (Gupta & Singhal, 2022).

3.2.2 Structure lightweight design

It is a way of creating and designing parts based on topology, shape, and parameter optimization. The goal is to change the shape and form in order to lose weight while increasing

or maintaining stiffness and/or strength. The use of all lightweighting strategies, that combine lightweighting design with numerically optimised structures, innovative lightweight materials, and fabrication techniques that are efficient for both the materials and the structures leads to the best possible lightweight (Kaluza et al., 2018). In order to reduce material consumption and improve structural performance, such as higher strength and stiffness, better crashworthiness, and better vibration performance, a component's size, shape, and topology are all factors in the structure design optimization process (Czerwinski, 2021).

3.2.3 Multimaterial Lightweight Design

A multi-material design approach necessitates the combination of different lightweight materials, which eventually need to bond together into a final assembly such as aluminium to CFRP, aluminium to aluminium, steel to CFRP and other material combinations (Gene Liao & State University, 2017). Modern vehicles must incorporate multi-material structures with highly integrated light metal applications, utilising the material with the optimum qualities for the specified requirements in a suitable location (Czerwinski, 2021). The current forefront of the lightweight design trend in the automobile industry is multi-material design, which is regarded as one of the techniques for improving production efficiency. The characteristics, manufacture, and end-of-life recyclability of the components can all be enhanced by combining various materials. It is well acknowledged that using a variety of materials with various properties during the design process results in a product that performs better in terms of its functionality, cost, manufacturability and aesthetics. It should be emphasised that the term "multi-material design" can apply to both the overall vehicle and its specific parts. They are referred to as smart or hybrid components, and their fundamental properties such as strength, ductility, or crashworthiness variate in different locations depending on the needs of the design. To fully utilise the property advantages of various materials, the smart/hybrid

components frequently combine two or more distinct types of materials, such as metallic alloy-carbon-fibre compositions. The design of multi-material vehicle components results in a variety of design possibilities and trade-offs between competing development goals, which makes the creation of appropriate lightweight solutions for mass production particularly difficult. As a result, the literature suggests a variety of alternatives. As Kleemann et al., suggested (Kleemann et al., 2017), the methodological approach for generating multi-material components, which includes characteristics property modelling (CPM), property-driven development (PDD), and extended mapping matrices (EMM), serves as a technique to identify approaches to design concepts. Figure 3.1 reveals materials commonly used in the vehicle (*CSR Europe on Twitter: "Do You Know How Many Raw Materials Are Needed to Make a Car or Another Vehicle? #DriveSustainability Aims to Improve Sustainability in Sourcing of These Raw Materials: Https://T.Co/LEyjEXAbh8 Https://T.Co/WVxTXovc83" / Twitter*, n.d.).

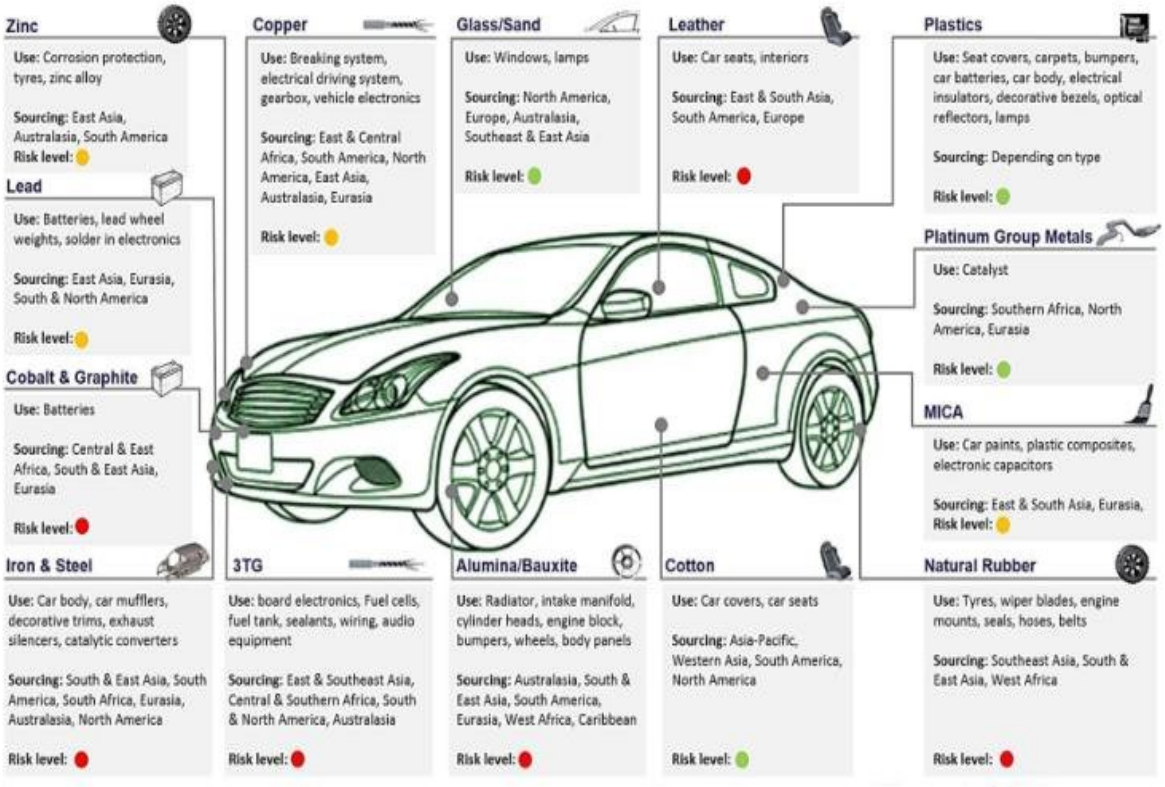

Note: Raw materials relevant for car manufacturing are also used in trucks, buses, motorbikes, and other vehicles.

Figure 3. 1: An Overview: Materials in the Automotive Industry (CSR Europe on Twitter: "Do You Know How Many Raw Materials Are Needed to Make a Car or Another Vehicle? #DriveSustainability Aims to Improve Sustainability in Sourcing of These Raw Materials : Https://T.Co/LEyjEXAbh8 Https://T.Co/WVxTXovc83" / Twitter, n.d.)

3.3 Polymer Composite materials

Polymer composite materials have been used as structural components since they offer a combination of good mechanical properties, low weight, stability and versatile processing techniques (Baekeland, 1909). Polymer matrix composites are divided into three main categories according to the matrix used, i.e. thermoplastic, thermoset and elastomers. Elastomers, thermoplastics, and thermosets are among the structural polymeric matrices for advanced nanocomposites that are widely employed due to their remarkable physical and chemical properties, which can be tailored to various applications (Ebewele, 2000; Natarajan, 2015; PAINTER & COLEMAN, 1997; Ram & Ram, 1997; Skura, 1980). Generally, thermosets are stiffer than thermoplastic matrices, have lower viscosity, have better creep resistance, and are suitable for moulding large parts with short, long or woven fibres and produce structural composites with high strength and modulus (Mallick, 2021b)(Saba & Jawaid, 2018). The function of the matrix is to link the reinforcing fibres, distribute the constraints, provide the chemical resistance of the structure and give the final product the desired shape (Arabpour et al., 2020)(S. Zheng et al., 2019).

Polymer-matrix composites are fabricated using a fibre filler (carbon or glass) and a matrix material (e.g. an epoxy polymer) that provides enhanced properties when combined with individual materials. The percentage of plastics by mass in an average vehicle has gone from 6% in 1970 to 16% in 2010 and is expected to reach 18% in 2020 (Miller et al., 2014). Figure 3. 2 illustrates the change in vehicle composition from 1970 to 2020 (Miller et al., 2014).

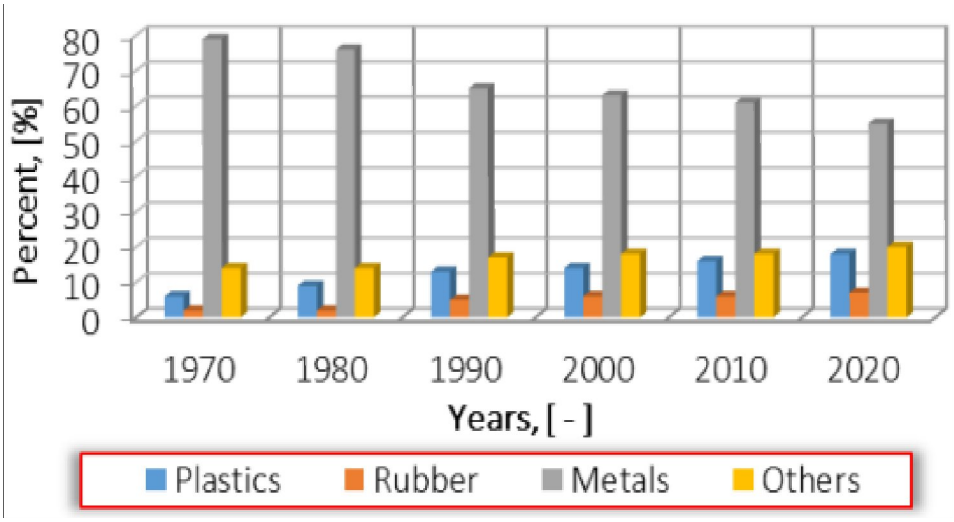

Figure 3. 3: Change in vehicle composition from 1970 to 2020 (Miller et al., 2014).

Improved material qualities have resulted from research on composite materials, reinforced plastics, and polymers, making them appropriate for automobiles' interior, exterior, and under-the-hood components. Bumpers, seating, dashboards, internal and external trims, and other automotive components use automotive composite materials (Todor & Kiss, 2016). Designers can increase durability, meet load-bearing requirements and reduce vehicle weight by carefully selecting certain automobile materials. Due to the modest nature of the automotive sector, research and development departments are working hard to develop suitable materials combinations for lightweight and reliable cars. Polymer Composites materials are lightweight and provide flexibility of better design compromise and improve the safety of vehicles.

Carbon fibres are characterised by low density and high mechanical properties, specific Ultimate tensile strength and modulus (Petersen, 2016). Polymers added to the carbon fibres provide a cohesive matrix in the desired geometric arrangement to form a carbon fibre reinforced polymer (CFRP). The polymer matrix transfers the load to the fibres and protects against mechanical and chemical damage, resulting in CFRP with a high strength-to-weight ratio, stiffness and durability (Ofoegbu et al., 2019). CFRP contains carbon fibres (CFs) of about 0.005-0.010 mm in width in polymeric matrices, promoting lightweight composite

structures (Pramanik et al., 2017). Carbon fibre reinforced polymer (CFRP) is one of the most significant materials for structural applications are utilised in numerous industries due to their remarkable mechanical, thermal and chemical properties. CFRPs have become the materials of choice for aerospace equipment due to their well-integrated design and manufacturing properties, including the ease of manufacturing large and complex components, their lightweight, and their joining capabilities (Hui Wang et al., 2020). Many researchers have developed CFRP/ metal different joining technology (Lim et al., 2018)(Pramanik et al., 2017). However, CFRP is a costly material mainly due to the cost of carbon fibre, which can be very expensive depending on the quality requirements of the product or the application (Hagnell & Åkermo, 2019)(Vo Dong et al., 2018).

3.4 Lightweight automotive composites

Adding a nanofiller such as graphene or related materials into polymer composites can improve the structure's mechanical properties. Fibrous reinforcement arranged in a continuous or non-continuous polymer matrix is used to make the majority of polymer composites. Glass, carbon, and aramid fibres are commonly employed to provide strength and stiffness to polymer matrices like polyester, polyurethane, epoxy, polypropylene, polyethylene, nylon, and others. Nanoparticles can also be added to a polymer matrix to create nanocomposites, higher-performance composites with outstanding mechanical properties and less weight. This is a good addition to the automotive industry, but still, more research is needed on Graphene/Polymer-based materials; there are many challenges related to filler dispersion, filler/matrix interaction, and stress transfer. Lithium-ion batteries with graphene enhancements might be utilized in far more energy-intensive applications, like electrically powered vehicles, or they could be used in smartphones, laptops, and tablet PCs as they are currently used, but with significantly smaller and lighter batteries. Although graphene-based batteries are not yet

entirely commercially viable, they have intriguing potential. R&D is intensive and should produce results in the future. Many businesses throughout the world (including Samsung, Huawei, and others) are creating various kinds of graphene-enhanced batteries, some of which are now hitting the market. The primary uses are in mobile devices and electric cars (SHARMA, 2022). Figure 3. 4 shows the global graphene battery market from 2022-2026 (SHARMA, 2022).

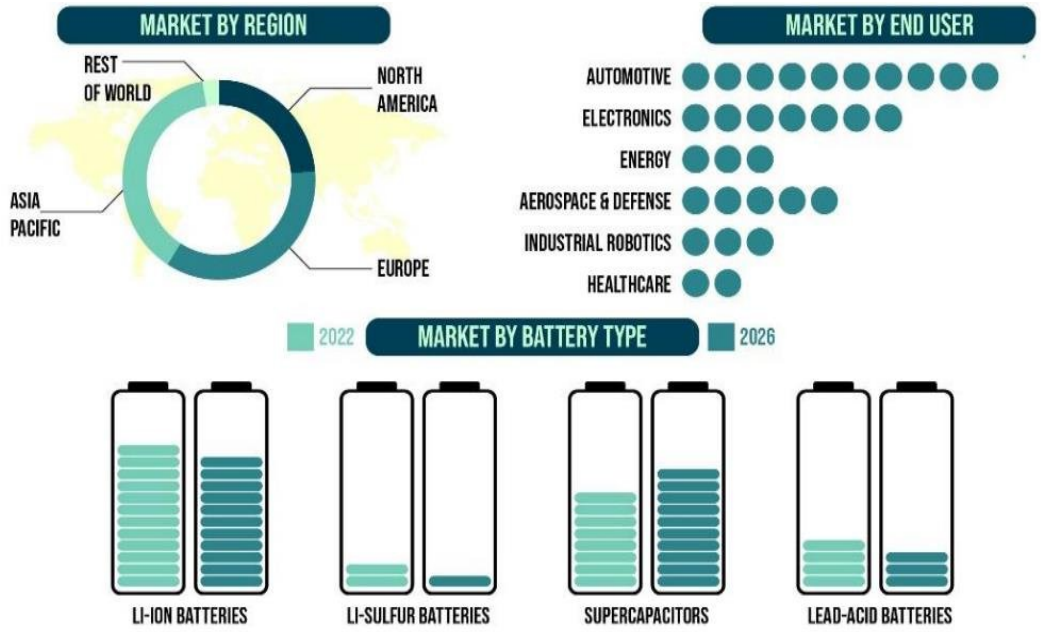

Figure 3. 5: Global Graphene battery market from 2022-2026 (SHARMA, 2022).

3.5 Epoxy polymer

In 1936, the Initial formulation of bisphenol-A-based epoxy resins was developed by Dr Pierre Castan in Switzerland and Dr S.O. Greenlee in the United States (Wei et al., 2015). The most generally used epoxy resins are based on the diglycidyl ether of bisphenol A (DGEBA). By combining the epoxy resin with a suitable curing agent, a three-dimensional cross-linked thermoset structure is achieved, which brings about the material with excellent mechanical and

thermal properties (L. Guadagno et al., 2015) (Kausar, Rafique, et al., 2016)(Barletta et al., 2016). As a result, epoxy is widely used in various engineering applications, i.e. automotive, aerospace, adhesives, biomedical devices, construction and marine (Quaresimin et al., 2016)(Rohem et al., 2016)(Wu et al., 2015)(Karger-Kocsis et al., 2015)(N. Li et al., 2006), because of their exceptionally advantageous properties, such as high adhesion strength and good processability.

Since the early 1980s, various studies have been directed to improve the fracture toughness properties of epoxy resin by utilising different strategies. Modification of the polymer matrix using nanofillers, for example, carbon nanotubes (CNT), silica nanoparticles, nano clays and nano alumina, was seen as a successful strategy to improve the mechanical performance of polymer composite (Ahmadi-Moghadam et al., 2015; Jumahat et al., 2012; Sapiai et al., 2018; Shaari & Jumahat, 2018; Shettar et al., 2017). On the other hand, synthetic polymers are mainly derived from petroleum and cannot break down biologically in nature, harming the environment. Therefore, natural polymers are employed instead of synthetic polymers.

3.5.1 Epoxy Properties

Epoxy resin has lots of properties; usually, we use low and medium viscosity epoxy resin so they can simply and rapidly cure at any temperature ranging from 5°C to 150°C. The curing of epoxy depends on the choice of curing agent. The most significant properties of epoxy have minor shrinkage through the curing process, which provides good quality samples and less cost so easily used in different applications to save the processing time and cost of the products. In addition, high electrical insulation and better chemical resistance improved mechanical properties and high adhesive strength. Unfortunately, the engineering applications of epoxies are narrowed by their brittle nature and poor thermal and electrical properties. To increase the applications of epoxy materials, the best method is to add some filler to improve their nature

and physical properties. Nowadays, different fillers have been explored, i.e. graphene, CNTs, thermoplastic polymers, fibres, clays and rubbers. In these fillers, most can reinforce epoxy well, but sometimes it diminishes properties if not appropriately done (Shivakumar Gouda et al., 2016).

3.5.2 Bisphenol-A epoxy resins

Bisphenol-A (BPA) epoxy resin is a form of epoxy resin (petroleum-based chemical) created by the reaction of epichlorohydrin with bisphenol-A in the presence of an essential catalyst. Their properties depend upon the number of monomers. Bisphenol-A epoxy resin has good mechanical, thermal, stability and toughness properties. However, excessive exposure to bisphenol A may lead to serious health problems since it has been recognised to be an endocrine disruptor (Ribeiro et al., 2017)(Rochester, 2013)(Vandenberg et al., 2007). The synthetic route to bisphenol A epoxy resin (DGEBA) shows in figure 3. 4.

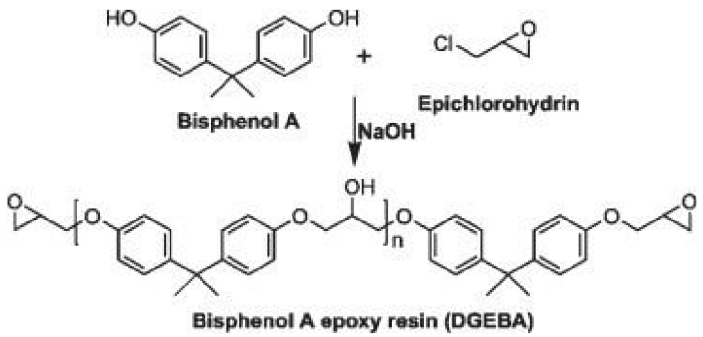

Figure 3. 6: Synthetic route to bisphenol A epoxy resin (DGEBA).

3.5.3 Bio-based epoxy resins

Bio-based thermosets are produced from natural sources. Recent years have seen an expanding necessity for renewable resource-derived polymers (biobased polymers) and their composites with natural fibre (biocomposites) inferable from expanding genuine concern and limited accessibility of petrochemical assets (Dai et al., 2019) (Gandini, 2011). Biopolymers are becoming all the more intriguing because better utilisation of green resources allows us to save fossil resources and reduce the environmental impact (Marefat Seyedlar et al., 2018)(Luckeneder et al., 2016). Researchers are replacing the building blocks for epoxy resins as well as the curing agents for such resins with molecules obtained from natural sources because commonly used bisphenols, such as BPA, it is a toxic endocrine-disrupting chemical that is spread into the environment through modern manufacturing practices (Tarafdar et al., 2022). Additionally a xenoestrogen, BPA harms living things by having geno- and cytotoxic, mutagenic, and carcinogenic properties (Tarafdar et al., 2022). As a result, recent research is focused on the synthesis of structure blocks derived from readily renewable sources, including epoxidised oils, natural polyphenols, terpenes, sugars and itaconic acids. Progress right now has broadly been assessed (Auvergne et al., 2014; Baroncini et al., 2016; S. Kumar et al., 2018; S. Ma & Webster, 2015). However, bisphenol A epoxy resin is a dangerous effect on human well-being, for which a few nations have restricted bisphenol A-based epoxy resins as crude material for the creation of polymer or polymeric items. Overall environmental issues compelled to research and industries for reasonable improvement in the polymer industry as bio-based epoxy resin. Extensive research has been completed on the production of epoxy resin utilising vegetable oils (Alam et al., 2014; Del Rio et al., 2010; Miao et al., 2014; Pfister et al., 2011), lignin (Asada et al., 2015; Calvo-Flores & Dobado, 2010; El Mansouri et al., 2011; Ferdosian et al., 2014), sugar (Niedermann et al., 2015)(Shibata et al., 2013) rosin (K. Huang et al., 2013), cardanol (Jaillet et al., 2014)(Kanehashi et al., 2013), or itaconic acid(S. Ma et al.,

2016) to replace bisphenol A-based epoxy resins and simultaneously to contribute. Considering the commercial significance of epoxy resin in different parts and the rise of manageable advancement, the research about just as the enterprises have moved their concentration towards incorporating bio-based epoxy resin and foreseen from renewable natural resources. For example, vegetable oil, lignin, sugars, rosin and itaconic acid due to their broad accessibility, economical and biodegradability. Moreover, new bio-based materials show properties proportionate to or more than commercial petroleum-based products (Ronda et al., 2013)(Auvergne et al., 2014).

3.5.4 Epoxy Application

Typically, epoxies are recognised for their different physical properties such as good high adhesion strength (de Morais et al., 2007), mechanical properties (S. Yamini & Young, 1980), electrical resistance (Joseph & Viney, 2000), impressive thermal stability (B. Guo et al., 2004) and solvent resistance (Wegmann, 1997). Epoxy nanocomposites have been proposed for several applications, extending from car bumpers to advanced optoelectronic devices (Crosby & Lee, 2007). Thermosetting resins have been widely used for automotive parts (Y. Wang et al., 2018)(Suay et al., 2003), aerospace (Liberata Guadagno et al., 2014a; Vandi et al., 2012), adhesives (Popineau et al., 2005)(Zhai et al., 2008), electronic materials (Zeng et al., 2016)(Reit et al., 2016), biomedical devices (IO, 2016)(Barua et al., 2014) and due to their excellent properties.

An essential application of epoxy-based materials in manufacturing Industries

There are many applications of epoxy-based materials; for example, Aerospace industry, Marine applications, Adhesives, Industrial tooling, Electronic materials, Biomedical systems, Paints and coatings, Consumer applications and Art. In this section few of the most important

are discussed:

3.5.4.1 Adhesives

Epoxy adhesives are being used in various applications such as aircraft, boats, automobiles, bicycles and snowboards. This is because of their great adhesion properties to different substrates, high modulus, low shrinkage and great corrosion resistance (Kasemsiri et al., 2015). In addition, there are usually cured at a high temperature to improve their strength and chemical bonding at the substrate and the adhesive interface (Vietri et al., 2014).

3.5.4.2 Aerospace industry

Epoxy resins are mostly used in structural adhesive applications in aerospace because of their high adhesive properties and low cost. Combined with high-strength reinforcing fillers such as glass, carbon, boron, and Kevlar fibres are promising materials for use in the aerospace industry(Azeez et al., 2013; Kandare et al., 2013). However, epoxy composites can satisfy the mechanical requirements of structural materials for military, aviation and civil applications, for example, wings, ducts, flooring boards and vertical and horizontal stabilisers (Ayad et al., 2012; Liberata Guadagno et al., 2014b; Shamsuddoha et al., 2013).

3.5.4.3 Electrical Systems and Electronics Materials

Epoxy-based material is also used in electrical and electronic applications such as motors, transformers, bushings, insulators, switchgear, semiconductor encapsulants and printed circuit boards. Epoxy resins are outstanding electrical insulators and help prevent short-circuiting, dust, and moisture. Epoxy moulding compounds are widely used for semiconductor encapsulants to protect the integrated circuit products from humidity and hostile environmental situations, for example, temperature, radiation, moisture, physical and mechanical damage (Ho & Wang, 1996; Lin et al., 1997). For electronic packaging applications, various fillers are combined with epoxy matrices. The most commonly used fillers are fused silica, glass powder, and minerals (Suh et al., 2012; Teh et al., 2008).

3.5.4.4 Industrial tooling

Epoxy resins are also used for the manufacturing of industrial tools. Epoxy is widely applied to produce moulds, master models, castings, laminates, and other industrial manufacturing aids. There are many benefits of these epoxy-based tools; usually, they enhance the efficiency of the process. Recently, epoxy-based tools have replaced various materials such as metal, wood and other traditional materials by improving overall performance. As discussed in reference (Lin et al., 1997; Quang Dao et al., 2013; Shamsuddoha et al., 2013), fibre-reinforced epoxy composites have proven effective in repairing metallic components and tubular pipes.

3.6 Graphene-based polymer matrix nanocomposites

To increase the application scope of polymer composites, graphene nanofillers can be used to enhance the properties of the final nanocomposites. Even with relatively low loadings, graphene can give significant reinforcement to the final material (Papageorgiou et al., 2017). Therefore, graphene/polymer nanocomposites have a competitive advantage in applications requiring light-weighting, such as automotive and aerospace. The effectiveness of graphene as a nanofiller in various polymeric systems such as epoxy, polystyrene, polyaniline, polyurethane, poly(vinylidene fluoride), poly(ethylene terephthalate) has been reported in a detailed review (Kuilla et al., 2010). The nanosheet configuration includes layer number, lateral size, and defect, all of which significantly impact graphene properties (T. Ma et al., 2017) (Zandiatashbar et al., 2014). Figure 3.5 shows some potential applications of graphene/polymer nanocomposite materials.

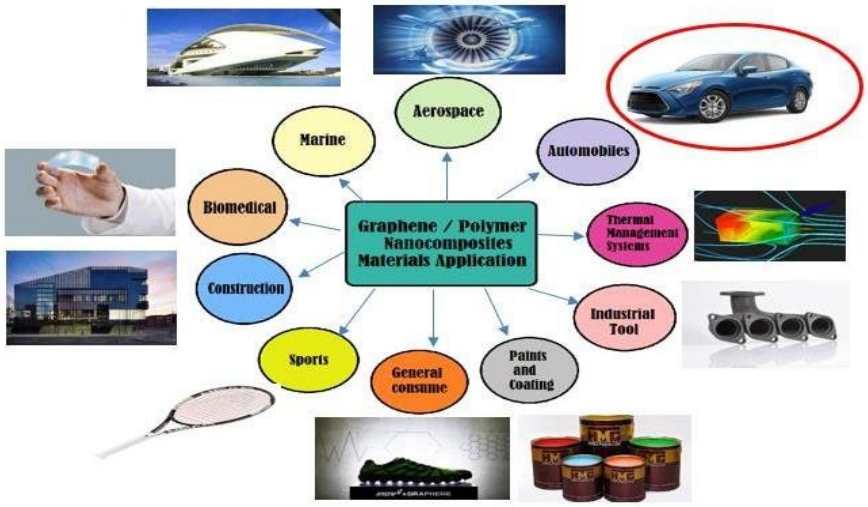

Figure 3. 7: Application of graphene/polymer nanocomposite materials.

3.7 Summary

Requirements for better fuel efficiency, weight reduction, environmental regulations, and customer needs force automotive manufacturing companies to develop new materials and structures or redesign existing ones. There are many factors involved in selecting automotive materials, such as cost, weight, safety, and recyclability/reuse.

Current trends for reducing vehicle weight include the use of low-density materials and multi-material lightweight design. Materials used in the automotive industry include steel, aluminium, magnesium, polymer composite materials, carbon fibre-reinforced polymers (CFRPs), and lightweight automotive composites. In addition to traditional materials, epoxy polymers are widely used for automotive, aerospace, adhesives, biomedical devices, construction and marine. Key applications for epoxy-based materials are adhesives, aerospace industry, electrical and electronics materials and industrial tooling. Furthermore, graphene structure for graphene derivatives as potential filler nanomaterials and graphene-based polymer matrix nanocomposites are useful for various day-to-day applications. Research methods formed for the GRM polymer nanocomposites are further discussed in the next chapter.

Chapter 4 Research methods

This chapter discusses the research methods, i.e., materials formulation techniques and characterisation techniques used in this thesis. The chapter presents mainly the methods, operating principles, and theory. The details of the particular experimental conditions used (e.g., processing time, materials concentration, etc.) will be reported in the following experimental chapters (chapters 5 and 6).

4. 1 Method of graphene production from graphite

There are various methods of graphene production from graphite. I will discuss a few solution-based processes, such as liquid-phase exfoliation (bath ultrasonication), high shear mixing and microfluidization.

4.1.1 Liquid-phase exfoliation

Liquid-phase exfoliation (LPE) is currently widely used by both the academic and industrial sectors as the primary method of producing two-dimensional (2D) materials like graphene in large quantities with a good balance between quality and cost. The shear forces produced by ultrasounds and their interaction with the solvent molecules have typically been assumed to be the exclusive causes of the fragmentation and exfoliation mechanisms involved (Li et al., 2020). There are three distinct steps in the transition from graphite flakes to graphene using ultrasonic LPE. First, sonication causes large flakes to break off and create kink band striations on their surfaces, generally in a zigzag direction. Second, cracks develop along these striations and, in conjunction with the intercalation of solvent, cause thin graphite strips to unzip and peel off, eventually exfoliating into graphene. The first reported LPE technique was based on sonication where stable few-layer graphene dispersions with concentrations as high as 0.01 mg/ml were obtained using 30 min bath sonication in *N*-methylpyrrolidone (NMP). The procedure relies on generating shock waves with ultrasound that are powerful enough to

rupture the van der Waals connections between the layers of graphite (Hernandez et al., 2008).

4.1.2 High Shear mixing

High-shear mixing of graphite is an economical solution processing method for making few-layer graphene dispersions. Shear forces are used in high-shear exfoliation to separate the graphene sheets. This method was initially developed by Chen et al. (Chen et al., 2012) by exfoliating graphite in a vortex fluidic system where the shearing resulted from the interaction of centrifugal and gravitational forces. The shear exfoliation technique was then demonstrated by Paton et al. using a laboratory mixer with a rotor-stator combination. They demonstrated the possibility for high-shear exfoliation to be applied on an industrial scale (Paton et al., 2014).

4.1.3 Microfluidization

Microfluidization is a homogenization process in which a fluid is subjected to high pressure (up to 207 MPa)(Panagiotou et al., 2008) and forced to flow through a microchannel with a Fixed geometry (diameter, $d < 100$ μm).

The main benefit over sonication and shear-mixing is that a high shear rate $\dot{\gamma} > 10^6 s^{-1}$ is applied to the entire fluid volume(Goldberg, 2008) not only locally. Exfoliation of graphite is made easy and scalable by using this method (Karagiannidis et al., 2017).

4.2 Production of rGOs (Solution Processing)

4.2.1 Preparation of GO

An aqueous suspension of graphite oxide (1.0 wt%) was prepared using a modified Hummers' method (Hummers & Offeman, 1958) as described in (Carosio et al., 2018). This dispersion was then ultrasonicated using a UP400S HIELCHER ultrasonicator equipped with an H22 sonotrode for 30min and freeze-dried to obtain GO powder.

4.2.2 Preparation of rGO

rGO was prepared from GO following a thermochemical reduction process (Gómez et al., 2017). Ascorbic acid (Vitamin C) was added into GO dispersion, and the mixture was refluxed

overnight at atmospheric pressure. The solid was filtered off and air-dried. Then the chemically reduced GO was heated in an oven under Ar atmosphere for 60 min at 200°C to obtain the thermochemically reduced rGO as a black solid with an apparent density of 0.002g/ml.

4.2.3 Preparation of GLYMO-rGO

50 g of rGO was suspended in one litre of ethanol/water (30/70 v/v) under stirring to homogenise the suspension. HCl 33%v/v was added dropwise until the pH was adjusted to 3.5. Then 50 mL of GLYMO was added and stirred at 60ºC for 24 h. A powder was collected by filtering and washed with water and ethanol 96% v/v to remove the unreacted silane molecules. The obtained powder was placed in an oven and dried at 80ºC for 24 h.

4.3 Materials fabrication techniques

Material fabrication techniques, including ultrasonication and wet lay/hand-up process, are discussed to explain the process.

4.3.1 Dispersion methods for GRMs/polymer matrix reinforcement

The dispersion of graphene and its derivatives into an epoxy polymer is a crucial step in the synthesis of nanocomposites. A good dispersion of the reinforcing agent ensures a maximum reinforced surface area, which will affect the polymer chains and consequently the properties of the whole matrix (Wei et al., 2015). There are several dispersion methods such as solution-based processing (Ultrasonication) (Kamal et al., 2021; S. Kim et al., 2009; Liang, Xu, et al., 2009; Ramanathan et al., 2007; Zaman et al., 2014; X. Zhao et al., 2010), melt-based processing (Kalaitzidou et al., 2007; Y. F. Zhao et al., 2007; W. Zheng et al., 2004) and in situ polymerization (Cassagneau & Fendler, 1998; D. Cho et al., 2005; X. S. Du et al., 2004; H. Kim, Miura, et al., 2010; Kulkarni et al., 2010; H. Li et al., 2011). Solution-based processing and melt-based processing are traditional methods. Recent reviews showed different preparation schemes for creating high-performing graphene-based composites (W. K. Chee et

al., 2015; Yan Li et al., 2019; Mittal, 2014; Papageorgiou et al., 2015, 2017). Solution mixing is most presumably the most extensively utilized technique for the preparation of low viscosity polymer nanocomposites at the laboratory level because of its flexibility with the utilization of different solvents and the opportunities for functionalization of the flakes alongside its speed and simplicity (Cheng et al., 2016; Lago et al., 2016; Vallés et al., 2016; H. Xu et al., 2016). Melt mixing is an industrial-friendly procedure for forming (mainly) thermoplastic-based nanocomposites since it is quick and economical. During melt blending, the polymer is heated over its melting/softening point, and afterwards, GRMs are included in the polymer melt (Bhawal et al., 2018; E. C. Cho et al., 2016; Liebscher et al., 2013; Y. Liu & Feng, 2017; Papageorgiou et al., 2016, 2018, 2019). In situ polymerization technique, intercalated monomers inside extended graphite clusters can advance their effective exfoliation into single sheets all through the polymer matrix brought about by catalysis reactions (H. Hu et al., 2010), which in this way prompts an expansion in the similarity between the components of the system and an improved interface (Luong et al., 2011; Milani et al., 2013; Xin Wang et al., 2011; Z. Xu & Gao, 2010). A significant downside of in situ polymerization procedure is the increase in viscosity with the advancement of the polymerization process which prevents manipulation and limits load fraction(An et al., 2010)(Verdejo et al., 2011). Furthermore, sometimes, the procedure is completed within the presence of solvents; hence the removal of the solvent is a critical issue correspondingly in solution-based processing (An et al., 2010).

The dispersion of nanoparticles is generally higher in solution and In situ polymerization procedures. Polymer particles gain enhanced mobility by thermal energy input and are mechanically mixed with fillers in melt mixing procedures (Jojibabu et al., 2020).

The most well-known dispersion process utilized for GRMs is sonication, in which vibrational energy is delivered to the flakes in order for them to escape from the constrained force around them (Seretis et al., 2018) (Shahdan et al., 2013). As explained in (R. S. Chen et al., 2019), It is

worth noting that the GNP layers are more winkled during sonication, and the ultimate Ultimate tensile strength of nanocomposites increases with the sonication time. Singh et al. (S. Singh et al., 2015) explored the mechanical properties of GNP/epoxy nanocomposite arranged to utilize a mechanical stirrer. The SEM micrographs tend to be reasoned that the mechanical stirrer was ineffective to disperse the GNP in the epoxy resin. GNP particles were agglomerated in the epoxy resin in this manner. This explains the powerless interfacial bonding among GNP and the matrix and simultaneously influences the composite's mechanical properties. Phua et al. (Phua et al., 2016) utilized the heat-assisted bath sonication strategy to enhance the dispersion of GNP in the epoxy matrix. From the SEM characterization, agglomeration is seen in high GNP loading, leading to the poor relationship between GNP and epoxy matrix, decreasing mechanical performance. The drawbacks of the solution-based method are that it is a time-consuming process due to the addition of the solvent, difficulty in solvent removal, and fundamental aggregation problems through mixing and solvent evaporation stages(Leroux & Besse, 2001; Stankovich, Piner, Chen, et al., 2006).

4.3.2 Ultrasonication Process

Bath Ultrasonication uses ultrasound waves (> 20 kHz) to create cavitation, i.e., bubbles grow and collapse in a liquid medium, generating significant shear forces. Bath ultrasonication is an effective tool to disperse particles in a solution or a low viscosity medium. The generated shear forces can accelerate the dissolution of solids in liquids. A strong vibration wave releases a large amount of energy into the cavitation field, thus disrupting molecular interactions, such as the interaction between water molecules. By applying ultrasonic waves to a solid-liquid mixture, the agglomeration of the nanoparticles can be removed, and homogenous dispersion of the nanoparticles can be achieved. In the sonication process, one has to consider the following essential parameters: power, frequency, time, the volume of resin container, viscosity and structure of the resin, temperature of the resin during sonication, the separation

between the tip (in probe sonication) and container and content of fillers are very important. During the ultrasonic process, cavitation is produced in the solution; bubbles quickly grow and collapse, producing shockwaves, breaking up the aggregates and separating the stacked graphene from each other (Si & Samulski, 2008)(Show et al., 2007). A standard method reported in the literature involves the dispersion of graphene in a suitable solvent for a period using an ultrasonic bath. Then the epoxy resin is added and sonicated for some time. Then the solvent is removed by evaporation (W. Li et al., 2013). In this research, both solvent-based and solvent-free approaches have been tested. Figure 4. 1 shows the Elmasonic P ultrasonication bath used in this study (University of Sunderland) for the sonication process.

Figure 4. 1: Elmasonic P ultrasonication bath used in this study (University of Sunderland) for the sonication process.

4.3.2.1 Comparison of Bath sonication with Tip sonication

There are two most popular sonication methods, i) bath sonication and ii) tip sonication. In the bath sonication method, the sample is placed in the ultrasonic bath in its own container, and the acoustic waves propagate from the water bath through the container and into the liquid dispersion/sample. The major benefit of this process is that the sample does not get

contaminated because it never comes into contact with anything during the sonication process. On the contrary, in the tip sonication method, the tip directly enters the sample to create ultrasonic waves. The benefit of this method is that high power can be directly delivered, but a drawback is that there may be contamination when the probe is moved between samples.

Furthermore, tip sonication cannot be easily scaled up to mass production (Moriche et al., 2015) (Zegeye et al., 2014) (Yuqi Li et al., 2013). In addition, the direct high power delivered in tip sonication may cause defects in GRMs. For these reasons, the bath sonication dispersion method was selected in this study (Montazeri & Chitsazzadeh, 2014) (Yu et al., 2012).

4.3.2.2 Wet lay/hand-up process

The hand lay-up method also called the wet lay-up method, is one of the most widely used methods in the composites industry. This is a straightforward method; each carbon-fibre layer can only be manipulated by hand and stacked layer by layer to achieve the required thickness (Elkington et al., 2015). Usually, this procedure is split into four steps: preparation of mould, gel coating, lay-up, and curing. First, the resin is manually impregnated between fibres, commonly done using rollers or brushes. Usually, a brush is used to distribute the resin on the fibres evenly, and a roller is used to remove air bubbles in the reinforcing material and ensure complete wetting (CRIPPS et al., 2000).

The hand roller is applied to roll the wet composite material to improve the interaction between the reinforcement and the matrix (Jamir et al., 2018). The wet lay-up process has several disadvantages, such as low production efficiency and slow speed production; because of the difference in workers' level and environmental conditions, it relies on the skills of the person who is executing the process. Figure 4. 2 represents the Lamination sheet of rGO/Carbon fibre/epoxy; prepared by the wet lay/hand-up process.

Figure 4. 2: Lamination sheet of rGO/Carbon fibre/epoxy; prepared by wet lay/hand-up process.

Preparation of Lap shear joints- Waterjet cutting

A waterjet cutting machine is the equipment used in the manufacturing industry to cut various materials using very high-pressure waterjets or a combination of water and abrasive substances. It is a non-thermal cutting method that uses only natural sand and water to cut almost any material. It is a quick and effective way to cut shapes out of materials that are impossible to cut by hand. The term abrasive jet refers to the use of water with abrasives to cut hard materials such as metal, glass, or stone, while pure waterjet cutting and pure water cutting refer to waterjet cutting without abrasives, which is typically used for softer materials such as wood or rubber. The waterjet cuts using a high-pressure jet of water mixed with a garnet abrasive at a pressure between 30,000 and 60,000psi. The cut accuracy tolerance is 0.3mm, the same as that of a rough sandblast finish. Tolerance "Waterjet Cutter NC" is a tool that cuts smooth and flat surface materials into random shapes using only one water stream (Index @ Www.Waterjetsweden.Co.Uk, n.d.). Figure 4. 3 represents the water Jet Cutting machine used in the present study (National Glass Centre, University of Sunderland).

Figure 4. 3: The water Jet Cutting machine used in the present study (National Glass Centre, University of Sunderland).

Waterjet cutter program

The machine works with IGEMS software to program AutoCAD (2000) files saved as .dwg and Adobe Illustrator files saved as .dxf. Could program directly on 3D models, visualise every toolpath, simulate with crash control, and nest your parts in this section of IGEMS CAD. Simply put, it's a 3D environment with automatic and customised CAM capabilities for as many axes as you require. For example, with the help of a software program, we can cut lap shear joint specimen sheets for bonding in a short time compared to cutting specimens individually, as indicated in figure 4. 4.

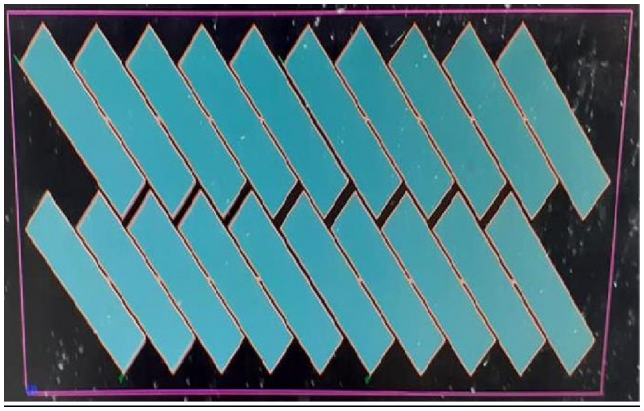

Figure 4. 4: Multiple lap shear joint specimens cut the design using a software program.

Key Benefits to Cutting Composites with Waterjet cutter

There are many advantages of using a waterjet cutter for cutting composite materials: no delamination, whiskers or fibre pulls during cutting, higher efficiency, quick cutting, raw material savings (decreased waste) with sharp cutting, and no thermal damage. In addition, the finely focused waterjet beam can cut reliably and accurately with incredible detail in any direction.

4.4 Characterisation Techniques

In this research, the following techniques were used to characterise the mechanical and thermal properties of the developed nanocomposites: Differential Scanning Calorimetry (DSC), Scanning Electron Microscopy (SEM), Thermogravimetric analysis (TGA), Tensile test, Hardness through Nanoindentation and Lap shear joint test.

4.4.1 Differential Scanning Calorimetry (DSC)

In a controlled environment, DSC measures the temperatures and heat flow associated with material transitions as a function of time or temperature. This technique offers qualitative and quantitative data on physical and chemical changes involving endothermic and exothermic processes (Thomas, 2010). With DSC, the energy absorbed or released by a sample is measured as heated or cooled. DSC generally has two sample pans, one for the sample under analysis and the other for reference. Figure 4. 5 shows a cross-section of a typical DSC sample holder. A small quantity of uncured sample (~10 mg) is placed into an aluminium pan and then covered with a lid. Then the sample pan is positioned on top of a single chrome alloy heating plate. The same empty aluminium pan is placed on the second chrome alloy heating pan as a reference for the experiment. The sample pan and the reference pan are each given their own amount of energy to match the heating rate of a predetermined temperature profile. As a result, the rate at which energy is delivered to the sample to heat it at a controlled rate is

proportional to its specific heat (Epoxy & Solutions, 2012).

The DSC method has been used to analyse the cure kinetics of various thermosetting resins (Um et al., 2002)(Karkanas, 1996)(Sourour & Kamal, 1976) (Sichina, 2000) (Abenojar et al., 2018). DSC can provide useful information such as the maximum rate of cure, the heat of cure, the onset and the completion of cure, and the degree of cure and glass transition temperature (T_g) of the sample under investigation.

The study of cure kinetics of resin systems is performed by dynamic measurements (temperature ramp) and isothermal measurements (with elapsing time at constant temperature). A thermoset resin cure is an exothermic reaction. As a result, the degree of cure can be evaluated by measuring the exothermic heat generation during cure and comparing it to the overall heat output of the reaction. In DSC analysis, the degree of cure (α) ranges from 0 to 1, with 0 representing a completely uncured sample and 1 showing a complete cured sample. In this research, DSC will be used to study the curing kinetics of epoxies and nanocomposites.

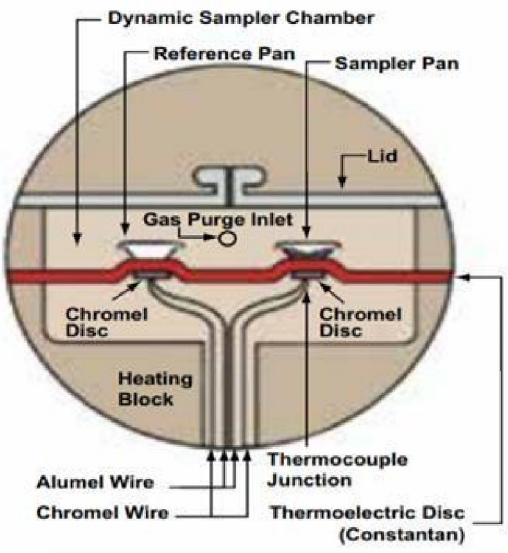

Figure 4. 5: Standard DSC Cell (Epoxy & Solutions, 2012).

If the material maintains the same physical state, the material's specific heat will only change slightly with temperature. However, when the heat distribution provided to the material causes the material to shift to a new state (for example, decomposition, melting, curing, etc.), the specific heat will change significantly. The energy that must be given to the sample to maintain the desired heating or cooling profile will change due to the immediate change in specific heat during the transition. The state change that absorbs energy is called endothermic change. Melting is an example of a change in the endothermic state.

Conversely, the state change that releases energy is the exothermic transition. The heat of curing (crosslinking) reaction and crystallisation are examples of exothermic transitions. Typical DSC transitions are shown in figure 4. 6 (Epoxy & Solutions, 2012).

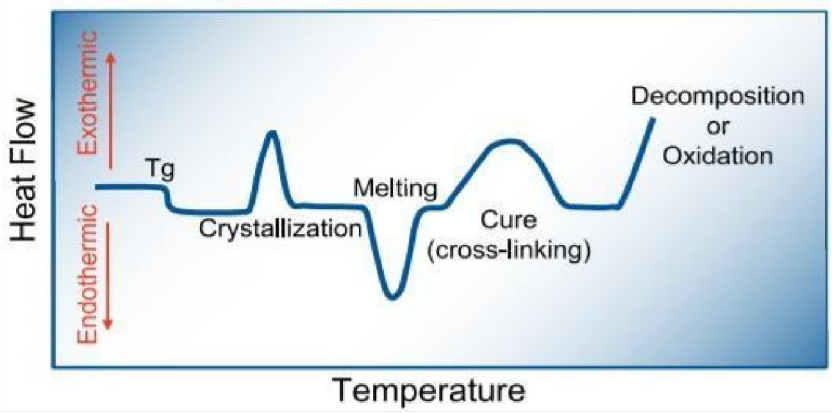

Figure 4. 6: Typical DSC transitions (Epoxy & Solutions, 2012).

This research investigated the curing kinetics of GRMs/polymer nanocomposite composites using DSC. DSC was also used to assess how long a material must be cured at a specific temperature to achieve the maximal degree of conversion at that temperature. This is achieved by measuring the exotherm curing peak of a material exposed to a constant temperature over time (isothermal scan). The neat epoxy system and nanocomposites DSC study was carried out using a Differential Scanning Calorimeter DSC Q10 from TA Instruments.

4.4.1.1 Cure Kinetic models

The curing process of a thermosetting resin is critical for the properties of the final composite. The study of cure kinetics provides the researcher, engineer, or procedure control manager with essential data that can be utilised to optimise processing conditions that affect the degree of cure and crosslinking density which determines properties. Kinetics refers to modelling the impacts of temperature and time upon completing the cure of a thermosetting resin. Kinetic parameters were dictated by fitting the information obtained from DSC to the kinetic model to additionally research the curing behaviours (Lv et al., 2020). Manufacturers give the information about the cure cycle; however, it is not essential to tail it precisely because it can be different because of different components and mould geometry. Thus, it is critical to contemplate the cure kinetics of the resin. There are different methods have been established to calculate the activation energy and pre-exponential factor of the sample.

The Kissinger method was used to calculate the activation energy in this research. Reactions require energy input to begin, referred to as activation energy (E_a). Activation energy is the amount of energy required to reach the transition state. The source of the activation energy needed to push reactions forward is typically heat energy from the surroundings. At the same time, a Model-Free Isoconversional method, the Ozawa-Flynn-Wall model, was used to calculate the pre-exponential factor and activation energy as a function of the degree of cure since these changes throughout the curing reactions.

4.4.1.2 Kissinger method

The Kissinger technique is a widely used approach for calculating the activation energy of thermally stimulated processes examined using differential scanning calorimetry (DSC). The lowest amount of energy required to activate the reactant molecules to a state where they can conduct the chemical transformation is known as the activation energy of a chemical reaction.

Kissinger (Kissinger, 1956) devised a method for estimating the activation energy of physical or chemical processes based on data from multiple nonisothermal tests carried out at constant heating rates (constant during each test, different among tests). The Kissinger technique is a quick and easy way to calculate mean activation energies, which is important in comparison studies, particularly those at constant heating rates with a known peak temperature. An examination of Kissinger plots can reveal the activation energy's temperature dependency and allow for the computation of local activation energy values at various stages of the process. In this way, it may be a less complicated alternative to complex isoconversional kinetic analysis based on the degree of phase transformation, at least for preliminary screening. The activation energy of isoconversional procedures is temperature dependent.

4.4.1.3 Model-Free Isoconversional Method: Ozawa-Flynn-Wall Analysis

Ozawa-Flynn-Wall's analysis makes a model-free evaluation of the activation energy from a series of nonisothermal measurements at different heating rates. The Flynn–Wall–Ozawa method is a straightforward method for determining the value of activation energy from a weight loss versus temperature curve at various heating rates (Pal & Katiyar, 2017). For all values of the degree of conversion α, the crucial assumption in this model is that the conversion function f(α) is independent of the change in heating rate. It follows the Arrhenius type of temperature dependence without making any assumptions about the kinetic equation's structure.

4.4.1.4 Curing mechanism and kinetics

The generally accepted mechanism scheme of the epoxy/primary amine cure involves three main addition reactions of epoxide as shown in Figure 4. 7 (Prime, 1997):

Primary amine reaction

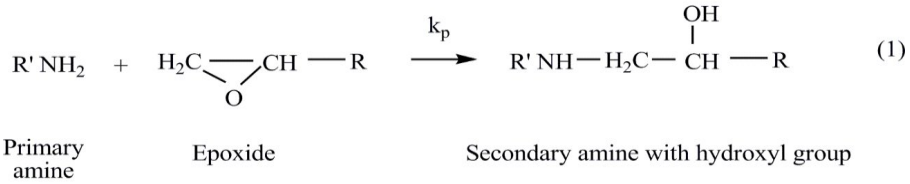

(1)

Primary amine | Epoxide | Secondary amine with hydroxyl group

Secondary amine reaction

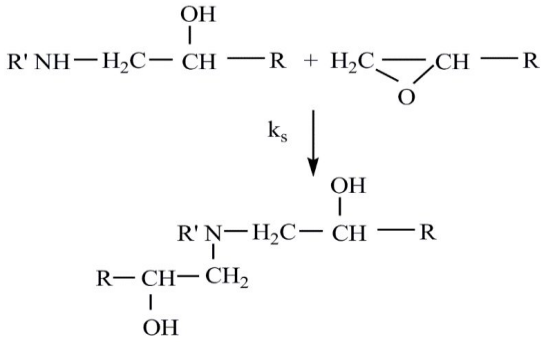

(2)

Tertiary amine with hydroxyl groups

Etherification reaction

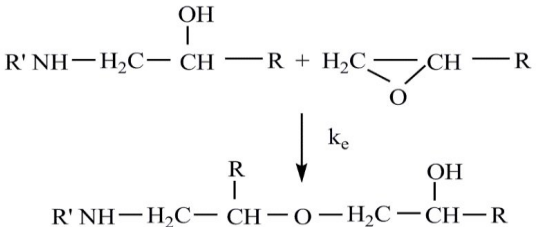

(3)

Figure 4. 7: Reactions may occur during the curing of an epoxide with a primary amine (Prime, 1997).

For 1:1 epoxy/amine stoichiometry or when the amine is present in excess, reaction (3) is generally insignificant to reactions (1) and (2). In most systems, the primary and secondary amines have similar reactivities, and one DSC cure exotherm is observed (Prime,1997) as in the system studied in this work. The kinetic model commonly employed for the epoxy/amine reactions (1) and (2) was originally derived by Smith (I. T. Smith, 1961). The corresponding reaction scheme (Eqs. (4)-(6)) is very simple if the following two assumptions are fulfilled: possible differences in the reactivity of primary and secondary amine can be neglected, and intentionally added catalytic species and/or catalytic impurities are missing.

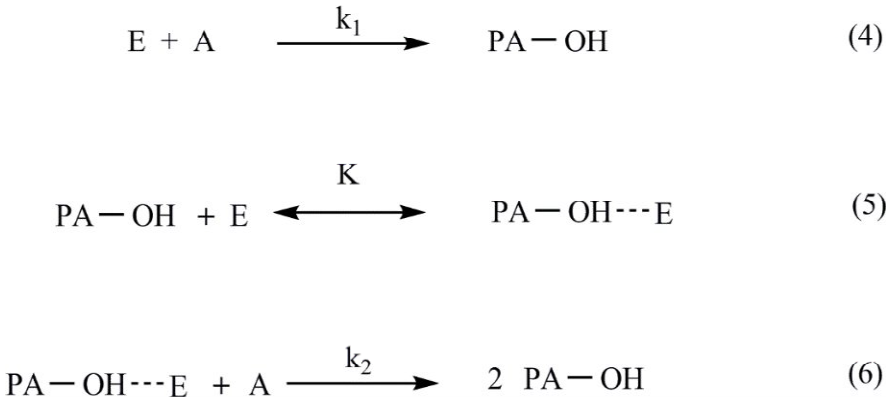

Figure 4. 8: Simplified kinetic model proposed by Smith (I. T. Smith, 1961) for the epoxy/amine reactions (1) and (2).

Where E, A and PA-OH are the epoxides, the amine and the reaction product are characterised as polyadduct containing hydroxyl groups, respectively. At the very beginning of the process, the non-catalysed reaction occurs (4) (primary amine reaction, Figure 4. 8). The formed polyadduct contains hydroxyl groups which form hydrogen bonds with the oxygen atom of epoxide (equilibrium reaction 5), facilitating the ring-opening and reaction with amine (Vyazovkin & Sbirrazzuoli, 1996). The rate-determining step is the autocatalysed reaction (6) (Flammersheim, 1998).

Kinetics deals with the measurement and parameterisation of the process rates. DSC is a widely used experimental technique to obtain a thorough understanding of the curing process. In the kinetic analysis by DSC, the rate of reaction is assumed to be proportional to the rate of heat generation and can be expressed as:

$$\frac{da}{dt} = \frac{1}{\Delta H_{total}}\left(\frac{dH}{dt}\right) \qquad (7)$$

Where α is the degree of cure, $d\alpha/dt$ is the rate of reaction, dH/dt the heat flow and ΔH_{total} is the exothermic heat expressed as heat per mole of reacting groups (kJ mol^{-1}). The degree of curing α at any time t is given by

$$a(t) = \frac{\Delta H(t)}{\Delta H_{total}} \qquad (8)$$

Where $\Delta H(t)$ is the heat generated up to time t. The ultimate degree of conversion is defined as

$$a_{ult} = \frac{\Delta H_{ult}}{\Delta H_{total}} \qquad (9)$$

The vast majority of kinetic methods used in the area of thermal analysis consider the rate to be a function of only two variables, α and the absolute temperature T.

$$\frac{d\alpha}{dt} = k(T)f(a) \qquad (10)$$

Where $d\alpha/dt$ is the rate of reaction, $k(T)$ is the temperature-dependent rate constant, and $f(\alpha)$ is the degree of conversion dependent reaction model.

Equation 10 describes the rate of a single-step process. It is worthy to note that if a process is found to obey a single-step equation, it does not mean that the process mechanism is made up of only one stage. The mechanism is most likely made up of numerous phases, but one of them

determines the overall kinetics. For example, this would be the case of two consecutive reactions, e.g. the first reaction is significantly slower than the second. Then the first reaction would determine the overall kinetics that would obey a single-step Eq. (10), whereas the mechanism involves two steps (Vyazovkin et al., 2011b).

The temperature dependence of the reaction rate is generally defined through an Arrhenius expression:

$$k(T) = Ae^{(-\frac{E_a}{RT})} \qquad (11)$$

Where A and E_α are kinetic parameters, the preexponential factor and the activation energy respectively, R is the universal gas constant and T.

Combining Eq. (10) and (11) yields:

$$\frac{d\alpha}{dt} = A\, e^{\left(-\frac{E_a}{RT}\right)} f(a) \qquad (12)$$

This equation applies to any temperature program, isothermal or nonisothermal.

For constant heating rate φ, and nonisothermal conditions, Eq. 12 is frequently rearranged:

$$\varphi \frac{da}{dT} = A\, e^{\left(-\frac{E_a}{RT}\right)} f(a) \qquad (13)$$

Among various multiple heating rate methods used for determining the curing kinetic parameters (E_α and A), the most extensively used method is that of Kissinger (Kissinger, 1957), because of its ease of use, in which both E_α and A are assumed to be constant (Vyazovkin et al., 2011b).

The basic equation of the method has been derived from eq. (12) under the condition of the maximum reaction rate. At this point, $d^2\alpha/dt^2$ is zero:

$$\frac{d^2a}{dt^2} = \left[\frac{E_a\varphi}{RT_p^2} + A\, f'(a_m)\, e^{\left(-\frac{E_a}{RT_p}\right)}\right]\left(\frac{da}{dt}\right)_m = 0 \qquad (14)$$

Where $f'(\alpha_m) = df(\alpha)/d\alpha$ and the subscript m denotes the values related to the rate maximum. It follows from Eq. (14) that:

$$\frac{E_a\,\varphi}{R\,T_p^2} = -A\, f'(a_m)\, e^{\left(-\frac{E_a}{RT_p}\right)} \qquad (15)$$

After simple rearrangements (Eq. 15) is transformed into the Kissinger equation:

$$ln\left(\frac{\varphi}{T_p^2}\right) = ln\left[\left(-\frac{AR}{E_a}\right) f'(a_m)\right] - \frac{E_a}{RT_p} \qquad (16)$$

Where T_p is the peak temperature. By plotting $ln(\varphi/T_p^2)$ versus $1/T_p$, the values of ' =and A can be estimated by calculating the slope of the linear fit and the y-intercept.

It is worth to note that one limitation of the method is associated with the fact that the determination of an accurate ' =value requires $f'(\alpha_m)$ to be independent of φ. Otherwise, the first term on the right-hand side of equation (16) would not be constant, and the plot of $ln(\varphi/T_p^2)$ versus $1/T_p$ would deviate systematically from a straight line, producing a systematic error in ' =(Vyazovkin et al., 2011b).

4.4.2 Thermogravimetric analysis (TGA)

Thermogravimetric analysis (TGA) is broadly used to research the thermal degradation of polymeric composites when the composite specimen is exposed to high thermal loads (Monteiro et al., 2012). The thermal stability of a material depicts its capacity to oppose mechanical deformation at higher temperatures (S. S. Chee et al., 2019). Figure 4. 9 illustrates

a TGA system used in this study (University of Sunderland and Schematic (Mohomed, 2016).

Thermal analysis is essential to many industries, including polymers, composites, pharmaceuticals, nourishments, petroleum, inorganic and organic chemicals, and numerous others. TGA is a methodology of thermal investigation where the mass of a sample is evaluated as a function of temperature or time changes in an environment of nitrogen, helium, air, other gas, or in a vacuum. Estimations are utilised principally to decide the composition of materials and to anticipate their thermal stability at temperatures up to 1200° C. The method can describe materials that display weight reduction or addition because of decomposition, oxidation, or dehydration. Inorganic materials, metals, polymers and plastics, composites, ceramics and glasses materials can be analyzed using this procedure. This estimation gives data about physical phenomena, such as phase transitions, absorption, and chemical phenomena, including thermal decomposition and solid-gas reactions (e.g., oxidation or reduction)(Coats & Redfern, 1963). TGA measurements give significant knowledge that can be applied to choose materials for specific end-use applications, predict product performance, and enhance product quality. TGA can be used to estimate the thermal stability of a material, oxidative stability of materials, the composition of multicomponent frameworks, filler content of materials, Estimated lifetime of a product and decomposition kinetics of materials (W.J. Sichina, 2011).

The TGA equipment is usually loaded with a sample mass in the range of (~2–20mg), contingent upon the density of the sample, the sample pan size, and the motivation behind the examination. Concerning the physical properties of the sample, these can influence the TG curves. For example, on account of an exothermic response, higher mass stacking may prompt higher onset temperature due to the higher heat discharged by the sample, which includes an abrupt local temperature increment (de Blasio, 2019).

Figure 4. 9: TGA system that was used in this study (University of Sunderland and Schematic (Mohomed, 2016).

This research will investigate the effects of different GRMs/polymer nanocomposites material on thermal stability. Curing takes place in controlled environment conditions (N_2 or air) at low temperatures (e.g. 150°C). A second temperature ramp-up to 1000°C determines the thermal stability of the materials. The thermal stability of nanocomposites has been investigated by thermogravimetric analysis using a TGA55 thermogravimetric analyser by TA Instruments.

4.4.3 Scanning Electron Microscopy (SEM)

Scanning electron microscopy (SEM) has become an incredible and adaptable tool for material characterisation, particularly nanoscale. SEM instruments use electrons for imaging; along these lines, light magnifying instruments utilise noticeable light. SEMs utilise a particular arrangement of coils to scan the beam in a raster-like pattern and utilise the electrons reflected or knocked off the close surface region of a sample to form an image. Since the wavelength of electrons is a lot littler than the wavelength of light, the goals of SEMs are better than that of a light microscope. Scanning electron microscopy can provide a range of imaging procedures

with resolutions in the range of 1µm to 1nm, depending on the microscope and the signal used to form the image (Henini, 2000). The SEM utilises a focussed beam of electrons, with energies regularly ranging from a few hundred eV to about 30 keV, which is raster across the surface of a sample in a rectangular scan pattern (Joy, 2003). In this research, SEM will be utilised to investigate the quality of dispersion of GRMs in the resins and identify correlations with their mechanical properties. Figure 4. 10 shows an illustration of an SEM system that was used in this study (University of Sunderland).

Figure 4. 10: SEM microscope that was used in this study (University of Sunderland).

4.4.4 Mechanical Properties

4.4.4.1 Tensile Test

The tensile test is one of the easiest and most extensively used mechanical tests. During the test, a test specimen is subjected to a controlled expanding elongation until failure. The properties that are precisely measured are the tensile stress and deformation (change in length). More specifically, Young's modulus and yield strength (yield point) and ultimate Ultimate tensile strength can be determined from these measurements. In addition, the results can be applied for quality control of materials for different purposes. The tensile tests were performed according to ASTM D638; dumbbell-shaped specimens were obtained 32mm long and 4mm thick for tensile measurements. Tensile tests were accomplished using a universal testing

machine Zwick Roell Z010 with a load cell of 10 kN at room temperature and a 5mm/min crosshead speed. The achieved results were processed with one-way ANOVA parametric analysis using a Tukey's range test. Figure 4. 11 shows the Zwick system, which was used for mechanical testing (University of Sunderland).

Figure 4. 11: Zwick system that was used in this study (University of Sunderland) for mechanical testing.

4.4.4.2 Hardness test

Hardness testing applies a consistent load through adjusted or pointed object-controlled conditions to form an indentation on a metal surface. This can be at that point measured to decide the hardness of the material. Hardness influences many physical characteristics, identifying the hardness of sample relationship between the total indentation load and displacement or area. Mainly, various hardness tests are used, such as Rockwell, Brinell, and Vickers.

4.4.4.3 Nanoindentation

The indentation test is a straightforward and efficient method to evaluate the mechanical properties of materials, for example, modulus and hardness of materials in various shapes, sizes, and scales, and it has been widely used in the latest century. Indentation technology assesses the material's mechanical properties by inserting an indenter into the surface of the material and then imaging the impression. Indentation hardness is widely used for material strength, and the Berkovich tip is one of them, which is a nanoindenter tip utilised for testing the indentation hardness of a material. Berkovich tip is unique in its shape with a three-sided pyramid and geometrically self-comparable. As it is three-sided, it is simpler to grind these tips to a sharp point as it is more promptly utilised for nanoindentation tests. Then the hardness of the examined material can be concluded based on the relationship between the total indentation load and the displacement or area (Haidou Wang et al., 2018). Hardness and E for all samples were obtained by instrumented indentation. For this purpose, nanoindentation measurements were performed with a Micromaterials NanoTest Vantage platform 3 using a diamond Berkovich indenter.

The samples were securely clamped to the nanoindenter, and a total of 100 indentations per sample were performed applying a maximum load of 10mN with an initial load of 0.1mN, a load time of 10 seconds, a dwell period of 20 seconds and an unloading time of 5 seconds. The indentations were performed using a 10 by 10 grid matrix with 100μm spacing between each indentation. All the tests were performed at a constant room temperature of 21ºC. The inbuilt NanoTest Vantage algorithms were used to calculate hardness. The elastic modulus was obtained using the following equation:

$$E = \frac{1 - {v_s}^2}{\frac{1}{E_r} - \frac{1 - {v_i}^2}{E_i}}$$

Where E is the Young's Modulus of the sample, v_s and v_i are the Poisson's ratios of the sample and the Berkovich indenter, E_i is the elastic modulus of the indenter and E_r is the reduced modulus of the sample after indentation. The obtained results were processed with one-way ANOVA parametric analysis using a Tukey's range test. Berkovich's Indentation process is shown in figure 4. 12.

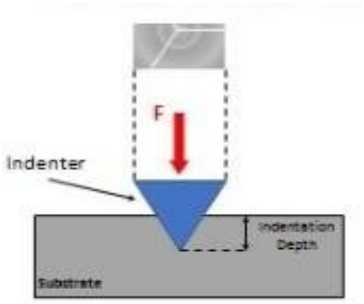

Figure 4. 12: Berkovich Indentation process.

4.4.5 Lap Shear Test

The lap shear strength test is usually executed because of its simplicity when a new adhesive is investigated in terms of its bond strength. Lap shear tests were conducted according to ASTM D5868. This test can determine the shear strength of the lap joint and check the failure mode; this allows the type of failure to be determined, adhesive or cohesive failure or adherent failure. The single-lap shear test contains two rectangular adherents, usually 25.4mm in width, 101mm long, and 1.5 to 2.0mm thick, bonded together, and the overlap length ranges from 12.7 to 25mm. The average shear stress decreases as the overlap length increases (Lucić et al., 2006). Figure 4. 13 represents a top view of the shear lap joint test showing adherents made of carbon fibre laminates with an overlapping bonding area of 25.4mm * 12.7mm.

$$\tau = \frac{P}{bl}$$

Where τ is ultimate shear strength, applied load (P), joint width (b) and overlap length (l) (L.F. M. da Silva et al., 2009).

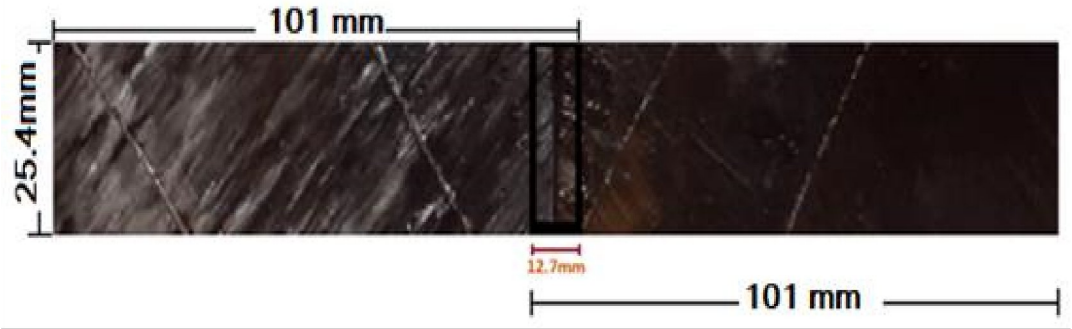

Figure 4. 13: The lap shear joint test's top view shows adherents made of carbon fibre laminates with an overlapping bonding area of 25.4mm * 12.7mm.

Failure mode of Adhesives bonding

There are three main types of bond failure: adhesive, cohesive, and substrate failure.

Adhesive failure

Adhesive failure is an interfacial bond failure between the adhesive and the adherend (Renart et al., 2015). This frequently indicates a lack of surface preparation or the presence of contaminants on the adherend surface.

Cohesive failure

A layer of adhesive remains on both surfaces when a fracture occurs, resulting in cohesive failure. Cohesive failure of the substrate occurs when the adherend fails before the adhesive. (Ebnesajjad & Landrock, 2015).

Substrate failure

The substrate is weaker than the forces transferred to it by adhesive and cohesive bonds. As a result, the material breaks apart, and the substrate is separated into pieces.

4.5 Summary

In this chapter, research methods used for this research are discussed where material fabrication techniques, including ultrasonication and wet lay/hand-up processes, are used. To characterise thermal and mechanical properties, characterisation techniques including differential scanning calorimetry (DSC), Scanning Electron Microscopy (SEM), Thermogravimetric analysis (TGA), Tensile test, Hardness through Nanoindentation and Shear Lap joint test are discussed in detail. Furthermore, failure modes of adhesive bonding, including adhesive failure and substrate failure, are provided. Effects of graphene nanoplatelets on cure kinetics, thermal and mechanical properties of graphene/Epilok 60-566 epoxy polymer nanocomposites are further discussed in chapter 5.

Chapter 5 Effects of graphene nanoplatelets on cure kinetics, thermal and mechanical properties of graphene/Epilok 60-566 epoxy polymer nanocomposites

In this work, novel nanocomposites with an epoxy/amine (Epilok 60-566/Curamine 32-494) reinforced with GNPs were prepared and studied; i.e. their cure kinetics, thermal stability and mechanical properties. The GRMs contain a low oxygen content that aided dispersion into the low viscosity liquid Curamine without using a solvent. The cure kinetics of the neat epoxy/Curamine system (100/30 w/w excess of amine) and the GRM/epoxy/Curamine system (1.5%wt of GRM) are studied by Differential Scanning Calorimetry (DSC) under non-isothermal conditions at different heating rates (2, 5, 10 and 20°C/min) and under isothermal conditions (50, 70 and 90°C). In addition, the mechanical properties *E* and *UTS* of the neat resin and nanocomposites (0-1wt% GRM) are determined.

5.1 Materials

GNPs Elicarb® were provided by Thomas Swan, UK. According to the manufacturer, the GNPs have a lateral size between 0.5-5μm, thickness in the range of 10-60nm and contain a non-ionic surfactant. Epilok 60-566 resin was provided by Bitrez, UK. This is a specially formulated liquid mixture of epoxy oligomers with low viscosity and intended to be used for the resin infusion process (0.7 Pa·s at 25°C) and contains a) oligo (bisphenol-A-co-epichlorydrin) (CAS number: 25068-38-6 and EC number: 500-033-5) with a number average molecular weight <700 (corresponding to n=0 or 1, Figure 5. 1a) in an amount 30-60%w/w; b) oligo[(phenyl glycidyl ether)-co-formaldehyde]) (CAS number: 28064-14-4 and EC number: 608-164-0) with a number average molecular weight about 345 (corresponding to n=0 or 1, Figure 5. 1b) in an amount 10-30%w/w; c) 1,6 hexane diol diglycidyl ether (CAS number: 16096-31-4 and EC number: 240-260-4) (Figure 5. 1c) in an amount 10-30%w/w. This epoxy

has good crystallization resistance, functionality and mechanical performance, and “post cured” systems offer excellent service. Epoxy resin has a wide range of applications, including composites, adhesives, structural, coatings, civil engineering and electronic. Curamine 32-494 curing agent (or hardener) was provided by Bitrez, UK. This is a specially formulated liquid amine-based curing agent that is low in viscosity (0.1 Pa·s at 25°C) and has moderate reactivity. This is 4,4’-methylenebis(cyclohexylamine) (Figure 5. 1d) (CAS number: 1761-71-3 and EC number: 217-168-8) (60-100%) MW=210.36284. The epoxide equivalent weight (EEW), defined as the grams of Epilok 60-566 containing 1gmol of epoxy groups, is reported by Bitrez to be minimum=170 g/eq and maximum 190 g/eq (average EEW=180 g/eq). The Curamine 32-494 amine hydrogen equivalent weight (AHEW) was calculated by using the following equation: AHEW=molecular weight of the amine/number of active amine hydrogens. The 4,4’-methylenebis(cyclohexylamine) with a molar mass 210.36284 g/mol contains four active amine hydrogen atoms and acts theoretically as a tetramine. Thus, the AHEW of the Curamine is equal to 210.36284/4= 52.5921 g/eq. Since it is assumed that one amine hydrogen reacts with one epoxy group, the stoichiometric ratio of Curamine to use with the Epilok is given by the ratio: AHEWx100/EEW of Epilok or 52.5921x100/180=29.22 phr (phr =parts by weight of Curamine per 100 parts by weight of Epilok). The supplier (Bitrez) of the system Epilok 60-566/ Curamine 32-494 recommends the use of phr=30, and this was used in the present work, which corresponds to the 1:1 stoichiometric ratio of curing agent to the available epoxy groups. Meguiars M-08 Maximum Mold Release Wax’’Mirror glaze" was obtained from East Coast Fibreglass Supplies, UK. It is specially formulated to provide the maximum number of releases and is especially useful for tooling and new moulds.

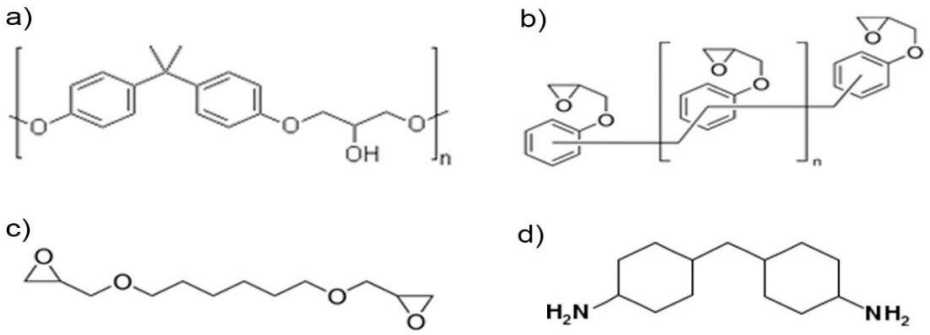

Figure 5. 1 (a-c) Chemical structure of epoxy compounds contained in Epilok resin 60-566: a) Oligo(bisphenol-A-co-epichlorohydrin) n=0 or 1, b) Oligo[(phenyl glycidyl ether)-co-formaldehyde] n=0 or 1, c) 1,6 Hexane diol diglycidyl ether. (d) chemical structure of 4,4'-methylenebis(cyclohexylamine) contained in curing agent Curamine 32-494.

Preparation of Nanocomposites

GNPs were first mixed with the Curamine using a bath ultrasonicator (Elmasonic P300) for 20 min. In the following ultrasonication, the epoxy resin was added via hand mixing for 3 min at a ratio Epilok: Curamine of 100:30. Samples were prepared for DSC, TGA, mechanical and nanomechanical testing. The methodology followed is summarised in Figure 5. 2.

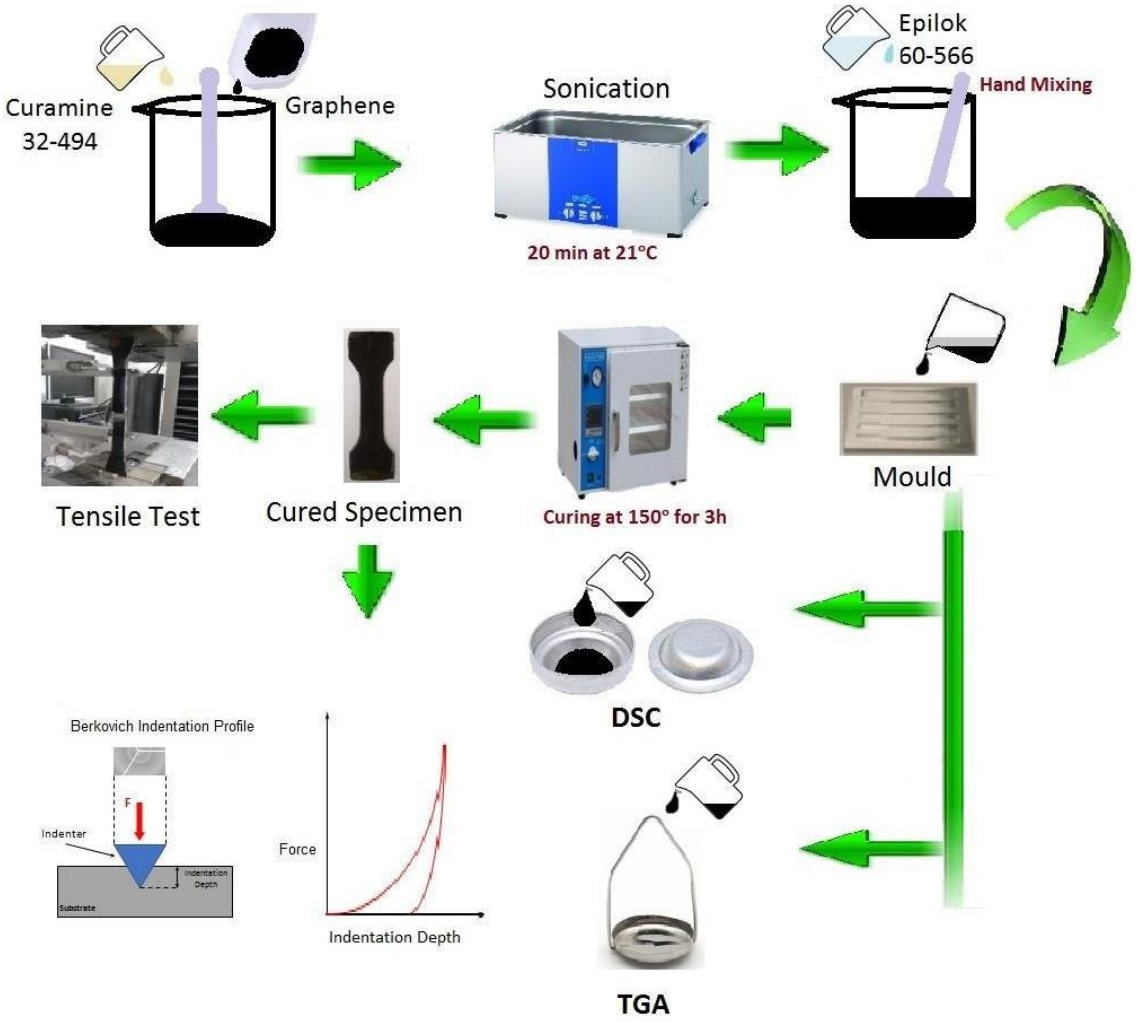

Figure 5. 2: Methodology followed for the preparation of GNPs/epoxy nanocomposites and their characterisation by DSC, TGA and mechanical testing.

5.2 Curing kinetics by DSC measurements

The DSC study of the neat epoxy system and nanocomposites was carried out using a Differential Scanning Calorimeter DSC Q10 from TA Instruments. The content of GNPs in these samples was 0.5 or 1.5%wt. About 10-15mg samples were weighed and sealed into aluminium hermetic DSC pans. The sample pan was then put in the DSC cell previously maintained at room temperature. All DSC runs were carried out under an N_2 atmosphere.

Non-isothermal scans were recorded from 20 to 300°C with four different heating rates of 2,5,

10 or 20°C/min. Isothermal scans were recorded at 50, 70 or 90°C. The DSC cell was quickly heated (50°C/min) to the desired cure temperature and then isothermally held at that temperature for 3h. Following this isothermal scan, the DSC cell was immediately cooled down to room temperature and then heated to 300°C at 10°C/min to obtain the residual heat of curing. This was determined by integrating over the exothermic peak with respect to time. The total heat of curing recorded isothermally (ΔH_{iso}) and the residual heat of curing recorded dynamically (ΔH_{dyn}) were used to determine the degree of curing (α) at various isothermal cure temperatures.

5.3 Thermal stability study by TGA

The thermal stability of the prepared nanocomposites was investigated by thermogravimetric analysis using a TGA55 thermogravimetric analyser by TA Instruments. Measurements were carried out from 20°C to 800°C, at a heating rate of 10°C/min under N_2 atmosphere.

5.4 Mechanical characterisation

Specimens were prepared for tensile tests (~15g/per sample) with GNPs content 0.3, 0.5, 0.7 or 1%wt. After adding Epilok resin into graphene/Curamine mixture, mechanical stirring was applied. Aluminium moulds were prepared using a CNC milling machine. Applied mirror glaze mould releases wax inside the mould. The final mixture was poured into the moulds and cured for 3h at 150°C (Figure 5. 2). Dumbbell-shaped specimens were obtained 32mm long and 4mm thick for tensile measurements. Tensile tests were performed using a universal testing machine Zwick Roell Z010 with a load cell of 10 kN at room temperature and a 5mm/min crosshead speed. Hardness and *E* for all samples were obtained by instrumented indentation. For this purpose, nanoindentation measurements were performed using a diamond Berkovich indenter with a Micromaterials NanoTest Vantage platform 3. The samples were securely clamped to the nanoindenter, and a total of 100 indentations, per sample, were performed

applying a maximum load of 10mN with an initial load of 0.1mN, a load time of 10s, a dwell period of the 20s and an unloading time of 5s. The indentations were performed using a 10 by 10 grid matrix with 100μm spacing between each indentation. All the tests were performed at room temperature.

5.5 SEM Characterisation

The dispersion of nanofiller in the epoxy resin using SEM (Hitachi S3000-N) manufactured by Hitachi High Technologies, Japan. Samples were submerged in a 1L Dewar filled with liquid nitrogen and left until bubbling had stopped. The sample was removed from the liquid nitrogen, placed on the edge of a bench and hit with a hammer. This shattered the sample revealing a fractured surface to be imaged. The sample was then mounted on an aluminium SEM Specimen Stub, using carbon adhesive discs (stubs and carbon adhesives were purchased from Agar Scientific, UK). The samples were then placed into a Quorum SC7620 Mini Sputter Coater with a gold/palladium target for coating. The process was carried out for 105seconds at 18-20mA. Giving us a coating of around 8nm.

5.6 Results and discussion

5.6.1 Dispersion of GNPs into Epilok /Curamine

This research initially identified the optimum dispersion of GNPs into Epilok /Curamine. GNPs were first attempted to be dispersed into epilok 60-566 using a bath ultrasonication process for 20min at room temperature, but without success. Secondly, GNPs were attempted to be dispersed in Curamine 32-494, which gave a much more uniform dispersion (Figure 5.3). One of the possible reasons for this is the lower viscosity of Curamine (0.1 Pa·s) compared to that of Epilok (0.7 Pa·s), which facilitated dispersion. Figure 5. 3 is a photograph of Epilok 60-566 (left) and Curamine 32-494 (right) with the addition of GNPs and shows the dispersion quality, which is much higher in Curamine 32-494.

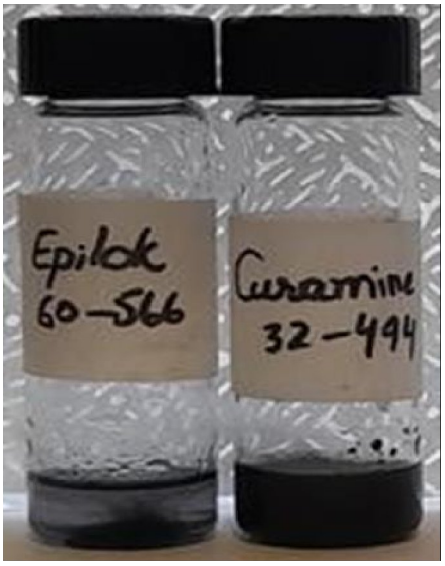

Figure 5. 3: Dispersion quality of GNP with epilok and curamine.

5.6.2 Effect of different Sonication Time and Frequency

The determination of the ideal ultrasonication time and power to obtain the best stability and mechanical properties is important. Although this was not the main focus of this study and chapter, a prescreening investigation was performed to determine the optimum processing conditions (i.e. time and frequency). Three different sonication times, 20, 40 and 90 min and two frequencies (37 kHz and 80 kHz) were investigated. The sonication power was kept constant at 100 W. Using DSC; it was found that 20 min sonication increased the exothermic curing peak area of GRMs/polymer nanocomposites hence releasing more energy (more crosslinking) than the 40 or 90-min sonication, which illustrates in figure 5. 4. It is also observed that the exothermic peak intensity decreased with increasing sonication time. In the ultrasonication process, nanoparticles are agitated by exerting ultrasound energy. The curing reactions are discussed in detail in section 5.6.3.

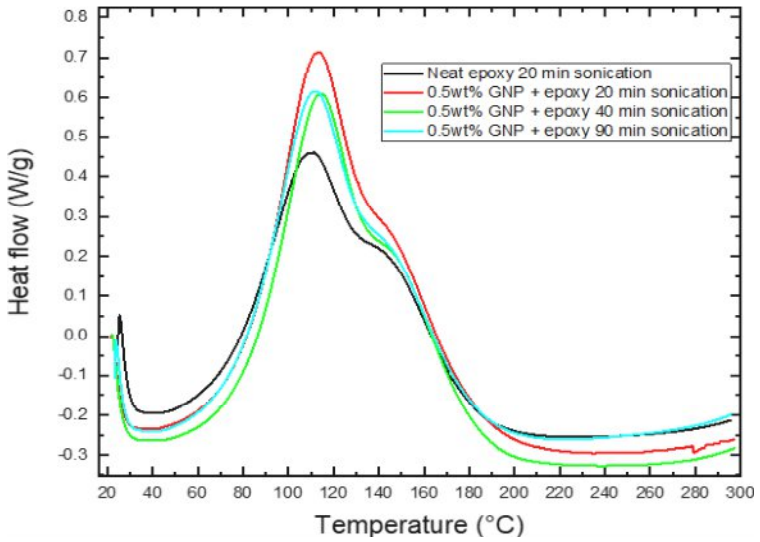

Figure 5. 4: Effect of different sonication time*s*.

The effects of GRMs sonication time, i.e. 20 and 40min with 37 and 80kHz sonication frequency, on the mechanical properties (*E* and *UTS*) are summarised in Table 5. 1. Twenty minutes, sonication gave the highest the *E* but decreased the *UTS* in 37KHZ. When the frequency changed to 80KHZ, it dropped the *E* and improved the *UTS.* The same trend was found with 40min sonication at 80kHz frequency. It has been reported that The longer the sonication duration, the more wrinkled the GNP structure becomes (Zegeye et al., 2014)(A. M. Pinto et al., 2013). Similar results were obtained by Singh et al., where the combined effects of various sonication times and power on 0.75wt% functionalised multi-layer Graphene (AF-MGL) in a polymer matrix were explored. Sonication times of 10, 40, and 70 minutes and powers of 20, 40, and 60W were utilised to guarantee appropriate dispersion of AF-MGL in the epoxy matrix (P. K. Singh et al., 2020). The Ultimate tensile strength was higher at 40 minutes of sonication with maximum power (60w); however, the tensile Modulus dropped as the sonication time, and power increased. Seretis et al. (Seretis et al., 2018) examined the influence of sonication process time on the mechanical performance of GNPs/glass fabric/epoxy nanocomposites; they tested three alternative times: 20, 40, and 60 minutes.

While sonication time increases, *UTS* shows the same increasing trend. For longer sonication times, however, the *UTS* rise values get higher. As a result, the most significant *UTS* rise was seen for the maximum sonication period, and GNPs content was investigated, namely 60 minutes of sonication and 5wt% GNPs. Hence, we used a 20min sonication time with a 37KHz frequency for improved *E*.

Table 5. 1: The effects of GRMs sonication times and frequencies on the mechanical properties.

wt% GRM	***E* at 37KHz (GPa)**		***UTS* at 37KHz (MPa)**		***E* at 80KHz (GPa)**		***UTS* at 80KHz (MPa)**	
	Sonication Time (min)		**Sonication Time (min)**		**Sonication Time (min)**		**Sonication Time (min)**	
	20	**40**	**20**	**40**	**20**	**40**	**20**	**40**
0.5	1.98	1.55	52.11	58.98	1.31	1.19	61.02	66.23

5.6.3 Curing study by DSC

The main reactions that take place during curing include the epoxide ring at the end of the epoxy resin chains with the primary amino groups (Figure 5. 5a), secondary amino groups (Figure 5. 5b) and etherification of oxirane ring with a pendant hydroxyl group (Figure 5. 5c). These reactions may take place, either simultaneously or sequentially, depending on the reactivity of reactants and the process temperature.

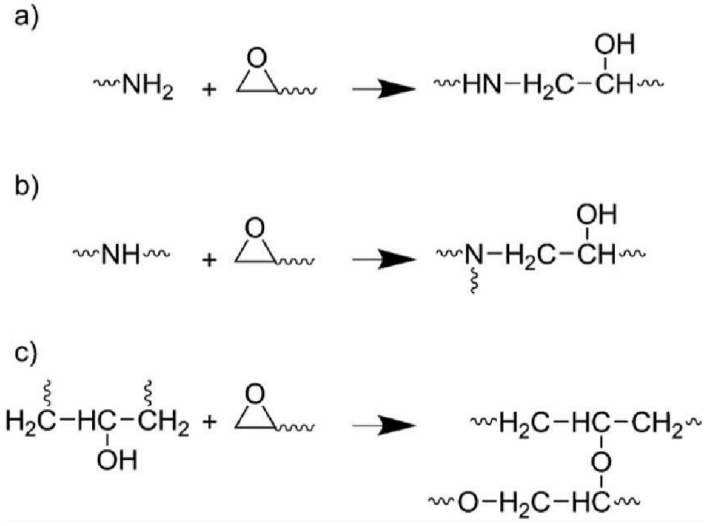

Figure 5. 5: Reactions that take place while curing a) epoxide ring at the end of the epoxy resin chains with the primary amino groups b) epoxide ring and secondary amino groups, and c) etherification of oxirane ring with a pendant hydroxyl group (Ramsdale-Capper & Foreman, 2018).

Horie et al. (Horie et al., 1970) observed that the primary amine reaction shows E_a of 58.2 kJ mol^{-1} (13.9 kcal mol^{-1}) and the secondary amine reaction 56.1 kJ mol^{-1} (13.4 kcal mol^{-1}). For 1:1 stoichiometry, as in our case, or when the amine is present in excess, reaction (c) (Figure 5. 5) is generally insignificant with respect to reactions (a) and (b). In most systems, the primary and secondary amines have similar reactivities, and one DSC cure exotherm is observed. In a few cases, e.g. with hindered amines (Duffy et al., 1987), the reactivity of secondary amine may be significantly lower, resulting in separate exotherms; one for the reaction of a primary amine with epoxy and the other for secondary amine with epoxy. Such cases are observed in hindered amines, in which the nitrogen atom of the amine molecule is partially shielded by neighbouring groups so that larger molecules cannot easily approach and react with the nitrogen. Etherification reaction (Figure 5. 5c) is usually much slower than the amine-epoxy reactions and only becomes significant in epoxy-rich systems above 150°C when the primary

amine is sufficiently depleted (Carmen C. Riccardi & Williams, 1986); two cure exotherms are typically observed in epoxy-rich systems.

Curing of epoxy resins is a highly exothermic process; hence reaction kinetics were monitored by recording the amount of heat released with time (rate of heat flow in Watts=J/s) by DSC under non-isothermal and isothermal conditions. The basic assumption underlying the application of DSC is that the measured rate of heat flow (*dH/dt*) is proportional to the reaction rate *dα/dt*:

$$\frac{da}{dt} = \frac{1}{\Delta H_{total}}\left(\frac{dH}{dt}\right) \qquad (2)$$

Where ΔH_{total} is the exothermic heat expressed as heat per mole of reacting groups (kJ mol^{-1}), in the ideal case, ΔH_{total} is the total heat liberated when an uncured resin is taken to complete cure, and this value is independent of temperature for a particular resin system. The degree of curing α at any time *t* is given by

$$a(t) = \frac{\Delta H(t)}{\Delta H_{total}} \qquad (3)$$

Where $\Delta H(t)$ is the heat generated up to time *t.* The ultimate degree of conversion is defined as

$$a_{ult} = \frac{\Delta H_{ult}}{\Delta H_{total}} \qquad (4)$$

For several amine-epoxy systems and model reactions, ΔH_{total} has been measured and found to be reasonably constant and equal to 25.6 ± 1 kcal mol^{-1} of epoxide (107±4 kJ mol^{-1} of epoxide); this value may be used as a standard value for analysing amine-epoxide systems (Verchère et al., 1990), (Prime, 1997). However, it was found from simultaneous DSC and FTIR measurements conflicting results for ΔH_{total}, that is 83 ± 2, 131 ± 9, and 65 ± 6 kJ mol^{-1} for primary amine (Figure 5. 5a), secondary amine (Figure 5. 5b) and hydroxyl (Figure 5. 5c) reactions with epoxide respectively; note that the average for the primary plus secondary amine

reactions is 107 kJ mol^{-1} (de Bakker et al., 1993). It is worth noting that values of 25.5±1.5 kcal mol^{-1} of epoxide are typically measured in epoxy systems with excess amine (e.g. up to 20%), but lower values are often observed for a 1:1 stoichiometric mixture suggesting that 100% conversion may be difficult to achieve in stoichiometric systems (C. C. Riccardi et al., 1984) (Simon & Gillham, 1992) (Simon & Gillham, 1994).

5.6.3.1 Non-isothermal scanning method

The non-isothermal DSC curves for the neat epoxy resin system and the composite with 0.5 or 1.5%wt of GNPs at different heating rates (2, 5, 10 and 20°C/min) were recorded. Characteristic curves illustrating the change of heat flow with temperature for the neat epoxy resin and the nanocomposite with 1.5%wt GNPs are shown in Figure 5. 6. Origin is a proprietary computer program that works on Microsoft Windows and allows users to graph and analyse scientific data. Statistics, curve fitting, peak analysis and signal processing are some of the key technical features in the Origin software. Origin is a graphical user interface (*GUI*) programme with a spreadsheet interface, and it is worksheet column-oriented, unlike popular spreadsheets in Excel. Each column has its features, such as a name, units, and other labels that users can customise. Origin calculation is based on column formula rather than cell formula. It accepts ASCII text, Excel and other supportive formats. It also exports the graph to JPEG, GIF and other image file formats.

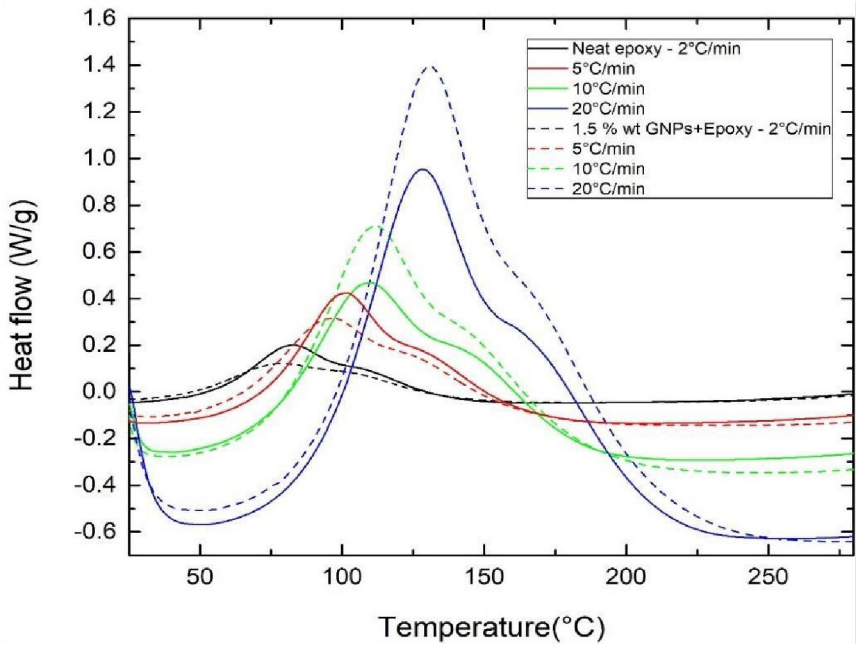

Figure 5. 6: Dynamic scans with different heating rates of 2-20°C/min for neat epoxy and with 1.5%wt GNPs.

All DSC curves showed a broad peak and a shoulder at the higher temperature, which will be referred to as peak-1 and peak-2. An analogous result was reported for the non-isothermal curing study by DSC of the commercial epoxy resin Epikote 828 based on diglycidyl ether of bisphenol A cured by isophorone diamine (Figure 5. 7). One peak was first observed, which was attributed to the reaction of the epoxy group with the aliphatic group $-CH_2NH_2$ and a shoulder attributed to the alicyclic group (Núñez et al., 1996).

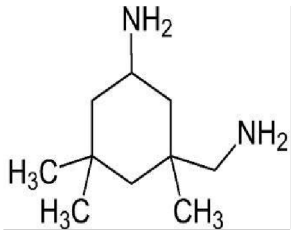

Figure 5. 7: Chemical structure of isophorone diamine a cycloaliphatic diamine (Núñez et al., 1996).

A non-isothermal curing study by DSC of two systems Epikote resin 816LV/Epikure F205 and Epikote resin 240/Epikure F205 (at stoichiometric ratio), was also reported in the literature (Achilias et al., 2012). The epoxy resin is based on a diglycidyl ether of bisphenol A, and the curing agent is based on isophorone diamine. In both cases, first a peak and then a shoulder was observed in all scans carried out at different scanning rates. Study of isothermal (30, 50 and 70°C) curing kinetics of these systems by Fourier Transform Infrared Spectroscopy (FTIR) showed that the reaction of hydroxyl groups with the epoxy groups does not seem to take place.

According to the literature data reported above, in our case, the first peak observed in DSC (Figure 5 .6) must correspond to the reaction of the primary amino group with the epoxy (Figure 5. 5a) and the second to the reaction of the secondary amino group with the epoxy group (Figure 5. 5b). It is worth to note that 4,4'-methylenebis(cyclohexylamine) contained in Curamine 32-494 is a hindered amine with the two amino groups -NH_2 connected with alicyclic groups (Figure 5.1 d); so the secondary amino group -NH- derived from reaction (a) (Figure 5. 5) shows much lower reactivity than the primary amino group -NH_2. Hence, reaction (b) (Figure 5.5) gives the shoulder at a higher temperature (Figure 5.6). Since we used a 1:1 stoichiometric mixture, the reaction between the hydroxyl group and epoxy (Figure 5.5c) does not occur.

The initial curing temperature (T_{init}), final (T_{final}) and the peak temperatures ($T_{peak\ -1}$) and ($T_{peak\ -2}$) shift to higher values with increasing heating rate β (Table 5.2). No significant peak shift is observed with the addition of graphene. From a practical standpoint, it may be desirable to define processing parameters such as T_{init} and T_{final}; for example, a practical definition of T_{final} could be the minimum cure temperature at which total (α=1) or final (α=α_{final}) conversion takes place in a reasonable time.

Table 5. 2: Characteristic temperatures of curing process obtained under non-isothermal conditions with different heating rates.

GNPs(%wt)	β (°C/min)	T_{init} (°C)	T_{final} (°C)	T_{final}-T_{int} (°C)	T_{peak-1} (°C)	T_{peak-2} (°C)
0	2	18.5	261.1	243.7	81.5	108.3
(neat epoxy)	5	20.9	273.0	252.0	99.8	130.8
	10	26.6	291.3	264.7	108.8	147.1
	20	35.8	298.4	262.6	129.9	171.6
0.5	2	17.9	278.5	260.6	82.8	108.1
	5	20.3	274.4	254.0	90.4	121.7
	10	21.3	285.2	263.9	112.2	149.0
	20	30.5	292.5	262.0	123.7	168.2
1.5	2	15.4	270.3	254.9	76.5	104.9
	5	25.8	284.6	258.8	94.5	127.8
	10	23.3	286.8	263.5	110.5	147.7
	20	36.6	291.3	254.7	129.9	171.4

The ultimate heat of curing ΔH_{1ult} (J/g) and ΔH_{2ult} (J/g) was determined by integrating peak-1 and peak-2 correspondingly. Taking into account that the EEW of epoxy resin used is an average 180 g/eq (=the grams of Epilok 60-566 containing 1gmol of epoxy groups), the values of $\Delta H1_{ult}$ (kJ/mol) and $\Delta H2_{ult}$ (kJ/mol) were calculated by $\Delta H1_{ult}$ (J/g)x180 and $\Delta H2_{ult}$ (J/g)x180

correspondingly. Figure 5.8 shows the plots between time and heat flow in Origin to calculate the ΔH_{ult}.

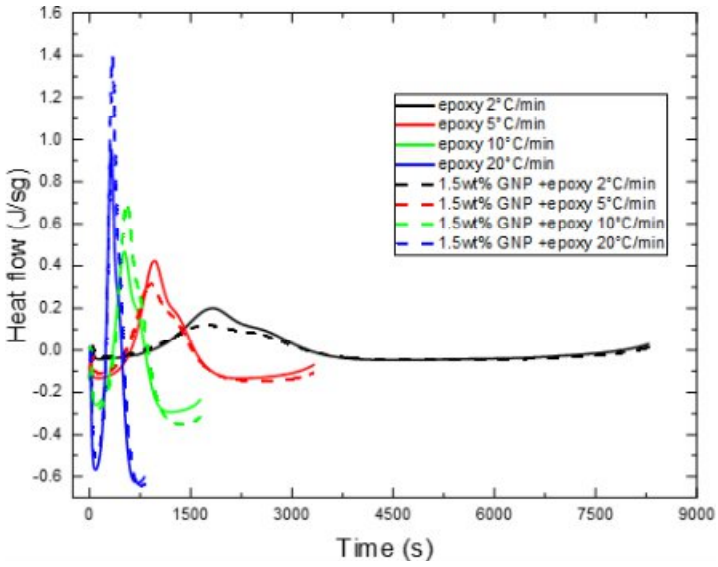

Figure 5. 8: Dynamic scans of different heating rates 2-20°C/min for neat epoxy and with 1.5%wt GNPs.

We can calculate area either using heat flow versus time or heat flow versus temperature. Heat flow versus time gives the area straight away; however, we need to divide the peak area with the heating rate when calculating the heat flow versus temperature.

Curve fitting

One of Origin's most powerful and extensively used analysis techniques is curve fitting. Curve fitting looks at the relationship between one or more predictors (independent variables) and a response variable (dependent variable) in order to find the "best fit" model. To calculate the area of multiple peaks using different models, such as the Lorentz and Gaussian fit models, we need to follow the steps for a proper fitting procedure.

1. Make a graph of the data.

2. Determine the model/formula that should be used to describe the data. This is not within the computer's control.

3. Determine which fit parameter is in charge of a specific fit line feature.

4. Based on the discovery thus far, make an educated guess about the fit parameters.

5. Use the guess to plot the fit function and see if it meets expectations.

6. Fine-tune guesses and repeat steps 1–6 until a model function curve closely resembles the data.

7. Finally, instruct the computer to do time-consuming refinements of estimated parameters, i.e. run the fit.

Lorentz Fit model

The Cauchy distribution, often known as the Lorentz distribution, is a mathematical distribution. The Lorentzian function, or Cauchy–Lorentz distribution, consists of continuous probabilistic distributions that resemble the normal curve family. While there is some resemblance, it has a higher peak than a regular. Its fat tails decay significantly more slowly than the typical distribution. A scale parameter (λ) and a location parameter (x0) are the two main components of the Cauchy distribution. The location parameter (x0) causes the graph to shift along the x-axis, while the scale parameter (λ) causes the graph to be shorter or taller. The curve becomes higher and thinner as the scale parameter is reduced. Figure 5.9 shows Lorentz fit for Peak-1 and Peak-2. Lorentz model shown is well fitted in experimental results which were applied with R^2 and adjusted reduced R^2 of 0.998, indicating a very good fit quality.

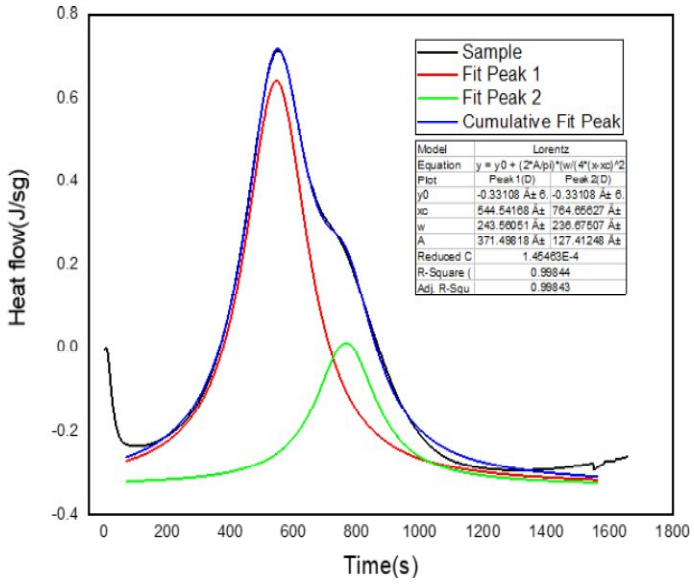

Figure 5. 9: Lorentz fit for Peak-1 and Peak-2.

The experimental peak curves were deconvoluted using OriginPro software, and an integration gadget is used to plot data and activate the graph window to calculate the peak area. Go to Gadgets; Integrate and click OK in the pop-up dialogue to bring up the Integration gadget's yellow Region of Interest (ROI) box. Drag to place and resize the box to the area to compute, and the ROI top will provide the Area and FWHM information. The x-coordinates will be labelled on each peak in the resulting plot. The Integration Resultn worksheet in the results output workbook displays the estimated result parameters for each peak, including peak regions. In addition, the Integrated_Curve_Datan worksheet contains data for the integral curve. For example, in figure 5. 10, Calculate the area of Peak-1 and Peak-2 using Integrate data plot over a region of interest.

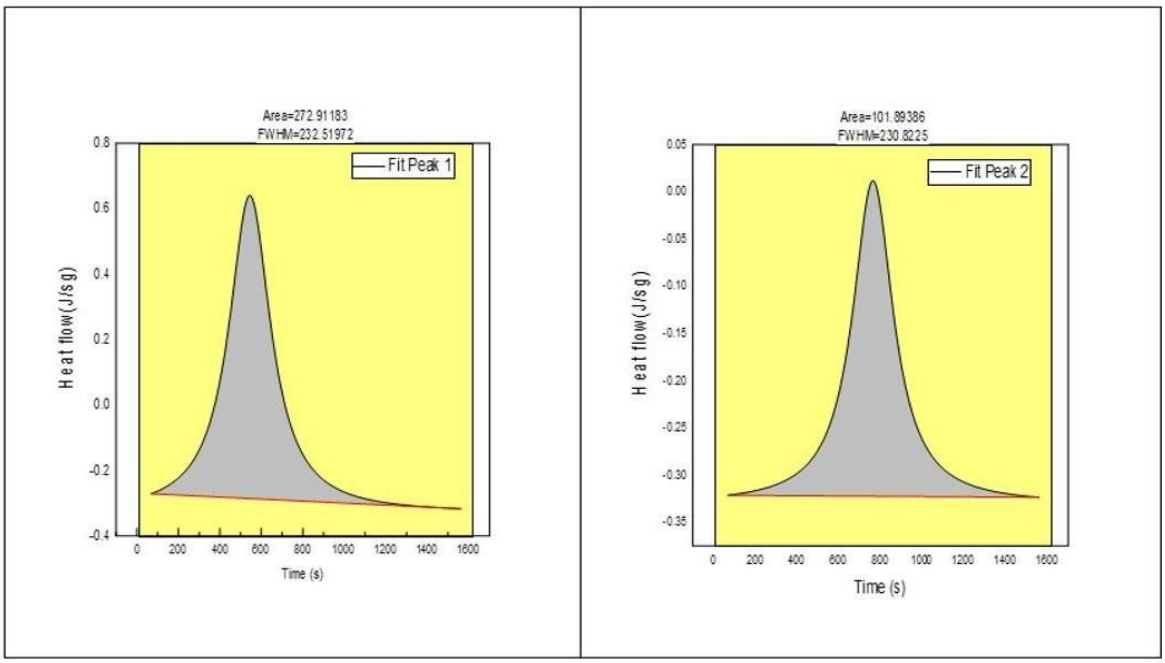

Figure 5. 10: Calculate the area of Peak-1 and Peak-2 using Integrate data plot over a region of interest.

Gaussian Fit model

Gaussian processes benefit from traits inherited from the normal distribution, making them valuable in statistical modelling. For example, a Gaussian model implies a two-dimensional normal distribution of concentration in both the crosswind and vertical directions, centred on the source point's downwind axis. Figure 5. 11 shows the Gaussian fit for Peak-1 and Peak-2.

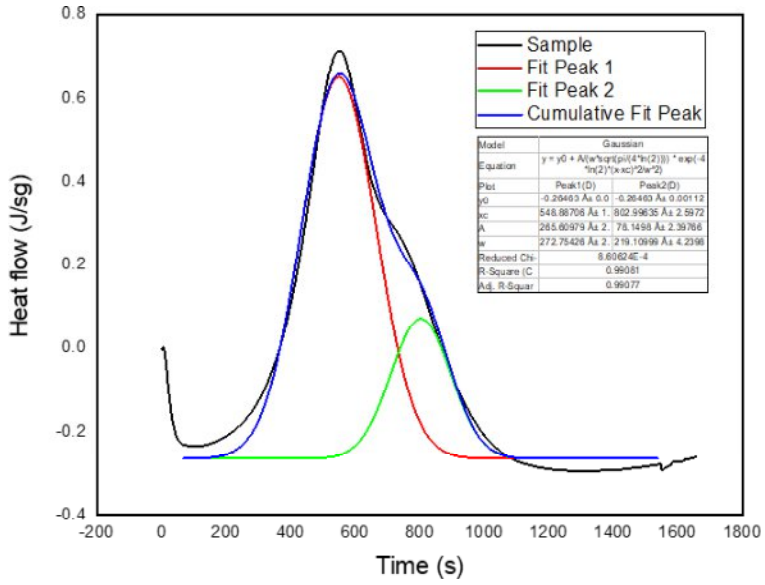

Figure 5. 11: Gaussian fit for Peak-1 and Peak-2.

In this study, the Lorentz fit is better than the Gaussian fit, so I used Lorentz fit model to calculate the area of the peaks.

Table 5. 3: Exothermic heat of curing (ΔH) and degree of curing (α) were obtained under non-isothermal conditions with different heating rates.

GNPs (%wt)	β (°C/min)	$\Delta H1_{ult}$ (J/g)[a]	$\Delta H1_{ult}$ (kJ/mol)[b]	$\Delta H2_{ult}$ (J/g)[a]	$\Delta H2_{ult}$ (kJ/mol)[b]	α_1 (%)	α_2 (%)	α (%)
0 (neat epoxy)	2	222.02	51.96	91.04	21.30	63	16	79
	5	244.31	57.18	108.66	25.43	69	19	88
	10	213.38	49.94	91.28	21.36	60	16	76
	20	241.44	56.51	88.33	20.67	68	16	84
0.5	2	210.91	49.36	103.08	24.12	59	18	77
	5	211.64	49.53	107.32	25.12	60	19	79
	10	272.91	63.88	101.89	23.84	77	18	95
	20	269.19	63.00	111.26	26.04	76	20	96
1.5	2	155.76	36.45	95.48	22.34	44	17	61
	5	227.01	53.13	108.32	25.35	64	19	83
	10	282.5	66.12	111.72	26.15	80	19	99
	20	293.25	68.64	96.06	22.48	83	17	100

[a] $\Delta H1_{ult}$ (J/g) refers to 1 gr of epoxy determined from the experimental value divided by 0.769.

[b] ΔH_{ult} (kJ/mol) calculated from ΔH_{ult} (kJ/g) x 180 (=EEW of Epilok 60–566).

The degree of curing was calculated from equation 4, where for peak-1 the value of ΔH_{total} =83 kJ/mol was used, and for peak-2 (shoulder), the value of ΔH_{total} =131 kJ/mol (de Bakker et al.,

1993). Thus, the total degree of curing is $\alpha = \alpha_1 + \alpha_2$ (Vyazovkin et al., 2011a)(Jubsilp et al., 2010) The lower α values obtained for the loading 0.5 and 1.5 %wt GNPs at low heating rates 2 and 5°C/min than the neat epoxy/amine system can be attributed to the steric hindrance of GNPs. The main reason is the low interaction between the GNPs and the matrix, generating a very weak interface (S. G. Prolongo et al., 2014). On the contrary, the higher α obtained for the loading of 0.5 and 1.5%wt GNPs at high heating rates 10 and 20°C/min than the α of the neat epoxy/amine system can be attributed to the high thermal conductivity of GNPs (Table 5.3). Figure 5. 12 represents $\Delta H_1 ult_1$ b) $\Delta H_1 ult_2$ at different heating rates 2-20°C/min for Peak-1 and Peak-2.

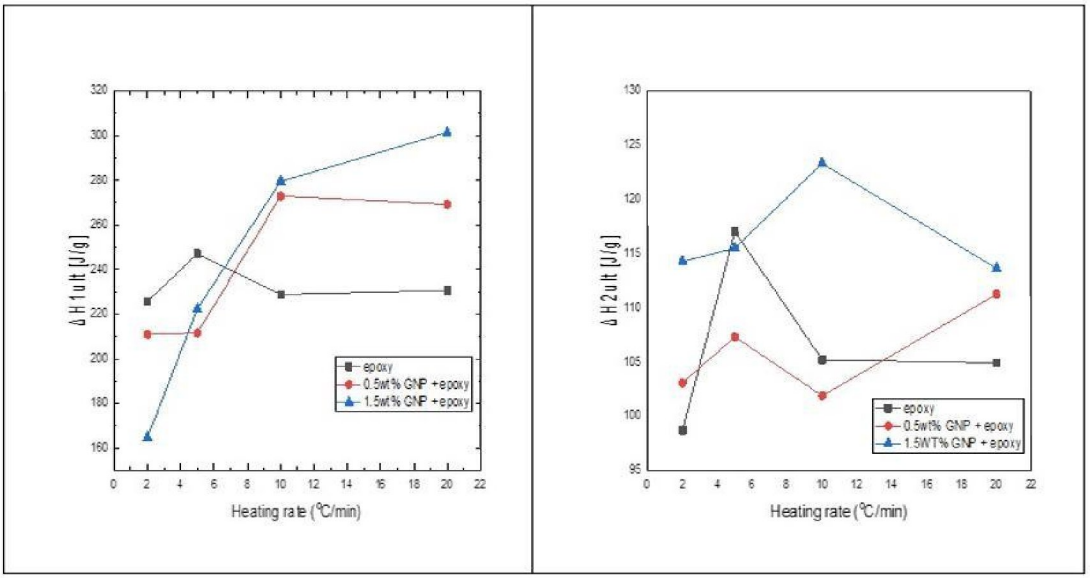

Figure 5. 12: Determination of $\Delta H_1 ult_1$ b) $\Delta H_1 ult_2$ at different heating rates 2-20°C/min for Peak-1 and Peak-2.

One of the most frequently used model-free methods which estimate E_a and the pre-exponential factor (A) in physical or chemical processes from data obtained at several non- isothermal tests conducted at constant heating rates (constant during each test, different among tests) is the Kissinger method (Kissinger, 1957), One crucial condition needed to apply the

Kissinger's method is that the conversion at the maximum reaction rate denoted as α must be very similar for all the heating rates (Lascano et al., 2019) and is identical to the ASTM Method E 698-79 (Hadad, 1988). Kissinger derived a useful expression that relates Ea and A for nth-order reactions to φ and peak temperature Tp (Núñez et al., 1996).

$$A = \frac{\varphi E e^{\frac{E_a}{RT_p}}}{RT_p^2\left[n\left(1-a_p\right)^{n-1}\right]} \qquad (5)$$

Kissinger argued that $n\left(1-a_{p_i}\right)^{n-1} \approx 1$ and is independent of the heating rate; by definition, this is true for a first-order reaction (Prime, 1973) and showed this quantity to be constant and only 2-4% greater than unity for an n^{th}-order cure reaction. Kissinger, in his study of reactions of any order n, observed that the peak shape of a reaction is independent of heating rate and the values of the kinetic constants and depends only on the reaction order *n*; to quantitatively describe the peak shape, a "shape index" (*S*) was proposed defined as the absolute value of the ratio of the slopes of tangents to the curve at the inflection points (S=a_1/a_2, Fig. 5. 13a). The shape index *S* is then a function only of the reaction order *n:*

$$S = 0.63n^2 \;\Rightarrow n = 1.26\,S^{1/2} \qquad (6)$$

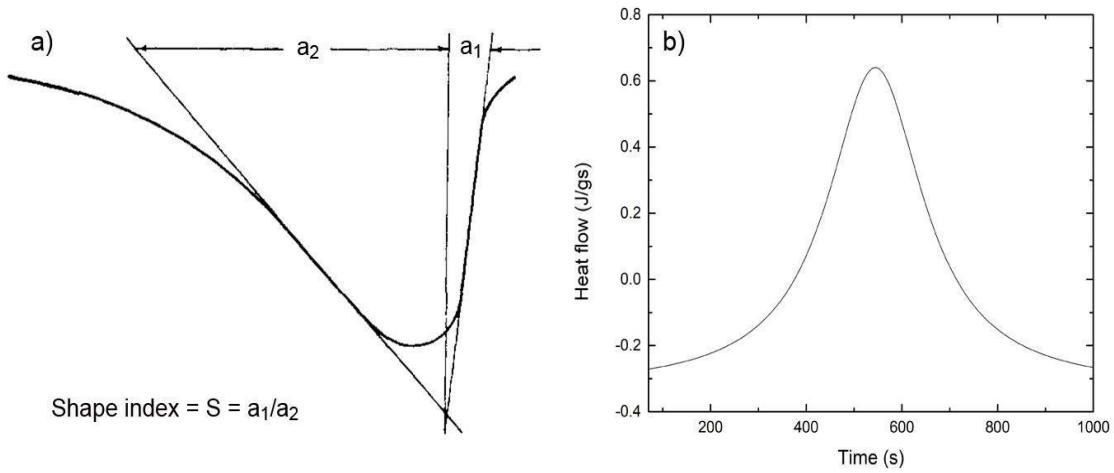

Figure 5. 13: Determination of shape index S of DSC curves (Kissinger, 1957), b) deconvoluted peak-1.

The shape index of curve peaks (representative peak-1 shown in Figure 5.13b) was found to be symmetrical, and so S=a_1/a_2=1 for all heating rates. Thus equation (6) leads to the result n=1.26. So, equation (5) can be written as:

$$A = \frac{\varphi E e^{\frac{E_a}{RT_p}}}{RT_p^2} \qquad (7)$$

And taking the logarithm of eq. (7) we take:

$$\ln\left(\frac{\varphi}{T_p^2}\right) = \ln\left(\frac{AR}{E_a}\right) - \frac{E_a}{RT_p} \qquad (8)$$

Where R is the universal gas constant (8.314×10^{-3} kJ/mol·K), by plotting $\ln(\varphi/T_p^2)$ versus $1/T_p$, Ea and the A values can be estimated from the slope of the linear fit and the y-intercept correspondingly. However, it must be noted that the Kissinger method is associated with the fact that the determination of accurate E_a values requires a_p (eq. 5) to be independent of φ. Otherwise, the plot of $\ln(\varphi/T^2)$ versus $1/T$ would deviate systematically from a straight line. It is reported that for other models, α at T_p may vary significantly with φ (Vyazovkin et al.,2011a). A variation of α at T_p with φ can be detected on visual inspection as a change in the peak shape with φ (Vyazovkin et al., 2011a). The peak shape of the studied epoxy/amine system in this work was found to be symmetrical and practically unchanged for all heating rates. The shape index (S) of peaks (representative peak-1 is shown in Figure 5.13b) was calculated as S= a_1+a_2, which corresponds based on eq. 6 to n=1.26.

From the plot of $\ln(\varphi/T_p^2)$ versus $1/T$ shown in Figure 5.14, the value of activation energy E_{a1} was determined for the neat epoxy to be 51.09±4.74 kJ/mol and A_1= 3489.9 s^{-1} and E_{a2} = 44.64±2.29 kJ/mol and A_2= 101.26 s^{-1} for peak-2. The values of E_{a1} and E_{a2} for primary and secondary amino groups of our system obtained by the Kissinger method are lower than those reported by Horie (Horie et al., 1970). Addition of 1.5%wt GNPs dropped values to E_{a1} = 44.10±1.48 kJ/mol and A_1= 357.69 s^{-1} and E_{a2} = 41.68±0.90 kJ/mol and A_1= 41.35 s^{-1}.

Table 5. 4: For Activation energy.

GNPs (%wt)	Heating Rate β [°C/min]	T_{peak-1} [°C]	ln(β/ Tpeak-$_1$^2) [°K]	1/ T_{peak-1} [°K]	T_{peak-2} [°C] Shoulder	ln(β/ Tpeak-$_2$^2)[°K]	1/ T_{peak-2} [°K]	E_{a1} [kJ/mol]	E_{a2} [kJ/mol]
0 (neat epoxy)	2	81.53	-11.04	.00281	108.30	-11.19	.00262	51.09± 4.74	44.64± 2.29
	5	99.73	-10.22	.00268	130.72	-10.38	.00247		
	10	108.83	-9.58	.00261	147.13	-9.77	.00237		
	20	129.89	-9.00	.00248	171.59	-9.19	.00224		
0.5	2	82.78	-11.05	.00280	108.12	-11.19	.00262	52.85± 4.48	50.16 ± 3.25
	5	90.36	-10.18	.00275	121.72	-10.34	.00253		
	10	112.16	-9.60	.00259	148.97	-9.78	.00236		
	20	123.66	-8.97	.00252	168.15	-9.18	.00226		
1.5	2	76.47	-11.02	.00286	104.88	-11.17	.00264	44.10± 1.48	41.68± 0.90
	5	94.48	-10.20	.00272	127.75	-10.37	.00249		
	10	110.45	-9.59	.00260	147.69	-9.78	.00237		
	20	129.88	-9.00	.00248	171.37	-9.19	.00224		

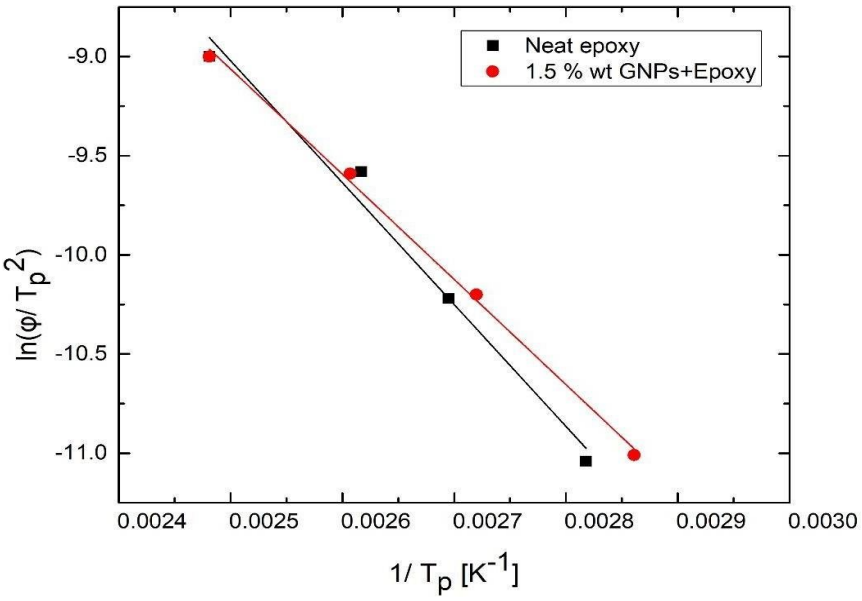

Figure 5. 14: Kissinger's plot to determine E_a from the slope of the linear fit and factor A from the y-intercept for peak-1.

E_α is the minimum energy requirement that must be met for a chemical reaction to occur; the factor A is an empirical relationship between temperate and rate constant k and depends on the quantity of molecules or groups in the reaction and their orientation. Both Eα and A connect with the reaction rate constant k with an Arrhenius-type expression:

$$k = Ae\left(-\frac{E_a}{RT}\right) \qquad (9)$$

Where k is the rate constant (for order one, the rate constant has units of s^{-1}), from E_a and A data based on the Arrhenius law, the rate constants k_1 and k_2 and ratio k_1/k_2 at different temperatures can be derived. The results obtained are shown in Table 5. 5. These results show that the values of E_a and A and k_1/k_2 are lower for the secondary imino -NH- group. As can be seen, as the temperature increases, both reactions proceed simultaneously; both constants k1 and k_2 increase with temperature, but the ratio k_1/k_2 remains constant. This shows that the participation ratio of the primary amino group and the secondary amino groups in the reactions

(Figure 5. 5a) and (Figure 5. 5b) correspondingly is constant, and the structure of the prepared polymer matrix does not depend on the curing temperature.

Table 5.5 shows that the loading of 1.5 %wt GNPs led to a significant decrease of k_1/k_2, which was due mainly to the significant decrease of k_1. Two opposite effects have to be considered to explain the epoxy curing in the presence of graphene, the steric hindrance of GNPs that impedes the mobility of the reactants decreasing the curing reaction rate and the high thermal conductivity of GNPs, which can explain the accelerating effect for high temperatures (M. G. Prolongo et al., 2016b). The significant decrease of k_1, an order of magnitude, and k_2 and so k_1/k_2 with the presence of 1.5 %wt GNPs can be attributed to the steric hindrance of GNPs.

Table 5. 5: Rate constants k_1 and k_2 and ratio k_1/k_2 at different temperatures.

T (K)	Neat epoxy			1.5%wt GNP + epoxy		
	k_1 (s^{-1})	k_2 (s^{-1})	k_1/k_2	k_1 (s^{-1})	k_2 (s^{-1})	k_1/k_2
298.15	3418.70	99.45	34.38	351.38	40.66	8.64
308.15	3420.99	99.51	34.38	351.58	40.68	8.64
318.15	3423.13	99.56	34.38	351.77	40.70	8.64
328.15	3425.15	99.61	34.39	351.95	40.72	8.64
338.15	3427.05	99.66	34.39	352.12	40.74	8.64
348.15	3428.84	99.71	34.39	352.28	40.75	8.64
358.15	3430.53	99.75	34.39	352.43	40.77	8.64
368.15	3432.13	99.79	34.39	352.57	40.79	8.64
378.15	3433.64	99.83	34.39	352.70	40.80	8.64
388.15	3435.08	99.86	34.40	352.83	40.81	8.64
398.15	3436.45	99.90	34.40	352.95	40.83	8.64

It is worth noting that although the Kissinger method produces specific Arrhenius parameters, it yields a single averaged pair of these parameters for the overall cure process in a manner similar to the model-fitting methods, which can be used however for comparative studies, e.g. the effect of GNPs on the epoxy resin curing. The resulting average values do not reflect changes in the reaction mechanism and kinetics with the curing temperature and α. However, the process of epoxy curing is known to involve multiple steps that are likely to have different E_α values. Then the contributions of these steps to the overall cure rate measured by DSC should vary with both temperature and α.

The amine-epoxy reactions (Figure 5.5.a-b) may be uncatalysed (n order) or catalysed by probable impurities (e.g. water, alcohols, phenols, acids) initially present in the reaction system (n order) or by the hydroxyl groups (OH) generated by the epoxy-amine reaction (autocatalysis) (m order) (Karkanas & Partridge, 2000)(Rozenberg, 1986)(Swier et al., 2005)(Flammersheim, 1998). During curing, the reaction system undergoes gelation (liquid-to-rubber) and vitrification (rubber-to glass) transitions. Intensive crosslinking occurring in the region between the above transitions reduces molecular mobility and cure changes from kinetic to diffusion (Vyazovkin & Sbirrazzuoli, 1996). In such cases where changes in the curing mechanism are associated with changes in the activation energy, the model-free isoconversional methods can be used to observe how the activation energy changes throughout the entire reaction. One of the model-free isoconversional methods, the Ozawa-Flynn-Wall analysis, provides a simple relationship between α-dependent E_α, φ and isoconversion temperature (T_i) (Hardis et al., 2013):

$$log\beta = -\frac{0.4567E_a}{RT_i} + A' \qquad (10)$$

for each relative degree of curing (α_r), A' is a constant that can be defined as:

$$A' = log\left(\frac{AE_a}{g(a)R}\right) - 2.315 \qquad (11)$$

Where g(α) is a conversion dependent function, in order to determine the corresponding E_α and A at each relative α, a plot first was drawn of the relative degree of cure (α_r) vs curing temperature (T) at each φ, as shown in Figure 5. 15a,b and Figure 5. 15c,d. for peak-1 and peak-2 correspondingly.

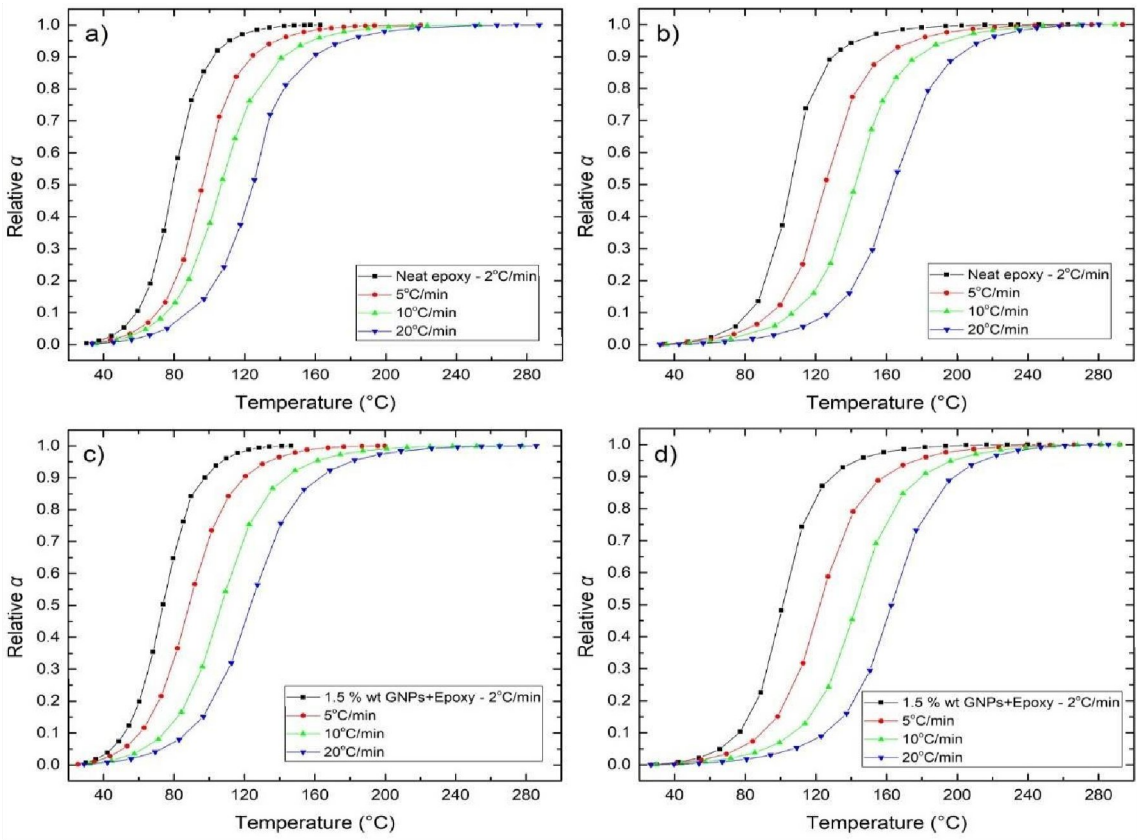

Figure 5. 15: Conversion α as a function of temperature at different heating rates for a) neat epoxy peak-1, b) neat epoxy peak-2, c) 1.5 %wt GNP/epoxy peak-1, and d) 1.5 %wt GNP/epoxy peak-2.

Then a plot of logβ vs T_i was drawn at each α_r as shown in Fig. 5. 16. a,b. The resulting slope is proportional to $E_{\alpha,}$ and the intercept is proportional to A'.

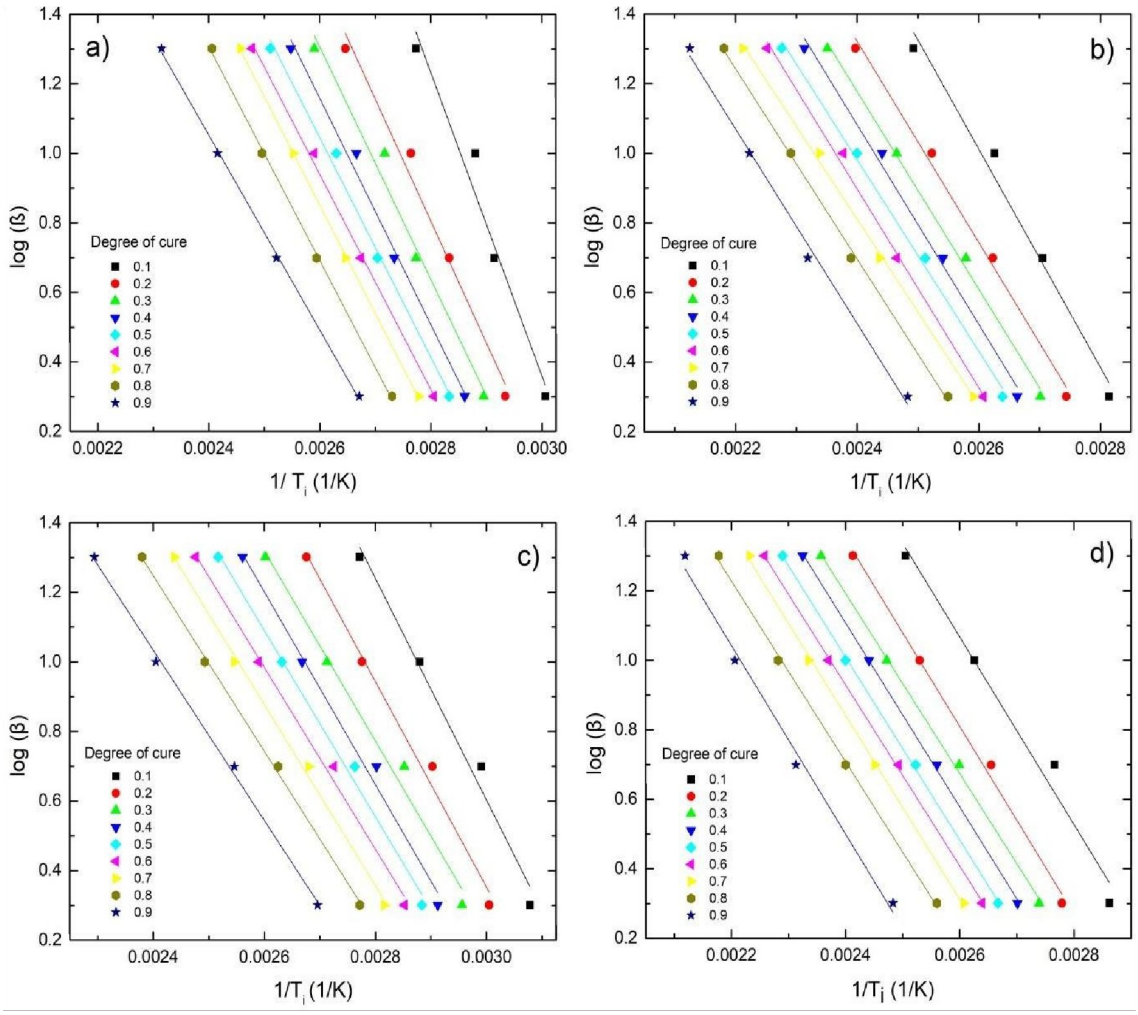

Figure 5. 16: Isoconversional plots for the logarithmic heating rate versus the reciprocal absolute temperature for a) neat epoxy peak-1, b) neat epoxy peak-2, c) 1.5%wt GNP/epoxy peak-1, and d) 1.5%wt GNP/epoxy peak-2.

In Figure 5. 17a,b, the E_α was plotted with α for neat epoxy resin and GNPs/epoxy composite with 1.5%wt GNPs for peak-1 and peak-2. The high effective value of E_α at the very beginning of curing at α=1 corresponds to the non-catalysed reaction of epoxy-amine. Since the hydroxyl groups formed during the curing facilitate the ring-opening (autocatalysis) and do other

probable impurities (HX)o, it is reasonable to expect a rapid decrease in E_α. When during the curing, the T_g of a partially cured system exceeds the curing temperature, the system verifies. The monomer molecules become frozen in their positions in the glassy state, resulting in the virtual cessation of curing (Sbirrazzuoli & Vyazovkin, 2002). Stutz et al. (Stutz et al., 1993) have studied the kinetics of epoxy-amine curing in the glass transition region and found that the process has very low E_α (few kJ mol^{-1}); this means that vitrification should cause a decrease in the effective activation energy with increasing the extent of reaction. The same effect was also observed during the curing of another epoxy-amine system using model-free isoconversional methods. In that study, it was found that as early as α=0.3, the curing starts to change from kinetically controlled to diffusion-controlled and diffusion at α=1 (Vyazovkin & Sbirrazzuoli, 1996). From Fig.10a-b, it was observed that $E_{\alpha 1}$ decreases from 79.5 to 51 kJ/mol for the neat epoxy and $E_{\alpha 2}$ from 57.1 to 50.9 kJ/mol. The nanocomposite contained 1.5wt% showed a decrease in $E_{\alpha 1}$ from 58.2 to 44.6 kJ/mol, and $E_{\alpha 2}$ is about 48 kJ/mol. The minimum values are close to the ones calculated by the Kissinger method.

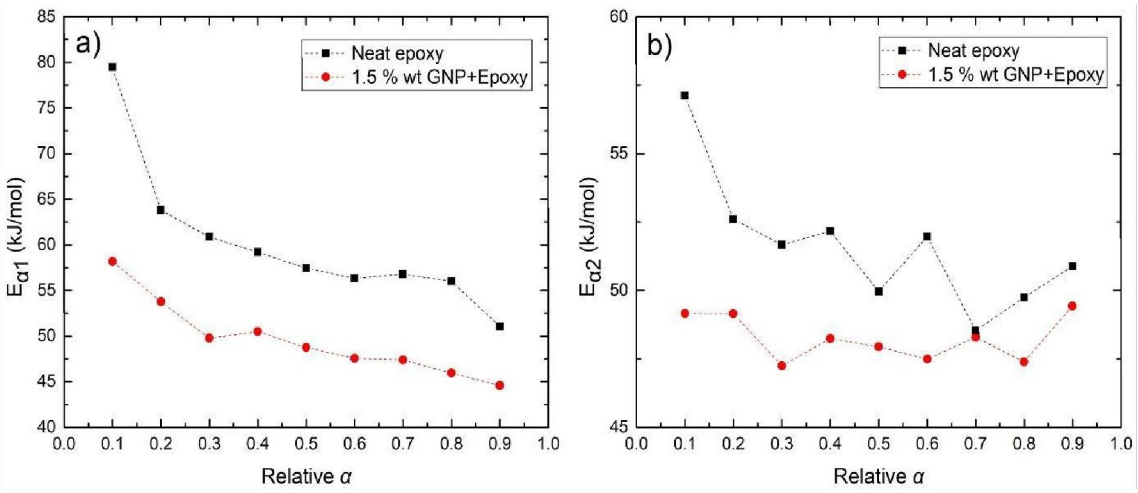

Figure 5. 17: Ozawa–Flynn–Wall's activation energy (Eα) as a function of the relative degree of cure α for a) peak-1 and b) peak-2.

5.6.3.2 Isothermal scanning method

Isothermal DSC curves at 50, 70 and 90ºC are presented in Figure 5. 18. A single exothermic peak was observed for each isothermal run which corresponds to the maximum curing rate. Figure 11 shows that the reaction rate at t=0 is zero, which indicates that the epoxy-amine reaction is non-catalysed (n-order) and then as the OH groups form facilitates the ring-opening (m-order) (autocatalysis) (Vyazovkin & Sbirrazzuoli, 1996). The peak value decreases in intensity and shifts to longer times at lower temperatures. Thus, the total curing enthalpy ΔH_{iso} at a specific temperature and time was determined.

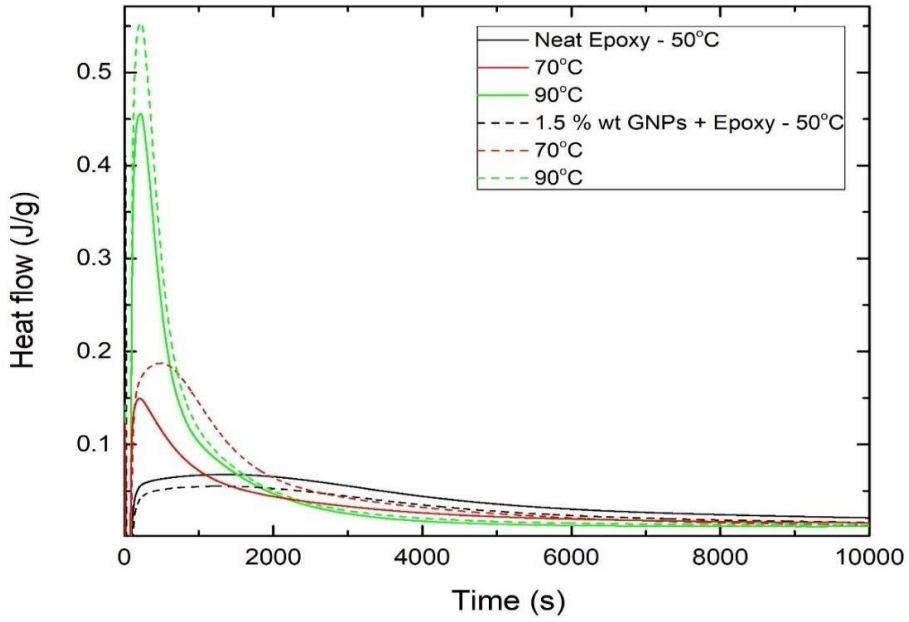

Figure 5. 18: Isothermal DSC thermograms for neat epoxy and nanocomposites containing 1.5%wt GNPs at different temperatures.

Following the isothermal scans, the samples immediately cooled at room temperature and then heated to 300ºC at 10°C/min. The curves obtained are shown in Figure 5. 19. From the data shown in Table 5.6, a relative degree of conversion α_1 can be calculated as:

$$\alpha_1 = \frac{\Delta H_{iso}}{\Delta H_{iso} + \Delta H_{dyn}} \qquad (12)$$

The degree of conversion was also calculated from equation 4, using ΔH_{tot} of 107 kJ/mol as the average enthalpy for primary and secondary reactions (de Bakker et al., 1993).

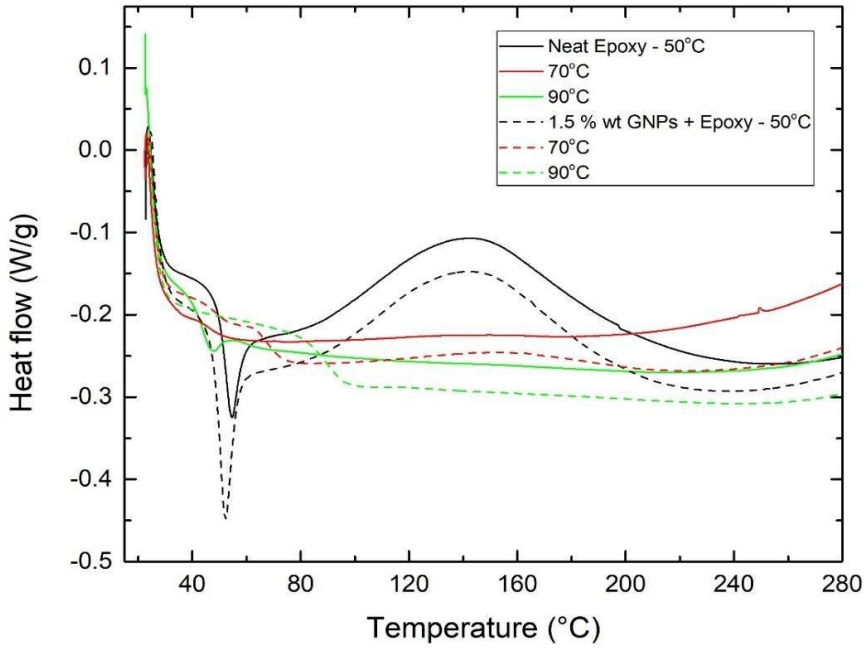

Figure 5. 19: Subsequent non-isothermal DSC scans at a constant heating rate of the partially cured samples derived from the isothermal scans.

Table 5. 6 summarises the obtained heat of curing values of the isothermal scans ΔH_{iso}, the dynamic ΔH_{dyn}, α_1 and a_2 and T_g. The isothermally cured neat epoxy and nanocomposite at 90°C did not show any residual enthalpy in the subsequent dynamic scan. As expected, α_1, a_2 and T_g increase with the increase of curing temperature. In addition, it can be seen that α increases with the addition of GNPs.

Table 5. 6: Exothermic heat of curing during the isothermal scans (*ΔHiso*), during subsequent dynamic scans (*ΔHdyn*), degree of curing (α) and glass transition temperature (T_g).

GNPs (%wt)	**T (°C)**	***ΔH*$_{iso}$*** **(kJ/mol)**	***ΔH*$_{dyn}$** **(kJ/mol)**	***α*$_1$ (%)**	***α*$_2$ (%)**	***T*$_g$ (°C)**
0	50	49.51	14.47	77.4	46.3	54.5
(neat epoxy)	70	52.17	1.57	97.1	48.7	72.1
	90	60.56	0	100	56.5	84.5
1.5	50	37.15	14.14	72.4	34.7	52.0
	70	72.82	1.14	98.4	68.0	78.5
	90	80.87	0	100	75.6	88.5

*ΔH_{ult} (kJ/mol) calculated from ΔH_{ult} (kJ/g) x 180 (=EEW of Epilok 60-566) where $\Delta H1_{ult}$ (kJ/g) refers to 1gr of epoxy determined from the experimental value divided by 0.769.

It is observed that the values of α_1 and α_2 for 1.5 %wt GNPs in the epoxy system were lower than those of neat epoxy from the isothermal DSC measurements under 50°C, which is different from the trends under 70°C and 90°C. At a low temperature of 50°C, the steric hindrance of GNPs interfered with the mobility of the reactive species. The higher temperatures of 70°C and 90°C prompted the mobility of the reacting species, increased the local density of the reacting species and prompted the curing reaction. On the other hand, the high thermal conductivity of the GNPs further weakened the retarding effect of the steric hindrance from the added GNPs. Analogous behaviour is reported in (Fu & Zhong, 2011).

5.6.4 Thermogravimetric analysis

Figure 5.20 presents TGA curves of the epoxy and the nanocomposites containing 1.5%wt GNPs. The initial decomposition temperature, which corresponds to 5% weight loss (Xiao Wang et al., 2016), decreased from 339℃ for the neat epoxy to 330℃ for the nanocomposite. This could result from the early decomposition of the interfacial epoxy chains, the cure of which was partially inhibited by the inclusion of GNPs (Xiao Wang et al., 2016). The dominant weight loss occurs above 350℃ due to the thermal decomposition of epoxy resin. The temperature of the maximum rate of degradation decreased from 392.3℃ of the neat epoxy resin to 378.6℃ in the case of the nanocomposite. The TGA curve of the GNP/epoxy nanocomposite was shifted in the range of 360-580℃ towards higher temperatures compared to that of pure epoxy, increasing the thermal stability of the cured epoxy composites. The % weight residue at 500℃ is 7.85% for the neat and 22.45% for the nanocomposite. TGA curve of the composites showed a shoulder between 450-550 degrees, which can cause additional chemical reactions. Table 5.7 illustrates thermal decomposition.

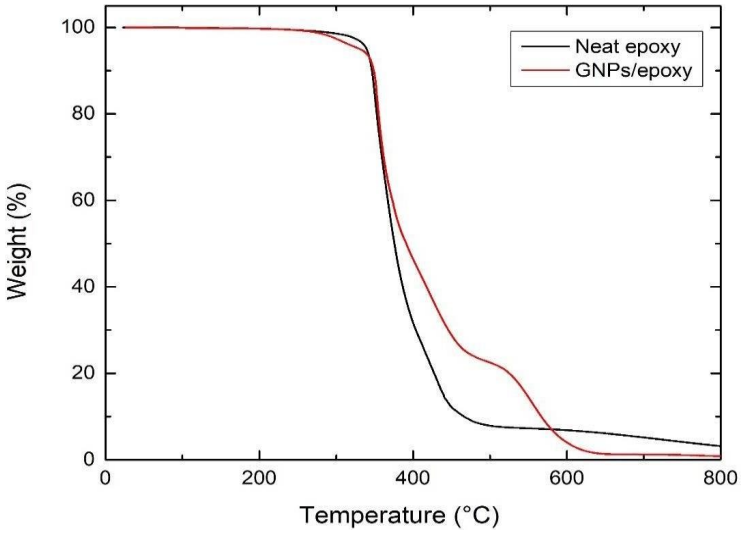

Figure 5. 20: TGA spectra were obtained from neat epoxy and cured nanocomposites containing 1.5%wt GNPs

Table 5. 7: TGA thermal decomposition.

GNPs(%wt)	ITD (°C)	T_{max} [°C]	Residue% at 450°C	Residue% at 500°C	Residue % at 600°C	Residue % at 700°C
0(neat epoxy)	339.49	392.33	12.08	7.85	6.38	5.15
1.5	330.45	378.64	28.78	22.45	3.42	1.22

5.6.5 Mechanical Properties

5.6.5.1 Tensile

Figure 5. 22 presents the mechanical properties of the prepared nanocomposites as a function of the %wt GNPs. The addition of graphene caused an increase in *E* at low filler content, which peaked at 0.5%wt and then decreased. The maximum enhancement in *E* was 37% (1.98 GPa compared to 1.58GPa of the neat epoxy). On the other hand, the addition of graphene flakes into the polymer matrix caused a reduction in *UTS* from 70.3MPa for the neat epoxy to 32.1MPa for 1%wt GNPs. The mechanical properties in graphene/epoxy nanocomposites are strongly dependent on the sample preparation conditions (dispersion steps, use of solvent etc.); hence a direct comparison with other reports is difficult. However, a similar trend in *E* and *UTS* was observed by I. Zaman et al. (Zaman et al., 2011) and Poutrel et al. (Poutrel et al., 2017), which was attributed to poor interfacial bonding between the epoxy and graphene. The dispersion of GNP in the epoxy resin is significant in tensile properties as inappropriate dispersion of nanofiller results in agglomeration or GNP irregularities that prompt a drop in the Ultimate tensile strength (Ghaleb et al., 2017). The agglomeration of nanofillers may induce an opposite effect on the properties of the nanocomposite. The dispersion status of GNP in the

epoxy resin is vital in tensile properties as inappropriate dispersion of nanofiller brings about agglomeration or GNP lumps that prompt a drop in the Ultimate tensile strength (Ghaleb et al., 2017). Figure 5. 12 shows the steel mould & dog bone specimen for tensile tests.

Figure 5. 21: Steel mould & dog bone specimen for tensile tests.

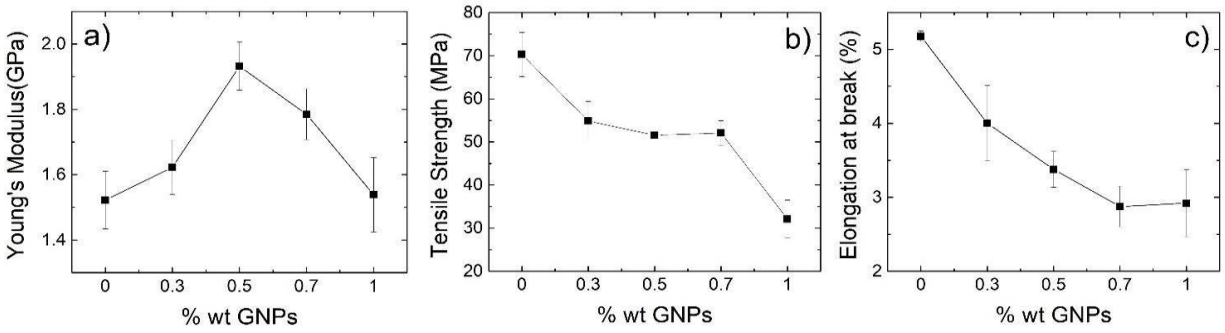

Figure 5. 22: Mechanical properties of cured nanocomposites; a) Young's Modulus, b) Ultimate tensile strength and c) Elongation at the break.

5.6.5.2 Nanoindentation

Figure 5. 23 shows that the nanoindentation test determines the hardness. Analysis of the data showed statistical differences between the samples, with the samples enriched with 0.7% GNPs showing a 9.4% improvement over the neat epoxy.

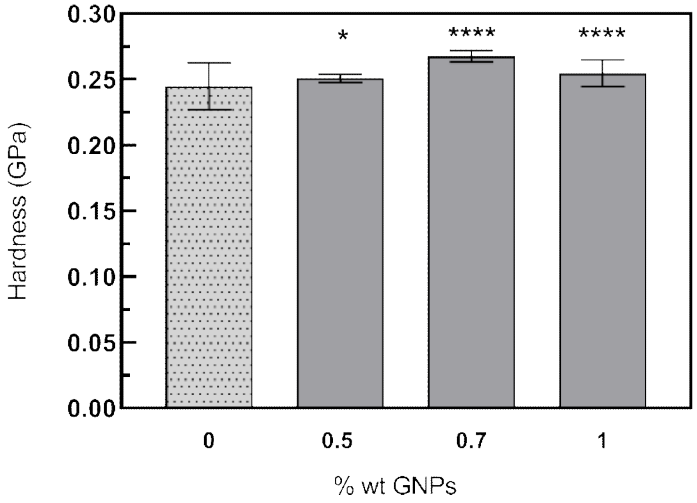

Figure 5. 23: Instrumented indentation hardness values for all samples. Values are means ±SD. P-values calculated by Tukey's range test: *p-value < 0.05; ****p < 0.0001.

Figure 5. 24 shows *E* as determined by the nanoindentation. Analysis of the data showed that there are statistical differences between the control sample and the 0.7% and 1%wt nanocomposites but not for the 0.5% wt. The improvement for the latter is in the range of 1.7% and increases to 4.5% and 5.6% for nanocomposites enriched with 0.7% and 1% GNPs. The *E* values determined by nanoindentation, although they follow the same trend, are higher than those obtained by macroscopic tensile tests. This is in agreement with other reports and is likely due to the pile-up of material around the contact impression (J. A. King et al., 2013)(Tranchida et al., 2007).

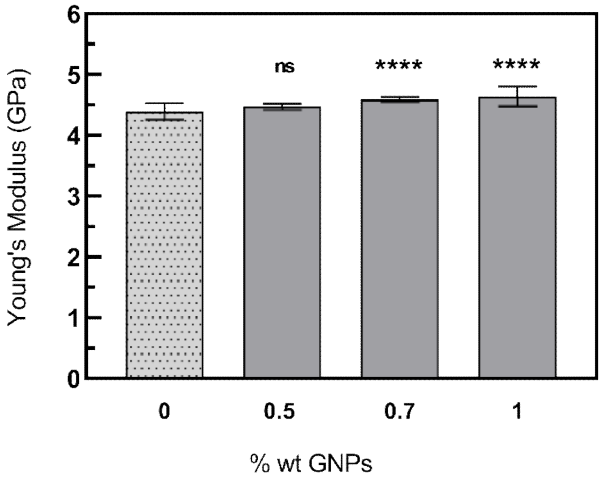

Figure 5. 24: Instrumented indentation elastic modules values for all samples. Values are means ±SD. P-values calculated by Tukey's range test: ns = no statistical significance; **p-value < 0.01; ****p < 0.0001.

5.6.6 Microscopical Investigation

Figure 5.25 shows the morphologies of the fractured surfaces of pure epoxy and GNPs/Epoxy nanocomposites which were studied using SEM to understand better the increase in mechanical properties of GNPs/Epoxy nanocomposites. Due to its brittle nature, pure epoxy has inferior mechanical qualities, as shown by the SEM image. The rougher fractured surfaces of the GNPs/Epoxy nanocomposites with 0.5 wt% graphene concentration, as illustrated in Figure 5. 25b), can be due to the strong interfacial interaction and good compatibility between the epoxy matrix and GNPs. Compared to pure epoxy, such strong interfacial interaction favours stress transfer from the epoxy matrix to the graphene, increasing *E* and *UTS*.

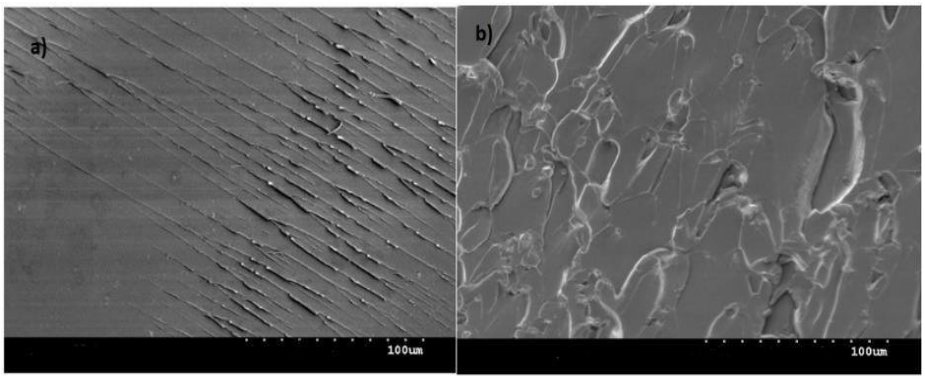

Figure 5. 25: SEM images of fractured surfaces of (a) neat epoxy, (b) nanocomposite with 0.5 wt% GNP.

5.7 Summary

This research studied the cure kinetics, thermal stability and mechanical properties of GNP/Epilok 60-566 prepared via a solvent-free facile approach by dispersing GNPs in the curing agent Curamine 32-494. DSC analysis showed that the degree of cure was increased with the addition of GNPs at high heating rates (10-20°C/min). It was found that the addition of 1.5%wt GNPs catalysed the curing reactions; E_a was found to decrease by 13.7% and by 6.6% for the reactions of the primary and secondary amino groups with the epoxy group, respectively. The GNPs also improved the thermal stability of the epoxy system in the range of 360-580°C. Young's Modulus increased in all nanocomposites containing GNPs from 0.3 to 0.7%wt with the maximum enhancement of 37% at 0.5%wt. Nanoindentation measurements showed a 9.4% improvement in hardness at 0.7%wt.

Chapter 6 Bio-based epoxy/amine reinforced with reduced graphene oxide (rGO) or GLYMO-rGO: study of curing kinetics, mechanical properties, lamination and bonding performance

The epoxy resins and the curing agents commonly used these days are derived from finite petrochemical resources. Biopolymers are becoming increasingly attractive, allowing a more sustainable production and growth. Hence, chapter 6 reports the synthesis and study of novel nanocomposites using a biobased epoxy/amine (Epilok 60-600G/Curamine 30-952) matrix, reinforced with reduced graphene oxide (rGO) or functionalised with 3-glycidoxypropyltrimethoxysilane (GLYMO-rGO). Epilok 60-600G and Curamine 30-952 have 36% and 66% bio-based renewable content, respectively. In this work, novel nanocomposites with a biobased epoxy/amine (Epilok 60-600G/Curamine 30-952) reinforced with rGO or GLYMO-rGO are prepared and studied; i.e. their cure kinetics, thermal stability, mechanical properties, SEM characterisation and development of 3-phase (graphene/carbon fibre/epoxy) for bonding performance. This research will help to improve joining technology towards a multi-material lightweight design. The GRMs contain a low oxygen content that aid dispersion into the low viscosity liquid Curamine without using a solvent. The cure kinetics of the neat epoxy/Curamine system (100/85 w/w excess of amine) and the GRM/epoxy/Curamine system (1.5%wt of GRM) are studied by Differential Scanning Calorimetry (DSC) under nonisothermal conditions at different heating rates (2, 5, 10 and 20°C/min) and under isothermal conditions (50, 70 and 90°C). In addition, the mechanical properties *E* and *UTS* ofthe neat resin and nanocomposites (0.05-0.7wt% GRM) are determined. The GRM enhanced resin (0.05-0.5wt% GRM) was used as a matrix system to prepare CFRP laminates and as an adhesive to prepare lap shear joints; CFRP/CFRP (similar adherents), and CFRP/Aluminium (dissimilar adherents).

6.1 Materials

Graphite powder was obtained from NGS-Naturgraphit. Concentrated H_2SO_4, $KMnO_4$, sodium nitrate, hydrochloric acid and ascorbic acid were purchased from Cofarcas (Spain). Epilok 60-600G resin and Curamine 30-952 hardener was provided by Bitrez (UK). This is a specially formulated two-part epoxy system designed for the bonding and lamination of composite parts. The system has components derived from biomass, such as plants and/or trees; Epilok 60-600G and Curamine 30-952 have 36% and 66% bio-based renewable content, respectively.

The usage of biocomposites in automotive applications has several advantages. Due to their inherent lightness, composites typically result in lower fuel consumption and greenhouse gas emissions. The superior acoustic and thermal characteristics of biocomposites over composites derived from non-renewable sources make them perfect for use in automotive interior components. In the automotive industry, biocomposites currently have a wide range of potential uses. Their characteristics make them excellent for the production of non-structural interior parts such as wood trim, seat backs, seat fillers, interior panels, headliners, dashboards, and thermoacoustic insulation (*Biocomposites in the Automotive Industry: Potential Applications and Benefits - Renewable Carbon News*, n.d.). Scientist Nicholas Rorrer of the National Renewable Energy Laboratory (NREL) said. "By using bio-based feedstocks instead of petrochemical feedstocks, we can drastically retool their chemistries without requiring additional energy. Rorrer continued. As a result, we are able to more precisely, affordably, and successfully design innovative materials with beneficial performance and environmental effects (*Plant-Based Epoxy Enables Recyclable Carbon Fiber | Plasticstoday.Com*, n.d.). Epilok 60-600G has low to moderate viscosity (100-145 Poise evaluated at 25°C) and mean epoxy equivalent weight (EEW=185 G/eq). It has CAS number 25068-38-6, which corresponds to the chemical structure shown in Fig.1. Its number average molecular weight is lower than 700. Curamine 30-952 is a liquid polyaminoamide-based curing agent with a small

amount (1-5%) triethylenetetramine. It has a low-moderate viscosity (100-145 Poise at 25°C). The Active Hydrogen Equivalent Weight (AHEW) of Curamine 30-952 is 100. It contains a 66% bio-based polyaminoamide curing agent. The mix ratio (parts per hundred of epoxy resin) by weight for a stoichiometric ratio is given by the relation: Mix stoichiometric ratio per 100 parts of epoxy resin= (AHEW of Curamine)/(EEW of epoxy resin)x100. For the above system, this ratio is 100:54. However, the provider suggests using a mix ratio of 100:85, that is, an excess of amine and this ratio was used in the present work. The manufacturer reports a higher level of amine hardener that increases the flexibility and toughness of the cured epoxy resin. Carbon Fibre Biaxial Tape 110mm wide, 410g per m² with +/- 45° fibre orientation was obtained from east coast fibreglass supplies, UK. Aluminium EN AW-7075 T6 was supplied by Alnan Aluminium Co Ltd, China.

6.2 Characterisation of GRM flakes

Raman spectra were recorded on a confocal Renishaw inVia Raman microscope at room temperature. The system is equipped with a CCD detector and a holographic notch filter, using an excitation wavelength of 532 nm. Scans were acquired from 1000 to 3500 cm^{-1}, performing maps of 25 spectra on a sample pellet prepared by pressing GRM powder in a 13 mm diameter mould at 5 Tonne/cm^2. X-ray photoelectron spectroscopy (XPS) analysis was carried out using an ESCAPROBE P (Omnicron) with non-monochromatised MgK radiation (1253.6 eV) spectrometer; the X-ray source operated at 300 W. The specific surface area (SSA) of GRMs was determined by Brunauer-Emmett-Teller (BET) using autosorb-6 Quantachrome instruments. The samples were degassed in an autosorb degasser (Quantachrome instruments) at 250ºC for 8h. Transmission electron microscopy (TEM) was performed using a JEOL microscope (JEM-2010), equipped with INCA Energy TEM 100 X-ray detector and a GATAN camera (SC600ORIUS). GRM samples were dispersed in isopropyl alcohol, then sonicated with a Hielscher UP200S sonicator for 15 minutes and drop casted onto copper grids. Scanning

electron microscopy (SEM) imaging was performed on GRM flakes using a Hitachi S-2400 (18kV) with XFash detector.

6.3 Preparation, characterisation and testing of GRM/polymer nanocomposites

This research initially identified the optimum dispersion of GRMs into Epilok /Curamine. GNPs were first attempted to disperse into epilok 60-600G using bath sonication process for 20min at room temperature, but without success. Secondly, GRMs were attempted to disperse in Curamine 30-952, which gave a much more uniform dispersion (Figure 6. 1). GRMs in powder form were first mixed with preheated (50°C) Curamine using a bath ultrasonicator (Elmasonic P300) for 20 min at 50°C. Following ultrasonication, Epilok was added via mechanical stirring for 5 min at a ratio Epilok:Curamine of 100:85. The mixture was degassed for 10 min to remove any trapped air. These GRM/Curamine/Epilok nanocomposites were prepared at different GRM content (wt%) and were used for DSC, thermogravimetric analysis (TGA), tensile and lap shear tests, as described in the next section. The overall methodology followed is summarised in Figure 6. 2.

Figure 6. 1: Dispersion quality of GRMs with epilok and curamine.

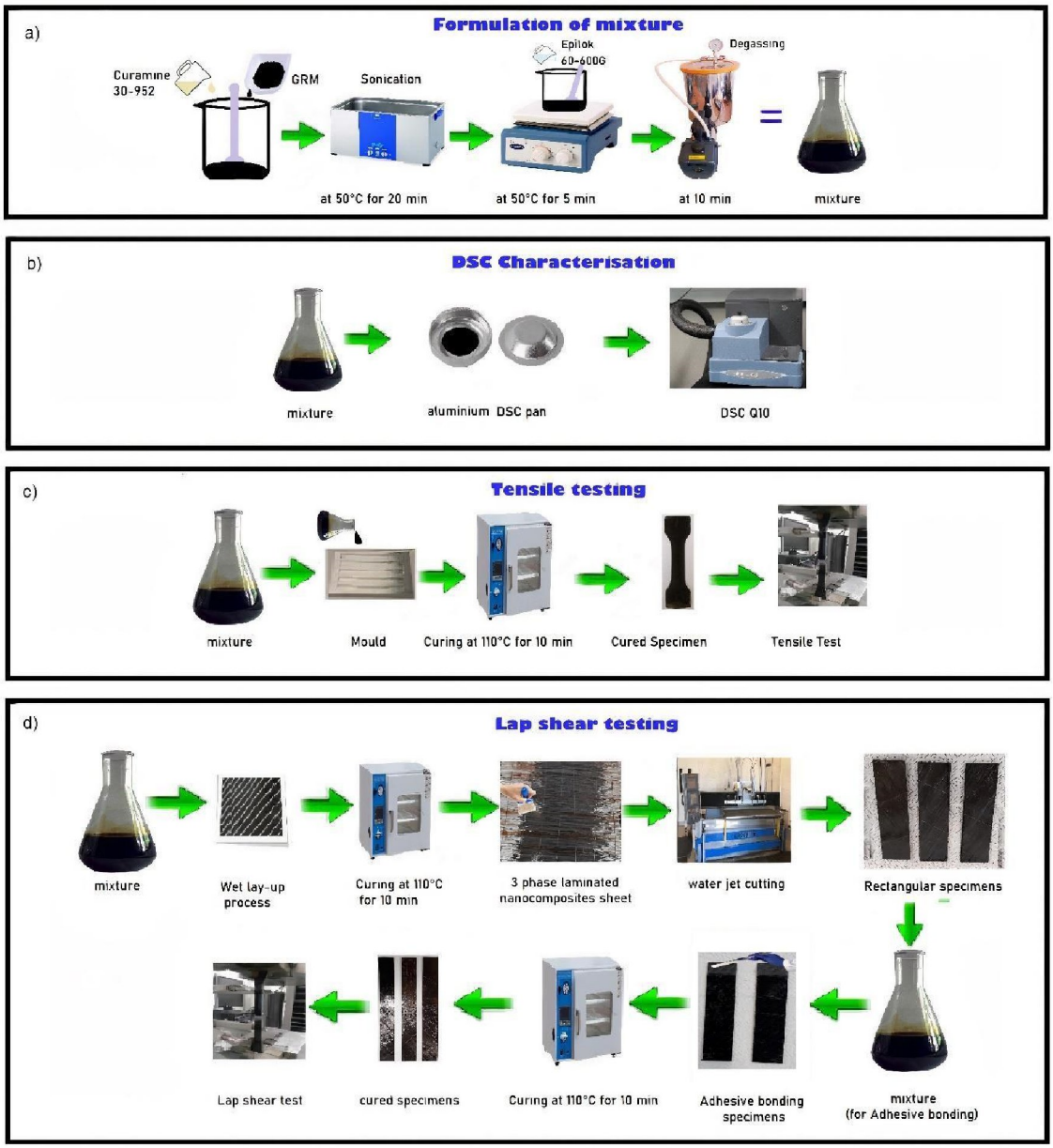

Figure 6. 2: Methodology followed for the Preparation and testing of nanocomposites: a) preparation of GRM/amine/epoxy mixture, b) curing study by DSC, c) fabrication of specimens and tensile testing, d) fabrication of laminates, lap shear joints and lap shear testing.

6.4 Characterisation Techniques

6.4.1 DSC Characterisation

The DSC study of the neat epoxy system and GRM/amine/epoxy nanocomposites was carried out using a DSC Q10 from TA Instruments (Figure 6 . 2b). The GRM content in these samples was 1.5 wt%. Samples about 10-15mg were weighted and sealed into aluminium hermetic DSC pans. The sample pan was then put in the DSC cell previously maintained at room temperature. All DSC runs were carried out under an N2 atmosphere. Nonisothermal scans were recorded from 20 to 300°C with four heating rates of 2, 5, 10 or 20°C/min. Isothermal scans were recorded at 50, 70 or 90°C. The DSC cell was quickly heated (50°C/min) to the desired cure temperature and then isothermally held at that temperature for 3h. Following this isothermal scan, the DSC cell was immediately cooled down to room temperature and then heated to 300oC at 10°C/min to obtain the residual heat of curing. This was determined by integrating over the exothermic peak with respect to time. The total heat of curing recorded isothermally (ΔHiso) and the residual heat of curing recorded dynamically (ΔHdyn) were used to determine the degree of curing (α) at various isothermal cure temperatures.

6.4.2 Tensile testing

Specimens were prepared for tensile tests (~15g/per sample) with rGOs content 0.05, 0.1, 0.3, 0.5 or 0.7 wt%. After the addition of Epilok resin into the GRM/Curamine mixture, mechanical stirring was applied. Aluminium moulds for tensile specimens were prepared using a CNC milling machine. The final mixture was poured into the moulds, degassed for 10min in a vacuum chamber and then cured for 10min at 110℃ in an oven. Dumbbell-shaped specimens were obtained, 10mm wide and 4mm thick for tensile testing. Tensile tests were performed using a universal testing machine Zwick Roell Z010 with a load cell of 10 kN at room temperature and a 5mm/min crosshead speed. The mechanical properties, *E* and *TS,* were determined according to the ASTM D638 standard.

6.4.3 SEM Characterisation

Specimens were submerged in liquid nitrogen and shattered. Samples were collected and mounted on an aluminium SEM specimen stub by using carbon adhesive discs; stubs and carbon adhesives were purchased from Agar Scientific, UK. A thin metal layer of around 8 nm was sputtered using a Quorum SC7620 Mini Sputter Coater with a gold/palladium target.

6.4.4 Fabrication of CFRP laminates lap shear joints and lap shear testing

Laminate specimens (3 plies) were prepared for lap shear testing, using ~55g of neat epoxy or 0.1 wt% GRM/epoxy mixture with 55g carbon fibres/per sheet. After the addition of the Epilok resin into the GRM/Curamine mixture, mechanical stirring was applied. The final mixture was applied onto the carbon fibre sheet via the wet lay-up process and then cured for 10min at 110℃. Rectangular shape specimens were cut 101mm long and 25.4mm wide, and 1.6mm thick using water jet cutting to be used as adherents. For the adhesive part of the lap joints, the same Epilok/Curamine system was used (with and without GRM) to bond the laminate

adherents. CFRP surfaces were rugged with sandpaper P60 and Aluminium surfaces with silicon carbide 1200. Then the surfaces were wiped with a dry cloth to remove particles and cleaned with acetone. Then the mixture of GRM/Curamine was applied to the substrate surfaces bonding them together and cured for 10min at 110℃. The joints' overlapping area was 12.7 mm x 25.4mm according to the ASTM D5868 standard. The thickness of the laminate sheet was 1.6mm, and the thickness of the adhesive was 0.2mm. The joints were tested using a Zwick Roell Z010 at room temperature with a 5mm/min crosshead speed.

6.5 Results and Discussion

6.5.1 Characterisation of GRMs

The following GRM characterisation was kindly provided by our collaboration (Sheikh Rehman et al., 2022). Figure 6. 3 shows the Raman spectra of the prepared rGO and GLYMO-rGO. It shows an intense D band (~1350 cm−1), which confirms lattice distortions, and the Gapp band (~1585 cm−1), which corresponds to the overlap of G and D' bands. Two-dimensional band (~2700 cm−1) and D+D' and 2D' bands, which are different overtone and combination bands of the previous ones, show very small intensity, in alignment with stage 2 defects. GLYMO-rGO shows higher ID/IGapp and lower values of full width at half maximum (FWHM) of D and G peaks when they are compared with the starting rGO (Table 6.1). This fact is in agreement with a decrease in oxygen content during the functionalisation of rGO (Gómez et al., 2017). Due to the low intensity in the second-order bands in agreement with highly defective rGO materials in Stage 2 defects, any tendency can be observed for I2D/ID and IDD'/I2D.

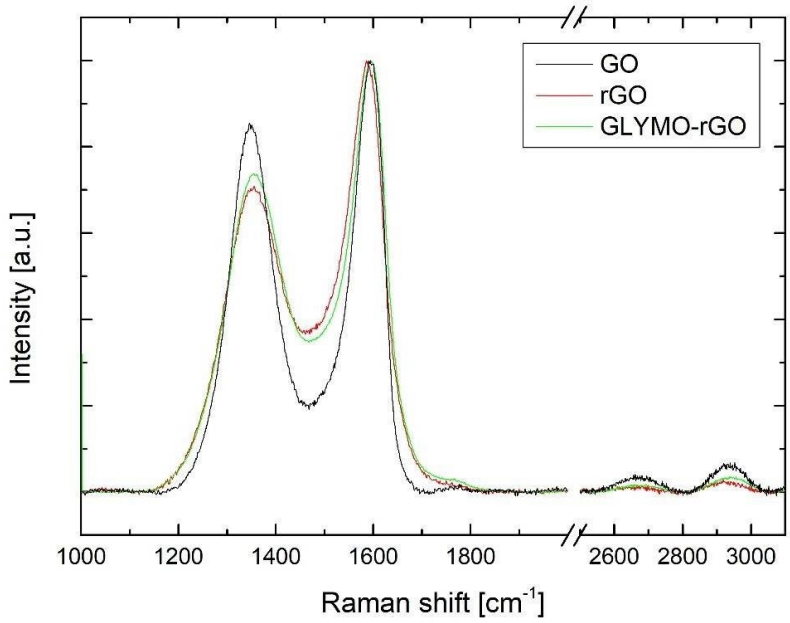

Figure 6. 3: Raman spectra of GO, rGO and GLYMO-rGO (Rehman et al., 2022).

Table 6. 1: Characteristic Raman peaks and intensity ratios for the GRMs used (Sheikh Rehman et al., 2022).

GRM	**D (cm^{-1})**	**G_{app} (cm^{-1})**	**I_D/I_{Gapp}**	**$FWHM_D$**	**$FWHM_G$**	**I_{2D}/I_D**	**$I_{DD'}/I_{2D}$**	**D'*inf***	**D'*inf*-G_{app}**
rGO	1363.9	1581.5	0.68	180.3	101.8	0.015	2.29	1588.7	3.89
GLYMO-rGO	1359.6	1588.0	0.74	146.6	92.8	0.010	2.44	1595.8	7.80

As mentioned by King et al. (A. A. K. King et al., 2016), the unreliability of the relationship between the ID/IGapp due to the overlap of G and D' peaks limits the utility of this relationship as a measure of the density of defects in rGO; for that reason, we have combined ID/IGapp, FWHM D and FWHM G. A second-order transition band 2D' has been recently

used to calculate the inferred energy of D' (D'inf) and the differences between 2D' (or D'inf) and Gapp.

Raman spectroscopy findings are also in agreement with those of XPS spectroscopy (Table 6.2). Higher C/O ratio and lower FWHM of D and Gapp were observed for GLYMO-rGO. The relation between D'-Gapp and the C/O ratio obtained by XPS is in good agreement with the data obtained by King et al. and by us for other rGO materials (Gómez et al., 2017). (D'inf-Gapp = 3.89 (rGO) and 7.8 (GLYMO-rGO) C/O 8.1 (rGO) and 12.8 (GLYMO-rGO)). The Si 2p peak originated from GLYMO confirms further the covalent functionalization of rGO with GLYMO. Moreover, the C/O ratio increased in the case of GLYMO because of the reaction of hydroxyl and epoxy groups containing oxygen atoms with groups of rGO. Figure 6.4 illustrates the (a) XPS spectrum of GLYMO-rGO, (b) high resolution deconvoluted O1s and (c) deconvoluted C1s spectra of GLYMO-rGO (Rehman et al., 2022).

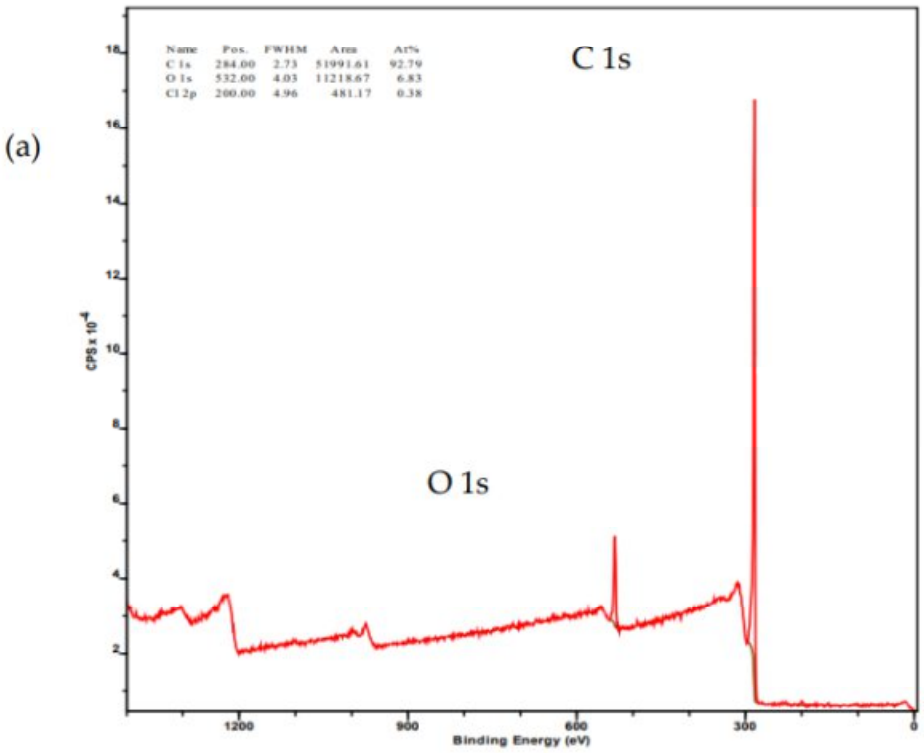

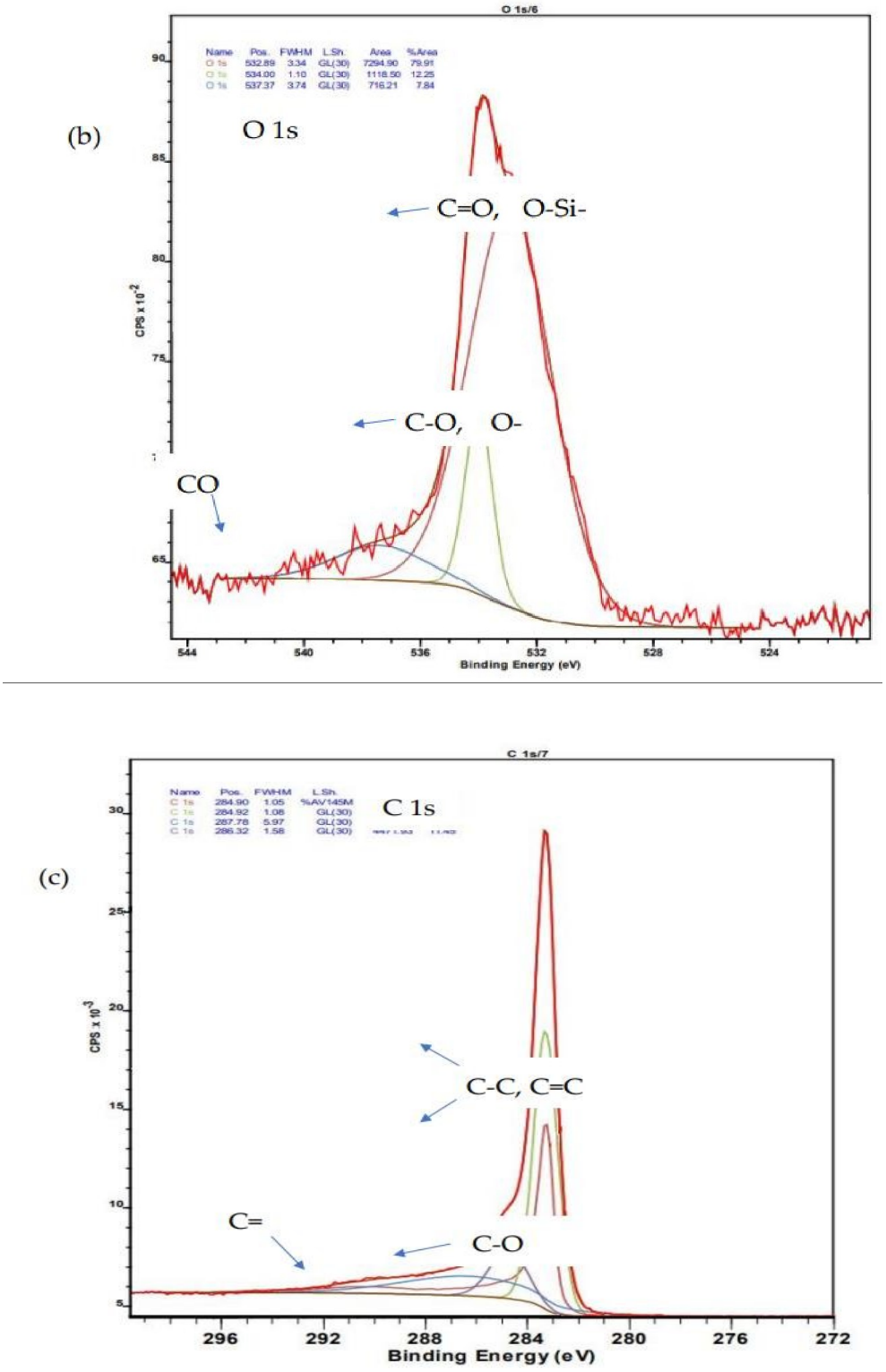

Figure 6. 4:(a) XPS spectrum of GLYMO-rGO, (b) high resolution deconvoluted O1s and (c) deconvoluted C1s spectra of GLYMO-rGO(Rehman et al., 2022).

Table 6. 2: Results obtained by XPS spectroscopy for GRMs (Sheikh Rehman et al., 2022).

GRM	C 1s (%)	O 1s (%)	Si 2p (%)	C/O
rGO	88.7	11.0	-	8.1
GLYMO-rGO	92.5	7.2	0.45	12.8

rGO showed high SSA, 778.4 m2/g, while GLYMO-rGO showed an important drop in surface area, 146.1 m2/g, in agreement with the lower accessible area due to compaction during the filtration process (F. Guo et al., 2014), producing non-accessible area loss. TEM imaging in Figure 6. 4a obtained from typical rGO flakes revealed low flake thickness in the range of 1 nm, in agreement with the large SSA observed. SEM imaging was used to assess the lateral size of the flakes and was found to be in the 20–50μm range (Figure 6. 7b). Further characterisation of GRMs, i.e., Figure 6.5 and 6.6 shows TEM micrographs obtained from rGO flakes and TEM micrographs of GLYMO-rGO respectively (Rehman et al., 2022). Figure 6.8 shows X-Ray diffraction patterns obtained from GO, rGO and GLYMO-rGO and figure 6.9 illustrates BET isotherms for rGO and GLYMO-rGO (Rehman et al., 2022).

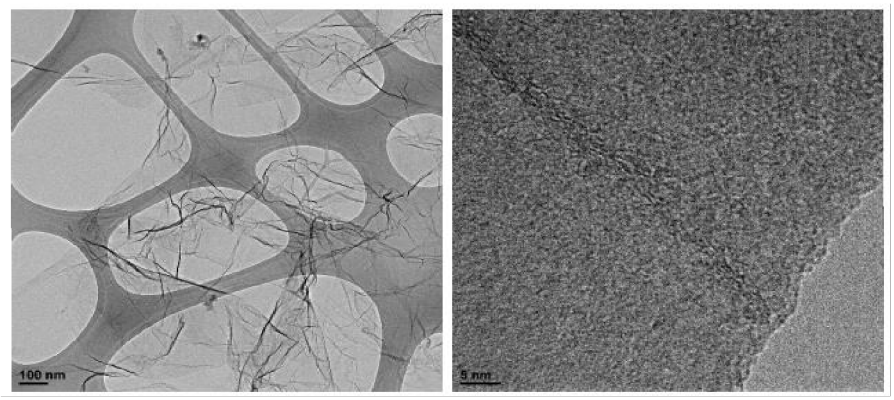

Figure 6. 5: TEM micrographs obtained from rGO flakes (Rehman et al., 2022).

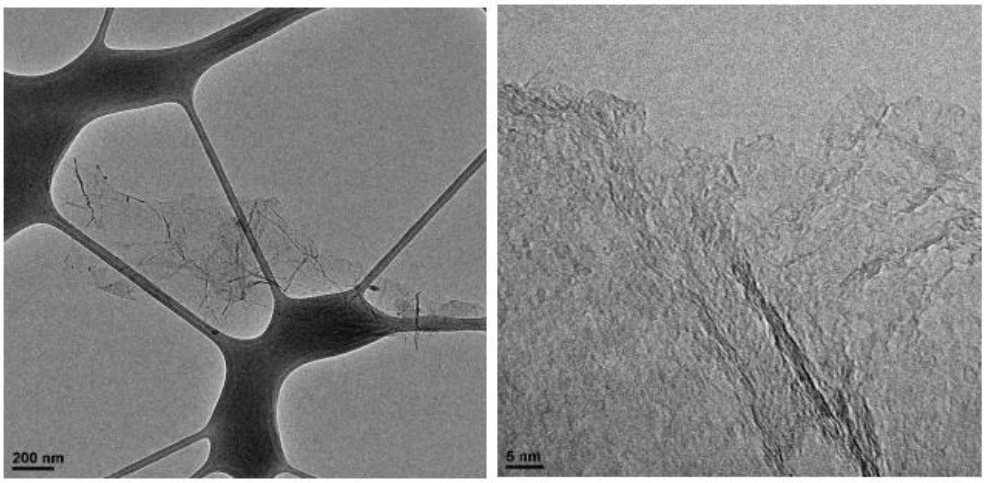

Figure 6. 6: TEM micrographs of GLYMO-rGO (Rehman et al., 2022).

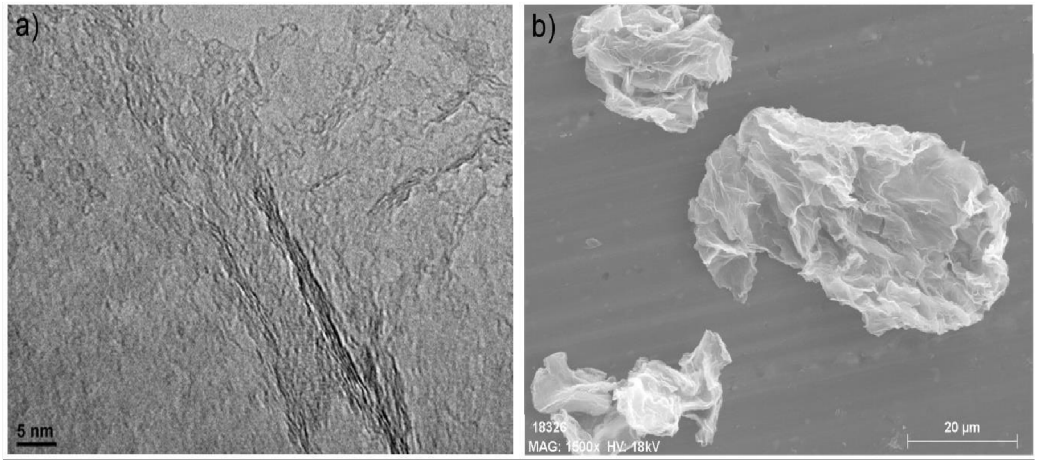

Figure 6. 7 a) TEM image obtained from typical rGO flakes and b) SEM representative image obtained from GLYMO-rGO flakes (Rehman et al., 2022).

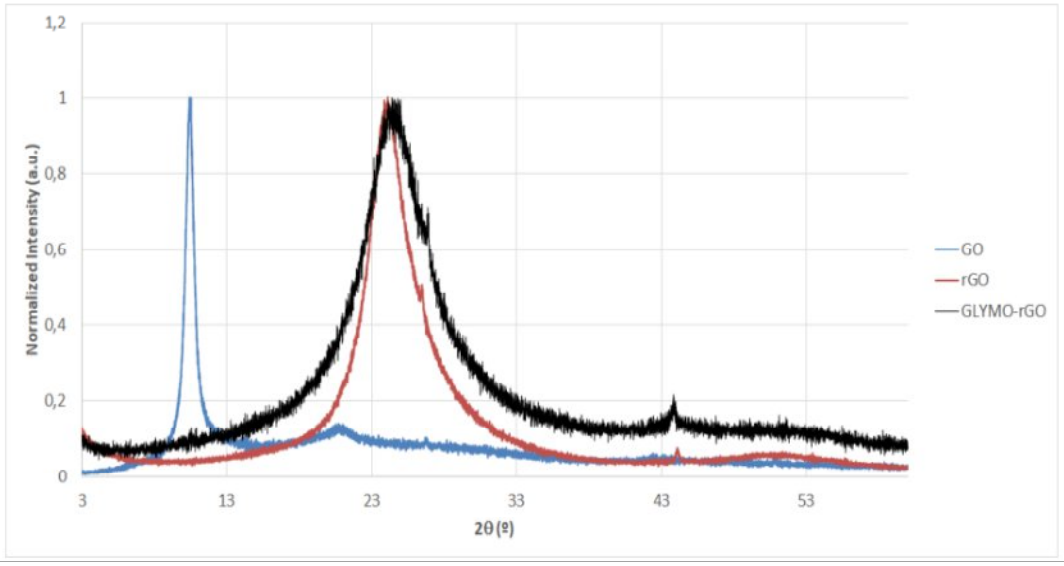

Figure 6. 8: X-Ray diffraction patterns obtained from GO, rGO and GLYMO-rGO flakes (Rehman et al., 2022)

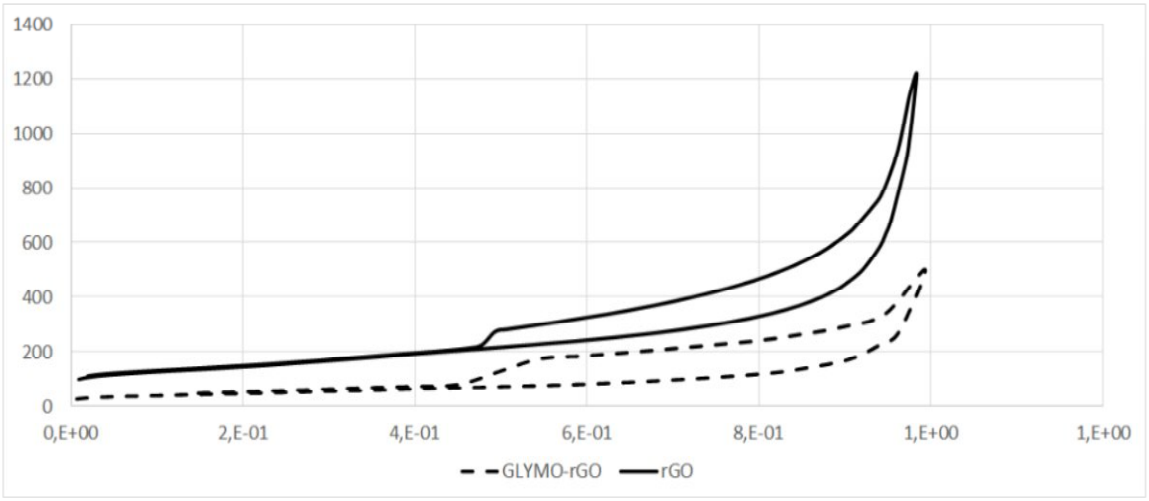

Figure 6. 9: BET isotherms for rGO and GLYMO-rGO (Rehman et al., 2022)

6.5.2 Curing study of GRM/polymer nanocomposites by DSC

6.5.2.1 Nonisothermal curing scanning method

The nonisothermal dynamic scanning method involves heating the sample at a constant rate over the desired temperature range. Figure 6. 10 shows the dynamic scans with different φ, 2, 5, 10

and 20ºC/min for neat epoxy with 1.5 wt% rGO or 1.5 wt% GLYMO-rGO.The initial curing temperature (T_{init}), final (T_{final}) and peak temperatures ($T_{peak\ -1}$) shift to higher values with increasing heating rate φ (Table 6.3). The inclusion of graphene does not cause any discernible peak shift. It may be useful to specify processing parameters like T_{init} and T_{final}; for example, a practical definition of T_{final} could be the minimum cure temperature at which total (α=1) or final (α=α_{final}) conversion takes place in a reasonable time. When a reaction releases heat, or is exothermic, the equilibrium will shift to the left as the temperature rises, leading the system to absorb heat and partially offsetting the temperature increase. When the temperature rises, endothermic processes have the opposite effect and are displaced to the right.

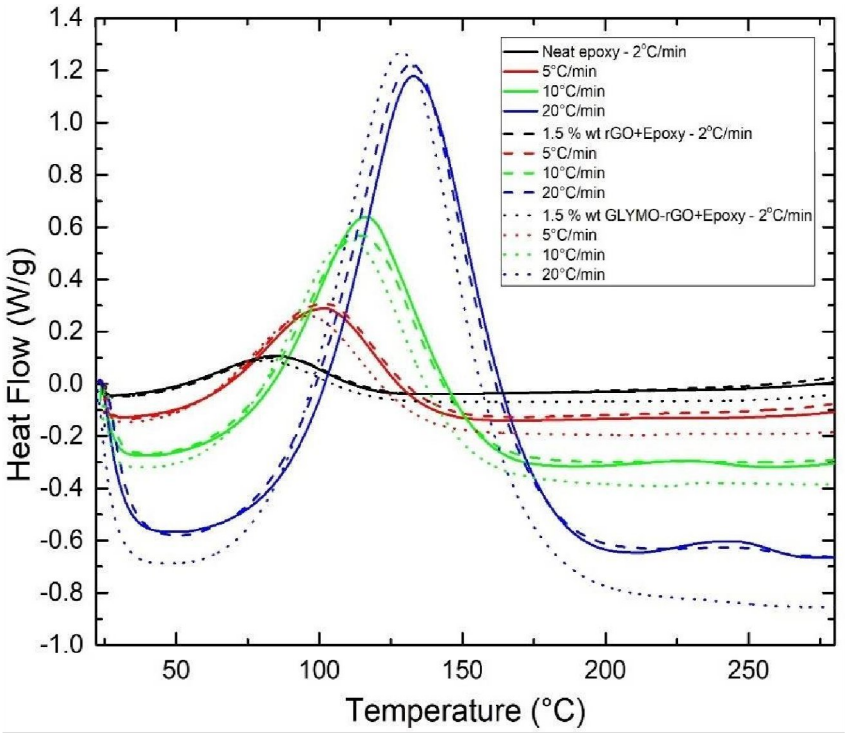

Figure 6. 10: Dynamic scans with different heating rates 2, 5, 10, 20°C/min for neat epoxy with 1.5 wt% rGO or 1.5 wt% GLYMO-rGO.

The results obtained for the initial cure (or onset) temperature (T_{init}), peak cure temperature (T_p), final cure temperature (Tf_{inal}), ultimate heat of curing (ΔH_{ult}) and degree of curing (α) for the studied samples under different heating rates are presented in Table 6. 3. It is observed that for all systems studied, the T_{init}, T_p and T_{final} increased with increasing φ because lower φ offered longer time for chemical groups to react, while at faster φ, less time is needed for the reaction of the groups. Figure 6. 11 shows the dynamic scans of different heating rates 2-20°C/min for neat epoxy and with 1.5wt% rGO and 1.5wt% f-rGO(GLYMO) for characteristic kinetic parameters of curing process: characteristic temperatures, exothermic heat of curing (ΔH) and degree of curing. Figure 6. 12 represents the area and degree of cure at different heating rates for neat epoxy and nanocomposites containing 1.5%wt rGO and 1.5%wt f-rGO(GLYMO).

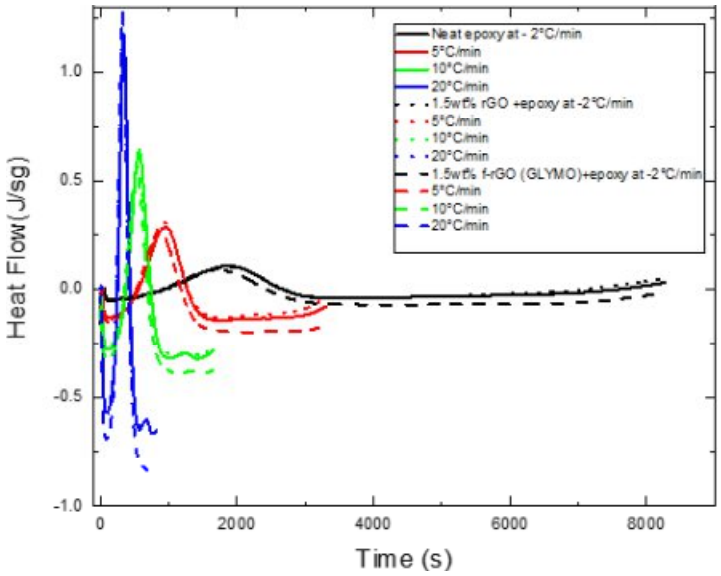

Figure 6. 11: Dynamic scans of different heating rates 2-20°C/min for neat epoxy and with 1.5wt% rGO and 1.5wt% f-rGO(GLYMO).

Table 6. 3: Characteristic kinetic parameters of curing process: characteristic temperatures, exothermic heat of curing (*ΔH*) and degree of curing (α) obtained under nonisothermal conditions with different heating rates φ.

GRM (wt%)	***φ*** **(°C/min)**	T_{init} **(°C)**	T_{final} **(°C)**	T_p **(°C)**	ΔH_{ult} [a] **(J/g)**	ΔH_{ult} [b] **(kJ/mol)**	***α*** **(%)**
0 (neat epoxy)	2	28.72	276.52	83.10	173.35	59.38	55.5
	5	30.12	283.06	100.56	243.62	83.46	78.0
	10	33.98	281.96	114.53	275.57	94.40	88.2
	20	42.025	258.16	132.83	275.80	94.48	88.3
1.5 rGO	2	27.77	278.22	84.71	193.98	66.45	62.1
	5	32.46	277.66	99.49	243.72	83.49	78.0
	10	36.74	284.59	112.78	268.47	91.97	86.0
	20	44.75	283.19	130.84	287.36	98.44	92.0
1.5 GLYMO-rGO	2	28.29	276.02	79.07	212.13	72.67	68.0
	5	30.15	284.91	93.99	276.61	94.76	88.6
	10	33.98	283.92	109.12	290.26	99.44	92.9
	20	37.74	287.78	127.35	312.32	106.99	100

a. ΔH_{ult} (J/g) refers to 1 gr mixture of epoxy determined from the experimental value divided by 0.540.

b. ΔH_{ult} (kJ/mol) calculated from ΔH_{ult} (kJ/g) x 185 (=EEW of Epilok 60–600G).

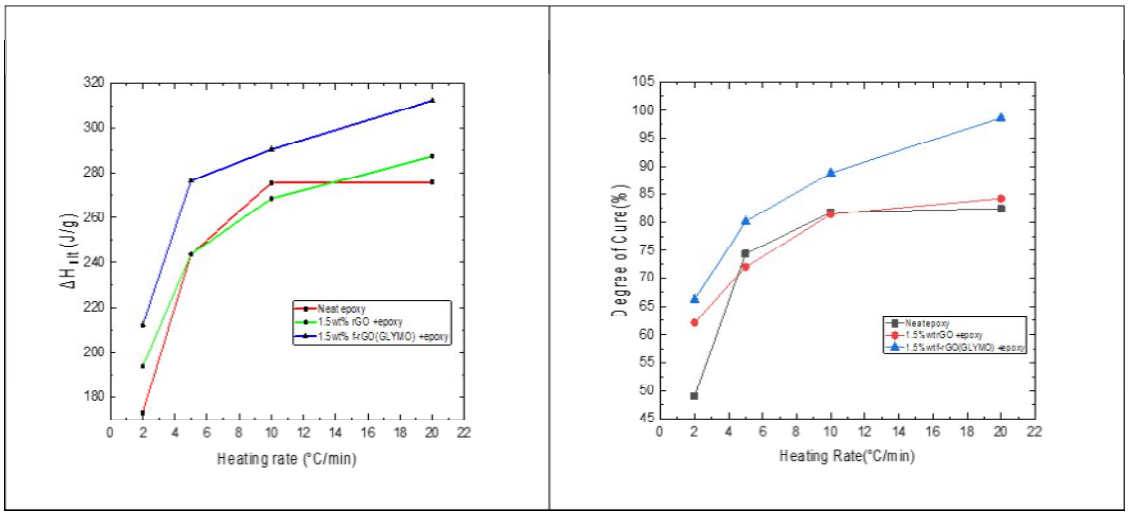

Figure 6. 12: Area and degree of cure at different heating rates for neat epoxy and nanocomposites containing 1.5%wt rGO and 1.5%wt f-rGO(GLYMO).

The DSC curves shift to a higher temperature to compensate for the reduced time (M. G. Prolongo et al., 2016c). T_p of 1.5 wt% rGO or GLYMO-rGO is slightly lower than T_p of neat epoxy. The ultimate heat of curing ΔH (J/g) was determined by the integration of the exothermic peak. Taking into account that we have used a ratio of 100 g epoxy resin to 85g of amine, 1 g of the mixture contains 0.540 g of epoxy resin, the value of ΔHult (J/g)epoxy was calculated from the experimental value (J/g)mixture divided by 0.540. Since the EEW of epoxy resin used is 185 g/eq (e.g. 185g of Epilok 60–600G is 1 gmol of epoxy groups), the value of ΔHult (kJ/mol)epoxy was calculated by ΔHult (kJ/g)epoxy x 185. ΔHtotal measured for several amine-epoxy systems and model reactions was found to be reasonably constant and equal to 107 ± 4 kJ mol of epoxide; this value may be used as a standard value for analysing amine-epoxide systems (Verchère et al., 1990)(Prime, 1997). The values of Ea were determined graphically by the Kissinger method, as described in our previous communication (S. Rehman et al., 2020). E_a is the minimum energy requirement that must be met for a chemical reaction to occur. E_a was found for the neat epoxy to be 49.68± 1.65 kJ/mol. The

addition of 1.5 wt% of rGO and rGO-GLYMO did not significantly affect E_a with values 53.88± 3.34 and 49.48± 2.89 kJ/mol, respectively. Table 6. 4 illustrates the E_a.

Table 6. 4: For Activation energy.

GRM wt%)	**Heating Rate β [°C/min]**	**Tpeak-$_1$ [°C]**	**ln(β/ Tpeak-$_1$^$_2$) [°K]**	**1/ Tpeak-$_1$ [°K]**	**E_{a1} [kJ/mol]**
0 (neat epoxy)	2	83.10	-11.05	.002807	-49.68± 1.65
	5	100.56	-10.23	.002675	
	10	114.53	-9.61	.002579	
	20	132.83	-9.01	.002463	
1.5 rGO	2	84.71	-11.06	.002794	-53.88± 3.341
	5	99.49	-10.23	.002683	
	10	112.78	-9.60	.002591	
	20	130.84	-9.00	.002475	
1.5 GLYMO-rGO	2	79.07	-11.03	.002839	-49.48± 2.892
	5	93.99	-10.20	.002723	
	10	109.12	-9.58	.002615	
	20	127.35	-8.98	.002496	

6.5.2.2 Isothermal scanning method

The isothermal DSC curves obtained at 50, 70 and 90°C and the subsequent dynamic scans are shown in Figure 6. 13 and Figure 6. 14, respectively. From these curves, the total curing enthalpy ΔH_{iso} at a specific temperature and time was determined (Table 6. 5). Following the isothermal scans, the samples immediately cooled at room temperature and then heated to 300°C at 10°C/min, and the dynamic ΔH_{dyn} were determined. From the data are shown in Table 6. 5, a relative degree of conversion α_1 can be calculated as:

$$\alpha_1 = \frac{\Delta H_{iso}}{\Delta H_{iso} + \Delta H_{dyn}}$$

The degree of conversion α_2 (Table 6.5) was calculated from eq. 9, using ΔH_{tot} of 107 kJ/mol is the average enthalpy for primary and secondary amine reactions (de Bakker et al., 1993).

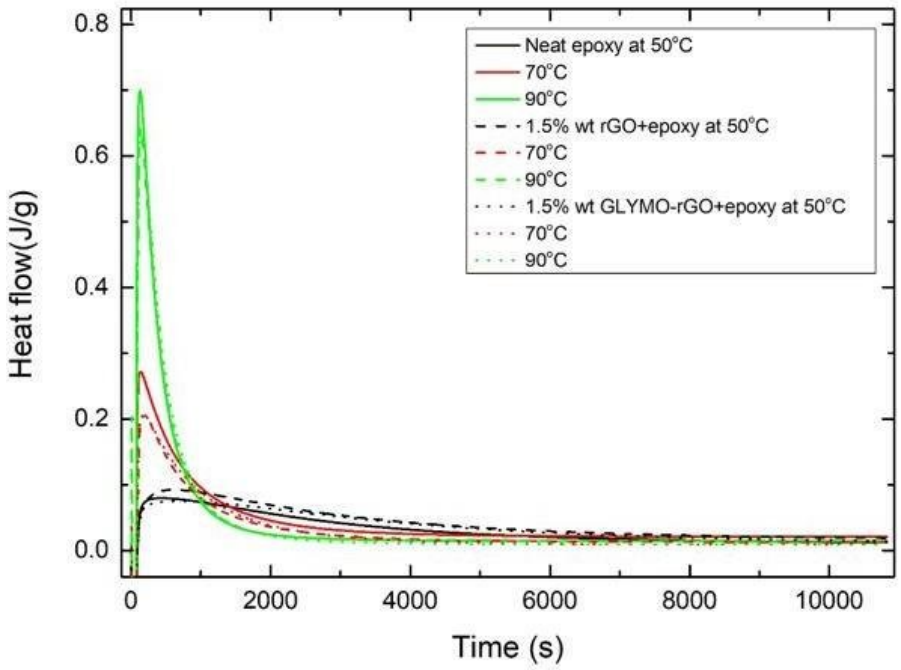

Figure 6. 13: Isothermal DSC thermograms for neat epoxy and nanocomposites containing 1.5 wt% rGO at different temperatures.

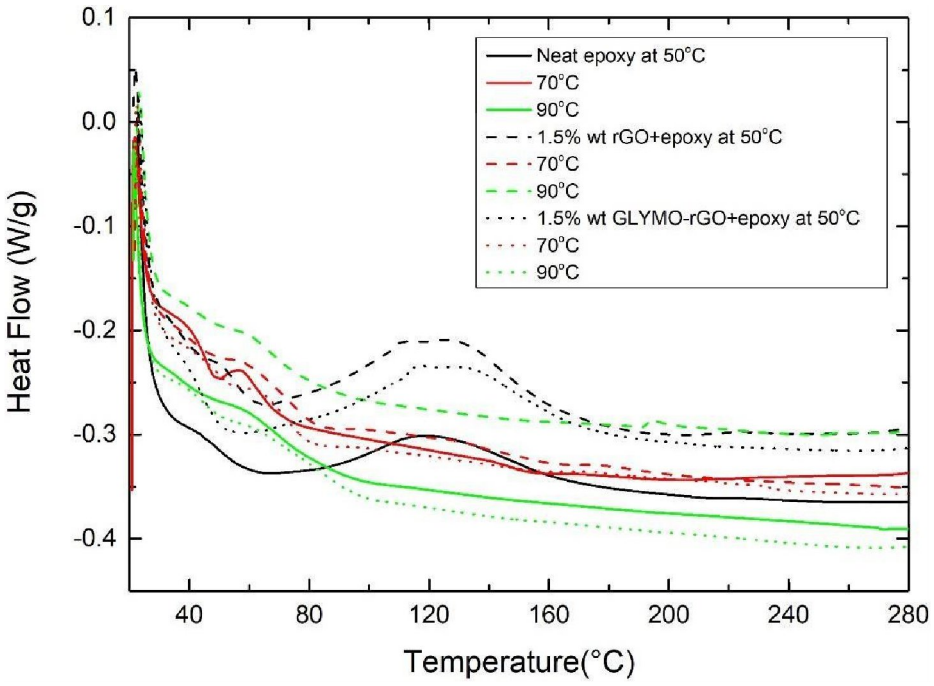

Figure 6. 14: Subsequent nonisothermal DSC scans at a constant heating rate of the partially cured samples derived from the isothermal scans.

All samples isothermally cured at 90°C did not show any residual enthalpy in the subsequent dynamic scan. As expected, α_1, α_2 and T_g increase with the increase of curing temperature. Furthermore, it can be seen that both α and T_g increase with the addition of GRM. For example, at 90°C isothermal curing, the degree of conversion α_2 increases from 83.6°C for the neat resin to 86.1°C and 93.4°C with the addition of 1.5 wt% rGO and GLYMO-rGO correspondingly due to the higher crosslinking density. Also, at 90°C isothermal curing, T_g increases from 83.6°C for the neat resin to 94.2°C and 97.5°C with the addition of 1.5 wt% rGO and GLYMO-rGO correspondingly improving thermal stability.

Table 6. 5: Exothermic heat of curing during the isothermal scans (*ΔHiso*), during subsequent dynamic scans (*ΔHdyn*), degree of curing (α) and glass transition temperature (T_g).

GRM (wt%)	T (°C)	$\Delta H1_{iso}$ [J/g]	ΔH_{iso}[a] (kJ/mol)	$\Delta H1_{dyn}$ [J/g]	ΔH_{dyn} (kJ/mol)	α_1 (%)	α_2 (%)	T_g (°C)
0 (neat epoxy)	50	209.16	71.65	35.22	12.06	85.6	66.7	53.1
	70	214.37	73.44	0.120	0.041	99.8	68.6	73.3
	90	261.21	89.48	0	0	100	83.6	83.6
1.5 rGO	50	242.63	83.12	26.09	8.92	96.5	77.7	64.5
	70	255.86	87.65	0.24	0.082	99.9	81.9	84.2
	90	268.94	92.13	0	0	100	86.1	94.2
1.5 GLYMO-rGO	50	243.30	83.35	24.35	8.33	96.7	77.9	55.9
	70	260.96	89.40	0.318	0.108	99.9	83.6	83.4
	90	291.66	99.92	0	0	100	93.4	97.5

ΔH_{iso}[a] (kJ/mol) calculated from ΔH_{ult} (kJ/g) x 185 (=EEW of Epilok 60-600G) where $\Delta H1_{ult}$ (kJ/g) refers to 1gr of epoxy determined from the experimental value divided by 0.540.

6.5.3 Thermogravimetric Analysis

Figure 6. 15 presents TGA curves of the epoxy and the nanocomposites containing 0.1 wt% rGO and 0.1 wt% GLYMO-rGO. The initial decomposition temperature, which corresponds to 5% weight loss (Xue et al., 2019), was found to decrease from 342.2 °C for neat epoxy, to 331.91°C for 0.1 wt% rGO and 339.7 °C for 0.1 wt% GLYMO-rGO. This could result from the early decomposition of interfacial epoxy chains, the cure of which was partially inhibited by the inclusion of the nanofiller (Xue et al., 2019). Dominant weight loss occurs above 350 °C

due to the thermal decomposition of epoxy resin. The temperature of the maximum rate of degradation decreases from 394.82°C of the neat epoxy resin to 386.04°C for 0.1 wt% rGO and 381.78 for GLYMO-rGO. The TGA curve of the nanocomposites was shifted in the range of 408–615°C towards higher temperatures compared to that of pure epoxy, increasing the thermal stability of cured epoxy nanocomposites. The percentage weight residue at 500°C is 7.1% for the neat resin, 10% for rGO and 13.3% for GLYMO-rGO. The increased residue confirmed the incorporation of rGO and GLYMO-rGO to improve thermal stability. The incorporation of GRMs also improves thermal stability and shifts the degradation temperature by more than 20 °C. Table 6. 5 represents TGA thermal decomposition obtained from neat epoxy and nanocomposites containing 0.1 wt% rGO and 0.1 wt% GLYMO-rGO.

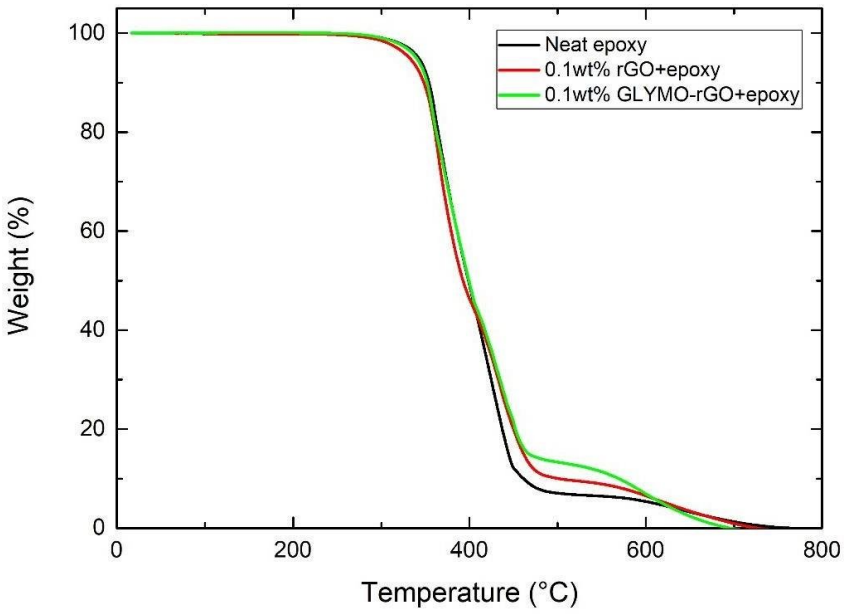

Figure 6. 15: TGA spectra obtained from neat epoxy and nanocomposites containing 0.1 wt% rGO and 0.1 wt% GLYMO-rGO.

6.5.4 Mechanical properties

6.5.4.1 Tensile testing GRM/polymer nanocomposites

The results obtained from tensile tests are shown in Figure 6. 16. The addition of only 0.05 wt% of rGO increased *E* from 1.52 GPa to 2.21 GPa and *UTS* from 51.1 MPa to 55.71 MPa, an increase of 45.39% and 9.02%, respectively. The addition of 0.05 wt% of GLYMO-rGO increased *E* to 2.43 GPa and *UTS* to 59.27 Mpa, an increase of 59.86% and 15.98%, respectively. A comparison of the results of this work with other literature reporting on rGO/epoxy nanocomposites is provided in Table 6. 6. This increase is due to chemical reactions between the functional groups of GRMs with the epoxy matrix resulting in covalent bonding of rGO and GLYMO-rGO groups with the epoxy matrix, thus improving stress transfer efficiency and mechanical properties at such low GRM content (Y.-J. Wan et al., 2014). In both GRMs, *E* and *UTS* decreased at higher filler content, probably due to poor dispersion of GRMs in the epoxy matrix (Y.-J. Wan et al., 2014). Figure 6. 17: Representative stress-strain curves obtained from neat epoxy and nanocomposites.

Table 6. 6: Literature data of studies on rGO/epoxy nanocomposites and their mechanical properties.

Reference	**Nanocomposite Preparation method**	**Solvent**	**Optimum filler content (wt%)**	***E* [GPa] (% change)**	***UTS* [MPa] (% change)**
(Ramos-Galicia et al., 2013b)	ultrasonication	-	0.4	1.2 (20% increase)	31 (0% change)
(M. Peng et al., 2016)	mechanical stirring in-situ thermal reduction	water	0.43	12.1 ± 0.6 (86% increase)	83.7 ± 8 (51% increase)
(Olowojoba et al., 2016)	three-roll mill, in-situ thermal reduction	water	2	3.29 (13.44% increase)	44.1 (35.8% decrease)
(Olowojoba et al., 2017)	mechanical stirring, in-situ thermal reduction	water	0.06	3.11 (7.24% increase)	10 (85.4% decrease)
(Aradhana et al., 2018)	mechanical stirring, ultrasonication	acetone	0.5	3.3 ± .076 (27.8% increase)	62.02 ± 7.6 (30.70% increase)

This work					
rGO/epoxy	ultrasonication, mechanical stirring	-	0.05	2.21 (45.39% increase)	55.71 (9.02% increase)
GLYMO-rGO/epoxy	ultrasonication, mechanical stirring	-	0.05	2.43 (60% increase)	59.27 (16% increase)

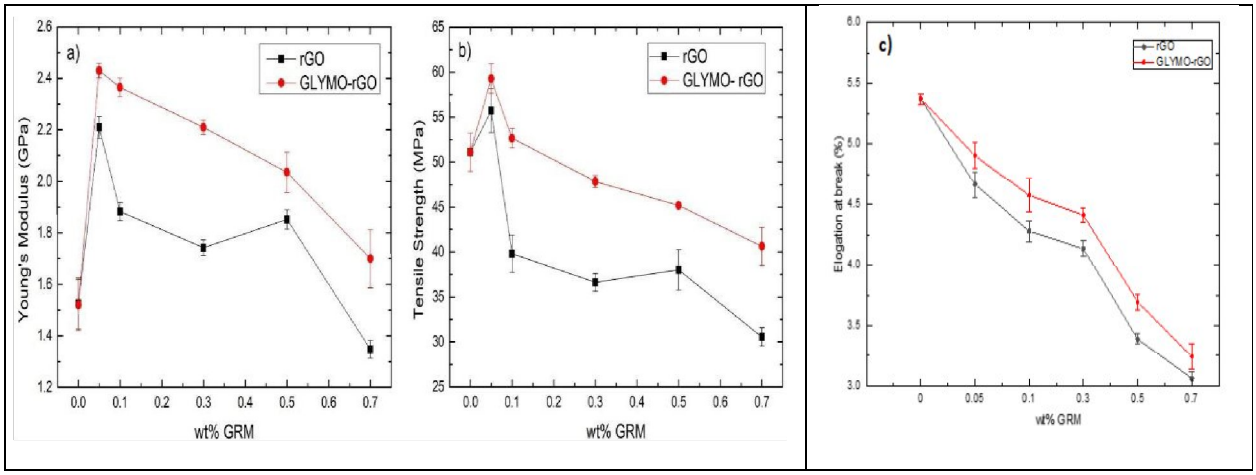

Figure 6. 16: Mechanical properties of cured nanocomposites reinforced with different amounts of GRMs; a) Young's modulus, b) Ultimate tensile strength, c) elongation at break.

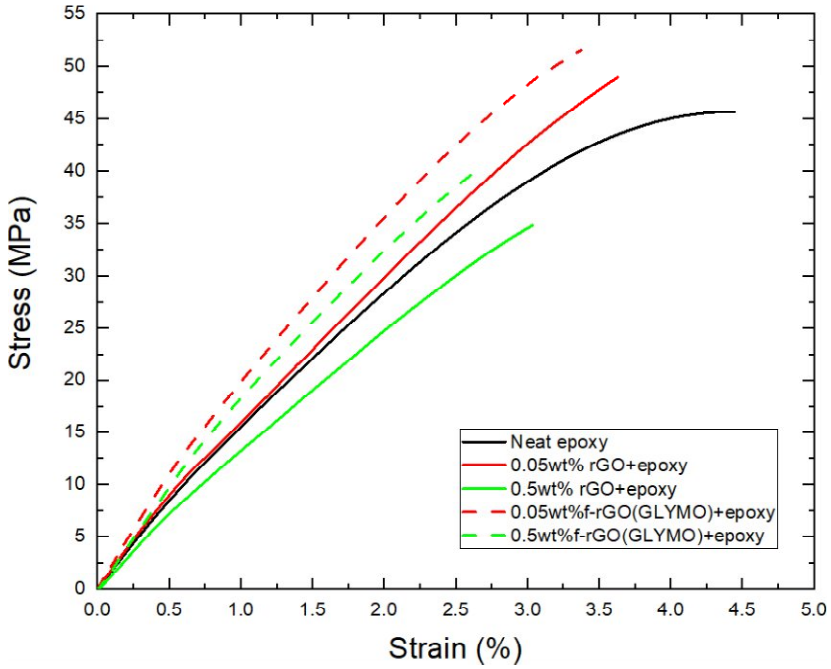

Figure 6. 17: Representative stress-strain curves obtained from neat epoxy and nanocomposites.

6.5.5 Microscopical Investigation

In order to understand the mechanisms of failure, the fracture surfaces were investigated using SEM. The neat epoxy resin exhibited a featureless image typical of a brittle fracture surface (Figure 6. 15a). The addition of 0.05 wt% rGO (Figure 6. 18b) shows a different morphology with a rougher surface, which indicates that higher energy was consumed to create a larger fractured surface (Marami et al., 2016). This morphology is in agreement with other rGO/epoxy reports (Aradhana et al., 2018), which suggest that when a crack front encounters any rigid rGO inclusion indicated with arrows, it deviates from its original path generating more fracture surface area. Nanocomposites with 0.1 wt% rGO shown in Figure 6. 15c present an even rougher surface. However, agglomerated clusters indicated with circles are present, which should be responsible for the decrease in mechanical properties as these can act as stress

concentration points for initiating rupture (Aradhana et al., 2018). Olowojoba et al. (Olowojoba et al., 2017) found agglomeration to be present above 0.06 wt%, which is in agreement with our results.

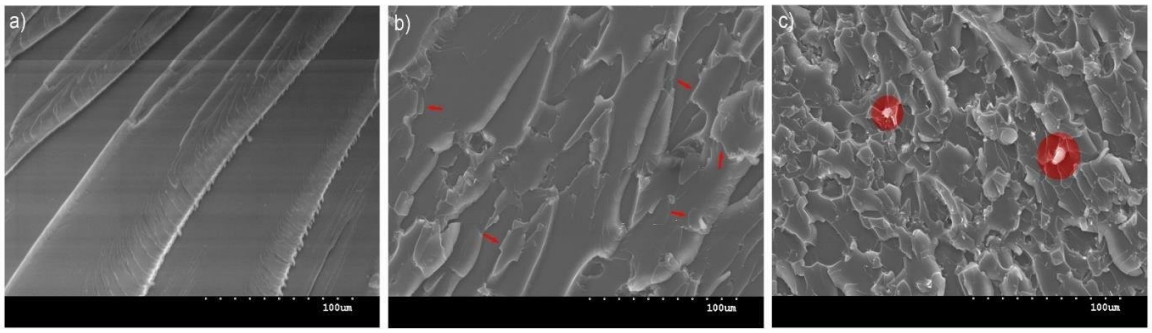

Figure 6. 18: SEM images of fractured surfaces of (a) neat epoxy, (b) nanocomposite with 0.05 wt% rGO and (c) nanocomposite with 0.1 wt% rGO.

6.5.6 Lap shear joints with CFRP/CFRP or CFRP/Aluminium laminate adherents

Lap shear joints were prepared and tested according to the ASTM D5868 standard test method for lap shear adhesion of fibre-reinforced plastic bonding. *LSS* was calculated from the peak load divided by the shear area of the joint. Figure 6. 19a) shows the *LSS* versus wt% of the GRM added in adhesive or adhesive and CFRP adherents. It is shown that the addition of 0.1 wt% rGO in the adhesive in joints with adherents made with neat epoxy increased *LSS* from 19.92 to 23.54 MPa (18.17% increase). Interestingly, the addition of 0.1 wt% rGO in the adhesive and CFRP adherents improved *LSS* further to 24.24 MPa (21.53% increase compared to neat). When GLYMO-rGO (0.1 wt%) was used in the adhesive only, *LSS* increased from 19.92 to 24.62 MPa (23.59% increase). The highest *LSS* of 25.45MPa was observed when 0.1 wt% GLYMO-rGO was added into both the adhesive and the adherents, which corresponds to a 24.08% increase compared to neat reference samples. Improvements in *LSS* can be attributed to better interaction between the adhesive and adherent; increased mechanical interlocking and

chemical bonding between the GRM and epoxy matrix. Consistent with tensile results, a higher concentration of GRM gave lower *LSS,* possibly due to the agglomeration of GRM. In the case of joints made with CFRP/Aluminium adherents, a similar trend is observed with samples showing the highest *LSS* at 0.1 wt% of GRM in the adhesive and CFRP adherent (Figure 6. 16b). The highest *LSS* obtained was 20.97MPa with 0.1% GLYMO-rGO, an improvement of 23.28% compared to the reference CFRP/Aluminium sample without GRM. *LSS* is lower in CFRP/Aluminium joints compared to CFRP/CFRP joints due to the weaker adhesive/Aluminium interface.

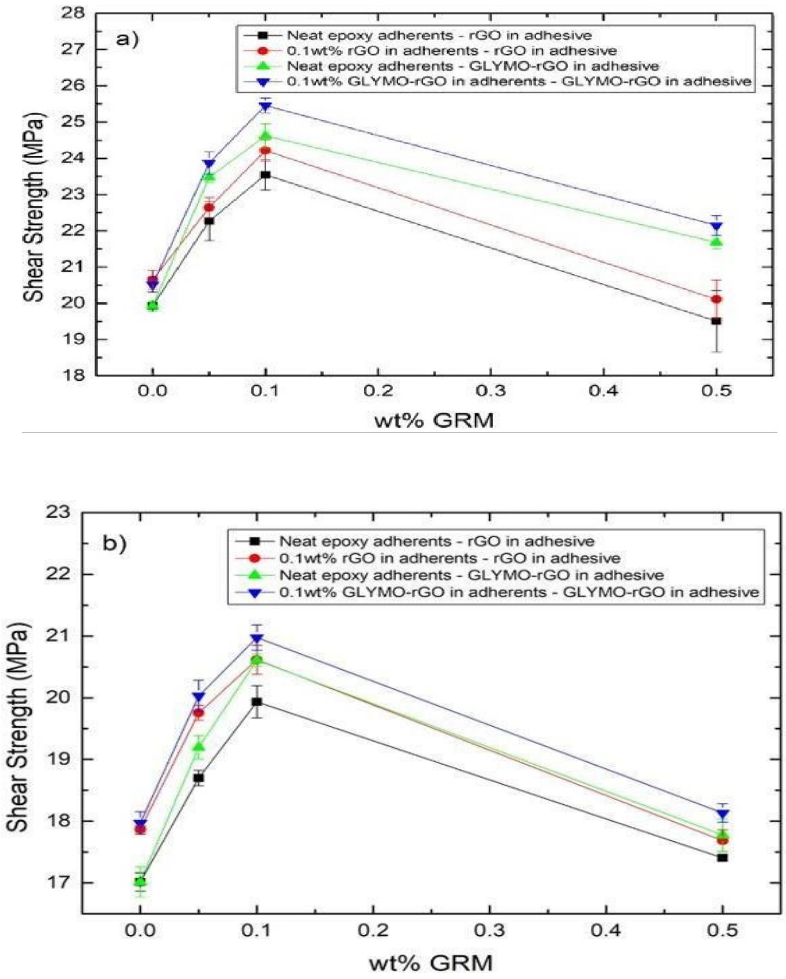

Figure 6. 19: Lap shear strength versus wt% of GRM in adhesive for a) CFRP/ CFRP adherents and b) CFRP/Aluminum adherents.

After lap shear testing, the fractured surfaces were investigated to elucidate the failure modes. In CFRP/CFRP samples, the typical failure was a combination of adhesive and cohesive modes, as shown in Figure 6. 20a. In CFRP/Al samples, when the neat adhesive was used, adhesive failure was observed at the Aluminium/adhesive interface (Figure 6. 20b). The addition of GRM improved the adhesive/Al interface and *LSS*. Figure 6. 20c shows cohesive failure with both adherents retaining the adhesive, which was reinforced with 0.1 wt% GLYMO-rGO.

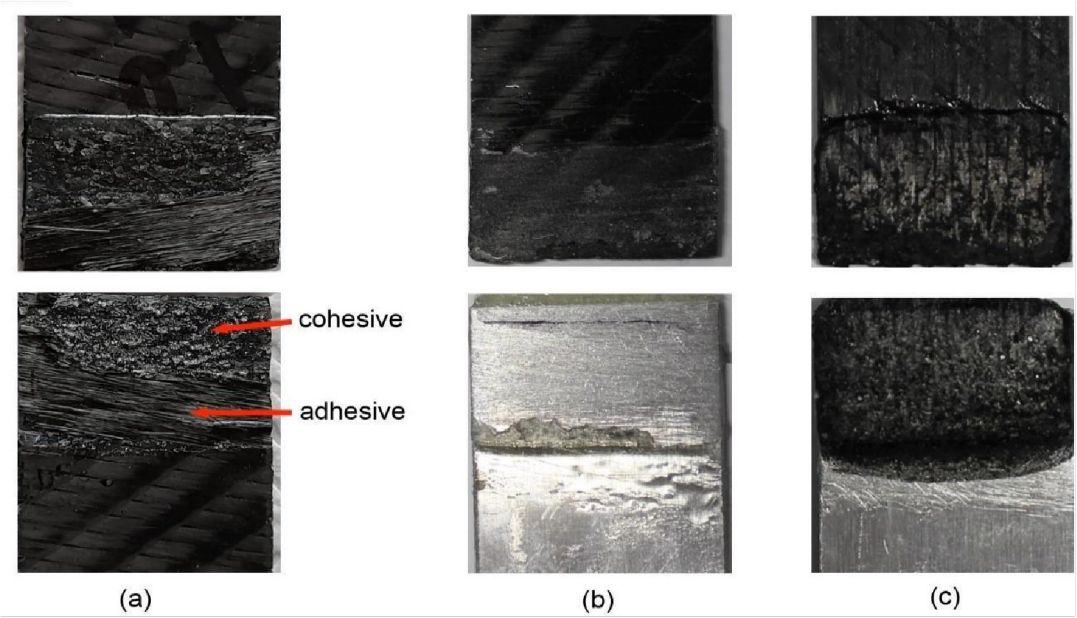

Figure 6. 20: Representative fracture surfaces of a) CFRP/CFRP joints, b) CFRP/Aluminium with neat adhesive and c) CFRP/Aluminium with 0.1 wt% GLYMO-rGO in adhesive.

6.6 Summary

In the present work, we successfully synthesised GRMs (rGO and GLYMO-rGO). Subsequently, we prepared new GRM/biobased epoxy nanocomposites and studied their cure kinetics, mechanical properties and bonding performance. These graphene-related materials (GRMs) were first dispersed into the curamine hardener using bath ultrasonication, followed by the addition of the epoxy resin. Curing kinetics were studied by DSC under nonisothermal and under isothermal conditions. The addition of 1.5 wt% of GLYMO-rGO into the epoxy matrix was found to increase the degree of cure by up to 12% and the glass transition temperature by 14°C. Mechanical testing showed that the addition of 0.05 wt% GLYMO-rGO improves *E* and *UTS* by 60% and 16%, respectively, compared to neat epoxy. The GRMs also improved the thermal stability of the epoxy system in the range of 408–615 °C. Carbon fibre reinforced polymer (CFRP) laminates were prepared via hand lay-up, using the nanocomposite system GRM/Epilok/Curamine as a matrix, and were cut as CFRP adherents for lap shear joints. The GRM/Epilok/Curamine was also used as adhesive to bond the CFRP/CFRP and CFRP/aluminium adherents. The addition of 0.1 wt% GLYMO-rGO into the adhesive and the CRFP adherents showed improved lap shear strength by 23.6% compared to the neat resin, while in the case of CFRP/Aluminium joints, the increase was 21.2%.

Chapter 7 Conclusions and Future Work

7.1 Conclusions

Due to the significant improvements in mechanical and thermal performance of GRMs/Epoxy nanocomposites at low graphene loadings, these materials have sparked a lot of research interest in academia and industry. They combine the advantages of the superior mechanical properties of graphene and the ease of processability of epoxies.

During processing, a solvent has been reported in the literature as necessary to facilitate the dispersion of graphene into the epoxy. Subsequently, solvent removal is typically associated with high expenditures and energy consumption. In addition solvent traces can remain and affect negatively mechanical properties. This could have significant consequences in end applications. Hazardous solvents are used in most chemical synthesis processes, which might have negative consequences for humans. Therefore, this research looked into various processing options to create solventless homogeneously dispersed GRMs/epoxy nanocomposites. GRMs/Epilok novel nanocomposites were prepared via a solvent-free facile approach by dispersing GNPs in the curing agent Curamine. Epilok and Curamine are trade names of epoxy and amine systems which were provided by Bitrez UK. Solvent-free processing, by simplifying the experimental procedure, and conserving labour, clearly reduces pollution and lower handling costs. These would be very useful in industrial settings.

In this research work, two different systems consisting of GRMs dispersed into epoxy polymer resins matrix were investigated. Used different methods for characterised the materials such as DSC, TGA, SEM, tensile test, and GRMs enhanced resin was used as a matrix system to prepare CFRP laminates and as adhesive to prepare lap shear joints; CFRP/CFRP (similar adherents), and CFRP/Aluminium (dissimilar adherents). Carbon fibre reinforced polymer (CFRP) laminates were prepared via a hand lay-up process.

In the first system, graphene nanoplatelets (GNPs) were combined with a low viscosity epoxy resin (Epilok 60-566/Curamine 32-494). The second is about reduced graphene oxide (rGO) and functionalised reduced graphene oxide (GLYMO) with a medium viscosity bio-based resin (Epilok 60-600G/Curamine 30-952).

Nanocomposites were prepared using graphene nanoplatelets (GNPs) and the low viscosity epoxy in the first system. The key findings are the following: i) the degree of curing increased with the addition of GNPs, while the activation energy decreased by 13.7% for the first exothermic peak and by 6.6% for the second peak as obtained from Kissinger model ii) The inclusion of GNPs increased thermal stability in the range of 360-580°C, as measured by TGA.

iii) in terms of mechanical properties, the addition of an optimum amount of 0.5%wt of GNPs in the hardener improved the E by 37%, iv) nanoindentation measurements showed 9.4% improvement in hardness at 0.7%wt GNPs.

Fossil fuel dominates the present energy and chemical supply chain. The widespread use and exploitation of fossil fuels have resulted in negative environmental consequences as well as resource exhaustion. As a result, using renewable feedstock for material preparation is a viable alternative that offers significant environmental benefits for the development of sustainable materials and circular energy. Because bio-based resins preparation has lower environmental consequences and production costs than petroleum-based resins, it is crucial for renewable material exploitation in the circular economy. Bio-based products' cost-effectiveness (performance) and environmental friendliness will determine how far they are developed and used in the industry and by consumers. Based on a review of the research, common strategies and commercial application, it appears that using bio-based materials as a tool to drive the transition to circularity, with the goal of increasing sustainability, is both viable and necessary. Renewable natural resources, for example, Plant oils and starches, have attracted attention as

polymer building blocks because to their inexpensive cost, eco-friendliness, and ability to be epoxidized, resulting in bio-based epoxy resins.

For the above reasons, the bio-based resin (medium viscosity) was used in the second system with reduced graphene oxide (rGO) and functionalised reduced graphene oxide (GLYMO). The curing behaviour and mechanical properties of rGO with bio-based resin (Epilok 60-600G/Curamine 30-952) are considered. The degree of curing increased slightly with the addition of rGOs, while no substantial change in activation energy was observed. Functionalised rGO, i.e. f-rGO (GLYMO), are being investigated as more compatible with the resin matrix. The addition of 1.5wt% GLYMO-rGO to the epoxy matrix increased the glass transition temperature by 14°C and degree of cure by up to 12%. The GRMs also increased the epoxy system's thermal stability in the 408–615 °C range. The featureless image of a brittle fracture surface was visible on the neat epoxy resin. The addition of 0.1 wt% GLYMO-rGO results in a more uniform distribution and a rougher fractured surface, which indicates that higher energy was consumed to create a larger fractured surface. In terms of mechanical properties, the addition of an optimum amount of only 0.05%wt of rGO in the hardener improved the *E* and *UTS* by 60% and 16%, respectively, compared to neat epoxy; a comparison of the results of this work with other literature reporting on rGO/epoxy nanocomposites is provided in Table 6. 7. Lap shear joints were prepared to investigate the effect of rGO on bonding performance. It was found that the addition of 0.1 wt% GLYMO-rGO into the adhesive and the CRFP adherents showed a 23.6% improvement in lap shear strength, while CFRP/Aluminum joints showed a 21.2% increase. *LSS* improvements can be attributed to better interaction between the adhesive and adherent; increased mechanical interlocking and chemical bonding between the GRM and epoxy matrix.

7.2 Future Work

Several challenges have been identified during the development of GRMs/Epoxy nanocomposites. The material properties are heavily influenced by the filler's content, manufacturing process, GRMs morphology on the properties of nanocomposites, and nanocomposite synthesis method. Concerns of petroleum dependence and environmental pollution prompt an urgent need for new sustainable approaches to polymeric product development. Biobased epoxy holds a lot of potential, but they will have to overcome many obstacles to get from an academic concept to real-world materials, starting with a scaled-up approach and working their way up to sustainable manufacturing to satisfy market demands. This step should address a variety of issues, including the availability and cost of biobased building blocks and the application area of this epoxy with GRMs. However, inconsistent chemistry and heterogeneous composition of biobased materials have functionality and consistent performance challenges.

Joining turns out to be increasingly significant as the body material changes from a single material to a blend of materials, since the similarity between various materials as far as their shared joinability, surface characteristics, corrosion, assembly, etc. May introduce various specific challenges and ought to be considered in the arrangement strategy and assurance of materials.

In the future, lap shear joints with similar or dissimilar materials should be further investigated to determine the optimum design for essential automotive parts such as inner panels, side panels, roof, battery-pack protection shield, protection firewall for passenger cabins, etc. Also, further investigated comparing the effect of the GRMs on adhesion properties such as GNP with rGO or LPE graphene.

Due to the simple geometry of the sample, the lap shear test is commonly used to evaluate joint

performance and is suitable for comparing the effect of various parameters on bond strength. However, the mixed-mode loads and tiny deformations can raise issues.

References

APPLICATIONS OF GRAPHENE POLYMER MATRIX COMPOSITES - The Graphene Council. (n.d.). Retrieved August 5, 2022, from https://www.thegraphenecouncil.org/blogpost/1501180/368117/APPLICATIONS-OF-GRAPHENE-POLYMER-MATRIX-COMPOSITES

Global transport CO2 emissions breakdown 2020 | Statista. (n.d.). Retrieved December 30, 2021, from https://www.statista.com/statistics/1185535/transport-carbon-dioxide-emissions-breakdown/

Global vehicle production forecast 2030 _ Statista. (n.d.).

How lightweight design saves costs in battery-electric vehicles. (n.d.). Retrieved June 24, 2022, from https://www.shapesbyhydro.com/en/sustainable-design/how-lightweight-design-saves-costs-in-battery-electric-vehicles/

Overview: Lightweighting Matters - just-auto magazine | Issue 6 | June 2020. (n.d.). Retrieved August 4, 2022, from https://justauto.nridigital.com/just-auto_magazine_jun20/overview_lightweighting_matte

Recycling - WorldAutoSteel. (n.d.). Retrieved July 23, 2022, from https://www.worldautosteel.org/life-cycle-thinking/recycling/

Vehicle weight. (n.d.). Retrieved August 20, 2022, from https://www.nrcan.gc.ca/energy-efficiency/transportation-alternative-fuels/personal-vehicles/choosing-right-vehicle/tips-buying-fuel-efficient-vehicle/factors-affect-fuel-efficiency/vehicle-weight/21024

Abbasi, H., Antunes, M., & Velasco, J. I. (2019). Recent advances in carbon-based polymer nanocomposites for electromagnetic interference shielding. In *Progress in Materials Science* (Vol. 103). https://doi.org/10.1016/j.pmatsci.2019.02.003

Abenojar, J., Del Real, J. C., Ballesteros, Y., & Martinez, M. A. (2018). Kinetics of curing process in carbon/epoxy nano-composites. *IOP Conference Series: Materials Science and Engineering*. https://doi.org/10.1088/1757-899X/369/1/012011

Abu-Okail, M., Alsaleh, N. A., Farouk, W. M., Elsheikh, A., Abu-Oqail, A., Abdelraouf, Y. A., & Ghafaar, M. A. (2021). Effect of dispersion of alumina nanoparticles and graphene nanoplatelets on microstructural and mechanical characteristics of hybrid carbon/glass fibers reinforced polymer composite. *Journal of Materials Research and Technology*, *14*. https://doi.org/10.1016/j.jmrt.2021.07.158

Achilias, D. S., Karabela, M. M., Varkopoulou, E. A., & Sideridou, I. D. (2012). Cure kinetics study of two epoxy systems with Fourier Tranform Infrared Spectroscopy (FTIR) and Differential Scanning Calorimetry (DSC). *Journal of Macromolecular Science, Part A: Pure and Applied Chemistry*. https://doi.org/10.1080/10601325.2012.696995

Adams, R. D. (2005). Adhesive bonding: Science, technology and applications. In *Adhesive Bonding: Science, Technology and Applications*. https://doi.org/10.1533/9781845690755

Adams, R. D., & Peppiatt, n. a. (1974). Stress analysis of adhesive-bonded lap joints. *The Journal of Strain Analysis for Engineering Design*, *9*(3). https://doi.org/10.1243/03093247V093185

Adams, Robert D., & Wake, W. C. (1984). Structural Adhesive Joints in Engineering. In *Structural Adhesive Joints in Engineering*. https://doi.org/10.1007/978-94-009-5616-2

Adderley, C. S. (1988). Adhesive Bonding. *Materials and Design*. https://doi.org/10.1016/0261-3069(88)90006-4

adhesive | Definition, Types, Uses, Materials, & Facts | Britannica. (n.d.). Retrieved December 30, 2021, from https://www.britannica.com/technology/adhesive

Advantages of Adhesive Bonding over Mechanical Fasteners. (n.d.). Retrieved January 4, 2022, from https://www.masterbond.com/enews/advantages-of-adhesive-bonding-over-mechanical-fasteners.html

Advantages of Structural Adhesives over Welding, Rivets and Traditional Fastening Methods. (n.d.). Retrieved January 4, 2022, from https://www.linkedin.com/pulse/advantages-structural-adhesives-over-welding-rivets-methods-richards

Agius Anastasi, A., Ritos, K., Cassar, G., & Borg, M. K. (2016). Mechanical properties of pristine and nanoporous graphene. *Molecular Simulation*. https://doi.org/10.1080/08927022.2016.1209753

Agrawal, A. K., & Mirzaeifar, R. (2019). Graphene-Nickel interaction in layered metal-matrix composites. *Surface Science*. https://doi.org/10.1016/j.susc.2019.05.003

Ahmadi-Moghadam, B., Sharafimasooleh, M., Shadlou, S., & Taheri, F. (2015). Effect of functionalization of graphene nanoplatelets on the mechanical response of graphene/epoxy composites. *Materials and Design*. https://doi.org/10.1016/j.matdes.2014.10.047

Ajayan, P. M., Schadler, L. S., Giannaris, C., & Rubio, A. (2000). Single-walled carbon nanotube-polymer composites: Strength and weakness. *Advanced Materials*, *12*(10). https://doi.org/10.1002/(SICI)1521-4095(200005)12:10<750::AID-ADMA750>3.0.CO;2-6

Alam, M., Akram, D., Sharmin, E., Zafar, F., & Ahmad, S. (2014). Vegetable oil based eco-friendly coating materials: A review article. In *Arabian Journal of Chemistry*. https://doi.org/10.1016/j.arabjc.2013.12.023

Alamusi, Li, H., Ning, Y., Gu, B., Hu, N., Yuan, W., Jia, F., Liu, H., Li, Y., Liu, Y., Ning, H., Wu, L., Fu, S., & Cai, Y. (2018). Molecular dynamics simulations of thermal expansion properties of single layer graphene sheets. *Molecular Simulation*. https://doi.org/10.1080/08927022.2017.1336664

Alexandre, M., & Dubois, P. (2000). Polymer-layered silicate nanocomposites: Preparation, properties and uses of a new class of materials. *Materials Science and Engineering R: Reports*. https://doi.org/10.1016/S0927-796X(00)00012-7

An, X., Simmons, T., Shah, R., Wolfe, C., Lewis, K. M., Washington, M., Nayak, S. K., Talapatra, S., & Kar, S. (2010). Stable aqueous dispersions of noncovalently functionalized graphene from graphite and their multifunctional high-performance applications. *Nano Letters*. https://doi.org/10.1021/nl903557p

Anon. (2000). Automotive materials. *Advanced Materials and Processes*, *158*(2), 50–52. https://doi.org/10.1016/b978-0-08-034720-2.50017-4

Anwar, Z., Kausar, A., Rafique, I., & Muhammad, B. (2016). Advances in Epoxy/Graphene Nanoplatelet Composite with Enhanced Physical Properties: A Review. In *Polymer - Plastics Technology and Engineering*. https://doi.org/10.1080/03602559.2015.1098695

Anyfantis, K. N., & Tsouvalis, N. G. (2012). Experimental parametric study of Single-Lap adhesive joints between dissimilar materials. *ECCM 2012 - Composites at Venice, Proceedings of the 15th European Conference on Composite Materials*.

Arabpour, A., Shockravi, A., Rezania, H., & Farahati, R. (2020). Investigation of anticorrosive properties of novel silane-functionalized polyamide/GO nanocomposite as steel coatings. *Surfaces and Interfaces*, *18*. https://doi.org/10.1016/j.surfin.2020.100453

Aradhana, R., Mohanty, S., & Nayak, S. K. (2018). Comparison of mechanical, electrical and thermal properties in graphene oxide and reduced graphene oxide filled epoxy nanocomposite adhesives. *Polymer*, *141*. https://doi.org/10.1016/j.polymer.2018.03.005

Arvidsson, R., Tillman, A. M., Sandén, B. A., Janssen, M., Nordelöf, A., Kushnir, D., & Molander, S. (2018a). Environmental Assessment of Emerging Technologies: Recommendations for Prospective LCA. In Journal of Industrial Ecology (Vol. 22, Issue 6). https://doi.org/10.1111/jiec.12690

Asada, C., Basnet, S., Otsuka, M., Sasaki, C., & Nakamura, Y. (2015). Epoxy resin synthesis using low molecular weight lignin separated from various lignocellulosic materials. *International Journal of Biological Macromolecules*. https://doi.org/10.1016/j.ijbiomac.2014.12.039

Atif, R., Shyha, I., & Inam, F. (2016). The degradation of mechanical properties due to stress concentration caused by retained acetone in epoxy nanocomposites. *RSC Advances*. https://doi.org/10.1039/c6ra00739b

Atif, Rasheed, Shyha, I., & Inam, F. (2016). Mechanical, thermal, and electrical properties of graphene-epoxy nanocomposites-A review. In *Polymers* (Vol. 8, Issue 8). https://doi.org/10.3390/polym8080281

Auvergne, R., Caillol, S., David, G., Boutevin, B., & Pascault, J. P. (2014). Biobased thermosetting epoxy: Present and future. In *Chemical Reviews*. https://doi.org/10.1021/cr3001274

Ayad, M. M., Abu El-Nasr, A., & Stejskal, J. (2012). Kinetics and isotherm studies of methylene blue adsorption onto polyaniline nanotubes base/silica composite. *Journal of Industrial and Engineering Chemistry*. https://doi.org/10.1016/j.jiec.2012.05.012

Ayatollahi, M. R., Moghimi Monfared, R., & Barbaz Isfahani, R. (2019). Experimental investigation on tribological properties of carbon fabric composites: effects of carbon nanotubes and nano-silica. *Proceedings of the Institution of Mechanical Engineers, Part L: Journal of Materials: Design and Applications*. https://doi.org/10.1177/1464420717714345

Aydin, M. D., Özel, A., & Temiz, Ş. (2005). The effect of adherend thickness on the failure of adhesively-bonded single-lap joints. *Journal of Adhesion Science and Technology*, *19*(8). https://doi.org/10.1163/1568561054890499

Azeez, A. A., Rhee, K. Y., Park, S. J., & Hui, D. (2013). Epoxy clay nanocomposites - Processing, properties and applications: A review. *Composites Part B: Engineering*. https://doi.org/10.1016/j.compositesb.2012.04.012

Baekeland, L. H. (1909). Original papers: The synthesis, constitution, and uses of bakelite. *Industrial and Engineering Chemistry*. https://doi.org/10.1021/ie50003a004

Bahl, S., Dolma, J., Singh, J. J., & Sehgal, S. (2020). Biodegradation of plastics: A state of the art review. *Materials Today: Proceedings*, *39*. https://doi.org/10.1016/j.matpr.2020.06.096

Bai, S., & Shen, X. (2012). Graphene-inorganic nanocomposites. In *RSC Advances*. https://doi.org/10.1039/c1ra00260k

Baker, A. A., & Chester, R. J. (1992). Minimum surface treatments for adhesively bonded repairs. *International Journal of Adhesion and Adhesives*. https://doi.org/10.1016/0143-7496(92)90026-R

Balandin, A. A., Ghosh, S., Bao, W., Calizo, I., Teweldebrhan, D., Miao, F., & Lau, C. N. (2008). Superior thermal conductivity of single-layer graphene. *Nano Letters*. https://doi.org/10.1021/nl0731872

Bandivadekar, A. E. A. (2008). On the Road in 2035 - Reducing transportation's petroleum consumption and GHG emissions. In *Massachusetts Institute of Technology (MIT)*. https://doi.org/Report No. LFEE 2008-05 RP

Banea, M. D., & Da Silva, L. F. M. (2009). Adhesively bonded joints in composite materials: An overview. In *Proceedings of the Institution of Mechanical Engineers, Part L: Journal of Materials: Design and Applications*. https://doi.org/10.1243/14644207JMDA219

Banea, M. D., Rosioara, M., Carbas, R. J. C., & da Silva, L. F. M. (2018). Multi-material adhesive joints for automotive industry. *Composites Part B: Engineering*. https://doi.org/10.1016/j.compositesb.2018.06.009

Banea, Mariana D. (2019). Influence of adherend properties on the strength of adhesively bonded joints. *MRS Bulletin*, *44*(8). https://doi.org/10.1557/mrs.2019.180

Banea, Mariana D., Da Silva, L. F. M., Campilho, R. D. S. G., & Sato, C. (2014). Smart adhesive joints: An overview of recent developments. *Journal of Adhesion*. https://doi.org/10.1080/00218464.2013.785916

Banea, Mariana D., da Silva, L. F. M., Carbas, R., & Campilho, R. D. S. G. (2017). Effect of material on the mechanical behaviour of adhesive joints for the automotive industry. *Journal of Adhesion Science and Technology*. https://doi.org/10.1080/01694243.2016.1229842

Bao, Y. Z., Cong, L. F., Huang, Z. M., & Weng, Z. X. (2008). Preparation and proton conductivity of poly(vinylidene fluoride)/layered double hydroxide nanocomposite gel electrolytes. *Journal of Materials Science*. https://doi.org/10.1007/s10853-007-2100-1

Barletta, M., Vesco, S., Puopolo, M., & Tagliaferri, V. (2016). Graphene reinforced UV-curable epoxy resins: Design, manufacture and material performance. *Progress in Organic Coatings*, *90*. https://doi.org/10.1016/j.porgcoat.2015.08.013

Baroncini, E. A., Kumar Yadav, S., Palmese, G. R., & Stanzione, J. F. (2016). Recent advances in bio-based epoxy resins and bio-based epoxy curing agents. In *Journal of Applied Polymer Science*. https://doi.org/10.1002/app.44103

Barua, S., Chattopadhyay, P., Phukan, M. M., Konwar, B. K., & Karak, N. (2015). Hyperbranched epoxy/MWCNT-CuO-nystatin nanocomposite as a high performance, biocompatible, antimicrobial material. *Materials Research Express*. https://doi.org/10.1088/2053-1591/1/4/045402

Barua, S., Dutta, N., Karmakar, S., Chattopadhyay, P., Aidew, L., Buragohain, A. K., & Karak, N. (2014). Biocompatible high performance hyperbranched epoxy/clay nanocomposite as an implantable material. *Biomedical Materials (Bristol)*. https://doi.org/10.1088/1748-6041/9/2/025006

Bedsole, R. W., Park, C., Bogert, P. B., & Tippur, H. V. (2015). A critical evaluation of the enhancement of mechanical properties of epoxy modified using CNTs. *Materials Research Express*. https://doi.org/10.1088/2053-1591/2/9/095020

BEIS. (2020). 2019 UK Greenhouse Gas Emissions, Final Figures. In *National Statistics* (Issue March 2020).

Bhattacharya, M. (2016). Polymer nanocomposites-A comparison between carbon nanotubes, graphene, and clay as nanofillers. In *Materials*. https://doi.org/10.3390/ma9040262

Bhawal, P., Ganguly, S., Das, T. K., Mondal, S., Choudhury, S., & Das, N. C. (2018). Superior electromagnetic interference shielding effectiveness and electro-mechanical properties of EMA-IRGO nanocomposites through the in-situ reduction of GO from melt blended EMA-GO composites. *Composites Part B: Engineering*. https://doi.org/10.1016/j.compositesb.2017.09.046

Bhowmik, K., Pramanik, S., Medda, S. K., & De, G. (2012). Covalently functionalized reduced graphene oxide by organically modified silica: a facile synthesis of electrically conducting black coatings on glass. *Journal of Materials Chemistry*, *22*(47), 24690–24697. https://doi.org/10.1039/C2JM35429B

Bindu Sharmila, T. K., Antony, J. V., Jayakrishnan, M. P., Sabura Beegum, P. M., & Thachil, E. T. (2016). Mechanical, thermal and dielectric properties of hybrid composites of epoxy and reduced graphene oxide/iron oxide. *Materials and Design*. https://doi.org/10.1016/j.matdes.2015.10.055

Biocomposites in the automotive industry: potential applications and benefits - Renewable Carbon News. (n.d.). Retrieved August 21, 2022, from https://renewable-carbon.eu/news/biocomposites-in-the-automotive-industry-potential-applications-and-benefits/

Bonaccorso, F., Sun, Z., Hasan, T., & Ferrari, A. C. (2010). Graphene photonics and optoelectronics. *Nature Photonics*. https://doi.org/10.1038/nphoton.2010.186

Botelho, E. C., Silva, R. A., Pardini, L. C., & Rezende, M. C. (2004). Evaluation of adhesion of continuous fiber-epoxy composite/aluminum laminates. *Journal of Adhesion Science and Technology*. https://doi.org/10.1163/1568561042708377

Botelho, Edson Cocchieri, Silva, R. A., Pardini, L. C., & Rezende, M. C. (2006). A review on the development and properties of continuous fiber/epoxy/aluminum hybrid composites for aircraft structures. In *Materials Research*. https://doi.org/10.1590/S1516-14392006000300002

Boutar, Y., Naïmi, S., Mezlini, S., Da Silva, L. F. M., Hamdaoui, M., & Ben Sik Ali, M. (2016). Effect of adhesive thickness and surface roughness on the shear strength of aluminium one-component polyurethane adhesive single-lap joints for automotive applications. *Journal of Adhesion Science and Technology*. https://doi.org/10.1080/01694243.2016.1170588

Budhe, S., Banea, M. D., de Barros, S., & da Silva, L. F. M. (2017). An updated review of adhesively bonded joints in composite materials. *International Journal of Adhesion and Adhesives*, *72*, 30–42. https://doi.org/10.1016/j.ijadhadh.2016.10.010

Bulut, M. (2017). Mechanical characterization of Basalt/epoxy composite laminates containing graphene nanopellets. *Composites Part B: Engineering*. https://doi.org/10.1016/j.compositesb.2017.04.013

Burkholder, G. L., Kwon, Y. W., & Pollak, R. D. (2011). Effect of carbon nanotube reinforcement on fracture strength of composite adhesive joints. *Journal of Materials Science*, *46*(10). https://doi.org/10.1007/s10853-010-

5225-6

Calvo-Flores, F. G., & Dobado, J. A. (2010). Lignin as renewable raw material. In *ChemSusChem*. https://doi.org/10.1002/cssc.201000157

Camargo, P. H. C., Satyanarayana, K. G., & Wypych, F. (2009). Nanocomposites: Synthesis, structure, properties and new application opportunities. In *Materials Research* (Vol. 12, Issue 1). https://doi.org/10.1590/S1516-14392009000100002

Campilho, R. D. S. G., Moura, D. C., Banea, M. D., & Da Silva, L. F. M. (2015). Adhesive thickness effects of a ductile adhesive by optical measurement techniques. *International Journal of Adhesion and Adhesives*, *57*. https://doi.org/10.1016/j.ijadhadh.2014.12.004

Carbas, R. J. C., Borges, C., Marques, E. A. S., Akhavan-Safar, A., & da Silva, L. F. M. (2021). Manufacture and testing. In *Advanced Joining Processes*. https://doi.org/10.1016/b978-0-12-820787-1.00008-5

Carosio, F., Maddalena, L., Gomez, J., Saracco, G., & Fina, A. (2018). Graphene Oxide Exoskeleton to Produce Self-Extinguishing, Nonignitable, and Flame Resistant Flexible Foams: A Mechanically Tough Alternative to Inorganic Aerogels. *Advanced Materials Interfaces*, *5*(23), 1801288. https://doi.org/https://doi.org/10.1002/admi.201801288

Cassagneau, T., & Fendler, J. H. (1998). High density rechargeable lithium-ion batteries self-assembled from graphite oxide nanoplatelets and polyelectrolytes. *Advanced Materials*. https://doi.org/10.1002/(SICI)1521-4095(199808)10:11<877::AID-ADMA877>3.0.CO;2-1

Cha, J., Kim, J., Ryu, S., & Hong, S. H. (2019). Comparison to mechanical properties of epoxy nanocomposites reinforced by functionalized carbon nanotubes and graphene nanoplatelets. *Composites Part B: Engineering*. https://doi.org/10.1016/j.compositesb.2018.11.011

Chandrasekaran, S., Sato, N., Tölle, F., Mülhaupt, R., Fiedler, B., & Schulte, K. (2014). Fracture toughness and failure mechanism of graphene based epoxy composites. *Composites Science and Technology*. https://doi.org/10.1016/j.compscitech.2014.03.014

Chang, T. D., & Brittain, J. O. (1982). Studies of epoxy resin systems: Part D: Fracture toughness of an epoxy resin: A study of the effect of crosslinking and sub-Tg aging. *Polymer Engineering & Science*, *22*(18). https://doi.org/10.1002/pen.760221809

Chatterjee, S., Wang, J. W., Kuo, W. S., Tai, N. H., Salzmann, C., Li, W. L., Hollertz, R., Nüesch, F. A., & Chu, B. T. T. (2012). Mechanical reinforcement and thermal conductivity in expanded graphene nanoplatelets reinforced epoxy composites. *Chemical Physics Letters*. https://doi.org/10.1016/j.cplett.2012.02.006

Chee, S. S., Jawaid, M., Sultan, M. T. H., Alothman, O. Y., & Abdullah, L. C. (2019). Evaluation of the hybridization effect on the thermal and thermo-oxidative stability of bamboo/kenaf/epoxy hybrid composites. *Journal of Thermal Analysis and Calorimetry*. https://doi.org/10.1007/s10973-018-7918-z

Chee, W. K., Lim, H. N., Huang, N. M., & Harrison, I. (2015). Nanocomposites of graphene/polymers: a review. *RSC Advances*. https://doi.org/10.1039/c5ra07989f

Chen, R. S., Hakim Mohd Ruf, M. F., Shahdan, D., & Ahmad, S. (2019). Enhanced mechanical and thermal properties of electrically conductive TPNR/GNP nanocomposites assisted with ultrasonication. *PLoS ONE*, *14*(9). https://doi.org/10.1371/journal.pone.0222662

Chen, X., Zhang, Z., Jin, X., Xiao, M., Guo, H., & Ma, Z. (2018). Simulation method for precision bonding structure with micron scale adhesive layer. *Procedia CIRP*, *76*. https://doi.org/10.1016/j.procir.2018.01.035

Chen, X., Dobson, J. F., & Raston, C. L. (2012). Vortex fluidic exfoliation of graphite and boron nitride. Chemical Communications, 48(31). https://doi.org/10.1039/c2cc17611d

Cheng, X., Kumar, V., Yokozeki, T., Goto, T., Takahashi, T., Koyanagi, J., Wu, L., & Wang, R. (2016). Highly conductive graphene oxide/polyaniline hybrid polymer nanocomposites with simultaneously improved mechanical properties. *Composites Part A: Applied Science and Manufacturing*. https://doi.org/10.1016/j.compositesa.2015.12.006

Chhipa, S. M., Kumar, P., Bagha, A. K., & Bahl, S. (2021). Removing fiber orientation uncertainty from the finite element model of a composite lamina with direct updating algorithm. *Physica Scripta*, *96*(12). https://doi.org/10.1088/1402-4896/ac445e

Chisholm, N., Mahfuz, H., Rangari, V. K., Ashfaq, A., & Jeelani, S. (2005). Fabrication and mechanical characterization of carbon/SiC-epoxy nanocomposites. *Composite Structures*, *67*(1). https://doi.org/10.1016/j.compstruct.2004.01.010

Chiu, Y. C., Huang, C. L., & Wang, C. (2016). Rheological and conductivity percolations of syndiotactic polystyrene composites filled with graphene nanosheets and carbon nanotubes: A comparative study. *Composites Science and Technology*, *134*. https://doi.org/10.1016/j.compscitech.2016.08.016

Cho, D., Lee, S., Yang, G., Fukushima, H., & Drzal, L. T. (2005). Dynamic mechanical and thermal properties of phenylethynyl-terminated polyimide composites reinforced with expanded graphite nanoplatelets. *Macromolecular Materials and Engineering*. https://doi.org/10.1002/mame.200400281

Cho, E. C., Huang, J. H., Li, C. P., Chang-Jian, C. W., Lee, K. C., Hsiao, Y. S., & Huang, J. H. (2016). Graphene-based thermoplastic composites and their application for LED thermal management. *Carbon*. https://doi.org/10.1016/j.carbon.2016.01.097

Coats, A. W., & Redfern, J. P. (1963). Thermogravimetric analysis. A review. *The Analyst*. https://doi.org/10.1039/AN9638800906

Coleman, J. N., Khan, U., Blau, W. J., & Gun'ko, Y. K. (2006). Small but strong: A review of the mechanical properties of carbon nanotube-polymer composites. In *Carbon*. https://doi.org/10.1016/j.carbon.2006.02.038

Compton, O. C., An, Z., Putz, K. W., Hong, B. J., Hauser, B. G., Catherine Brinson, L., & Nguyen, S. T. (2012). Additive-free hydrogelation of graphene oxide by ultrasonication. *Carbon*. https://doi.org/10.1016/j.carbon.2012.01.061

CRIPPS, D., SEARLE, T. J., & SUMMERSCALES, J. (2000). Open Mold Techniques for Thermoset Composites. In Comprehensive Composite Materials. https://doi.org/10.1016/b0-08-042993-9/00188-1

CSR Europe on Twitter: "Do you know how many raw materials are needed to make a car or another vehicle? #DriveSustainability aims to improve sustainability in sourcing of these raw materials: https://t.co/lEyjEXAbh8 Retrieved August 27, 2022, from https://twitter.com/CSREuropeOrg/status/935447625024835585

Crosby, A. J., & Lee, J. Y. (2007). Polymer nanocomposites: The "nano" effect on mechanical properties. *Polymer Reviews*. https://doi.org/10.1080/15583720701271278

Czerwinski, F. (2021). Current trends in automotive lightweighting strategies and materials. *Materials*, *14*(21). https://doi.org/10.3390/ma14216631

da Silva, L. F. M., & Adams, R. D. (2007). Adhesive joints at high and low temperatures using similar and dissimilar adherends and dual adhesives. *International Journal of Adhesion and Adhesives*. https://doi.org/10.1016/j.ijadhadh.2006.04.002

da Silva, L. F. M., das Neves, P. J. C., Adams, R. D., Wang, A., & Spelt, J. K. (2009). Analytical models of adhesively bonded joints-Part II: Comparative study. *International Journal of Adhesion and Adhesives*, *29*(3). https://doi.org/10.1016/j.ijadhadh.2008.06.007

da Silva, L. F. M., Öchsner, A., & Adams, R. D. (2018a). Handbook of Adhesion Technology: Second Edition. In *Handbook of Adhesion Technology: Second Edition*. https://doi.org/10.1007/978-3-319-55411-2

da Silva, L. F. M., Öchsner, A., & Adams, R. D. (2018b). Introduction to adhesive bonding technology. In *Handbook of Adhesion Technology: Second Edition*. https://doi.org/10.1007/978-3-319-55411-2_1

da Silva, L. F. M., Rodrigues, T. N. S. S., Figueiredo, M. A. V., de Moura, M. F. S. F., & Chousal, J. A. G. (2006). Effect of adhesive type and thickness on the lap shear strength. *Journal of Adhesion*. https://doi.org/10.1080/00218460600948511

Dadkhah, M., Saboori, A., & Fino, P. (2019). An Overview of the Recent Developments in Metal Matrix Nanocomposites Reinforced by Graphene. *Materials*. https://doi.org/10.3390/ma12172823

Dai, J., Teng, N., Liu, J., Feng, J., Zhu, J., & Liu, X. (2019). Synthesis of bio-based fire-resistant epoxy without addition of flame retardant elements. *Composites Part B: Engineering*, *179*. https://doi.org/10.1016/j.compositesb.2019.107523

de Bakker, C. J., St John, N. A., & George, G. A. (1993). Simultaneous differential scanning calorimetry and near-infra-red analysis of the curing of tetraglycidyldiaminodiphenylmethane with diaminodiphenylsulphone. *Polymer*. https://doi.org/10.1016/0032-3861(93)90353-C

de Blasio, C. (2019). Thermogravimetric analysis (TGA). In *Green Energy and Technology*. https://doi.org/10.1007/978-3-030-11599-9_7

de Morais, A. B., Pereira, A. B., Teixeira, J. P., & Cavaleiro, N. C. (2007). Strength of epoxy adhesive-bonded stainless-steel joints. *International Journal of Adhesion and Adhesives*. https://doi.org/10.1016/j.ijadhadh.2007.02.002

Debelak, B., & Lafdi, K. (2007). Use of exfoliated graphite filler to enhance polymer physical properties. *Carbon*. https://doi.org/10.1016/j.carbon.2007.05.010

Deepak, V., & Senal, I. (2019). Natural fiber-reinforced polymer composites: Feasibiliy study for sustainable automotive industries. *Biomass, Biopolymer-Based Materials, and Bioenergy*. https://doi.org/10.1016/B978-0-08-102426-3.00006-0

Del Rio, E., Lligadas, G., Ronda, J. C., Galià, M., & Cádiz, V. (2010). Biobased polyurethanes from polyether polyols obtained by ionic-coordinative polymerization of epoxidized methyl oleate. *Journal of Polymer Science, Part A: Polymer Chemistry*. https://doi.org/10.1002/pola.24296

Delogu, M., Zanchi, L., Dattilo, C. A., & Pierini, M. (2017). Innovative composites and hybrid materials for electric vehicles lightweight design in a sustainability perspective. Materials Today Communications, 13. https://doi.org/10.1016/j.mtcomm.2017.09.012

Design Flexibility - Benefits of Composites | Composites Lab. (n.d.). Retrieved December 30, 2021, from http://compositeslab.com/benefits-of-composites/design-flexibility/

Dikin, D. A., Stankovich, S., Zimney, E. J., Piner, R. D., Dommett, G. H. B., Evmenenko, G., Nguyen, S. T., & Ruoff, R. S. (2007). Preparation and characterization of graphene oxide paper. *Nature*. https://doi.org/10.1038/nature06016

Domun, N., Hadavinia, H., Zhang, T., Liaghat, G., Vahid, S., Spacie, C., Paton, K. R., & Sainsbury, T. (2017). Improving the fracture toughness properties of epoxy using graphene nanoplatelets at low filler content. *Nanocomposites*. https://doi.org/10.1080/20550324.2017.1365414

Dow Automotive Systems. (2015). *Structural Bonding of Lightweight Cars*. 12. http://msdssearch.dow.com/PublishedLiteratureDOWCOM/

Dr Elmar Witten, T. K. (2014). *Composites Market Report 2014*. *September*, 1–44.

Du, X. S., Xiao, M., & Meng, Y. Z. (2004). Synthesis and characterization of polyaniline/graphite conducting nanocomposites. *Journal of Polymer Science, Part B: Polymer Physics*. https://doi.org/10.1002/polb.20102

Du, Xu, Skachko, I., Barker, A., & Andrei, E. Y. (2008). Approaching ballistic transport in suspended graphene. *Nature Nanotechnology*. https://doi.org/10.1038/nnano.2008.199

Du, Xusheng, Zhou, H., Sun, W., Liu, H. Y., Zhou, G., Zhou, H., & Mai, Y. W. (2017). Graphene/epoxy interleaves for delamination toughening and monitoring of crack damage in carbon fibre/epoxy composite laminates. *Composites Science and Technology*, *140*. https://doi.org/10.1016/j.compscitech.2016.12.028

Duffy, J. V., Hui, E., & Hartmann, B. (1987). Reaction kinetics for hindered amine/epoxides by DSC. *Journal of Applied Polymer Science*. https://doi.org/10.1002/app.1987.070330828

Ebewele, R. O. (2000). Polymer science and technology. In *Polymer Science and Technology*.

Ebnesajjad, S., & Landrock, A. H. (2015). Introduction and Adhesion Theories. In *Adhesives Technology Handbook*. https://doi.org/10.1016/b978-0-323-35595-7.00001-2

Eigler, S., & Hirsch, A. (2014). Chemistry with graphene and graphene oxide - Challenges for synthetic chemists. In *Angewandte Chemie - International Edition* (Vol. 53, Issue 30). https://doi.org/10.1002/anie.201402780

El-Kassas, A. M., & Elsheikh, A. H. (2021). A new eco-friendly mechanical technique for production of rice straw fibers for medium density fiberboards manufacturing. *International Journal of Environmental Science and Technology*, *18*(4). https://doi.org/10.1007/s13762-020-02886-8

El Mansouri, N. E., Yuan, Q., & Huang, F. (2011). Synthesis and characterization of kraft lignin-based epoxy resins. *BioResources*. https://doi.org/10.15376/biores.6.3.2492-2503

Electric Vehicles to Increase Aluminum Demand | Secondary A356.2. (n.d.). Retrieved June 23, 2022, from https://eccomelt.com/electric-vehicles-transform-aluminum-demand-2035/

Elkington, M., Bloom, D., Ward, C., Chatzimichali, A., & Potter, K. (2015). Hand layup: understanding the manual process. *Advanced Manufacturing: Polymer and Composites Science*, *1*(3). https://doi.org/10.1080/20550340.2015.1114801

Elmarakbi, A., & Azoti, W. (2018). State of the Art on Graphene Lightweighting Nanocomposites for Automotive Applications. In *Experimental Characterization, Predictive Mechanical and Thermal Modeling of Nanostructures and Their Polymer Composites*. https://doi.org/10.1016/B978-0-323-48061-1.00001-4

Encinas, N., Oakley, B. R., Belcher, M. A., Blohowiak, K. Y., Dillingham, R. G., Abenojar, J., & Martínez, M. A. (2014). Surface modification of aircraft used composites for adhesive bonding. *International Journal of Adhesion and Adhesives*, *50*. https://doi.org/10.1016/j.ijadhadh.2014.01.004

Epoxy, I., & Solutions, A. (2012). Epoxy Adhesive Application Guide. *Brochure*, 10–19. www.EPOTEK.com

European Aluminum Association (EAA). (2013). Aluminium in Cars. Unlocking the Light-Weighting Potential. In *Journal of Chemical Information and Modeling* (Vol. 53, Issue 9).

Evci, C., & Gülgeç, M. (2012). An experimental investigation on the impact response of composite materials. International Journal of Impact Engineering, 43. https://doi.org/10.1016/j.ijimpeng.2011.11.009

2030 climate & energy framework - Climate Action, 2030 Climate & Energy Framework (2018).

FEATURE: Light Speed – How electric cars are driving a new wave of lightweighting. (n.d.). Retrieved June 24, 2022, from https://www.imeche.org/news/news-article/feature-light-speed-how-electric-cars-are-driving-a-new-wave-of-lightweighting

Ferdosian, F., Yuan, Z., Anderson, M., & Xu, C. (2014). Synthesis of lignin-based epoxy resins: Optimization of reaction parameters using response surface methodology. *RSC Advances*. https://doi.org/10.1039/c4ra03978e

Ferrari, A. C., Bonaccorso, F., Fal'ko, V., Novoselov, K. S., Roche, S., Bøggild, P., Borini, S., Koppens, F. H. L., Palermo, V., Pugno, N., Garrido, J. A., Sordan, R., Bianco, A., Ballerini, L., Prato, M., Lidorikis, E., Kivioja, J., Marinelli, C., Ryhänen, T., … Kinaret, J. (2015). Science and technology roadmap for graphene, related two-dimensional crystals, and hybrid systems. *Nanoscale*. https://doi.org/10.1039/c4nr01600a

Ferreira, V., Merchán, M., Egizabal, P., García De Cortázar, M., Irazustabarrena, A., López-Sabirón, A. M., & Ferreira, G. (2019). Technical and environmental evaluation of a new high performance material based on magnesium alloy reinforced with submicrometre-sized TiC particles to develop automotive lightweight components and make transport sector more sustainable. *Journal of Materials Research and Technology*. https://doi.org/10.1016/j.jmrt.2019.02.012

Fertier, L., Koleilat, H., Stemmelen, M., Giani, O., Joly-Duhamel, C., Lapinte, V., & Robin, J. J. (2013). The use of renewable feedstock in UV-curable materials-A new age for polymers and green chemistry. In *Progress in Polymer Science* (Vol. 38, Issue 6). https://doi.org/10.1016/j.progpolymsci.2012.12.002

Flammersheim, H. J. (1998). Kinetics and mechanism of the epoxide–amine polyaddition1Presented at the Twelfth Ulm-Freiberg Conference, Freiberg, Germany, 19–21 March 19971. *Thermochimica Acta*, *310*(1), 153–159. https://doi.org/https://doi.org/10.1016/S0040-6031(97)00225-6

Friedrich, K., & Almajid, A. A. (2013). Manufacturing aspects of advanced polymer composites for automotive applications. *Applied Composite Materials*. https://doi.org/10.1007/s10443-012-9258-7

Fu, Y., & Zhong, W.-H. (2011). Cure kinetics behavior of a functionalized graphitic nanofiber modified epoxy resin. *Thermochimica Acta*, *516*(1), 58–63. https://doi.org/https://doi.org/10.1016/j.tca.2011.01.016

Galpaya, D. G. D., Fernando, J. F. S., Rintoul, L., Motta, N., Waclawik, E. R., Yan, C., & George, G. A. (2015). The effect of graphene oxide and its oxidized debris on the cure chemistry and interphase structure of epoxy nanocomposites. *Polymer*. https://doi.org/10.1016/j.polymer.2015.06.054

Galpaya, D., Wang, M., Liu, M., Motta, N., Waclawik, E., & Yan, C. (2012). Recent Advances in Fabrication and Characterization of Graphene-Polymer Nanocomposites. *Graphene*. https://doi.org/10.4236/graphene.2012.12005

Galvez, P., Quesada, A., Martinez, M. A., Abenojar, J., Boada, M. J. L., & Diaz, V. (2017). Study of the behaviour of adhesive joints of steel with CFRP for its application in bus structures. *Composites Part B: Engineering*. https://doi.org/10.1016/j.compositesb.2017.07.018

Gandini, A. (2011). The irruption of polymers from renewable resources on the scene of macromolecular science and technology. In *Green Chemistry*. https://doi.org/10.1039/c0gc00789g

Gao, Z., LaClair, T., Ou, S., Huff, S., Wu, G., Hao, P., Boriboonsomsin, K., & Barth, M. (2019). Evaluation of electric vehicle component performance over eco-driving cycles. Energy, 172. https://doi.org/10.1016/j.energy.2019.02.017

García, N. J., & Bazán, J. C. (2009). Electrical conductivity of montmorillonite as a function of relative humidity: La-montmorillonite. *Clay Minerals*. https://doi.org/10.1180/claymin.2009.044.1.81

Gardyński, L., Caban, J., & Barta, D. (2018). RESEARCH OF COMPOSITE MATERIALS USED IN THE CONSTRUCTION OF VEHICLE BODYWORK. Advances in Science and Technology Research Journal, 12(3). https://doi.org/10.12913/22998624/92096

Garg, A. C., & Mai, Y. W. (1988). Failure mechanisms in toughened epoxy resins-A review. *Composites Science and Technology*, *31*(3). https://doi.org/10.1016/0266-3538(88)90009-7

Geim, A. K. (2009). Graphene: Status and prospects. In *Science*. https://doi.org/10.1126/science.1158877

Geim, A. K., & Novoselov, K. S. (2007). The rise of graphene. *Nature Materials*. https://doi.org/10.1038/nmat1849

Gene Liao, Y., & State University, W. (2017). *Advanced Automotive Technology*. http://automobiles.honda.com/images/2009/civic-sedan/safety/safety-header.jpg

Ghaleb, Z. A., Mariatti, M., & Ariff, Z. M. (2017). Graphene nanoparticle dispersion in epoxy thin film composites for electronic applications: effect on tensile, electrical and thermal properties. *Journal of Materials Science: Materials in Electronics*. https://doi.org/10.1007/s10854-016-5594-y

Giampieri, A., Ling-Chin, J., Taylor, W., Smallbone, A., & Roskilly, A. P. (2019). Moving towards low-carbon manufacturing in the UK automotive industry. *Energy Procedia*. https://doi.org/10.1016/j.egypro.2019.01.946

Giannelis, E. P., Krishnamoorti, R., & Manias, E. (1999). Polymer-silicate nanocomposites: Model systems for confined polymers and polymer brushes. *Advances in Polymer Science*. https://doi.org/10.1007/3-540-69711-x_3

Gibson, G. (2017). *Chapter 27 - Epoxy Resins* (M. B. T.-B. P. M. (Eighth E. Gilbert (Ed.); pp. 773–797). Butterworth-Heinemann. https://doi.org/https://doi.org/10.1016/B978-0-323-35824-8.00027-X

Gkikas, G., Barkoula, N. M., & Paipetis, A. S. (2012). Effect of dispersion conditions on the thermo-mechanical and toughness properties of multi walled carbon nanotubes-reinforced epoxy. *Composites Part B: Engineering*. https://doi.org/10.1016/j.compositesb.2012.01.070

Gkikas, G., Lekatou, A., Sioulas, D., & Paipetis, A. S. (2014). Effect of carbon nanotube enhanced adhesives on degradation of bonded joints in corrosive environments. *Plastics, Rubber and Composites*. https://doi.org/10.1179/1743289814Y.0000000085

Godovsky, D. Y. (2000). Device applications of polymer-nanocomposites. In *Advances in Polymer Science*. https://doi.org/10.1007/3-540-46414-x_4

Goldberg, S. (2008). Mechanical/physical methods of cell disruption and tissue homogenization. In Methods in molecular biology (Clifton, N.J.) (Vol. 424). https://doi.org/10.1007/978-1-60327-064-9_1

Gómez, J., Villaro, E., Navas, A., & Recio, I. (2017). Testing the influence of the temperature, RH and filler type and content on the universal power law for new reduced graphene oxide TPU composites. *Materials Research Express*. https://doi.org/10.1088/2053-1591/aa8e11

Gong, X., Kang, H., Liu, Y., & Wu, S. (2015). Decomposition mechanisms and kinetics of amine/anhydride-cured DGEBA epoxy resin in near-critical water. *RSC Advances*. https://doi.org/10.1039/c5ra03828f

Gov.uk. (2019). UK becomes first major economy to pass net zero emissions law. In *Department for Business Energy & Industrial Strategy*.

Granado, L., Tavernier, R., Foyer, G., David, G., & Caillol, S. (2018). Comparative curing kinetics study of high char yield formaldehyde- and terephthalaldehyde-phenolic thermosets. *Thermochimica Acta*. https://doi.org/10.1016/j.tca.2018.06.013

Grant, L. D. R., Adams, R. D., & da Silva, L. F. M. (2009). Experimental and numerical analysis of single-lap joints for the automotive industry. *International Journal of Adhesion and Adhesives*, *29*(4). https://doi.org/10.1016/j.ijadhadh.2008.09.001

Graphene - What Is It? | Graphenea. (n.d.). Retrieved August 19, 2022, from https://www.graphenea.com/pages/graphene#.Yv-75i7MJPZ

Gu, H., Ma, C., Gu, J., Guo, J., Yan, X., Huang, J., Zhang, Q., & Guo, Z. (2016). An overview of multifunctional epoxy nanocomposites. In *Journal of Materials Chemistry C*. https://doi.org/10.1039/c6tc01210h

Gu, J., Liang, C., Zhao, X., Gan, B., Qiu, H., Guo, Y., Yang, X., Zhang, Q., & Wang, D. Y. (2017). Highly thermally conductive flame-retardant epoxy nanocomposites with reduced ignitability and excellent electrical conductivities. *Composites Science and Technology*. https://doi.org/10.1016/j.compscitech.2016.12.015

Guadagno, L., Raimondo, M., Vertuccio, L., Mauro, M., Guerra, G., Lafdi, K., De Vivo, B., Lamberti, P., Spinelli, G., & Tucci, V. (2015). Optimization of graphene-based materials outperforming host epoxy matrices. *RSC Advances*, *5*(46). https://doi.org/10.1039/c5ra04558d

Guadagno, Liberata, Raimondo, M., Vittoria, V., Vertuccio, L., Naddeo, C., Russo, S., De Vivo, B., Lamberti, P., Spinelli, G., & Tucci, V. (2014a). Development of epoxy mixtures for application in aeronautics and aerospace. *RSC Advances*. https://doi.org/10.1039/c3ra48031c

Guadagno, Liberata, Raimondo, M., Vittoria, V., Vertuccio, L., Naddeo, C., Russo, S., De Vivo, B., Lamberti, P., Spinelli, G., & Tucci, V. (2014b). Development of epoxy mixtures for application in aeronautics and aerospace. *RSC Advances*. https://doi.org/10.1039/c3ra48031c

Guadagno, Liberata, Sarno, M., Vietri, U., Raimondo, M., Cirillo, C., & Ciambelli, P. (2015). Graphene-based structural adhesive to enhance adhesion performance. *RSC Advances*. https://doi.org/10.1039/c5ra00819k

Gültekin, K., Akpinar, S., Gürses, A., Eroglu, Z., Cam, S., Akbulut, H., Keskin, Z., & Ozel, A. (2016). The effects of graphene nanostructure reinforcement on the adhesive method and the graphene reinforcement ratio on the failure load in adhesively bonded joints. *Composites Part B: Engineering*. https://doi.org/10.1016/j.compositesb.2016.05.039

Guo, B., Jia, D., & Cai, C. (2004). Effects of organo-montmorillonite dispersion on thermal stability of epoxy resin nanocomposites. *European Polymer Journal*. https://doi.org/10.1016/j.eurpolymj.2004.03.027

Guo, F., Creighton, M., Chen, Y., Hurt, R., & Külaots, I. (2014). Porous structures in stacked, crumpled and pillared graphene-based 3D materials. *Carbon*. https://doi.org/10.1016/j.carbon.2013.09.024

Guo, L., Liu, J., Xia, H., Li, X., Zhang, X., & Yang, H. (2021). Effects of surface treatment and adhesive thickness on the shear strength of precision bonded joints. *Polymer Testing*, *94*. https://doi.org/10.1016/j.polymertesting.2021.107063

Gupta, M. K., & Singhal, V. (2022). Review on materials for making lightweight vehicles. Materials Today: Proceedings, 56. https://doi.org/10.1016/j.matpr.2022.02.517

Hadad, D. K. (1988). Physical and Chemical Characterization of Epoxy Resins. In C. A. May (Ed.), *Epoxy Resins Chemistry and Technology* (Second). Taylor & Francis Inc , CRC Press Inc.

Hagnell, M. K., & Åkermo, M. (2019). The economic and mechanical potential of closed loop material usage and recycling of fibre-reinforced composite materials. *Journal of Cleaner Production*, *223*. https://doi.org/10.1016/j.jclepro.2019.03.156

Han, S., Meng, Q., Araby, S., Liu, T., & Demiral, M. (2019). Mechanical and electrical properties of graphene and carbon nanotube reinforced epoxy adhesives: Experimental and numerical analysis. *Composites Part A: Applied Science and Manufacturing*, *120*, 116–126. https://doi.org/https://doi.org/10.1016/j.compositesa.2019.02.027

Hardis, R., Jessop, J. L. P., Peters, F. E., & Kessler, M. R. (2013). Cure kinetics characterization and monitoring of an epoxy resin using DSC, Raman spectroscopy, and DEA. *Composites Part A: Applied Science and Manufacturing*. https://doi.org/10.1016/j.compositesa.2013.01.021

Hasheminia, S. M., Park, B. C., Chun, H. J., Park, J. C., & Chang, H. S. (2019). Failure mechanism of bonded joints with similar and dissimilar material. *Composites Part B: Engineering*. https://doi.org/10.1016/j.compositesb.2018.11.016

Hashim, U. R., & Jumahat, A. (2019). Improved tensile and fracture toughness properties of graphene nanoplatelets filled epoxy polymer via solvent compounding shear milling method. *Materials Research Express*. https://doi.org/10.1088/2053-1591/aaeaf0

He, B., & Ge, D. (2017). Dynamic strength of adhesively bonded composite joints with similar and dissimilar assembled adherends. *Journal of Reinforced Plastics and Composites*. https://doi.org/10.1177/0731684417724891

He, H., & Gao, C. (2010). General Approach to Individually Dispersed, Highly Soluble, and Conductive Graphene Nanosheets Functionalized by Nitrene Chemistry. *Chemistry of Materials*, *22*(17), 5054–5064. https://doi.org/10.1021/cm101634k

Henini, M. (2000). Scanning electron microscopy: An introduction. *III-Vs Review*. https://doi.org/10.1016/S0961-1290(00)80006-X

Hernandez, Y., Nicolosi, V., Lotya, M., Blighe, F. M., Sun, Z., De, S., McGovern, I. T., Holland, B., Byrne, M., Gun'Ko, Y. K., Boland, J. J., Niraj, P., Duesberg, G., Krishnamurthy, S., Goodhue, R., Hutchison, J., Scardaci, V., Ferrari, A. C., & Coleman, J. N. (2008). High-yield production of graphene by liquid-phase exfoliation of graphite. *Nature Nanotechnology*, *3*(9), 563–568. https://doi.org/10.1038/nnano.2008.215

Heuss, R., Müller, N., van Sintern, W., Starke, A., Tschiesner, A., Sintern, W. Van, Starke, A., Tschiesner, A., van Sintern, W., Starke, A., & Tschiesner, A. (2012). Lightweight, heavy impact. *McKinsey & Co*. https://doi.org/10.1016/j.bbadis.2004.11.017

Higgins, A. (2000). Adhesive bonding of aircraft structures. *International Journal of Adhesion and Adhesives*, *20*(5). https://doi.org/10.1016/S0143-7496(00)00006-3

High-Strength Adhesives are Replacing Mechanical Fasteners for Durable, Low-Cost Bonds. (n.d.). Retrieved January 4, 2022, from www.fabrico.com

Ho, T. H., & Wang, C. S. (1996). Modification of epoxy resins with polysiloxane thermoplastic polyurethane for electronic encapsulation: 1. *Polymer*. https://doi.org/10.1016/0032-3861(96)87635-X

Horie, K., Hiura, H., Sawada, M., Mita, I., & Kambe, H. (1970). Calorimetric investigation of polymerization reactions. III. Curing reaction of epoxides with amines. *Journal of Polymer Science Part A-1: Polymer Chemistry*. https://doi.org/10.1002/pol.1970.150080605

Hsieh, T. H., Chen, W. J., Chiang, C. L., & Shen, M. Y. (2018). Environmental aging effect on interlaminar properties of graphene nanoplatelets reinforced epoxy/carbon fiber composite laminates. *Journal of Reinforced Plastics and Composites*, *37*(19). https://doi.org/10.1177/0731684416637219

Hu, H., Wang, X., Wang, J., Wan, L., Liu, F., Zheng, H., Chen, R., & Xu, C. (2010). Preparation and properties of graphene nanosheets-polystyrene nanocomposites via in situ emulsion polymerization. *Chemical Physics Letters*. https://doi.org/10.1016/j.cplett.2009.11.024

Hu, J., Yuan, P., Zeng, K., & Yang, G. (2014). Study of the curing kinetics of a benzimidazole/phthalonitrile resin system. *Thermochimica Acta*. https://doi.org/10.1016/j.tca.2014.06.006

Huang, K., Zhang, P., Zhang, J., Li, S., Li, M., Xia, J., & Zhou, Y. (2013). Preparation of biobased epoxies using tung oil fatty acid-derived C21 diacid and C22 triacid and study of epoxy properties. *Green Chemistry*. https://doi.org/10.1039/c3gc40622a

Huang, M., & Li, Z. (2006). Influences of particle size and interface energy on the stress concentration induced by the oblate spheroidal particle and the void nucleation mechanism. *International Journal of Solids and Structures*, *43*(14–15). https://doi.org/10.1016/j.ijsolstr.2005.04.015

Huang, X., Qi, X., Boey, F., & Zhang, H. (2012). Graphene-based composites. In *Chemical Society Reviews*. https://doi.org/10.1039/c1cs15078b

Hummers, W. S., & Offeman, R. E. (1958). Preparation of Graphitic Oxide. *Journal of the American Chemical Society*. https://doi.org/10.1021/ja01539a017

Hussain, F., Hojjati, M., Okamoto, M., & Gorga, R. E. (2006). Review article: Polymer-matrix nanocomposites, processing, manufacturing, and application: An overview. *Journal of Composite Materials*, *40*(17). https://doi.org/10.1177/0021998306067321

index @ www.waterjetsweden.co.uk. (n.d.). https://www.waterjetsweden.co.uk/

IO, O. (2016). Development of Bone Particulate Reinforced Epoxy Composite For Biomedical Application. *Journal of Applied Biotechnology & Bioengineering*. https://doi.org/10.15406/jabb.2016.01.00006

Iqbal, H. M. S., Bhowmik, S., & Benedictus, R. (2010). Surface modification of high performance polymers by atmospheric pressure plasma and failure mechanism of adhesive bonded joints. *International Journal of Adhesion and Adhesives*, *30*(6). https://doi.org/10.1016/j.ijadhadh.2010.02.007

Jaillet, F., Darroman, E., Ratsimihety, A., Auvergne, R., Boutevin, B., & Caillol, S. (2014). New biobased epoxy materials from cardanol. *European Journal of Lipid Science and Technology*. https://doi.org/10.1002/ejlt.201300193

Jamir, M. R. M., Majid, M. S. A., & Khasri, A. (2018). Natural lightweight hybrid composites for aircraft structural applications. In *Sustainable Composites for Aerospace Applications*. https://doi.org/10.1016/B978-0-08-102131-6.00008-6

Jasiński, D., Meredith, J., & Kirwan, K. (2016). A comprehensive framework for automotive sustainability assessment. *Journal of Cleaner Production*. https://doi.org/10.1016/j.jclepro.2016.07.027

Jee, S. M., Ahn, C.-H., Park, J. H., Kim, T. A., & Park, M. (2020). Solvent-free encapsulation of curing agents for high performing one-component epoxy adhesives. *Composites Part B: Engineering*, *202*, 108438. https://doi.org/https://doi.org/10.1016/j.compositesb.2020.108438

Ji, Z., Zhang, L., Xie, G., Xu, W., Guo, D., Luo, J., & Prakash, B. (2020). Mechanical and tribological properties of nanocomposites incorporated with two-dimensional materials. In Friction (Vol. 8, Issue 5). https://doi.org/10.1007/s40544-020-0401-4

Johnsen, B. B., Kinloch, A. J., Mohammed, R. D., Taylor, A. C., & Sprenger, S. (2007). Toughening mechanisms of nanoparticle-modified epoxy polymers. *Polymer*, *48*(2). https://doi.org/10.1016/j.polymer.2006.11.038

Jojibabu, P., Jagannatham, M., Haridoss, P., Janaki Ram, G. D., Deshpande, A. P., & Bakshi, S. R. (2016a). Effect of different carbon nano-fillers on rheological properties and lap shear strength of epoxy adhesive joints. *Composites Part A: Applied Science and Manufacturing*. https://doi.org/10.1016/j.compositesa.2015.12.003

Jojibabu, P., Ram, G. D. J., Deshpande, A. P., & Bakshi, S. R. (2017). Effect of carbon nano-filler addition on the degradation of epoxy adhesive joints subjected to hygrothermal aging. *Polymer Degradation and Stability*. https://doi.org/10.1016/j.polymdegradstab.2017.04.017

Jojibabu, P., Zhang, Y. X., & Prusty, B. G. (2020). A review of research advances in epoxy-based nanocomposites as adhesive materials. *International Journal of Adhesion and Adhesives*. https://doi.org/10.1016/j.ijadhadh.2019.102454

Jouyandeh, M., Yarahmadi, E., Didehban, K., Ghiyasi, S., Paran, S. M. R., Puglia, D., Ali, J. A., Jannesari, A., Saeb, M. R., Ranjbar, Z., & Ganjali, M. R. (2019). Cure kinetics of epoxy/graphene oxide (GO) nanocomposites: Effect of starch functionalization of GO nanosheets. *Progress in Organic Coatings*. https://doi.org/10.1016/j.porgcoat.2019.105217

Joy, D. C. (2003). Introduction to the Scanning Electron Microscope. *Microscopy and Microanalysis*. https://doi.org/10.1017/s1431927603447788

Jubsilp, C., Punson, K., Takeichi, T., & Rimdusit, S. (2010). Curing kinetics of Benzoxazine–epoxy copolymer investigated by non-isothermal differential scanning calorimetry. *Polymer Degradation and Stability*, *95*(6), 918–924. https://doi.org/https://doi.org/10.1016/j.polymdegradstab.2010.03.029

Jumahat, A., Soutis, C., Abdullah, S. A., & Kasolang, S. (2012). Tensile properties of nanosilica/epoxy nanocomposites. *Procedia Engineering*. https://doi.org/10.1016/j.proeng.2012.07.361

Kalaitzidou, K., Fukushima, H., & Drzal, L. T. (2007). A new compounding method for exfoliated graphite-polypropylene nanocomposites with enhanced flexural properties and lower percolation threshold. *Composites Science and Technology*. https://doi.org/10.1016/j.compscitech.2006.11.014

Kaluza, A., Fröhlich, T., Kleemann, S., Walk, W., Herrmann, C., Krinke, S., & Vietor, T. (2018). Conceptual Development of Hybrid Structures Towards Eco-Efficient Vehicle Lightweighting. In Designing Sustainable Technologies, Products and Policies. https://doi.org/10.1007/978-3-319-66981-6_21

Kamal, A., Ashmawy, M., S, S., Algazzar, A. M., & Elsheikh, A. H. (2021). Fabrication techniques of polymeric nanocomposites: A comprehensive review. *Proceedings of the Institution of Mechanical Engineers, Part C: Journal of Mechanical Engineering Science*. https://doi.org/10.1177/09544062211055662

Kamarian, S., Bodaghi, M., Isfahani, R. B., Shakeri, M., & Yas, M. H. (2019). Influence of carbon nanotubes on thermal expansion coefficient and thermal buckling of polymer composite plates: experimental and numerical investigations. *Mechanics Based Design of Structures and Machines*. https://doi.org/10.1080/15397734.2019.1674664

Kandare, E., Kandola, B. K., & Myler, P. (2013). Evaluating the influence of varied fire-retardant surface coatings on post-heat flexural properties of glass/epoxy composites. *Fire Safety Journal*. https://doi.org/10.1016/j.firesaf.2013.01.009

Kanehashi, S., Yokoyama, K., Masuda, R., Kidesaki, T., Nagai, K., & Miyakoshi, T. (2013). Preparation and characterization of cardanol-based epoxy resin for coating at room temperature curing. *Journal of Applied Polymer Science*. https://doi.org/10.1002/app.39382

Kanerva, M., & Saarela, O. (2013). The peel ply surface treatment for adhesive bonding of composites: A review. In *International Journal of Adhesion and Adhesives* (Vol. 43). https://doi.org/10.1016/j.ijadhadh.2013.01.014

Kanerva, M., Sarlin, E., Hoikkanen, M., Rämö, K., Saarela, O., & Vuorinen, J. (2015). Interface modification of glass fibre-polyester composite-composite joints using peel plies. *International Journal of Adhesion and Adhesives*, *59*. https://doi.org/10.1016/j.ijadhadh.2015.01.016

Kango, S., Kalia, S., Celli, A., Njuguna, J., Habibi, Y., & Kumar, R. (2013). Surface modification of inorganic nanoparticles for development of organic-inorganic nanocomposites - A review. In *Progress in Polymer Science*. https://doi.org/10.1016/j.progpolymsci.2013.02.003

Karagiannidis, P. G., Hodge, S. A., Lombardi, L., Tomarchio, F., Decorde, N., Milana, S., Goykhman, I., Su, Y., Mesite, S. V., Johnstone, D. N., Leary, R. K., Midgley, P. A., Pugno, N. M., Torrisi, F., & Ferrari, A. C. (2017). Microfluidization of Graphite and Formulation of Graphene-Based Conductive Inks. *ACS Nano*, *11*(3). https://doi.org/10.1021/acsnano.6b07735

Karger-Kocsis, J., Mahmood, H., & Pegoretti, A. (2015). Recent advances in fiber/matrix interphase engineering for polymer composites. In *Progress in Materials Science*. https://doi.org/10.1016/j.pmatsci.2015.02.003

Karkanas, P. I. (1996). Modelling the cure of a commercial epoxy resin for applications in resin transfer moulding. *Polymer International*, *41*(2). https://doi.org/10.1002/(SICI)1097-0126(199610)41:2<183::AID-PI621>3.0.CO;2-F

Karkanas, P. I., & Partridge, I. K. (2000). Cure modeling and monitoring of epoxy/amine resin systems. I. Cure kinetics modeling. *Journal of Applied Polymer Science*, *77*(7), 1419–1431. https://doi.org/10.1002/1097-4628(20000815)77:7<1419::AID-APP3>3.0.CO;2-N

Kasemsiri, P., Neramittagapong, A., & Chindaprasirt, P. (2015). Curing kinetic, thermal and adhesive properties of epoxy resin cured with cashew nut shell liquid. *Thermochimica Acta*. https://doi.org/10.1016/j.tca.2014.11.031

Kausar, A. (2020). A review of high performance polymer nanocomposites for packaging applications in electronics and food industries. In *Journal of Plastic Film and Sheeting*. https://doi.org/10.1177/8756087919849459

Kausar, A., Anwar, Z., & Muhammad, B. (2016). Recent Developments in Epoxy/Graphite, Epoxy/Graphene, and Epoxy/Graphene Nanoplatelet Composites: A Comparative Review. In *Polymer - Plastics Technology and Engineering*. https://doi.org/10.1080/03602559.2016.1163589

Kausar, A., Rafique, I., Anwar, Z., & Muhammad, B. (2016). Recent Developments in Different Types of Flame Retardants and Effect on Fire Retardancy of Epoxy Composite. In *Polymer - Plastics Technology and Engineering* (Vol. 55, Issue 14). https://doi.org/10.1080/03602559.2016.1163607

Khanna, V., & Bakshi, B. R. (2009). Carbon nanofiber polymer composites: Evaluation of life cycle energy use. Environmental Science and Technology. https://doi.org/10.1021/es802101x

Kim, H., Abdala, A. A., & Macosko, C. W. (2010). Graphene/Polymer Nanocomposites. Macromolecules, 43, 6515–6530.

Kim, H., Miura, Y., & MacOsko, C. W. (2010). Graphene/polyurethane nanocomposites for improved gas barrier and electrical conductivity. *Chemistry of Materials*. https://doi.org/10.1021/cm100477v

Kim, J., Cha, J., Jun, G. H., Yoo, S. C., Ryu, S., & Hong, S. H. (2018). Fabrication of Graphene Nanoplatelet/Epoxy Nanocomposites for Lightweight and High-Strength Structural Applications. *Particle and Particle Systems Characterization*. https://doi.org/10.1002/ppsc.201700412

Kim, S., Do, I., & Drzal, L. T. (2009). Multifunctional xGnP/LLDPE nanocomposites prepared by solution compounding using various screw rotating systems. *Macromolecular Materials and Engineering*. https://doi.org/10.1002/mame.200800319

King, A. A. K., Davies, B. R., Noorbehesht, N., Newman, P., Church, T. L., Harris, A. T., Razal, J. M., & Minett, A. I. (2016). A new raman metric for the characterisation of graphene oxide and its derivatives. *Scientific Reports*, *6*. https://doi.org/10.1038/srep19491

King, J. A., Klimek, D. R., Miskioglu, I., & Odegard, G. M. (2013). Mechanical properties of graphene nanoplatelet/epoxy composites. *Journal of Applied Polymer Science*. https://doi.org/10.1002/app.38645

Kissinger, H. E. (1956). Variation of peak temperature with heating rate in differential thermal analysis. *Journal of Research of the National Bureau of Standards*, *57*(4). https://doi.org/10.6028/jres.057.026

Kissinger, H. E. (1957). Reaction Kinetics in Differential Thermal Analysis. *Analytical Chemistry*. https://doi.org/10.1021/ac60131a045

Kleemann, S., Fröhlich, T., Türck, E., & Vietor, T. (2017). A Methodological Approach Towards Multi-material Design of Automotive Components. Procedia CIRP, 60. https://doi.org/10.1016/j.procir.2017.01.010

Klimek-McDonald, D. R., King, J. A., Miskioglu, I., Pineda, E. J., & Odegard, G. M. (2018). Determination and Modeling of Mechanical Properties for Graphene Nanoplatelet/Epoxy Composites. *Polymer Composites*. https://doi.org/10.1002/pc.24137

Koffler, C. (2014). Life cycle assessment of automotive lightweighting through polymers under US boundary conditions. *The International Journal of Life Cycle Assessment*, *19*(3), 538–545. https://doi.org/10.1007/s11367-013-0652-7

Kong, C., Lee, H., & Park, H. (2016). Design and manufacturing of automobile hood using natural composite structure. *Composites Part B: Engineering*, *91*. https://doi.org/10.1016/j.compositesb.2015.12.033

Kreling, S., Fischer, F., Delmdahl, R., Gäbler, F., & Dilger, K. (2013). Analytical characterization of CFRP laser treated by excimer laser radiation. *Physics Procedia*, *41*. https://doi.org/10.1016/j.phpro.2013.03.080

Krieg, A. S., King, J. A., Jaszczak, D. C., Miskoglu, I., Mills, O. P., & Odegard, G. M. (2018). Tensile and conductivity properties of epoxy composites containing carbon black and graphene nanoplatelets. *Journal of Composite Materials*, *52*(28). https://doi.org/10.1177/0021998318771460

Kuan, C. F., Chiang, C. L., Lin, S. H., Huang, W. G., Hsieh, W. Y., & Shen, M. Y. (2018). Characterization and properties of graphene nanoplatelets/XNBR nanocomposites. *Polymers and Polymer Composites*, *26*(1). https://doi.org/10.1177/096739111802600107

Kuila, T., Srivastava, S. K., Bhowmick, A. K., & Saxena, A. K. (2008). Thermoplastic polyolefin based polymer - blend-layered double hydroxide nanocomposites. *Composites Science and Technology*. https://doi.org/10.1016/j.compscitech.2008.08.003

Kuilla, T., Bhadra, S., Yao, D., Kim, N. H., Bose, S., & Lee, J. H. (2010). Recent advances in graphene based polymer composites. In *Progress in Polymer Science (Oxford)*. https://doi.org/10.1016/j.progpolymsci.2010.07.005

Kulkarni, D. D., Choi, I., Singamaneni, S. S., & Tsukruk, V. V. (2010). Graphene oxide - Polyelectrolyte nanomembranes. ACS Nano. https://doi.org/10.1021/nn101204d

Kumanan, A., Varadarajan, S., & Narayanan, K. (2021). Lightweighting in Electric Vehicles: Review of the Design Strategies Based on Patents and Publications. Smart Innovation, Systems and Technologies, 223. https://doi.org/10.1007/978-981-16-0084-5_21

Kumar, A., Sharma, K., & Dixit, A. R. (2020). A review on the mechanical and thermal properties of graphene and graphene-based polymer nanocomposites: understanding of modelling and MD simulation. *Molecular Simulation*. https://doi.org/10.1080/08927022.2019.1680844

Kumar, S., Samal, S. K., Mohanty, S., & Nayak, S. K. (2018). Recent Development of Biobased Epoxy Resins: A Review. In *Polymer - Plastics Technology and Engineering*. https://doi.org/10.1080/03602559.2016.1253742

Lago, E., Toth, P. S., Pugliese, G., Pellegrini, V., & Bonaccorso, F. (2016). Solution blending preparation of polycarbonate/graphene composite: Boosting the mechanical and electrical properties. *RSC Advances*. https://doi.org/10.1039/c6ra21962d

Lascano, D., Quiles-Carrillo, L., Balart, R., Boronat, T., & Montanes, N. (2019). Kinetic analysis of the curing of a partially biobased epoxy resin using dynamic differential scanning calorimetry. *Polymers*. https://doi.org/10.3390/polym11030391

Lathabai, S. (2011). Joining of aluminium and its alloys. *Fundamentals of Aluminium Metallurgy: Production, Processing and Applications*, 607–654. https://doi.org/10.1533/9780857090256.3.607

Le, B., Khaliq, J., Huo, D., Teng, X., & Shyha, I. (2020). A review on nanocomposites. Part 1: Mechanical properties. *Journal of Manufacturing Science and Engineering, Transactions of the ASME*, *142*(10). https://doi.org/10.1115/1.4047047

Lee, C., Wei, X., Kysar, J. W., & Hone, J. (2008a). Measurement of the elastic properties and intrinsic strength of monolayer graphene. *Science*. https://doi.org/10.1126/science.1157996

Lee, C., Wei, X., Kysar, J. W., & Hone, J. (2008b). Measurement of the elastic properties and intrinsic strength of monolayer graphene. *Science*. https://doi.org/10.1126/science.1157996

Lee, J. U., Yoon, D., & Cheong, H. (2012). Estimation of young's modulus of graphene by Raman spectroscopy. *Nano Letters*. https://doi.org/10.1021/nl301073q

Lei, L., Xia, Z., Zhang, L., Zhang, Y., & Zhong, L. (2016). Preparation and properties of amino-functional reduced graphene oxide/waterborne polyurethane hybrid emulsions. *Progress in Organic Coatings*, *97*, 19–27. https://doi.org/https://doi.org/10.1016/j.porgcoat.2016.03.011

Leroux, F., & Besse, J. (2001). Polymer interleaved layered double hydroxide: A new emerging class of nanocomposites. In *Chemistry of Materials*. https://doi.org/10.1021/cm0110268

Li, C., Adamcik, J., & Mezzenga, R. (2012). Biodegradable nanocomposites of amyloid fibrils and graphene with shape-memory and enzyme-sensing properties. *Nature Nanotechnology*. https://doi.org/10.1038/nnano.2012.62

Li, D., Müller, M. B., Gilje, S., Kaner, R. B., & Wallace, G. G. (2008). Processable aqueous dispersions of graphene nanosheets. *Nature Nanotechnology*. https://doi.org/10.1038/nnano.2007.451

Li, H., Pang, S., Wu, S., Feng, X., Müllen, K., & Bubeck, C. (2011). Layer-by-layer assembly and UV photoreduction of graphene-polyoxometalate composite films for electronics. *Journal of the American Chemical Society*. https://doi.org/10.1021/ja201594k

Li, N., Huang, Y., Du, F., He, X., Lin, X., Gao, H., Ma, Y., Li, F., Chen, Y., & Eklund, P. C. (2006). Electromagnetic Interference (EMI) shielding of single-walled carbon nanotube epoxy composites. *Nano Letters*. https://doi.org/10.1021/nl0602589

Li, P., Kim, N. H., Bhadra, S., & Lee, J. H. (2009). Electroresponsive property of novel poly(acrylate-acryloyloxyethyl trimethyl ammonium chloride)/clay nanocomposite hydrogels. *Advanced Materials Research*. https://doi.org/10.4028/www.scientific.net/AMR.79-82.2263

Li, Q., Park, O. K., & Lee, J. H. (2009). Positive temperature coefficient behavior of HDPE/EVA blends filled with carbon black. *Advanced Materials Research*. https://doi.org/10.4028/www.scientific.net/AMR.79-82.2267

Li, W., Dichiara, A., & Bai, J. (2013). Carbon nanotube-graphene nanoplatelet hybrids as high-performance multifunctional reinforcements in epoxy composites. *Composites Science and Technology*. https://doi.org/10.1016/j.compscitech.2012.11.015

Li, Yan, Feng, Z., Huang, L., Essa, K., Bilotti, E., Zhang, H., Peijs, T., & Hao, L. (2019). Additive manufacturing high performance graphene-based composites: A review. In *Composites Part A: Applied Science and Manufacturing*. https://doi.org/10.1016/j.compositesa.2019.105483

Li, Yunfeng, Zhu, J., Wei, S., Ryu, J., Sun, L., & Guo, Z. (2011). Poly(propylene)/graphene nanoplatelet nanocomposites: Melt rheological behavior and thermal, electrical, and electronic properties. *Macromolecular Chemistry and Physics*. https://doi.org/10.1002/macp.201100263

Li, Yunfeng, Zhu, J., Wei, S., Ryu, J., Wang, Q., Sun, L., & Guo, Z. (2011). Poly(propylene) nanocomposites containing various carbon nanostructures. *Macromolecular Chemistry and Physics*. https://doi.org/10.1002/macp.201100364

Li, Yuqi, Pan, D., Chen, S., Wang, Q., Pan, G., & Wang, T. (2013). In situ polymerization and mechanical, thermal properties of polyurethane/graphene oxide/epoxy nanocomposites. Materials and Design, 47. https://doi.org/10.1016/j.matdes.2012.12.077

Li, Z., Young, R. J., Backes, C., Zhao, W., Zhang, X., Zhukov, A. A., Tillotson, E., Conlan, A. P., Ding, F., Haigh, S. J., Novoselov, K. S., & Coleman, J. N. (2020). Mechanisms of Liquid-Phase Exfoliation for the Production of Graphene. ACS Nano, 14(9). https://doi.org/10.1021/acsnano.0c03916

Liang, J., Huang, Y., Zhang, L., Wang, Y., Ma, Y., Cuo, T., & Chen, Y. (2009). Molecular-level dispersion of graphene into poly(vinyl alcohol) and effective reinforcement of their nanocomposites. *Advanced Functional Materials*, *19*(14), 2297–2302. https://doi.org/10.1002/adfm.200801776

Liang, J., Xu, Y., Huang, Y., Zhang, L., Wang, Y., Ma, Y., Li, F., Guo, T., & Chen, Y. (2009). Infrared-triggered actuators from graphene-based nanocomposites. *Journal of Physical Chemistry C*. https://doi.org/10.1021/jp901284d

Liebscher, M., Blais, M. O., Pötschke, P., & Heinrich, G. (2013). A morphological study on the dispersion and selective localization behavior of graphene nanoplatelets in immiscible polymer blends of PC and SAN. *Polymer*. https://doi.org/10.1016/j.polymer.2013.08.009

Lightweight Materials for Cars and Trucks | Department of Energy. (n.d.). Retrieved December 30, 2021, from https://www.energy.gov/eere/vehicles/lightweight-materials-cars-and-trucks

Lim, Y. C., Park, H., Jang, J., McMurray, J. W., Lokitz, B. S., Keum, J. K., Wu, Z., & Feng, Z. (2018). Dissimilar materials joining of carbon fiber polymer to dual phase 980 by friction bit joining, adhesive bonding, and weldbonding. Metals, 8(11). https://doi.org/10.3390/met8110865

Lin, L. L., Ho, T. H., & Wang, C. S. (1997). Synthesis of novel trifunctional epoxy resins and their modification with polydimethylsiloxane for electronic application. Polymer. https://doi.org/10.1016/S0032-3861(96)00713-6

Lipman, T. E., & Maier, P. (2021). Advanced materials supply considerations for electric vehicle applications. In MRS Bulletin (Vol. 46, Issue 12). https://doi.org/10.1557/s43577-022-00263-z

Liu, M., Guo, Y., Wang, J., & Yergin, M. (2018). Corrosion avoidance in lightweight materials for automotive applications. In npj Materials Degradation (Vol. 2, Issue 1). https://doi.org/10.1038/s41529-018-0045-2

Liu, S., Fan, X., & He, C. (2016). Improving the fracture toughness of epoxy with nanosilica-rubber core-shell nanoparticles. *Composites Science and Technology*. https://doi.org/10.1016/j.compscitech.2016.01.009

Liu, Y., & Feng, J. (2017). An attempt towards fabricating reduced graphene oxide composites with traditional polymer processing techniques by adding chemical reduction agents. *Composites Science and Technology*. https://doi.org/10.1016/j.compscitech.2016.12.026

Liu, Z., Duan, X., Qian, G., Zhou, X., & Yuan, W. (2013). Eco-friendly one-pot synthesis of highly dispersible functionalized graphene nanosheets with free amino groups. *Nanotechnology*, *24*(4), 45609. https://doi.org/10.1088/0957-4484/24/4/045609

Lu, Y., Biswas, M. C., Guo, Z., Jeon, J. W., & Wujcik, E. K. (2019). Recent developments in bio-monitoring via advanced polymer nanocomposite-based wearable strain sensors. In *Biosensors and Bioelectronics*. https://doi.org/10.1016/j.bios.2018.08.037

Lucić, M., Stoić, a., & Kopač, J. (2006). Investigation of aluminum single lap adhesively bonded joints. *Journal of Achievements in Materials and Manufacturing Engineering*, *15*(1).

Luckeneder, P., Gavino, J., Kuchernig, R., Petutschnigg, A., & Tondi, G. (2016). Sustainable phenolic fractions as basis for furfuryl alcohol-based co-polymers and their use as wood adhesives. *Polymers*. https://doi.org/10.3390/polym8110396

Luong, N. D., Hippi, U., Korhonen, J. T., Soininen, A. J., Ruokolainen, J., Johansson, L. S., Nam, J. Do, Sinh, L. H., & Seppälä, J. (2011). Enhanced mechanical and electrical properties of polyimide film by graphene sheets via in situ polymerization. *Polymer*. https://doi.org/10.1016/j.polymer.2011.09.033

Lv, J., Hong, J., Liang, B., Zhao, E., Zeng, K., Chen, M., Hu, J., & Yang, G. (2020). Study of the curing kinetics of melamine/phthalonitrile resin system. *Thermochimica Acta*. https://doi.org/10.1016/j.tca.2019.178442

Ma, S., Li, T., Liu, X., & Zhu, J. (2016). Research progress on bio-based thermosetting resins. In *Polymer International*. https://doi.org/10.1002/pi.5027

Ma, S., & Webster, D. C. (2015). Naturally Occurring Acids as Cross-Linkers To Yield VOC-Free, High-Performance, Fully Bio-Based, Degradable Thermosets. *Macromolecules*. https://doi.org/10.1021/acs.macromol.5b01923

Ma, T., Liu, Z., Wen, J., Gao, Y., Ren, X., Chen, H., Jin, C., Ma, X. L., Xu, N., Cheng, H. M., & Ren, W. (2017). Tailoring the thermal and electrical transport properties of graphene films by grain size engineering. *Nature Communications*, *8*. https://doi.org/10.1038/ncomms14486

Maghsoudlou, M. A., Barbaz Isfahani, R., Saber-Samandari, S., & Sadighi, M. (2019). Effect of interphase, curvature and agglomeration of SWCNTs on mechanical properties of polymer-based nanocomposites: Experimental and numerical investigations. *Composites Part B: Engineering*. https://doi.org/10.1016/j.compositesb.2019.107119

Maleki Moghadam, R., Saber-Samandari, S., & Hosseini, S. A. (2016). On the tensile behavior of clay-epoxy nanocomposite considering interphase debonding damage via mixed-mode cohesive zone material. *Composites Part B: Engineering*. https://doi.org/10.1016/j.compositesb.2015.11.043

Mallick, P. K. (2021a). Joining for lightweight vehicles. In *Materials, Design and Manufacturing for Lightweight Vehicles*. https://doi.org/10.1016/b978-0-12-818712-8.00008-2

Mallick, P. K. (2021b). Thermoset matrix composites for lightweight automotive structures. In *Materials, Design and Manufacturing for Lightweight Vehicles*. https://doi.org/10.1016/b978-0-12-818712-8.00006-9

Manta, A. (2019). *Design and Simulation of Graphene/Epoxy Nanocomposites: A Multi-Scale Approach on Mechanical, Thermal and Electrical Behaviour*. 1–256.

Marami, G., Nazari, S. A., Faghidian, S. A., Vakili-Tahami, F., & Etemadi, S. (2016). Improving the mechanical

behavior of the adhesively bonded joints using RGO additive. *International Journal of Adhesion and Adhesives*, *70*. https://doi.org/10.1016/j.ijadhadh.2016.07.014

Marefat Seyedlar, R., Imani, M., & Mirabedini, S. M. (2018). Curing of polyfurfuryl alcohol resin catalyzed by a homologous series of dicarboxylic acid catalysts. II. Swelling behavior and thermal properties. *Journal of Applied Polymer Science*. https://doi.org/10.1002/app.45770

Marouf, B. T., Mai, Y. W., Bagheri, R., & Pearson, R. A. (2016). Toughening of epoxy nanocomposites: Nano and hybrid effects. In *Polymer Reviews*. https://doi.org/10.1080/15583724.2015.1086368

Marques, A. C., Mocanu, A., Tomić, N. Z., Balos, S., Stammen, E., Lundevall, A., Abrahami, S. T., Günther, R., de Kok, J. M. M., & de Freitas, S. T. (2020). Review on adhesives and surface treatments for structural applications: Recent developments on sustainability and implementation for metal and composite substrates. In *Materials* (Vol. 13, Issue 24). https://doi.org/10.3390/ma13245590

Marzi, S., Biel, A., & Stigh, U. (2011). On experimental methods to investigate the effect of layer thickness on the fracture behavior of adhesively bonded joints. *International Journal of Adhesion and Adhesives*, *31*(8). https://doi.org/10.1016/j.ijadhadh.2011.08.004

Miao, S., Wang, P., Su, Z., & Zhang, S. (2014). Vegetable-oil-based polymers as future polymeric biomaterials. In Acta Biomaterialia. https://doi.org/10.1016/j.actbio.2013.08.040

Milani, M. A., González, D., Quijada, R., Basso, N. R. S., Cerrada, M. L., Azambuja, D. S., & Galland, G. B. (2013). Polypropylene/graphene nanosheet nanocomposites by in situ polymerization: Synthesis, characterization and fundamental properties. Composites Science and Technology. https://doi.org/10.1016/j.compscitech.2013.05.001

Miller, L., Soulliere, K., Sawyer-Beaulieu, S., Tseng, S., & Tam, E. (2014). Challenges and alternatives to plastics recycling in the automotive sector. In Materials (Vol. 7, Issue 8). https://doi.org/10.3390/ma7085883

Milner, J., Hamilton, I., Woodcock, J., Williams, M., Davies, M., Wilkinson, P., & Haines, A. (2020). Health benefits of policies to reduce carbon emissions. *The BMJ*, *368*. https://doi.org/10.1136/bmj.l6758

Mirabedini, A., Anderson, L., Antiohos, D., Ang, A., Nikzad, M., Fuss, F. K., & Hameed, N. (2022). Scalable Production and Thermoelectrical Modeling of Infusible Functional Graphene/Epoxy Nanomaterials for Engineering Applications. Industrial and Engineering Chemistry Research, 61(15). https://doi.org/10.1021/acs.iecr.1c04621

Mirabedini, A., Ang, A., Nikzad, M., Fox, B., Lau, K. T., & Hameed, N. (2020). Evolving Strategies for Producing Multiscale Graphene-Enhanced Fiber-Reinforced Polymer Composites for Smart Structural Applications. In *Advanced Science* (Vol. 7, Issue 11). https://doi.org/10.1002/advs.201903501

Mittal, V. (2014). Functional polymer nanocomposites with graphene: A review. In *Macromolecular Materials and Engineering*. https://doi.org/10.1002/mame.201300394

Mohan, J., Ramamoorthy, A., Ivanković, A., Dowling, D., & Murphy, N. (2014). Effect of an atmospheric pressure plasma treatment on the mode I fracture toughness of a co-cured composite joint. *Journal of Adhesion*, *90*(9). https://doi.org/10.1080/00218464.2013.772053

Mohan, V. B., Brown, R., Jayaraman, K., & Bhattacharyya, D. (2015). Characterisation of reduced graphene oxide: Effects of reduction variables on electrical conductivity. *Materials Science and Engineering B: Solid-State Materials for Advanced Technology*. https://doi.org/10.1016/j.mseb.2014.11.002

Mohomed, K. (2016). Thermogravimetric Analysis (TGA) Theory and Applications. *TA Instruments*, 4–235. http://webcache.googleusercontent.com/search?q=cache:2tG2B4rkrtwJ:www.tainstruments.com/wp-content/uploads/CA-2016-TGA.pdf+&cd=20&hl=en&ct=clnk&client=firefox-b

Mokhtari, M., Madani, K., Belhouari, M., Touzain, S., Feaugas, X., & Ratwani, M. (2013). Effects of composite adherend properties on stresses in double lap bonded joints. *Materials and Design*, *44*. https://doi.org/10.1016/j.matdes.2012.08.001

Montazeri, A., & Chitsazzadeh, M. (2014). Effect of sonication parameters on the mechanical properties of multi-walled carbon nanotube/epoxy composites. *Materials and Design*, *56*. https://doi.org/10.1016/j.matdes.2013.11.013

Monteiro, S. N., Calado, V., Rodriguez, R. J. S., & Margem, F. M. (2012). Thermogravimetric behavior of natural fibers reinforced polymer composites-An overview. *Materials Science and Engineering A*. https://doi.org/10.1016/j.msea.2012.05.109

Monteserín, C., Blanco, M., Aranzabe, E., Aranzabe, A., & Vilas, J. L. (2017). Effects of graphene oxide and chemically reduced graphene oxide on the curing kinetics of epoxy amine composites. *Journal of Applied Polymer Science*. https://doi.org/10.1002/app.44803

Moriche, R., Prolongo, S. G., Sánchez, M., Jiménez-Suárez, A., Chamizo, F. J., & Ureña, A. (2016). Thermal conductivity and lap shear strength of GNP/epoxy nanocomposites adhesives. *International Journal of Adhesion and Adhesives*. https://doi.org/10.1016/j.ijadhadh.2015.12.012

Moriche, R., Prolongo, S. G., Sánchez, M., Jiménez-Suárez, A., Sayagués, M. J., & Ureña, A. (2015). Morphological changes on graphene nanoplatelets induced during dispersion into an epoxy resin by different methods. *Composites Part B: Engineering*, *72*. https://doi.org/10.1016/j.compositesb.2014.12.012

Nair, R. R., Blake, P., Grigorenko, A. N., Novoselov, K. S., Booth, T. J., Stauber, T., Peres, N. M. R., & Geim, A. K. (2008). Fine structure constant defines visual transparency of graphene. *Science*, *320*(5881). https://doi.org/10.1126/science.1156965

Nascimento, H., dos Reis, M. O., Monteiro, E. C., & Ávila, A. F. (2021). An investigation on industrial adhesive nano-modified by graphene nanoplatelets under extreme environmental conditions. *International Journal of Adhesion and Adhesives*, *111*, 102982. https://doi.org/https://doi.org/10.1016/j.ijadhadh.2021.102982

Naskar, A. K., Keum, J. K., & Boeman, R. G. (2016). Polymer matrix nanocomposites for automotive structural components. In *Nature Nanotechnology*. https://doi.org/10.1038/nnano.2016.262

Natarajan, S. (2015). Fundamental Principles of Polymeric Materials by Christopher S. Brazel and Stephen L. Rosen . *Materials and Manufacturing Processes*. https://doi.org/10.1080/10426914.2015.1059079

Nemati Giv, A., Ayatollahi, M. R., Ghaffari, S. H., & da Silva, L. F. M. (2018). Effect of reinforcements at different scales on mechanical properties of epoxy adhesives and adhesive joints: a review. In *Journal of Adhesion*. https://doi.org/10.1080/00218464.2018.1452736

Niedermann, P., Szebényi, G., & Toldy, A. (2015). Novel high glass temperature sugar-based epoxy resins: Characterization and comparison to mineral oil-based aliphatic and aromatic resins. *Express Polymer Letters*. https://doi.org/10.3144/expresspolymlett.2015.10

Njuguna, J. (2016). Lightweight Composite Structures in Transport: Design, Manufacturing, Analysis and Performance. In *Lightweight Composite Structures in Transport: Design, Manufacturing, Analysis and Performance*. https://doi.org/10.1016/C2014-0-02646-9

Njuguna, James, & Pielichowski, K. (2003). Polymer Nanocomposites for Aerospace Applications: Properties. In *Advanced Engineering Materials*. https://doi.org/10.1002/adem.200310101

Novoselov, K. S., Geim, A. K., Morozov, S. V., Jiang, D., Zhang, Y., Dubonos, S. V., Grigorieva, I. V., & Firsov, A. A. (2004). Electric field in atomically thin carbon films. *Science*. https://doi.org/10.1126/science.1102896

Núñez, L., Fraga López, F., Fraga Grueiro, L., & Rodriguez Añón, J. A. (1996). Activation energies and rate constants for an epoxy/cure agent reaction: Variation in peak exotherm temperature. *Journal of Thermal* Analysis. https://doi.org/10.1007/BF01981809

Özgül, F., & Bektaş, N. B. (2019). Investigation of the effects of additives on mechanical properties of E-glass reinforced thermoset composites. Acta Physica Polonica A, 135(5). https://doi.org/10.12693/APhysPolA.135.915

Odian, G. (2004). Principles of Polymerization. In *Principles of Polymerization*. https://doi.org/10.1002/047147875x

Ofoegbu, S. U., Ferreira, M. G. S., & Zheludkevich, M. L. (2019). Galvanically stimulated degradation of carbon-

fiber reinforced polymer composites: A critical review. In *Materials* (Vol. 12, Issue 4). https://doi.org/10.3390/ma12040651

Olowojoba, G. B., Eslava, S., Gutierrez, E. S., Kinloch, A. J., Mattevi, C., Rocha, V. G., & Taylor, A. C. (2016). In situ thermally reduced graphene oxide/epoxy composites: thermal and mechanical properties. *Applied Nanoscience (Switzerland)*, *6*(7). https://doi.org/10.1007/s13204-016-0518-y

Olowojoba, G. B., Kopsidas, S., Eslava, S., Gutierrez, E. S., Kinloch, A. J., Mattevi, C., Rocha, V. G., & Taylor, A. C. (2017). A facile way to produce epoxy nanocomposites having excellent thermal conductivity with low contents of reduced graphene oxide. *Journal of Materials Science*, *52*(12). https://doi.org/10.1007/s10853-017-0969-x

Osokoya, O. (2017). An evaluation of polymer composites for car bumper beam. *International Journal of Automotive Composites*. https://doi.org/10.1504/ijautoc.2017.086521

PAINTER, P., & COLEMAN, M. M. (1997). FUNDAMENTALS OF POLYMER SCIENCE. In *CRC Press LLC* Originally Published by Technomic Publishing.

Pal, A. K., & Katiyar, V. (2017). Theoretical and analyzed data related to thermal degradation kinetics of poly (L-lactic acid)/chitosan-grafted-oligo L-lactic acid (PLA/CH-g-OLLA) bionanocomposite films. *Data in Brief*, *10*. https://doi.org/10.1016/j.dib.2016.11.100

Palmieri, F. L., Belcher, M. A., Wohl, C. J., Blohowiak, K. Y., & Connell, J. W. (2016). Laser ablation surface preparation for adhesive bonding of carbon fiber reinforced epoxy composites. International Journal of Adhesion and Adhesives, 68. https://doi.org/10.1016/j.ijadhadh.2016.02.007

Panagiotou, T., Mesite, S. V, Bernard, J. M., Chomistek, K. J., Fisher, R. J., & Corporation, M. (2008). Production of Polymer Nanosuspensions Using Microfluidizer ® Processor Based Technologies Massachusetts Institute of Technology , Cambridge , MA , USA. Technology, 1.

Panigrahi, S. K., & Zhang, Y. X. (2011). Investigation of damage growth in single lap joints of composite laminates. *Journal of Adhesion Science and Technology*, *25*(11). https://doi.org/10.1163/016942410X537170

Papageorgiou, D. G., Kinloch, I. A., & Young, R. J. (2015). Graphene/elastomer nanocomposites. In *Carbon*. https://doi.org/10.1016/j.carbon.2015.08.055

Papageorgiou, D. G., Kinloch, I. A., & Young, R. J. (2016). Hybrid multifunctional graphene/glass-fibre polypropylene composites. *Composites Science and Technology*. https://doi.org/10.1016/j.compscitech.2016.10.018

Papageorgiou, D. G., Kinloch, I. A., & Young, R. J. (2017). Mechanical properties of graphene and graphene-based nanocomposites. In *Progress in Materials Science*. https://doi.org/10.1016/j.pmatsci.2017.07.004

Papageorgiou, D. G., Liu, M., Li, Z., Vallés, C., Young, R. J., & Kinloch, I. A. (2019). Hybrid poly(ether ether ketone) composites reinforced with a combination of carbon fibres and graphene nanoplatelets. *Composites Science and Technology*. https://doi.org/10.1016/j.compscitech.2019.03.006

Papageorgiou, D. G., Terzopoulou, Z., Fina, A., Cuttica, F., Papageorgiou, G. Z., Bikiaris, D. N., Chrissafis, K., Young, R. J., & Kinloch, I. A. (2018). Enhanced thermal and fire retardancy properties of polypropylene reinforced with a hybrid graphene/glass-fibre filler. *Composites Science and Technology*. https://doi.org/10.1016/j.compscitech.2017.12.019

Park, J. B., Okabe, T., & Takeda, N. (2003). New concept for modeling the electromechanical behavior of unidirectional carbon-fiber-reinforced plastic under tensile loading. *Smart Materials and Structures*. https://doi.org/10.1088/0964-1726/12/1/312

Park, M. V. D. Z., Bleeker, E. A. J., Brand, W., Cassee, F. R., Van Elk, M., Gosens, I., De Jong, W. H., Meesters, J. A. J., Peijnenburg, W. J. G. M., Quik, J. T. K., Vandebriel, R. J., & Sips, A. J. A. M. (2017). Considerations for Safe Innovation: The Case of Graphene. In *ACS Nano* (Vol. 11, Issue 10). https://doi.org/10.1021/acsnano.7b04120

Park, S., & Ruoff, R. S. (2009). Chemical methods for the production of graphenes. *Nature Nanotechnology*. https://doi.org/10.1038/nnano.2009.58

Patel, J. K., Patel, A., & Bhatia, D. (2021). Introduction to Nanomaterials and Nanotechnology. In *Emerging Technologies for Nanoparticle Manufacturing*. https://doi.org/10.1007/978-3-030-50703-9_1

Patel, M., Pardhi, B., Chopara, S., & Pal, M. (2018). Lightweight Composite Materials for Automotive - A Review. *Concepts Journal of Applied Research*, *3*(7).

Paton, K. R., Varrla, E., Backes, C., Smith, R. J., Khan, U., O'Neill, A., Boland, C., Lotya, M., Istrate, O. M., King, P., Higgins, T., Barwich, S., May, P., Puczkarski, P., Ahmed, I., Moebius, M., Pettersson, H., Long, E., Coelho, J., … Coleman, J. N. (2014). Scalable production of large quantities of defect-free few-layer graphene by shear exfoliation in liquids. *Nature Materials*, *13*(6), 624–630. https://doi.org/10.1038/nmat3944

Pavlidou, S., & Papaspyrides, C. D. (2008). A review on polymer-layered silicate nanocomposites. In *Progress in Polymer Science (Oxford)*. https://doi.org/10.1016/j.progpolymsci.2008.07.008

Pei, S., & Cheng, H.-M. (2012). The reduction of graphene oxide. *Carbon*, *50*(9), 3210–3228. https://doi.org/https://doi.org/10.1016/j.carbon.2011.11.010

Peng, M., Tang, X., & Zhou, Y. (2016). Fast phase transfer of graphene oxide from water to triglycidyl para-aminophenol for epoxy composites with superior nanosheet dispersion. *Polymer*, *93*, 1–8. https://doi.org/https://doi.org/10.1016/j.polymer.2016.03.016

Peng, Y., Wang, Z., & Zou, K. (2015). Friction and Wear Properties of Different Types of Graphene Nanosheets as Effective Solid Lubricants. *Langmuir*, *31*(28). https://doi.org/10.1021/acs.langmuir.5b00422

Petersen, R. (2016). Carbon fiber biocompatibility for implants. *Fibers*, *4*(1). https://doi.org/10.3390/fib4010001

Pfister, D. P., Xia, Y., & Larock, R. C. (2011). Recent advances in vegetable oil-based polyurethanes. In *ChemSusChem*. https://doi.org/10.1002/cssc.201000378

Phiri, J., Gane, P., & Maloney, T. C. (2017). General overview of graphene: Production, properties and application in polymer composites. In *Materials Science and Engineering B: Solid-State Materials for Advanced Technology*. https://doi.org/10.1016/j.mseb.2016.10.004

Phua, J. L., Teh, P. L., Ghani, S. A., & Yeoh, C. K. (2016). Effect of Heat Assisted Bath Sonication on the Mechanical and Thermal Deformation Behaviours of Graphene Nanoplatelets Filled Epoxy Polymer Composites. *International Journal of Polymer Scien*ce. https://doi.org/10.1155/2016/9767183

Pinto, A. M., Cabral, J., Tanaka, D. A. P., Mendes, A. M., & Magalhães, F. D. (2013). Effect of incorporation of graphene oxide and graphene nanoplatelets on mechanical and gas permeability properties of poly(lactic acid) films. Polymer International, 62(1). https://doi.org/10.1002/pi.4290

Pinto, A. M. G., Magalhães, A. G., Campilho, R. D. S. G., de Moura, M. F. S. F., & Baptista, A. P. M. (2009). Single-lap joints of similar and dissimilar adherends bonded with an acrylic adhesive. Journal of Adhesion. https://doi.org/10.1080/00218460902880313

Plant-Based Epoxy Enables Recyclable Carbon Fiber | plasticstoday.com. (n.d.). Retrieved August 21, 2022, from https://www.plasticstoday.com/automotive-and-mobility/plant-based-epoxy-enables-recyclable-carbon-fiber

Popineau, S., Rondeau-Mouro, C., Sulpice-Gaillet, C., & Shanahan, M. E. R. (2005). Free/bound water absorption in an epoxy adhesive. *Polymer*. https://doi.org/10.1016/j.polymer.2005.09.008

Potts, J. R., Dreyer, D. R., Bielawski, C. W., & Ruoff, R. S. (2011). Graphene-based polymer nanocomposites. *Polymer*, *52*(1), 5–25. https://doi.org/https://doi.org/10.1016/j.polymer.2010.11.042

Poutrel, Q. A., Wang, Z., Wang, D., Soutis, C., & Gresil, M. (2017). Effect of pre and Post-Dispersion on Electro-Thermo-Mechanical Properties of a Graphene Enhanced Epoxy. *Applied Composite Materials*. https://doi.org/10.1007/s10443-016-9541-0

Pradeep, S. A., Iyer, R. K., Kazan, H., & Pilla, S. (2017). Automotive Applications of Plastics: Past, Present, and Future. In Applied Plastics Engineering Handbook: Processing, Materials, and Applications: Second Edition. https://doi.org/10.1016/B978-0-323-39040-8.00031-6

Pramanik, A., Basak, A. K., Dong, Y., Sarker, P. K., Uddin, M. S., Littlefair, G., Dixit, A. R., & Chattopadhyaya, S. (2017). Joining of carbon fibre reinforced polymer (CFRP) composites and aluminium alloys – A review. In

Composites Part A: Applied Science and Manufacturing. https://doi.org/10.1016/j.compositesa.2017.06.007

Pramanik, A. (2014). Developments in the non-traditional machining of particle reinforced metal matrix composites. In International Journal of Machine Tools and Manufacture. https://doi.org/10.1016/j.ijmachtools.2014.07.003

Prasad, S. V. S., Prasad, S. B., Verma, K., Mishra, R. K., Kumar, V., & Singh, S. (2022). The role and significance of Magnesium in modern day research-A review. In Journal of Magnesium and Alloys (Vol. 10, Issue 1). https://doi.org/10.1016/j.jma.2021.05.012

Prime, R. B. (1973). Differential scanning calorimetry of the epoxy cure reaction. *Polymer Engineering & Science*. https://doi.org/10.1002/pen.760130508

Prime, R. B. (1997). Thermosets. In E. A. Turi (Ed.), *Thermal Characterization of Polymeric Materials* (Second, pp. 1380–1744). Academic Press, San Diego.

Prolongo, M. G., Salom, C., Arribas, C., Sánchez-Cabezudo, M., Masegosa, R. M., & Prolongo, S. G. (2016a). Influence of graphene nanoplatelets on curing and mechanical properties of graphene/epoxy nanocomposites. *Journal of Thermal Analysis and Calorimetry*. https://doi.org/10.1007/s10973-015-5162-3

Prolongo, M. G., Salom, C., Arribas, C., Sánchez-Cabezudo, M., Masegosa, R. M., & Prolongo, S. G. (2016b). Influence of graphene nanoplatelets on curing and mechanical properties of graphene/epoxy nanocomposites. *Journal of Thermal Analysis and Calorimetry*. https://doi.org/10.1007/s10973-015-5162-3

Prolongo, M. G., Salom, C., Arribas, C., Sánchez-Cabezudo, M., Masegosa, R. M., & Prolongo, S. G. (2016c). Influence of graphene nanoplatelets on curing and mechanical properties of graphene/epoxy nanocomposites. *Journal of Thermal Analysis and Calorimetry*, *125*(2). https://doi.org/10.1007/s10973-015-5162-3

Prolongo, S. G., Moriche, R., Jiménez-Suárez, A., Sánchez, M., & Ureña, A. (2014). Advantages and disadvantages of the addition of graphene nanoplatelets to epoxy resins. *European Polymer Journal*, *61*, 206–214. https://doi.org/https://doi.org/10.1016/j.eurpolymj.2014.09.022

Prucha, T. (2012a). Materials - The foundation for the clean energy age. *International Journal of Metalcasting*, *6*(2), 5.

Prucha, T. (2012b). Materials - The foundation for the clean energy age. In *International Journal of Metalcasting*.

Prusty, R. K., Ghosh, S. K., Rathore, D. K., & Ray, B. C. (2017). Reinforcement effect of graphene oxide in glass fibre/epoxy composites at in-situ elevated temperature environments: An emphasis on graphene oxide content. *Composites Part A: Applied Science and Manufacturing*, *95*. https://doi.org/10.1016/j.compositesa.2017.01.001

Pullicino, E., Zou, W., Gresil, M., & Soutis, C. (2017). The Effect of Shear Mixing Speed and Time on the Mechanical Properties of GNP/Epoxy Composites. *Applied Composite Materials*, *24*(2). https://doi.org/10.1007/s10443-016-9559-3

Punetha, V. D., Rana, S., Yoo, H. J., Chaurasia, A., McLeskey, J. T., Ramasamy, M. S., Sahoo, N. G., & Cho, J. W. (2017). Functionalization of carbon nanomaterials for advanced polymer nanocomposites: A comparison study between CNT and graphene. In *Progress in Polymer Science* (Vol. 67). https://doi.org/10.1016/j.progpolymsci.2016.12.010

Qi, W., Zhang, X., & Wang, H. (2018). Self-assembled polymer nanocomposites for biomedical application. In *Current Opinion in Colloid and Interface Science*. https://doi.org/10.1016/j.cocis.2018.01.003

Qiu, S. L., Wang, C. S., Wang, Y. T., Liu, C. G., Chen, X. Y., Xie, H. F., Huang, Y. A., & Cheng, R. S. (2011). Effects of graphene oxides on the cure behaviors of a tetrafunctional epoxy resin. *Express Polymer Letters*. https://doi.org/10.3144/expresspolymlett.2011.79

Quang Dao, D., Luche, J., Richard, F., Rogaume, T., Bourhy-Weber, C., & Ruban, S. (2013). Determination of characteristic parameters for the thermal decomposition of epoxy resin/carbon fibre composites in cone calorimeter. *International Journal of Hydrogen Energy*. https://doi.org/10.1016/j.ijhydene.2012.05.116

Quaresimin, M., Schulte, K., Zappalorto, M., & Chandrasekaran, S. (2016). Toughening mechanisms in polymer nanocomposites: From experiments to modelling. In *Composites Science and Technology*. https://doi.org/10.1016/j.compscitech.2015.11.027

Rafiee, M. A., Rafiee, J., Wang, Z., Song, H., Yu, Z. Z., & Koratkar, N. (2009). Enhanced mechanical properties of nanocomposites at low graphene content. *ACS Nano*. https://doi.org/10.1021/nn9010472

Rajagopal, R. R., Rajarao, R., Cholake, S. T., & Sahajwalla, V. (2017). Sustainable composite panels from non-metallic waste printed circuit boards and automotive plastics. *Journal of Cleaner Production*. https://doi.org/10.1016/j.jclepro.2016.12.139

Rajak, D. K., Pagar, D. D., Menezes, P. L., & Linul, E. (2019). Fiber-reinforced polymer composites: Manufacturing, properties, and applications. In Polymers (Vol. 11, Issue 10). https://doi.org/10.3390/polym11101667

Rajak, D. K., Pagar, D. D., Kumar, R., & Pruncu, C. I. (2019). Recent progress of reinforcement materials: A comprehensive overview of composite materials. Journal of Materials Research and Technology, 8(6). https://doi.org/10.1016/j.jmrt.2019.09.068

Ram, A., & Ram, A. (1997). The Chemistry of Polymers. In *Fundamentals of Polymer Engineering*. https://doi.org/10.1007/978-1-4899-1822-2_2

Ramanathan, T., Abdala, A. A., Stankovich, S., Dikin, D. A., Herrera-Alonso, M., Piner, R. D., Adamson, D. H., Schniepp, H. C., Chen, X., Ruoff, R. S., Nguyen, S. T., Aksay, I. A., Prud'Homme, R. K., & Brinson, L. C. (2008). Functionalized graphene sheets for polymer nanocomposites. *Nature Nanotechnology*. https://doi.org/10.1038/nnano.2008.96

Ramanathan, T., Stankovich, S., Dikin, D. A., Liu, H., Shen, H., Nguyen, S. T., & Brinson, L. C. (2007). Graphitic nanofillers in PMMA nanocomposites - An investigation of particle size and dispersion and their influence on nanocomposite properties. *Journal of Polymer Science, Part B: Polymer Physics*. https://doi.org/10.1002/polb.21187

Ramos-Galicia, L., Mendez, L. N., Martínez-Hernández, A. L., Espindola-Gonzalez, A., Galindo-Esquivel, I. R., Fuentes-Ramirez, R., & Velasco-Santos, C. (2013a). Improved performance of an epoxy matrix as a result of combining graphene oxide and reduced graphene. *International Journal of Polymer Science*. https://doi.org/10.1155/2013/493147

Ramos-Galicia, L., Mendez, L. N., Martínez-Hernández, A. L., Espindola-Gonzalez, A., Galindo-Esquivel, I. R., Fuentes-Ramirez, R., & Velasco-Santos, C. (2013b). Improved performance of an epoxy matrix as a result of combining graphene oxide and reduced graphene. *International Journal of Polymer Science*, *2013*. https://doi.org/10.1155/2013/493147

Ramsdale-Capper, R., & Foreman, J. P. (2018). Internal antiplasticisation in highly crosslinked amine cured multifunctional epoxy resins. Polymer. https://doi.org/10.1016/j.polymer.2018.05.048

Ray, S. S., & Okamoto, M. (2003). Polymer/layered nanocomposites: a review from preparation to processing. Prog. Polym. Sci.

Reghat, M., Mirabedini, A., Tan, A. M., Weizman, Y., Middendorf, P., Bjekovic, R., Hyde, L., Antiohos, D., Hameed, N., Fuss, F. K., & Fox, B. (2021). Graphene as a piezo-resistive coating to enable strain monitoring in glass fiber composites. Composites Science and Technology, 211. https://doi.org/10.1016/j.compscitech.2021.108842

Rehman, S., Akram, S., Kanellopoulos, A., Elmarakbi, A., & Karagiannidis, P. G. (2020). Development of new graphene/epoxy nanocomposites and study of cure kinetics, thermal and mechanical properties. *Thermochimica Acta*, *694*. https://doi.org/10.1016/j.tca.2020.178785

Rehman, Sheikh, Gomez, J., Villaro, E., Cossey, D., & Karagiannidis, P. G. (2022). *Bio-Based Epoxy / Amine Reinforced with Reduced Graphene Oxide (rGO) or GLYMO-rGO : Study of Curing Kinetics , Mechanical Properties , Lamination and Bonding Performance*.

Reit, R., Abitz, H., Reddy, N., Parker, S., Wei, A., Aragon, N., Ho, M., Weittenhiller, A., Kang, T., Ecker, M., & Voit, W. E. (2016). Thiol-epoxy/maleimide ternary networks as softening substrates for flexible electronics. *Journal of Materials Chemistry B*. https://doi.org/10.1039/c6tb01082b

Renart, J., Costa, J., Sarrado, C., Budhe, S., Turon, A., & Rodríguez-Bellido, A. (2015). Mode I fatigue behaviour and fracture of adhesively-bonded fibre-reinforced polymer (FRP) composite joints for structural repairs. In

Fatigue and Fracture of Adhesively-Bonded Composite Joints. https://doi.org/10.1016/B978-0-85709-806-1.00005-7

Rhee, K. Y., & Yang, J. H. (2003). A study on the peel and shear strength of aluminum/CFRP composites surface-treated by plasma and ion assisted reaction method. *Composites Science and Technology*. https://doi.org/10.1016/S0266-3538(02)00145-8

Ribeiro, E., Ladeira, C., & Viegas, S. (2017). Occupational exposure to Bisphenol A (BPA): A reality that still needs to be unveiled. In *Toxics*. https://doi.org/10.3390/toxics5030022

Riccardi, C. C., Adabbo, H. E., & Williams, R. J. J. (1984). Curing reaction of epoxy resins with diamines. *Journal of Applied Polymer Science*. https://doi.org/10.1002/app.1984.070290805

Riccardi, Carmen C., & Williams, R. J. J. (1986). A kinetic scheme for an amine-epoxy reaction with simultaneous etherification. *Journal of Applied Polymer Science*. https://doi.org/10.1002/app.1986.070320208

Rochester, J. R. (2013). Bisphenol A and human health: A review of the literature. In *Reproductive Toxicology* (Vol. 42). https://doi.org/10.1016/j.reprotox.2013.08.008

Rohem, N. R. F., Pacheco, L. J., Budhe, S., Banea, M. D., Sampaio, E. M., & de Barros, S. (2016). Development and qualification of a new polymeric matrix laminated composite for pipe repair. *Composite Structures*. https://doi.org/10.1016/j.compstruct.2016.05.091

Ronda, J. C., Lligadas, G., Galià, M., & Cádiz, V. (2013). A renewable approach to thermosetting resins. *Reactive and Functional Polymers*. https://doi.org/10.1016/j.reactfunctpolym.2012.03.015

Rosenthal, S., Maaß, F., Kamaliev, M., Hahn, M., Gies, S., & Tekkaya, A. E. (2020). Lightweight in Automotive Components by Forming Technology. *Automotive Innovation*, *3*(3). https://doi.org/10.1007/s42154-020-00103-3

Rośkowicz, M., Godzimirski, J., Komorek, A., & Jasztal, M. (2021). The effect of adhesive layer thickness on joint static strength. *Materials*, *14*(6). https://doi.org/10.3390/ma14061499

Rozenberg, B. A. (1986). *Kinetics, thermodynamics and mechanism of reactions of epoxy oligomers with amines BT - Epoxy Resins and Composites II* (K. Dušek (Ed.); pp. 113–165). Springer Berlin Heidelberg.

Rudrapati, R. (2020). Graphene: Fabrication Methods, Properties, and Applications in Modern Industries. In *Graphene Production and Application*. https://doi.org/10.5772/intechopen.92258

Ryu, S. H., Sin, J. H., & Shanmugharaj, A. M. (2014). Study on the effect of hexamethylene diamine functionalized graphene oxide on the curing kinetics of epoxy nanocomposites. *European Polymer Journal*. https://doi.org/10.1016/j.eurpolymj.2013.12.014

Saba, N., & Jawaid, M. (2018). A review on thermomechanical properties of polymers and fibers reinforced polymer composites. In *Journal of Industrial and Engineering Chemistry* (Vol. 67). https://doi.org/10.1016/j.jiec.2018.06.018

Saber-Samandari, S., Khatibi, A. A., & Basic, D. (2007). An experimental study on clay/epoxy nanocomposites produced in a centrifuge. *Composites Part B: Engineering*. https://doi.org/10.1016/j.compositesb.2006.03.010

Saboori, A., Moheimani, S. K., Pavese, M., Badini, C., & Fino, P. (2017). New nanocomposite materials with improved mechanical strength and tailored coefficient of thermal expansion for electro-packaging applications. *Metals*. https://doi.org/10.3390/met7120536

Sainsbury, T., Gnaniah, S., Spencer, S. J., Mignuzzi, S., Belsey, N. A., Paton, K. R., & Satti, A. (2017). Extreme mechanical reinforcement in graphene oxide based thin-film nanocomposites via covalently tailored nanofiller matrix compatibilization. *Carbon*. https://doi.org/10.1016/j.carbon.2016.11.061

Salom, C., Prolongo, M. G., Toribio, A., Martínez-Martínez, A. J., de Cárcer, I. A., & Prolongo, S. G. (2018). Mechanical properties and adhesive behavior of epoxy-graphene nanocomposites. *International Journal of Adhesion and Adhesives*, *84*, 119–125. https://doi.org/https://doi.org/10.1016/j.ijadhadh.2017.12.004

Samyal, R., Bagha, A. K., Bedi, R., Bahl, S., Saxena, K. K., & Sehgal, S. (2021). Predicting the effect of fiber orientations and boundary conditions on the optimal placement of PZT sensor on the composite structures.

Materials Research Express, *8*(7). https://doi.org/10.1088/2053-1591/ac0de9

Sapiai, N., Jumahat, A., & Mahmud, J. (2018). Mechanical properties of functionalised CNT filled kenaf reinforced epoxy composites. *Materials Research Express*. https://doi.org/10.1088/2053-1591/aabb63

Sbirrazzuoli, N., & Vyazovkin, S. (2002). Learning about epoxy cure mechanisms from isoconversional analysis of DSC data. *Thermochimica Acta*. https://doi.org/10.1016/S0040-6031(02)00053-9

Schubbe, J. J., & Mall, S. (1999). Investigation of a cracked thick aluminum panel repaired with a bonded composite patch. *Engineering Fracture Mechanics*. https://doi.org/10.1016/S0013-7944(99)00032-6

Seretis, G. V., Theodorakopoulos, I. D., Manolakos, D. E., & Provatidis, C. G. (2018). Effect of sonication on the mechanical response of graphene nanoplatelets/glass fabric/epoxy laminated nanocomposites. *Composites Part B: Engineering*. https://doi.org/10.1016/j.compositesb.2018.04.034

Shaari, N., & Jumahat, A. (2018). Unhole and open hole compressive behaviours of hybrid Kevlar/glass fibre reinforced silica nanocomposites. *Materials Research Express*. https://doi.org/10.1088/2053-1591/aac667

Shadlou, S., Ahmadi-Moghadam, B., & Taheri, F. (2014). The effect of strain-rate on the tensile and compressive behavior of graphene reinforced epoxy/nanocomposites. *Materials and Design*. https://doi.org/10.1016/j.matdes.2014.03.020

Shah, R., Kausar, A., Muhammad, B., & Shah, S. (2015). Progression from Graphene and Graphene Oxide to High Performance Polymer-Based Nanocomposite: A Review. *Polymer - Plastics Technology and Engineering*. https://doi.org/10.1080/03602559.2014.955202

Shahdan, D., Ahmad, S. H., & Flaifel, M. H. (2013). Effect of ultrasonic treatment on tensile properties of PLA/LNR/NiZn ferrite nanocomposite. *AIP Conference Proceedings*. https://doi.org/10.1063/1.4858633

Shamsuddoha, M., Islam, M. M., Aravinthan, T., Manalo, A., & Lau, K. tak. (2013). Characterisation of mechanical and thermal properties of epoxy grouts for composite repair of steel pipelines. Materials and Design. https://doi.org/10.1016/j.matdes.2013.05.068

Sharma, D. (2022). Submitted By : مسبد الله ا نمحرلا ميحرلا. Academia.Edu, January, 1–189. https://minerva-access.unimelb.edu.au/handle/11343/56627%0Ahttp://www.academia.edu/download/39541120/performance_culture.doc

Shen, M. Y., Chang, T. Y., Hsieh, T. H., Li, Y. L., Chiang, C. L., Yang, H., & Yip, M. C. (2013). Mechanical properties and tensile fatigue of graphene nanoplatelets reinforced polymer nanocomposites. *Journal of Nanomaterials*, *2013*. https://doi.org/10.1155/2013/565401

Sherwani, S. F. K., Sapuan, S. M., Leman, Z., Zainuddin, E. S., & Ilyas, R. A. (2021). Application of polymer composite materials in motorcycles: A comprehensive review. In *Biocomposite and Synthetic Composites for Automotive Applications*. https://doi.org/10.1016/b978-0-12-820559-4.00015-8

Shettar, M., Achutha Kini, U., Sharma, S. S., & Hiremath, P. (2017). Study on Mechanical Characteristics of Nanoclay Reinforced Polymer Composites. *Materials Today: Proceedings*. https://doi.org/10.1016/j.matpr.2017.08.081

Shibata, M., Yoshihara, S., Yashiro, M., & Ohno, Y. (2013). Thermal and mechanical properties of sorbitol-based epoxy resin cured with quercetin and the biocomposites with wood flour. *Journal of Applied Polymer Science*. https://doi.org/10.1002/app.38438

Shivakumar Gouda, P. S., Williams, J. D., Yasaee, M., Chatterjee, V., Jawali, D., Rahatekar, S. S., & Wisnom, M. R. (2016). Drawdown prepreg coating method using epoxy terminated butadiene nitrile rubber to improve fracture toughness of glass epoxy composites. *Journal of Composite Materials*. https://doi.org/10.1177/0021998315583317

Shokrian, M. D., Shelesh-Nezhad, K., & Najjar, R. (2019). The effects of Al surface treatment, adhesive thickness and microcapsule inclusion on the shear strength of bonded joints. *International Journal of Adhesion and Adhesives*, *89*. https://doi.org/10.1016/j.ijadhadh.2019.01.001

Show, K. Y., Mao, T., & Lee, D. J. (2007). Optimisation of sludge disruption by sonication. *Water Research*, *41*(20).

https://doi.org/10.1016/j.watres.2007.07.017

Showaib, E. A., & Elsheikh, A. H. (2020). Effect of surface preparation on the strength of vibration welded butt joint made from PBT composite. *Polymer Testing*, *83*. https://doi.org/10.1016/j.polymertesting.2019.106319

Si, Y., & Samulski, E. T. (2008). Synthesis of water soluble graphene. *Nano Letters*, *8*(6). https://doi.org/10.1021/nl080604h

Sichina, W. J. (2000). Characterization of Epoxy Resins Using DSC. *PerkinElmer Instruments*, 2–5.

Silva, M. R. G., Marques, E. A. S., & da Silva, L. F. M. (2016). Behaviour under impact of mixed adhesive joints for the automotive industry. *Latin American Journal of Solids and Structures*. https://doi.org/10.1590/1679-78252762

Simon, S. L., & Gillham, J. K. (1992). Reaction kinetics and TTT cure diagrams for off-stoichiometric ratios of a high-Tg epoxy/amine system. *Journal of Applied Polymer Science*. https://doi.org/10.1002/app.1992.070460714

Simon, S. L., & Gillham, J. K. (1994). Thermosetting cure diagrams: Calculation and application. *Journal of Applied Polymer Science*. https://doi.org/10.1002/app.1994.070530601

Singh, P. K., Singh, P. K., Sharma, K., & Saraswat, M. (2020). Effect of sonication parameters on mechanical properties of in-situ amine functionalized multiple layer graphene/epoxy nanocomposites. *Journal of Scientific and Industrial Research*, *79*(11).

Singh, S., Srivastava, V. K., & Prakash, R. (2015). Influences of carbon nanofillers on mechanical performance of epoxy resin polymer. *Applied Nanoscience (Switzerland)*. https://doi.org/10.1007/s13204-014-0319-0

Skura, J. (1980). Book Review: Macromolecules. An Introduction to Polymer Science. Edited by F. A. Bovey and F. A. Winslow. *Angewandte Chemie International Edition in English*. https://doi.org/10.1002/anie.198006571

Smith, A. T., LaChance, A. M., Zeng, S., Liu, B., & Sun, L. (2019). Synthesis, properties, and applications of graphene oxide/reduced graphene oxide and their nanocomposites. *Nano Materials Science*. https://doi.org/10.1016/j.nanoms.2019.02.004

Smith, I. T. (1961). The mechanism of the crosslinking of epoxide resins by amines. *Polymer*, *2*, 95–108. https://doi.org/https://doi.org/10.1016/0032-3861(61)90010-6

Sorrentino, L., Polini, W., Bellini, C., & Parodo, G. (2018). Surface treatment of CFRP: influence on single lap joint performances. *International Journal of Adhesion and Adhesives*. https://doi.org/10.1016/j.ijadhadh.2018.06.008

Sourour, S., & Kamal, M. R. (1976). Differential scanning calorimetry of epoxy cure: isothermal cure kinetics. *Thermochimica Acta*, *14*(1–2). https://doi.org/10.1016/0040-6031(76)80056-1

Soutis, C. (2005). Carbon fiber reinforced plastics in aircraft construction. *Materials Science and Engineering A*, *412*(1–2). https://doi.org/10.1016/j.msea.2005.08.064

Spitalsky, Z., Tasis, D., Papagelis, K., & Galiotis, C. (2010). Carbon nanotube-polymer composites: Chemistry, processing, mechanical and electrical properties. In *Progress in Polymer Science (Oxford)*. https://doi.org/10.1016/j.progpolymsci.2009.09.003

Srivastava, V. K. (2011). Effect of carbon nanotubes on the strength of adhesive lap joints of C/C and C/CSiC ceramic fibre composites. *International Journal of Adhesion and Adhesives*. https://doi.org/10.1016/j.ijadhadh.2011.03.006

Stankovich, S., Dikin, D. A., Dommett, G. H. B., Kohlhaas, K. M., Zimney, E. J., Stach, E. A., Piner, R. D., Nguyen, S. B. T., & Ruoff, R. S. (2006). Graphene-based composite materials. *Nature*. https://doi.org/10.1038/nature04969

Stankovich, S., Piner, R. D., Chen, X., Wu, N., Nguyen, S. T., & Ruoff, R. S. (2006). Stable aqueous dispersions of graphitic nanoplatelets via the reduction of exfoliated graphite oxide in the presence of poly(sodium 4-styrenesulfonate). *Journal of Materials Chemistry*. https://doi.org/10.1039/b512799h

Stankovich, S., Piner, R. D., Nguyen, S. T., & Ruoff, R. S. (2006). Synthesis and exfoliation of isocyanate-treated graphene oxide nanoplatelets. *Carbon*, *44*(15), 3342–3347.

https://doi.org/https://doi.org/10.1016/j.carbon.2006.06.004

Stazi, F., Giampaoli, M., Rossi, M., & Munafò, P. (2015). Environmental ageing on GFRP pultruded joints: Comparison between different adhesives. *Composite Structures*, *133*. https://doi.org/10.1016/j.compstruct.2015.07.067

Stoller, M. D., Park, S., Yanwu, Z., An, J., & Ruoff, R. S. (2008). Graphene-Based ultracapacitors. *Nano Letters*. https://doi.org/10.1021/nl802558y

Stutz, H., Mertes, J., & Neubecker, K. (1993). Kinetics of thermoset cure and polymerization in the glass transition region. *Journal of Polymer Science Part A: Polymer Chemistry*. https://doi.org/10.1002/pola.1993.080310726

Suay, J. J., Rodríguez, M. T., Izquierdo, R., Kudama, A. M., & Saura, J. J. (2003). Rapid Assessment of Automotive Epoxy Primers by Electrochemical Techniques. *Journal of Coatings Technology*. https://doi.org/10.1007/bf02720157

Suh, S. W., Kim, J. J., Kim, S. H., & Park, B. K. (2012). Effect of pi film surface on printing of pd(ii) catalytic ink for electroless copper plating in the printed electronics. *Journal of Industrial and Engineering Chemistry*. https://doi.org/10.1016/j.jiec.2011.11.003

Suhaib Kamran, S., Haleem, A., Bahl, S., Javaid, M., Prakash, C., & Budhhi, D. (2022). Artificial intelligence and advanced materials in automotive industry: Potential applications and perspectives. Materials Today: Proceedings, 62, 4207–4214. https://doi.org/10.1016/J.MATPR.2022.04.727

Sun, L., Xiao, M., Liu, J., & Gong, K. (2006). A study of the polymerization of styrene initiated by K-THF-GIC system. European Polymer Journal. https://doi.org/10.1016/j.eurpolymj.2005.07.014

Swier, S., Van Assche, G., Vuchelen, W., & Van Mele, B. (2005). Role of Complex Formation in the Polymerization Kinetics of Modified Epoxy−Amine Systems. *Macromolecules*, *38*(6), 2281–2288. https://doi.org/10.1021/ma047796x

Systems, C. C. (2015). *EAA Aluminiu*m Automotive Manual – Joining. 1–42.

Szeluga, U., Kumanek, B., & Trzebicka, B. (2015). Synergy in hybrid polymer/nanocarbon composites. A review. In Composites Part A: Applied Science and Manufacturing. https://doi.org/10.1016/j.compositesa.2015.02.021

Tang, L. C., Wan, Y. J., Yan, D., Pei, Y. B., Zhao, L., Li, Y. B., Wu, L. Bin, Jiang, J. X., & Lai, G. Q. (2013). The effect of graphene dispersion on the mechanical properties of graphene/epoxy composites. Carbon. https://doi.org/10.1016/j.carbon.2013.03.050

Tarafdar, A., Sirohi, R., Balakumaran, P. A., Reshmy, R., Madhavan, A., Sindhu, R., Binod, P., Kumar, Y., Kumar, D., & Sim, S. J. (2022). The hazardous threat of Bisphenol A: Toxicity, detection and remediation. Journal of Hazardous Materials, 423. https://doi.org/10.1016/j.jhazmat.2021.127097

Taub, A., De Moor, E., Luo, A., Matlock, D. K., Speer, J. G., & Vaidya, U. (2019). Materials for Automotive Lightweighting. *Annual Review of Materials Research*. https://doi.org/10.1146/annurev-matsci-070218-010134

Teh, P. L., Jaafar, M., Akil, H. M., Seetharamu, K. N., Wagiman, A. N. R., & Beh, K. S. (2008). Thermal and mechanical properties of particulate fillers filled epoxy composites for electronic packaging application. *Polymers for Advanced Technologies*. https://doi.org/10.1002/pat.1014

Tewatia, A., Hendrix, J., Nosker, T., & Lynch-Branzoi, J. (2017). Multi-scale carbon (micro/nano) fiber reinforcement of polyetheretherketone using high shear melt-processing. Fibers, 5(3). https://doi.org/10.3390/fib5030032

Thomas, L. C. (2010). Interpreting Unexpected Events and Transitions in DSC Results. *Government Information Quarterly*, *27*(4), 423–430.

Thostenson, E. T., Ren, Z., & Chou, T. W. (2001). Advances in the science and technology of carbon nanotubes and their composites: A review. *Composites Science and Technology*. https://doi.org/10.1016/S0266-3538(01)00094-X

Tiwari, S. K., Kumar, V., Huczko, A., Oraon, R., Adhikari, A. De, & Nayak, G. C. (2016). Magical Allotropes of Carbon: Prospects and Applications. In *Critical Reviews in Solid State and Materials Sciences* (Vol. 41, Issue

4). https://doi.org/10.1080/10408436.2015.1127206

Tiwari, S. K., Mishra, R. K., Ha, S. K., & Huczko, A. (2018). Evolution of Graphene Oxide and Graphene: From Imagination to Industrialization. In *ChemNanoMat* (Vol. 4, Issue 7). https://doi.org/10.1002/cnma.201800089

Tiwari, S. K., Sahoo, S., Wang, N., & Huczko, A. (2020). Graphene research and their outputs: Status and prospect. In *Journal of Science: Advanced Materials and Devices* (Vol. 5, Issue 1). https://doi.org/10.1016/j.jsamd.2020.01.006

Tong, Y. (2019). Application of New Materials in Sports Equipment. *IOP Conference Series: Materials Science and Engineering*, *493*(1). https://doi.org/10.1088/1757-899X/493/1/012112

Tranchida, D., Piccarolo, S., Loos, J., & Alexeev, A. (2007). Mechanical characterization of polymers on a nanometer scale through nanoindentationn. A study on pile-up and viscoelasticity. *Macromolecules*. https://doi.org/10.1021/ma062140k

Tutunchi, A., Kamali, R., & Kianvash, A. (2015). Adhesive strength of steel-epoxy composite joints bonded with structural acrylic adhesives filled with silica nanoparticles. *Journal of Adhesion Science and Technology*. https://doi.org/10.1080/01694243.2014.981469

Um, M. K., Daniel, I. M., & Hwang, B. S. (2002). A study of cure kinetics by the use of dynamic differential scanning calorimetry. *Composites Science and Technology*, *62*(1). https://doi.org/10.1016/S0266-3538(01)00188-9

Urbańczyk, E., Maciej, A., Stolarczyk, A., Basiaga, M., & Simka, W. (2019). The electrocatalytic oxidation of urea on nickel-graphene and nickel-graphene oxide composite electrodes. *Electrochimica Acta*. https://doi.org/10.1016/j.electacta.2019.03.045

Vallés, C., Beckert, F., Burk, L., Mülhaupt, R., Young, R. J., & Kinloch, I. A. (2016). Effect of the C/O ratio in graphene oxide materials on the reinforcement of epoxy-based nanocomposites. *Journal of Polymer Science, Part B: Polymer Physics*. https://doi.org/10.1002/polb.23925

Vandenberg, L. N., Hauser, R., Marcus, M., Olea, N., & Welshons, W. V. (2007). Human exposure to bisphenol A (BPA). In *Reproductive Toxicology* (Vol. 24, Issue 2). https://doi.org/10.1016/j.reprotox.2007.07.010

Vandi, L. J., Hou, M., Veidt, M., Truss, R., Heitzmann, M., & Paton, R. (2012). Interface diffusion and morphology of aerospace grade epoxy co-cured with thermoplastic polymers. *28th Congress of the International Council of the Aeronautical Sciences 2012, ICAS 2012*.

Verchère, D., Sautereau, H., Pascault, J. P., Riccardi, C. C., Moschiar, S. M., & Williams, R. J. J. (1990). Buildup of epoxycycloaliphatic amine networks. Kinetics, vitrification, and gelation. *Macromolecules*. https://doi.org/10.1021/ma00205a006

Verdejo, R., Bernal, M. M., Romasanta, L. J., & Lopez-Manchado, M. A. (2011). Graphene filled polymer nanocomposites. *Journal of Materials Chemistry*. https://doi.org/10.1039/c0jm02708a

Vietri, U., Guadagno, L., Raimondo, M., Vertuccio, L., & Lafdi, K. (2014). Nanofilled epoxy adhesive for structural aeronautic materials. *Composites Part B: Engineering*. https://doi.org/10.1016/j.compositesb.2014.01.032

Vo Dong, P. A., Azzaro-Pantel, C., & Cadene, A. L. (2018). Economic and environmental assessment of recovery and disposal pathways for CFRP waste management. *Resources, Conservation and Recycling*, *133*. https://doi.org/10.1016/j.resconrec.2018.01.024

Vyazovkin, S., Burnham, A. K., Criado, J. M., Pérez-Maqueda, L. A., Popescu, C., & Sbirrazzuoli, N. (2011a). ICTAC Kinetics Committee recommendations for performing kinetic computations on thermal analysis data. In *Thermochimica Acta*. https://doi.org/10.1016/j.tca.2011.03.034

Vyazovkin, S., Burnham, A. K., Criado, J. M., Pérez-Maqueda, L. A., Popescu, C., & Sbirrazzuoli, N. (2011b). ICTAC Kinetics Committee recommendations for performing kinetic computations on thermal analysis data. *Thermochimica Acta*, *520*(1), 1–19. https://doi.org/https://doi.org/10.1016/j.tca.2011.03.034

Vyazovkin, S., & Sbirrazzuoli, N. (1996). Mechanism and kinetics of epoxy-amine cure studied by differential scanning calorimetry. *Macromolecules*. https://doi.org/10.1021/ma951162w

W.J. Sichina. (2011). Characterization of Polymers Using TGA. *Thermal Analysis Application Note*, 1–4.

Wan, H., Lin, J., & Min, J. (2018). Effect of laser ablation treatment on corrosion resistance of adhesive-bonded Al alloy joints. *Surface and Coatings Technology*. https://doi.org/10.1016/j.surfcoat.2018.03.087

Wan, Y.-J., Gong, L.-X., Tang, L.-C., Wu, L.-B., & Jiang, J.-X. (2014). Mechanical properties of epoxy composites filled with silane-functionalized graphene oxide. *Composites Part A: Applied Science and Manufacturing*, *64*, 79–89. https://doi.org/https://doi.org/10.1016/j.compositesa.2014.04.023

Wang, D., Zhou, K., Yang, W., Xing, W., Hu, Y., & Gong, X. (2013). Surface modification of graphene with layered molybdenum disulfide and their synergistic reinforcement on reducing fire hazards of epoxy resins. *Industrial and Engineering Chemistry Research*. https://doi.org/10.1021/ie402441g

Wang, Haidou, Zhu, L., & Xu, B. (2018). Principle and Methods of Nanoindentation Test. In *Residual Stresses and Nanoindentation Testing of Films and Coatings*. https://doi.org/10.1007/978-981-10-7841-5_2

Wang, Hui, Pei, Z. J., & Cong, W. (2020). A mechanistic cutting force model based on ductile and brittle fracture material removal modes for edge surface grinding of CFRP composites using rotary ultrasonic machining. *International Journal of Mechanical Sciences*, *176*. https://doi.org/10.1016/j.ijmecsci.2020.105551

Wang, P. N., Hsieh, T. H., Chiang, C. L., & Shen, M. Y. (2015). Synergetic effects of mechanical properties on graphene nanoplatelet and multiwalled carbon nanotube hybrids reinforced epoxy/carbon fiber composites. *Journal of Nanomaterials*. https://doi.org/10.1155/2015/838032

Wang, Xiao, Jin, J., Song, M., & Lin, Y. (2016). Effect of graphene oxide sheet size on the curing kinetics and thermal stability of epoxy resins. *Materials Research Express*. https://doi.org/10.1088/2053-1591/3/10/105303

Wang, Xin, Hu, Y., Song, L., Yang, H., Xing, W., & Lu, H. (2011). In situ polymerization of graphene nanosheets and polyurethane with enhanced mechanical and thermal properties. *Journal of Materials Chemistry*. https://doi.org/10.1039/c0jm03710a

Wang, Xin, Xing, W., Song, L., Yu, B., Hu, Y., & Yeoh, G. H. (2013). Preparation of UV-curable functionalized graphene/polyurethane acrylate nanocomposite with enhanced thermal and mechanical behaviors. *Reactive and Functional Polymers*, *73*(6), 854–858. https://doi.org/https://doi.org/10.1016/j.reactfunctpolym.2013.03.003

Wang, Y., Liu, W., Qiu, Y., & Wei, Y. (2018). A one-component, fast-cure, and economical epoxy resin system suitable for liquid molding of automotive composite parts. *Materials*. https://doi.org/10.3390/ma11050685

Wegmann, A. (1997). Chemical resistance of waterborne epoxy/amine coatings. *Progress in Organic Coatings*. https://doi.org/10.1016/S0300-9440(97)00062-3

Wei, J., & Inam, F. (2017). Processing of Epoxy/Graphene Nanocomposites: Effects of Surfactants. *J Polym Sci Appl*.

Wei, J., Saharudin, M. S., Vo, T., & Inam, F. (2017). Dichlorobenzene: An effective solvent for epoxy/graphene nanocomposites preparation. *Royal Society Open Science*. https://doi.org/10.1098/rsos.170778

Wei, J., Vo, T., & Inam, F. (2015). Epoxy/graphene nanocomposites - processing and properties: a review. *RSC Advances*. https://doi.org/10.1039/c5ra13897c

Whitby, R. L. D. (2014). Chemical control of graphene architecture: Tailoring shape and properties. In *ACS Nano*. https://doi.org/10.1021/nn504544h

Wichmann, M. H. G., Schulte, K., & Wagner, H. D. (2008). On nanocomposite toughness. *Composites Science and Technology*. https://doi.org/10.1016/j.compscitech.2007.06.027

Woltornist, S. J., Carrillo, J. M. Y., Xu, T. O., Dobrynin, A. V., & Adamson, D. H. (2015). Polymer/pristine graphene based composites: From emulsions to strong, electrically conducting foams. *Macromolecules*. https://doi.org/10.1021/ma5024236

Wu, Z., Li, J., Huang, C., & Li, L. (2015). Effect of matrix modification on interlaminar shear strength of glass fibre reinforced epoxy composites at cryogenic temperature. *Physics Procedia*. https://doi.org/10.1016/j.phpro.2015.06.202

Xiao, M., Sun, L., Liu, J., Li, Y., & Gong, K. (2002). Synthesis and properties of polystyrene/graphite

nanocomposites. *Polymer*. https://doi.org/10.1016/S0032-3861(02)00022-8

Xu, H., Gong, L. X., Wang, X., Zhao, L., Pei, Y. B., Wang, G., Liu, Y. J., Wu, L. Bin, Jiang, J. X., & Tang, L. C. (2016). Influence of processing conditions on dispersion, electrical and mechanical properties of graphene-filled-silicone rubber composites. *Composites Part A: Applied Science and Manufacturing*. https://doi.org/10.1016/j.compositesa.2016.09.011

Xu, J., Li, H., Zeng, K., Li, G., Zhao, X., & Zhao, C. (2019). Curing kinetics and thermal stability of novel siloxane-containing benzoxazines. *Thermochimica Acta*. https://doi.org/10.1016/j.tca.2018.11.016

Xu, W., & Wei, Y. (2012). Strength and interface failure mechanism of adhesive joints. *International Journal of Adhesion and Adhesives*. https://doi.org/10.1016/j.ijadhadh.2011.12.004

Xu, W., & Wei, Y. (2013). Influence of adhesive thickness on local interface fracture and overall strength of metallic adhesive bonding structures. *International Journal of Adhesion and Adhesives*, *40*. https://doi.org/10.1016/j.ijadhadh.2012.07.012

Xu, Z., & Gao, C. (2010). In situ polymerization approach to graphene-reinforced nylon-6 composites. *Macromolecules*. https://doi.org/10.1021/ma1009337

Xue, G., Zhang, B., Sun, M., Zhang, X., Li, J., Wang, L., & Song, C. (2019). Morphology, thermal and mechanical properties of epoxy adhesives containing well-dispersed graphene oxide. *International Journal of Adhesion and Adhesives*, *88*, 11–18. https://doi.org/https://doi.org/10.1016/j.ijadhadh.2018.10.011

Yamini, G., Shakeri, A., Vafayan, M., Zohuriaan-Mehr, M. J., Kabiri, K., & Zolghadr, M. (2019). Cure kinetics of modified lignosulfonate/epoxy blends. *Thermochimica Acta*. https://doi.org/10.1016/j.tca.2019.03.003

Yamini, S., & Young, R. J. (1980). The mechanical properties of epoxy resins. *Journal of Materials Science*. https://doi.org/10.1007/bf00550603

YAN, J., CHEN, G., CAO, J., YANG, W., XIE, B., & YANG, M. (2012). Functionalized graphene oxide with ethylenediamine and 1,6-hexanediamine. *New Carbon Materials*, *27*(5), 370–376. https://doi.org/https://doi.org/10.1016/S1872-5805(12)60022-5

Yang, S., Feng, X., & Müllen, K. (2011). Sandwich-like, graphene-based titania nanosheets with high surface area for fast lithium storage. *Advanced Materials*. https://doi.org/10.1002/adma.201101599

Young, R. J., Kinloch, I. A., Gong, L., & Novoselov, K. S. (2012). The mechanics of graphene nanocomposites: A review. In *Composites Science and Technology*. https://doi.org/10.1016/j.compscitech.2012.05.005

Young, R. J., Liu, M., Kinloch, I. A., Li, S., Zhao, X., Vallés, C., & Papageorgiou, D. G. (2018). The mechanics of reinforcement of polymers by graphene nanoplatelets. *Composites Science and Technology*, *154*. https://doi.org/10.1016/j.compscitech.2017.11.007

Yu, H., Hermann, S., Schulz, S. E., Gessner, T., Dong, Z., & Li, W. J. (2012). Optimizing sonication parameters for dispersion of single-walled carbon nanotubes. *Chemical Physics*, *408*. https://doi.org/10.1016/j.chemphys.2012.08.020

Zakaria, M. R., Abdul Kudus, M. H., Md. Akil, H., & Mohd Thirmizir, M. Z. (2017). Comparative study of graphene nanoparticle and multiwall carbon nanotube filled epoxy nanocomposites based on mechanical, thermal and dielectric properties. *Composites Part B: Engineering*. https://doi.org/10.1016/j.compositesb.2017.03.023

Zaman, I., Manshoor, B., Khalid, A., Meng, Q., & Araby, S. (2014). Interface modification of clay and graphene platelets reinforced epoxy nanocomposites: A comparative study. *Journal of Materials Science*. https://doi.org/10.1007/s10853-014-8296-y

Zaman, I., Phan, T. T., Kuan, H. C., Meng, Q., Bao La, L. T., Luong, L., Youssf, O., & Ma, J. (2011). Epoxy/graphene platelets nanocomposites with two levels of interface strength. *Polymer*. https://doi.org/10.1016/j.polymer.2011.02.003

Zandiatashbar, A., Lee, G. H., An, S. J., Lee, S., Mathew, N., Terrones, M., Hayashi, T., Picu, C. R., Hone, J., & Koratkar, N. (2014). Effect of defects on the intrinsic strength and stiffness of graphene. *Nature Communications*, *5*. https://doi.org/10.1038/ncomms4186

Zegeye, E., Ghamsari, A. K., & Woldesenbet, E. (2014). Mechanical properties of graphene platelets reinforced syntactic foams. *Composites Part B: Engineering*, *60*. https://doi.org/10.1016/j.compositesb.2013.12.040

Zeng, X., Ye, L., Guo, K., Sun, R., Xu, J., & Wong, C. P. (2016). Fibrous Epoxy Substrate with High Thermal Conductivity and Low Dielectric Property for Flexible Electronics. *Advanced Electronic Materials*. https://doi.org/10.1002/aelm.201500485

Zhai, L. L., Ling, G. P., & Wang, Y. W. (2008). Effect of nano-Al2O3 on adhesion strength of epoxy adhesive and steel. *International Journal of Adhesion and Adhesives*. https://doi.org/10.1016/j.ijadhadh.2007.03.005

Zhang, C., Garrison, T. F., Madbouly, S. A., & Kessler, M. R. (2017). Recent advances in vegetable oil-based polymers and their composites. In *Progress in Polymer Science* (Vol. 71). https://doi.org/10.1016/j.progpolymsci.2016.12.009

Zhang, X. C., Peng, H. X., Limmack, A. P., & Scarpa, F. (2014). Viscoelastic damping behaviour of cup stacked carbon nanotube modified epoxy nanocomposites with tailored interfacial condition and re-agglomeration. *Composites Science and Technology*. https://doi.org/10.1016/j.compscitech.2014.09.020

Zhang, Z., Shi, Q., Peng, J., Song, J., Chen, Q., Yang, J., Gong, Y., Ji, R., He, X., & Lee, J. H. (2006). Partial delamination of the organo-montmorillonite with surfactant containing hydroxyl groups in maleated poly(propylene carbonate). *Polymer*. https://doi.org/10.1016/j.polymer.2006.09.041

Zhao, X., Zhang, Q., Chen, D., & Lu, P. (2010). Enhanced mechanical properties of graphene-based polyvinyl alcohol composites. *Macromolecules*. https://doi.org/10.1021/ma902862u

Zhao, Y. F., Xiao, M., Wang, S. J., Ge, X. C., & Meng, Y. Z. (2007). Preparation and properties of electrically conductive PPS/expanded graphite nanocomposites. *Composites Science and Technology*. https://doi.org/10.1016/j.compscitech.2006.12.009

Zheng, R., Lin, J., Wang, P. C., Zhu, C., & Wu, Y. (2015). Effect of adhesive characteristics on static strength of adhesive-bonded aluminum alloys. *International Journal of Adhesion and Adhesives*. https://doi.org/10.1016/j.ijadhadh.2014.10.007

Zheng, S., Bellido-Aguilar, D. A., Hu, J., Huang, Y., Zhao, X., Wang, Z., Zeng, X., Zhang, Q., & Chen, Z. (2019). Waterborne bio-based epoxy coatings for the corrosion protection of metallic substrates. *Progress in Organic Coatings*, *136*. https://doi.org/10.1016/j.porgcoat.2019.105265

Zheng, W., Lu, X., & Wong, S. C. (2004). Electrical and mechanical properties of expanded graphite-reinforced high-density polyethylene. *Journal of Applied Polymer Science*. https://doi.org/10.1002/app.13460

Zhongliang, M., Le, Q., Wei, H., & Liming, H. (2019). A novel approach on the study of cure kinetics for rheological isothermal and non-isothermal methods. *Composites Part B: Engineering*. https://doi.org/10.1016/j.compositesb.2018.10.066

Zhou, W., Yu, D., Wang, C., An, Q., & Qi, S. (2008). Effect of filler size distribution on the mechanical and physical properties of alumina-filled silicone rubber. *Polymer Engineering and Science*, *48*(7). https://doi.org/10.1002/pen.21113

Zhu, Y., Murali, S., Cai, W., Li, X., Suk, J. W., Potts, J. R., & Ruoff, R. S. (2010). Graphene and graphene oxide: Synthesis, properties, and applications. *Advanced Materials*. https://doi.org/10.1002/adma.201001068

Zolghadr, M., Zohuriaan-Mehr, M. J., Shakeri, A., & Salimi, A. (2019). Epoxy resin modification by reactive bio-based furan derivatives: Curing kinetics and mechanical properties. *Thermochimica Acta*. https://doi.org/10.1016/j.tca.2019.01.025